The modulation of Transient Receptor Potential A1 channel by natural and novel

semi-synthetic compounds via non-covalent modification.

Jonathan David Knaggs

PhD

The University of Hull and the University of York

Hull York Medical School

September 2016

I. Abstract

Transient Receptor Potential A1 (TRPA1) is commonly known as the detector of a broad range of noxious chemical agents both exogenous and endogenous. TRPA1 detects these chemicals through a reversible covalent modification mechanism that allows most electrophilic compounds to activate the channel; hence one of the channel's key roles is to protect the respiratory system from harmful irritants by activating the cough reflex. It has been proposed that TRPA1 is involved in chronic inflammatory diseases of the respiratory system and has been highlighted as a potential drug target for this as well as general pain and inflammation.

TRPA1 is also activated by non-covalent mechanisms, which are less well understood. I therefore aimed to gain a further understanding of non-covalent mechanisms of TRPA1 modulation via structure-activity relationship studies using several groups of diverse compounds based on existing TRPA1 agonists.

The results reported have shown that compounds based on thymol, carvacrol and fenamic acid have a diverse effect on TRPA1 dependent on small alterations in structure. This highlights the delicate nature of the TRPA1 non-covalent binding sites. The derivatives tested all share one common structural feature; they all have two phenyl rings which are linked via different functional groups and different lengths. It was found that the length of the linker had an effect on the potency of the modulation of TRPA1. In addition to these results NDGA and its semi-synthetic derivative M4N were potent TRPA1 agonists, yet unlike other similar compounds do not desensitise TRPA1, possibly due to their folded structure. Throughout the results, the importance of hydrogen bonding was shown with different functional groups capable of acting as donors or acceptors.

Overall the results reported expand the group of non-covalent modulators of TRPA1 and indicated important structural features that must be considered in any future TRPA1 drug development projects.

II. Contents

III. List of figures

xi

IV. List of tables

V. Abbreviations

AITC - allylisothiocyanate

ARD - ankyrin repeat domains

BK – bradykinin

CaI - Calcium Ionophore (A23187)

%CaI – percentage of Calcium Ionophore response

CGRP - calcitonin gene-related peptide

COPD - chronic obstructive pulmonary disorder

CNS - central nervous system

DAG - diacylglycerol

DCM - Dichlromethane

DFC – Diclofenac

DMAP - dimethylaminopyrodine

DMSO - Dimethylsulfoxide

DRG - dorsal root ganglion

EDC - ethyl-(N',N'-dimethylamino)propylcarbodiimide hydrochloride

EM - electron microscopy

eNOS - endothelial nitric oxide synthase

FFA - Flufenamic acid

GC-MS – Gas Chromatography – Mass spectrometry

GPCRs - G protein-coupled receptors

hTRPA1 - Human TRPA1

MFA - Mefanamic acid

M4N - Terameprocol/Methylated Nordihydroguaiaretic acid

NDGA - Nordihydroguaiaretic acid

NFA – Niflumic acid

NG - nodose ganglion

NMM - N-methyl maleimide

NMR - Nuclear Magnetic Resonance spectroscopy

NSAIDs - Non-steroidal anti-inflammatory drugs

PER - proboscis extension response

ROS - Reactive oxygen species

RNS – Reactive nitrogen species

SCG - superior cervical ganglia

SP - Substance P

S5 – Transmembrane unit 5

S6 – Transmembrance unit 6

TG - trigeminal ganglion

TRP - Transient Receptor Potential

TRPA1 - Transient Receptor Potential A1

4-HNE - 4-hydroxynonenal

4-ONE - 4-oxononenal

VI. Acknowledgements

I would like to take this opportunity to thank my PhD supervisor Dr. Laura R. Sadofsky for the support, guidance and knowledge she has provided throughout my post graduate course. Whenever I have needed help no matter how big or small she was always ready and willing to help. I would also like to thank Dr. Andrew N. Boa for all of his expert guidance and advice in his role as secondary supervisor.

It has been a great opportunity to carry out my research as part of the Respiratory Medicine group, everyone in the group has been so helpful when I have sought guidance. In addition, the efforts of two undergraduate students, Sam Atkinson and Ashley Dickson, in carrying out parts of the experimentation, have been of great help.

Finally, I would like to thank my sweet wife, Dawn Knaggs, for her invaluable support throughout my academic life, without her I would not have had the motivation to achieve the things I have achieved.

VII. Authors Declaration

I confirm that this work is original and that if any passage(s) or diagram(s) have been copied from academic papers, books, the internet or any other sources these are clearly identified by the use of quotation marks and the reference(s) is fully cited. I certify that, other than where indicated, this is my own work and does not breach the regulations of HYMS, the University of Hull or the University of York regarding plagiarism or academic conduct in examinations. I have read the HYMS Code of Practice on Academic Misconduct, and state that this piece of work is my own and does not contain any unacknowledged work from any other sources'.

1 Introduction

TRPA1 is a member of the TRP superfamily of ion channels. It is expressed throughout the human body, but is mostly found in sensory neurons of the dorsal root ganglion (DRG), nodose ganglion (NG) and trigeminal ganglion neurons (TG). Due to its expression in nociceptor neurons, TRPA1 has been identified as a potential target for drug development due to its role in pain sensing, cough and itch(1). It is hypothesised that TRPA1 functions as a chemical irritant receptor, for harmful electrophilic compounds such as icilin, as a thermoreceptor by sensing temperatures below 17°C and as mechanosensor due to its unusually large amount of ankyrin repeat domains, up to 18 repeats, in the N-terminus. Of particular interest is the expression of TRPA1 in sensory neurons that innervate the airways and pulmonary epithelial cells. TRPA1 has been implicated in the pathogenesis of several respiratory diseases such as chronic obstructive pulmonary disorder (COPD), asthma and chronic cough(2). To further understand the role that TRPA1 plays in pain and inflammatory disease, more research is required to fully understand the structure and function of this channel.

1.1 TRP superfamily of ion channels

Transient Receptor Potential (TRP) channels are a superfamily of cation permeable channels that consists of seven subfamilies. The discovery of the first TRP channel begins with the observations reported by Cosens and Manning in 1969 of a mutant strain *Drosophila melanogaster*(3). They reported that the mutant fruit flies showed an abnormal electroretinogram response to light(3). The mutant flies showed a unique transient response to light rather than a sustained response hence the name Transient receptor potential channels. It was another 20 years later until the mutant gene was discovered by Montell and Rubin in 1989 who successfully isolated, sequenced and cloned the *trp* gene from *Drosophila* flies and showed it to encode a 1275 amino acid protein(4). Hardie and Minke in 1993 identified the TRP channel to be essential for visual transduction in *Drosophila* and showed the channel to be part of a phospholipase C-dependent process(5).

The TRP (Transient Receptor Potential) superfamily of ion channels comprises 28 different proteins subdivided into 7 classes based on sequence homology. Despite variations in sequence homology they all have six transmembrane domains and are permeable to cations(6). TRP channels, when compared to other ion channel families, are unique in the fact that they show a diverse range of cation selectivity and specific activation mechanisms, and many TRP channels have been found to have several different activation mechanisms (such as TRPA1). TRP channels have been found to respond to all major external stimuli such as light, sound, chemical, temperature and touch as well as many internal and local stimuli such as alterations in osmolarity. As a result of this diversity, TRP channels have been found to play critical roles in many cellular processes such as controlling the gating of voltage dependent ion channels, modulating the activity of calcium sensitive effector proteins and transcriptional regulation, migration and proliferation(6).
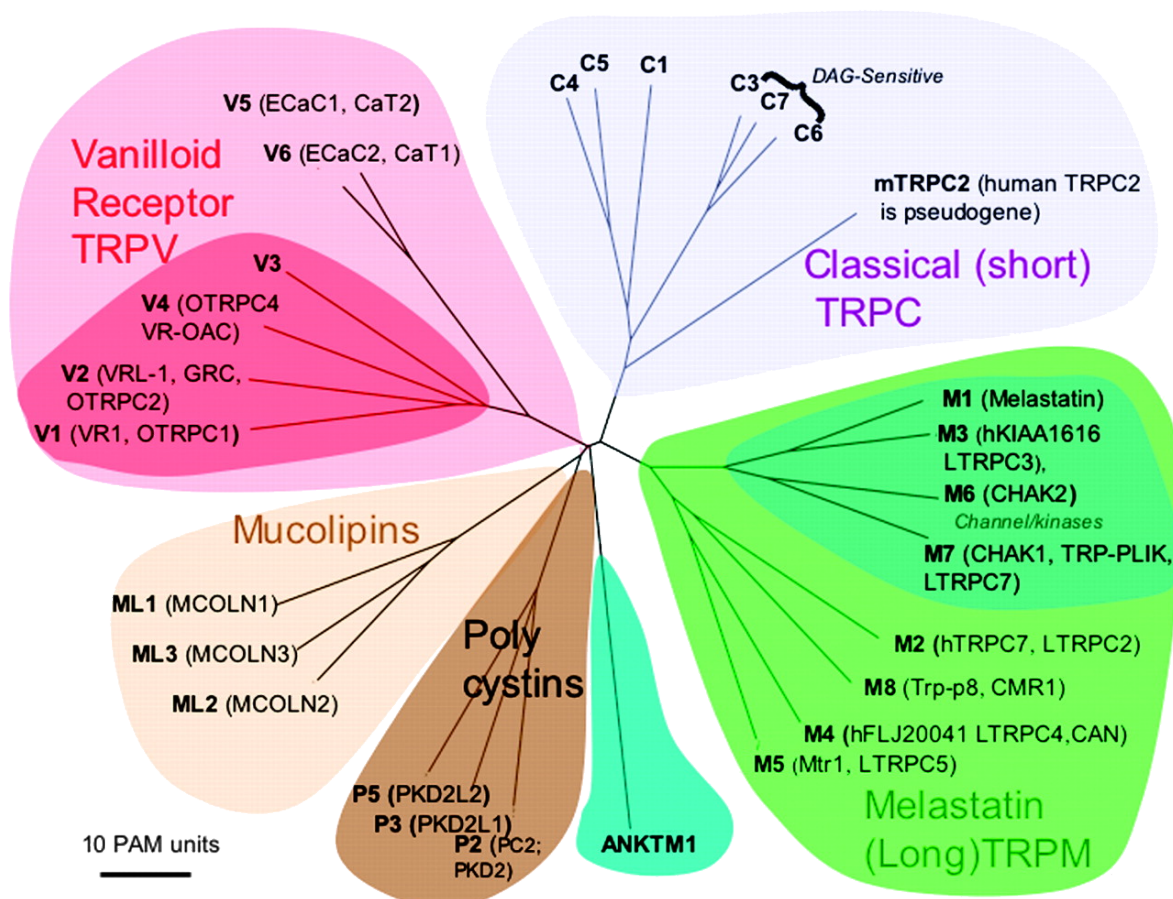
Figure 1 Mammalian TRP family tree adapted from Clapham et al.(7)

Since these initial discoveries, TRP channels have been found in many different species including humans. To date the search for mammalian TRP homologs has produced 28 TRP

channels. The 28 members that form the superfamily of mammalian TRP cation channels have been organised into six subfamilies: TRPA (Ankyrin), TRPC (Canonical), TRPM (Melastatin), TRPML (Mucolipin), TRPP (Polycystin) and TRPV (Vanilloid). The division into subfamilies is, unlike other protein channel families, based on amino acid sequence homology, see Figure 2 for comparison of amino acid sequence between families. The sequence has been found to be highly conserved for approximately 500 million years with all TRP channel members originating from the same ancestral point[8] (Figure 1).
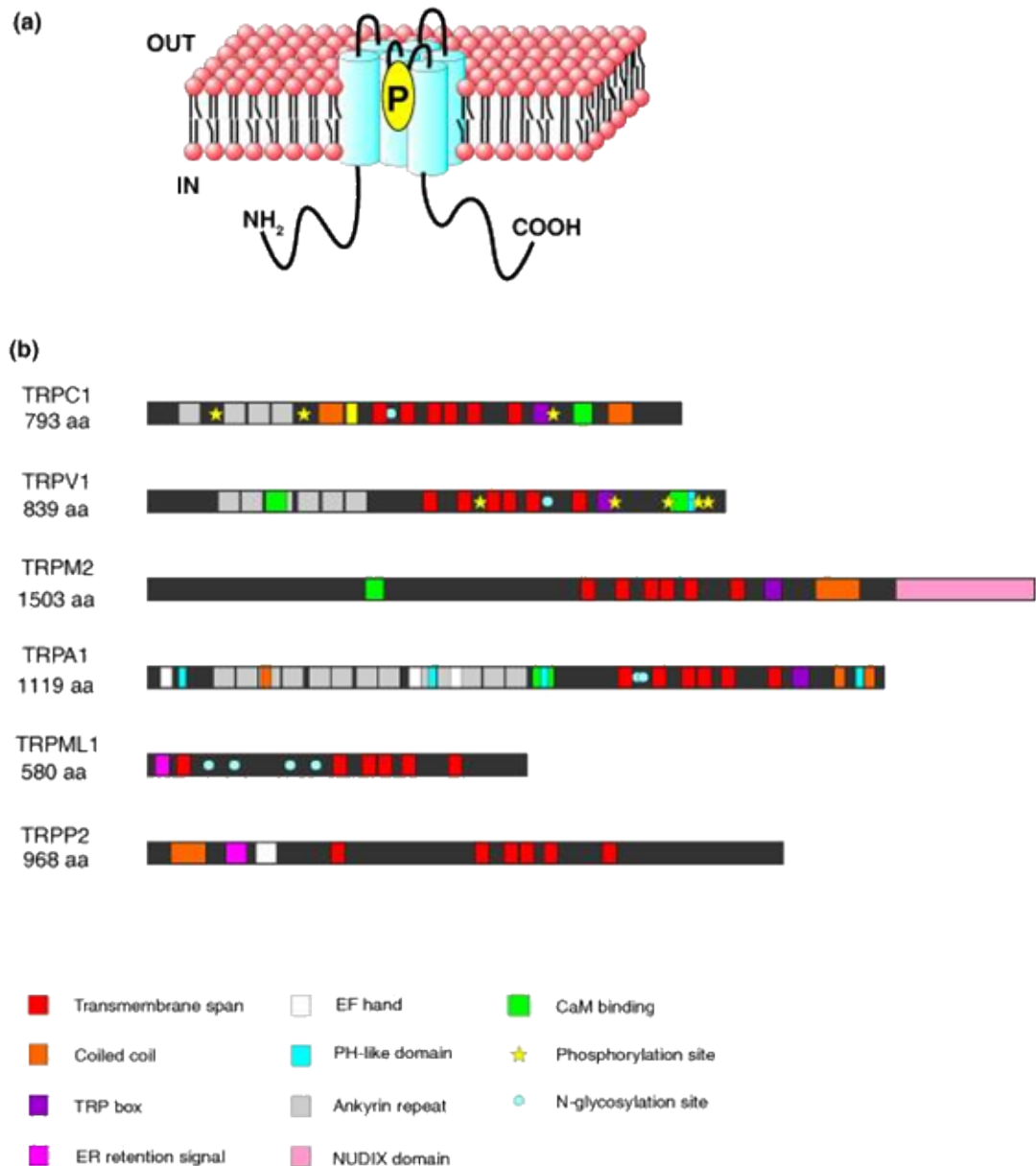
Figure 2 (a) General structure of TRP protein (b) Comparison of amino acid sequences of representative TRP channels from each family adapted from Nilius et al.(9)

The structure of TRP channels is yet to be fully understood, there is still a great deal to be uncovered. However, a general basic structure of TRP channels is generally accepted based

on sequence similarity and low resolution cryo-electron microscopy (EM) structures(10–12). It is expected that all TRP channels are similar in shape to voltage gated potassium channels, which have four subunits surrounding a centrally located pore. Each subunit of the homotetrameric structures has 6 transmembrane domains and both the N and C-termini are located intracellularly. It is the differences in the N and C-termini that differentiate the 28 TRP channel members into the six subfamilies.

1.1.1   TRPC

The TRPC family currently consists of seven mammalian proteins (TRPC1-7). The family can be further subdivided into three subgroups based on sequence homology. These are C1/C4/C5, C3/C6/C7 and C2 (*TrpC2* is a pseudogene in humans). The mammalian TRPC family all tend to be potentiated by stimulation of G-protein coupled receptors and receptor tyrosine kinases.

The seven mammalian TRPC channels share an invariant sequence in the C-terminal tail called a TRP box (EWK- FAR), as well as 3–4 N-terminal ankyrin repeats [23].

1.1.1.1   TRPC1/4/5 Subgroup

The existence of TRPC1 homomeric channels in the plasma membrane is yet to be determined however there is strong evidence to suggest TRPC1 coassembles with TRPC4 and TRPC5 to form heteromeric channels consisting of TRPC1 and either TRPC4 or TRPC5 subunits(13,14).

TRPC4 and TRPC5 are closely related sharing 64 % amino acid sequence identity. Both proteins contain a C-terminal PDZ-binding motif (VTTRL), and it has been reported that PDZ domain scaffolding proteins coimmunoprecipitate with TRPC4 and TRPC5(15). They also share similar functional characteristics such as potentiation by GPCRs that couple to $G\alpha_{q/11}$, activation by trivalent cations La^{3+} and Gd^{3+} as well as potentiation via intracellular Ca^{2+} (TRPC5 is more sensitive than TRPC4)(16–18).

All members of this subgroup are expressed in the brain mainly in the hippocampus, cortex, olfactory bulb and amygdala as well as in the heart, lung, liver, spleen and testis(6). Knockout studies in mice have shown TRPC1(-/-) mice to be increased in weight and have impaired salivary gland fluid secretion(19). TRPC4(-/-) mice showed impaired vascular

function and altered 5 HT-mediated GABA release(20). TRPC5(-/-) mice show a reduced anxiety-like behavioural phenotype(21).

1.1.1.2   TRPC3/6/7 Subgroup

TRPC3, TRPC6 and TRPC7 have been grouped due to each protein having roughly 75 % identical amino acid sequences. They all are potentiated by $G_{q/11}$-coupled receptors and by direct application of diacylglycerol (DAG) analogs(22). All three channels show a relatively low selectivity for Ca^{2+} over Na^+ and are sensitive to intracellular Ca^{2+}. TRPC3 and TRPC6 are activated by increases in intracellular Ca^{2+} concentrations whereas TRPC7 is inhibited. This subgroup is believed to act as downstream effectors for a wide range of hormone and neurotransmitter receptors(13,23).

TRPC3 is present in the brain, specifically in higher concentrations in the cerebellum, cortex, and hippocampus. In hippocampal neurons it has been reported that TRPC3 is activated via the following; through a pathway that is initiated by the binding of TrkB and a brain-derived neurotrophic factor, engagement of PLCγ, and activation of the inositol triphosphate receptor(24,25).

TRPC6 is abundant in smooth and cardiac muscle cells, and therefore is a candidate for the receptor activated non-selective cation channels long known to exist in these cells(26). TRPC7 is widely expressed. It has been reported to play a role in inducing myocardial apoptosis, due to its activation by angiotensin II causing Ca^{2+} overload(27).

In knockout studies TRPC3(-/-) mice showed normal brain development however negative changes in walking behaviour have been reported indicating a critical role for TRPC3 in motor coordination(28). TRPC6(-/-) mice show agonist-induced contractility of cerebral arteries(29). TRPC6 is reported to affect dendritic growth, synaptic formation and neuronal survival however brain development appears normal in TRPC6(-/-) mice(30,31).

1.1.2   TRPV

The TRPV subfamily is named after vanilloid receptor 1, commonly known as TRPV1(32). Six mammalian TRPV receptors have been identified and have been subdivided into two subgroups TRPV1-4 and TRPV5-6 based on sequence homology, functional similarities, and calcium selectivity. All TRPV channels contain 3-5 N-terminal ankyrin repeats, which has

been suggested to promote channel tetramerization and regulate channel activity(12,33). TRPV channels also share ~25 % homology with TRPC channels between S5 and S6.

TRPV1-4 are non-selective cation channels, which are modestly permeable to Ca^{2+} over Na^+ with PCa/PNa values ranging between ~1 and ~10(7). TRPV1-4 have been reported to be activated by a range of different stimuli, and interestingly 2-APB, which has been reported to block some TRPC and TRPM channels, activates TRPV3 and to a lesser extent TRPV2 and TRPV1 but not TRPV4(34,35). All four channels have been discovered to be thermosensitive, and all but TRPV2 are thought to be involved in thermoregulation of some sort in humans. TRPV2 is believed to be involved in innate immunity. TRPV1 is involved in the development of thermal hyperalgesia following inflammation and may contribute to the detection of noxious heat. TRPV4 has been claimed to be mechanosensitive but has not been established to be within physiological range in a native environment(36,37).

TRPV5 and 6 are highly calcium selective channels with PCa/PNa values of over a 100 reported. They share ~74 % identity with each other but only ~25 % with the rest of the TRPV subfamily(38). Unlike the rest of the TRPV channels TRPV5 and 6 are not heat sensitive. Both channels inactivate due to Ca^{2+} overload although through different mechanisms. TPRV5 is expressed in a number of tissues, most commonly in the kidney, more specifically in the distal convoluted and connecting tubule where it is important for transcellular transport and active reabsorption of Ca^{2+}(39). TRPV6 is more widely expressed than TRPV5 and carries out a similar function in the kidneys(40). It is also reported that in the intestines TRPV6, which is localised to the brush border membrane of enterocytes, mediates transcellular Ca^{2+} entry(41).

1.1.3   TRPM

The TRPM ("Melastatin") subfamily consists of 8 mammalian members and subdivided into 4 subclasses based on sequence homology; TRPM1/3, TRPM2/8, TRPM4/5, and TRPM6/7. The TRPM subfamily shares approximately 20 % sequence homology with the TRPC subfamily(42). Unlike TRPC, TRPV and TRPA channels TRPM members do not contain any ankyrin repeats. The C-terminal of TRPMs all have a TRP domain and can be divided into two regions: a coiled coil domain and a second variable region. TRPM2/6 and 7 uniquely contain enzymatically active protein domains in their C-termini and are termed

"chanzymes"(43,44). The N-termini of TRPM channels is considerably longer than that of the TRPV and TRPC members and contains a large TRPM homology region ~700aa long. The biological significance of this region is currently unknown(45).

TRPM1 is highly expressed in the brain. It has been reported to play a role in normal melanocyte pigmentation and is a visual transduction channel in retinal ON bipolar cells(46). TRPM3 has been purported to contribute to the detection of noxious heat and shows widespread expression but is most highly expressed in the brain and pituitary(47,48).

1.1.4   TRPML and TRPP

The TRP superfamily can be broadly split into two groups, group 1 consists of TRPC, TRPV, TRPM and TRPA subfamilies, the second group comprises of TRPML and TRPP.

The TRPML (Mucolipin) family consists of three mammalian channel proteins TRPML1-3(49,50). All three members are believed to be restricted to intracellular vesicles and are not thought to be part of the plasma membrane. TRPML1 is reported to be important for the sorting and transport of endosomes in the late endocytotic pathway and specifically fusion between endosome-lysosome hybrid vesicles. Mutations in the gene encoding the TRPML1 protein are one cause of the neurodegenerative disorder mucolipidosis type IV (MLIV) in man. TRPML3 plays a role in hair cell maturation, stereocilia maturation and intracellular vesicle transport. The function of TRPML2 has remained elusive until recently it has been suggested that TRPML2 may play a role in the regulation of the innate immune response in mammals(51).

The TRPP (Polycystin) subfamily is often referred to as the PKD2 and comprises three mammalian members TRPP1-3. PKD2, polycystic kidney disease 2, proteins are a subset of polycystins, which also include PKD1 proteins(52).

1.1.5   TRPA

The TRPA subfamily consists of one member, TRPA1. The following section 1.2 is an in depth review of the current understanding of this complex channel.

1.2 TRPA1

1.2.1   The *trpa1* gene

The *trpa1* gene was first identified by Jaquemar *et al*. (53) in 1999, who found mRNA in cultured fibroblasts that was not present in SV40 transformed cells, as well as many mesynchemal tumour cell lines. The corresponding gene, located on human chromosome 8 in band 8q13, consists of 55701 base pairs and is composed of 27 exons. The open reading frame of the mRNA encodes a protein of 1119 amino acids with two distinct domains: the N-terminal which contained 18 ankyrin repeat domains (ARD) and the C-terminal which contained seven hydrophobic segments of about 20 amino acids each They postulated that six of these segments may act as transmembrane units, and the remaining segment as a pore loop domain (which contains several charged residues) and only partially spans the membrane. Jaquemar *et al.* hypothesised that the protein product of the gene they had identified functions as an ion channel, due to the similarities of the C-terminal to other ion channels i.e. the six transmembrane domains and pore loop domain. They noted the unusual combination of features of an ion channel and the long chain of ankyrin repeat domains, which they postulated to act as a cytoskeletal anchor similar to that of anion exchanger proteins of the erythrocyte membrane. Due to the low expression levels, they determined under physiological conditions that the protein product may play a regulatory function. Combined with the structural features identified, they proposed an involvement in signal transduction.

The *trpa1* gene can be found in a wide range of animals from vertebrates such as humans to invertebrates such as *D. melanogaster* and beyond to *C. elegans.* The vertebrate TRPA subfamily has only one member, however non-vertebrates show a variety of different TRPA proteins, there are four subtypes in fruit flies, 2 in zebrafish and 2 in *C. elegans.* The activation via covalent modification of reactive cysteine residues on hTRPA1 has been shown to be a highly conserved sensory mechanism, conserved across ~500 million years of animal evolution. Kang *et al.* (8) have shown that fly and mosquito TRPA1 orthologs are molecular sensors of electrophiles using a mechanism conserved with vertebrate TRPA1s. *In vivo* testing of *Drosophila melanogaster* showed an inhibition of a normally robust and reliable response to food (proboscis extension response or PER) when it had been spiked

with reactive electrophiles such as ally isothiocyanate, NMM and cinnamaldehyde. The inhibition of PER was not present when only leg contact with the food was permitted which indicated that the response was gustatory and not an olfactory mechanism, suggesting that chemosensors along the food tract were responsible for reactive electrophile detection. Protein expression of dTRPA1 was detected in the mouthparts and in neurons innervating pores that open onto the oesophagus lumen, which indicates the possible role of dTRPA1 in reactive electrophile sensing in *D. melanogaster*. Kang *et al.* then went on to confirm this suspicion that dTRPA1 was crucial to the inhibition of PER when exposed to spiked food, by carrying out loss of function studies which showed that dTRPA1 loss of function mutants showed no reduction in inhibition of PER when spiked food was offered. Alternatively, *Painless* (a gene encoding a protein belonging to the TRPA subfamily, painless is considered a basal TRPA as it is not activated via the covalent modification of cysteine residues) loss of function mutants showed no effect over wildtype. Previously it was thought that activation of TRPA1 via covalent modification was only apparent in TRPA1 proteins of vertebrate species and not invertebrate species such as *D. melanogaster*(54,55). Hamada *et al.* (56) revealed that these previous results, which showed a distinct loss of function between vertebrate TRPA1 and invertebrate TRPA1, are slightly misguiding as the dTRPA1 cDNA used was found to contain a partial inactivation mutation. Hamada *et al.* went on to show that when wildtype dTRPA1 orthologs were expressed in Xenopus oocytes, the TRPA1 was activated by multiple reactive electrophiles. In addition, they also showed that TRPA1 from two other Drosophila and the malaria mosquito responded similarly. The similarities in the response between that of the dTRPA1 and hTRPA1 to reactive electrophiles suggest similar activation mechanisms. Kang *et al.* constructed a phylogeny of TRPA proteins (see Figure 3). They showed that with confidence that both electrophile sensitive vertebrate and invertebrate TRPA1 proteins are derived from a common ancestor and belong to the same monophyletic clade, the TRPA1 clade, which is distinct from other TRPAs which have been termed basal TRPAs. It is hard to believe that such a seemingly basic sensory mechanism has remained relatively unchanged and not evolved as species have diversified is a testament to the very basic need of animals to avoid naturally occurring harmful reactive molecule, see section 1.2.5.1 for a detailed review of activation via covalent modification of TRPA1.
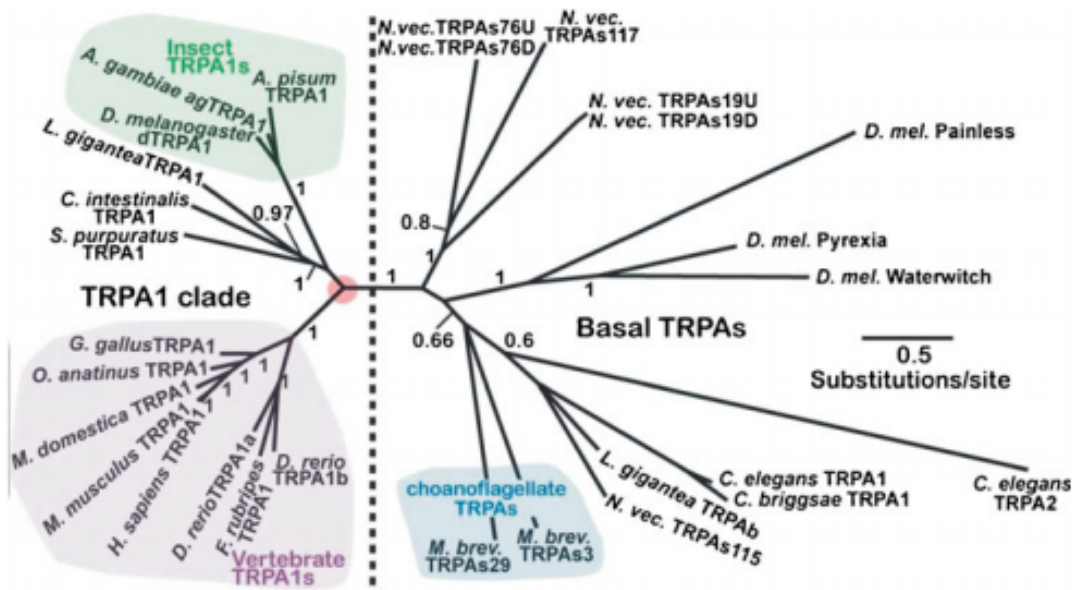
Figure 3 Phylogeny of TRPA channels(8)

1.2.2   Protein Structure of TRPA1

1.2.2.1   Basic Structure

Human TRPA1 (hTRPA1) is a 1119 aa protein with a mass of ~120-150kDa. TRPA1 proteins are believed to function as a homotetramer, much like the majority of other TRP channels. The predicted TRPA1 protein structure is similar to the generalised TRP channel protein structure and is made up of six putative transmembrane domains (S1-S6). In between the 5th and 6th transmembrane domain (S5-S6) is the putative ion-permeable site(57).

1.2.2.2   N-terminus

The N-terminus contains up to 18 ankyrin repeat domains (ARD). Ankyrin repeats are 33 aa motifs consisting of two alpha helices; they typically fold together to form a single linear structure which is termed an ankyrin repeat domain. Deletion of the ARDs from the TRPA1 structure negatively affects the insertion of the protein into the plasma membrane(58). The multiple ARD in the N-terminal are believed to be heavily involved in the gating mechanism of the channel(59).   Within the ARD are several key cysteine residues which have been shown to react with noxious chemical irritants resulting in channel activation (see 1.2.2.2.1 for full discussion). There is also an EF-hand domain which is located between ARD11 and ARD12. An EF-hand domain is a 12 aa helix-loop-helix motif, termed after its resemblance

to the thumb and forefinger of the human hand, that is capable of binding with calcium ions. The EF-hand domain has been reported to be involved in intracellular Ca^{2+} dependent activation[60][61]. It has been shown in modelling experiments by Zayats *et al.* [62]that the 'springy' multiple ARD can change dramatically upon Ca^{2+} binding with the EF-hand domain[62]. They have predicted that the calcium bound state is more rigid than the calcium free state and the end-end distance can change by almost 50 %. Zayats *et al*. postulate that the change in the physical properties of the N-terminus when exposed to stimuli causes an interaction with the transmembrane domains that ultimately affects the gating of the channel. Further studies of the EF-hand revealed that point mutations in the region only had small effects on the Ca^{2+} dependent activation mechanism. However, it was shown that deletions had an effect on trafficking of the truncated channel to the plasma membrane[58].

More specifically the residue N855, which is located in the loop between S4 and the S4-S5 connecting helix, forms stable hydrogen bonds with the N-terminus of S1 while all other interactions are hydrophobic in nature. This interaction shows a direct link between the N-terminus and the S4-S5 connecting helix. The N855 residue has been associated with familial episodic pain syndrome; it is the N855S mutant which is thought to be the root cause of the hereditary disease. The serine side chain is less polar than that of asparagine and has a lower hydrogen bonding capability. This has a knock on consequence of loosening the mechanical coupling to the ankyrin repeats. Zayats *et al.*[62] focused on the physical changes to the ankyrin repeats when calcium binding occurs, however they have commented on how irreversible covalent modification of cysteine residues may follow a similar route to effect the gating of the channel i.e. through a direct force link through the N855 residue[62] see below in Figure 4 and Figure 5 for N855 site.
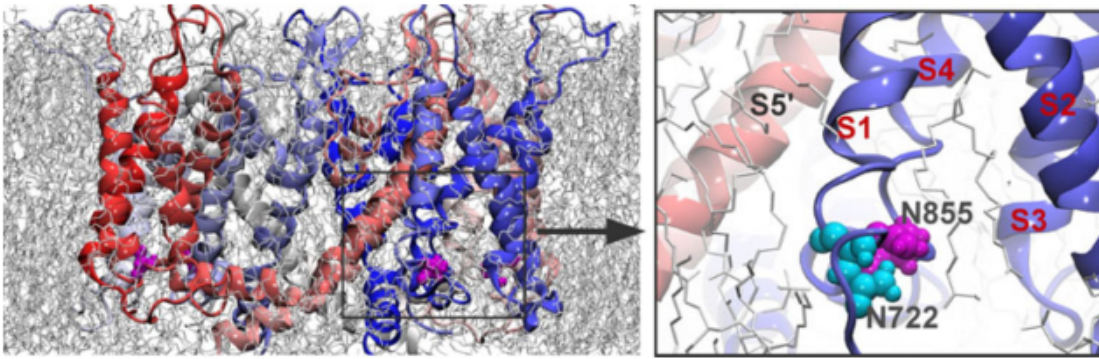
Figure 4 All four subunits of TRPA1 coloured differently in the membrane (left) Close up of N855 residue located between S4 and the S4-S5 linker helix, its position allows interaction with S1(62)
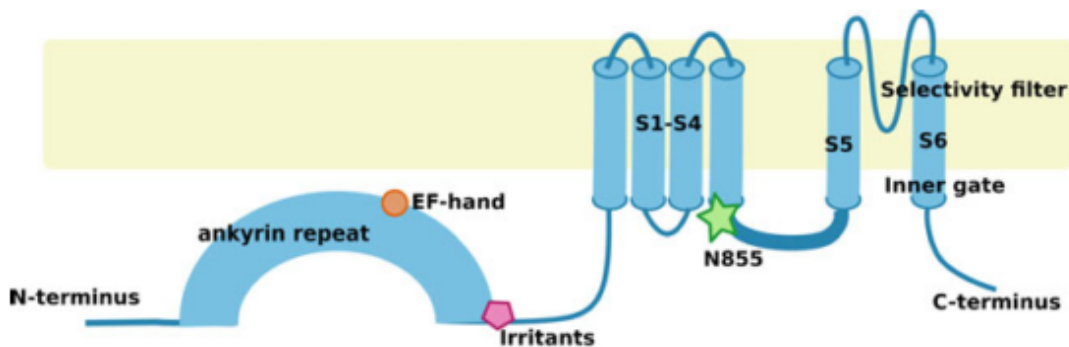
Figure 5 Model of TRPA1 subunit with position of N855 residue highlighted with a green star(62)

1.2.2.2.1 Important cysteine residues

TRPA1 activation by noxious chemical irritants occurs through a covalent modification of N-terminal cysteines. So far five cysteine residues have been identified as playing an important role in sensing these electrophilic irritants; in human TRPA1 (hTRPA1) these are Cys-415, Cys-422, Cys-622, Cys-642 and Cys-666(63,64). Mutation studies have shown that when these cysteine residues are replaced with non-reactive residues activation of the TRPA1 channel by electrophilic compounds is abolished. However, activation by non-electrophilic agonists was not affected by these mutations, highlighting another mode of activation. Experimentally it has been suggested that Cys-415 is important to the response to both reactive and non-reactive agonists(65). Cys-422 has been shown to be key to the response caused by human inflammatory mediators. In modelling experiments, it has been hypothesised that cysteine residues from different TRPA1 subunits can interact to form a cysteine pocket. Cys-415 and Cys-422 from one subunit, which may interact with Cys-622 located on a flexible loop on the adjacent subunit, Cys-642 and Cys-666 are also located on the same flexible loop as Cys-622 and they may also interact with this cysteine pocket(66).

So far there has been no definitive experimental data to determine how covalent modification of cysteine residues translates to protein activation. It may be reasonable to predict that covalent modifications may perturb this hypothesised cysteine pocket therefore facilitating or disturbing interactions between subunits leading to structural changes in the cytoplasmic domains that can potentially lead to channel gating(67).
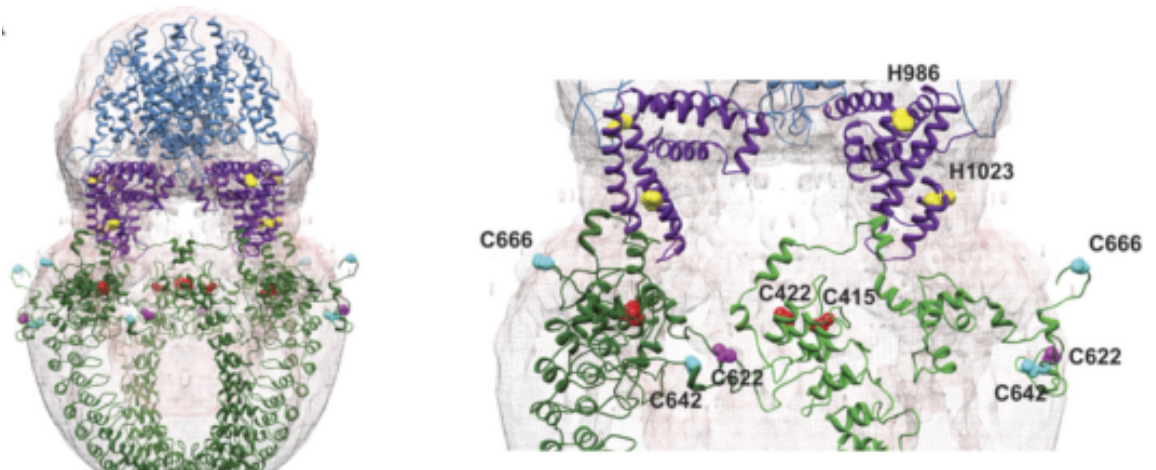
Figure 6 Model of homotetramer TRPA1 (left) Location of important cysteine residues on two subunits forming cystiene pocket (right)(66)

1.2.3   Protein expression

TRPA1 was originally thought to be expressed in the nociceptive sensory neurons of the DRG, TG and NG which respond to a vast range of chemical irritants and noxious cold (below 17°C)(68)'(69). To add to this TRPA1 was thought to function as a transduction channel found in the inner ear involved in hearing(70). In recent times there have been reports that suggest that TRPA1 is widely expressed throughout the human body, present in many organs and tissues such as the brain, heart, lung, small intestine and pancreas(71).

1.2.3.1   In the nervous system

1.2.3.1.1   Sensory Neurons and peripheral nervous system

TRPA1 is highly expressed throughout sensory neurons and the peripheral nervous system, as well as in the autonomic nervous system. In TG it is expressed in small myelinated axons, A(δ), axons and unmyelinated C axons. More than 25 % of the neurons that express TRPA1 are peptidergic and release substance P and calcitonin gene-related peptide (CGRP). Trigeminal sensory nuclei, the largest of the cranial nerve nuclei, express TRPA1 as well as

the spinal dorsal horn, superficial laminae of the trigeminal caudal nucleus (Vc). TRPA1 is also expressed in the autonomic nervous system, in particularly the sympathetic superior cervical ganglia (SCG) which contains neurons that are cold-sensitive and express TRPA1(72). TRPA1 is also expressed in nodose and jugular oesophageal nociceptors where it plays an important role in the activation of these neurons by bradykinin(73–75).

TRPA1 has been found to be expressed in vagal sensory nerves that innervate both the heart and the airways. The role it plays differs substantially in the neurons innervating the heart; here TRPA1 is involved with vasovagal reflexes, whereas in the airway neurons TRPA1 is key to sensing a wide range of harmful environmental irritants causing an action potential to occur in airway afferent C-fibers, which results in the propagation of the cough reflex(76). TRPA1 is highly expressed in the nociceptive neurons innervating the respiratory tract(77–79).

Other sensory neurons that express TRPA1 have been found to innervate:

- the colon: activation of TRPA1 inhibits contractility in the colon and is involved in the inhibition of spontaneous neurogenic contractions(80)
- the bladder: expression of TRPA1 is linked to bladder afferent transduction(81)
- the prostate: TRPA1 may act as a mediator of mechanoafferent signals, epithelial homeostasis, emission, or inflammation of the human prostate(82)

1.2.3.1.2   Central Nervous System Expression

TRPA1 has been found to be expressed throughout the central nervous system (CNS). It has been connected with the activation of the cannabinoid receptor CB1 in the hippocampus(83). It is coexpressed with TRPV1 in neurons of the nucleus supraopticus, which is a nucleus of magnocellular neurosecretory cells in the hypothalamus, where it is involved with excitatory synaptic inputs(84). TRPA1 is involved with regulation of glutamate release in the brain stem were it is expressed in the visceral afferent pathway(85).

1.2.3.2   Inner ear

Due to TRPA1's multiple ankyrin repeat domains located in the N-terminus, it has been suggested that TRPA1 may function as a mechanosensitive channel in the inner ear as the ankyrin repeats are thought to act like a spring capable of interacting with mechanical

stimuli(86). Specifically it has been found to be expressed in the stria vascularis, the organ of corti and in the outer and inner hair cells of the cochlea(87,88).

1.2.3.3   Cardiovascular System

TRPA1 is expressed in vascular endothelial cells and in perivascular nerves. It is believed that activation of TRPA1 plays a role in arterial dilation. Two pathways through which TRPA1 activation can lead to arterial dilation have been found. Firstly, TRPA1 expression is concentrated at myoendothelial junction sites where upon activation the influx of Ca^{2+} causes endothelium-dependent smooth muscle cell hyperpolarization. Secondly, TRPA1 channels in the perivascular nerves mediate vasodilation through a mechanism requiring the release of calcitonin gene-related peptide(89,90).

1.2.3.4   Gastrointestinal tract

TRPA1 is expressed throughout the small intestinal and colonic mucosa. Due to TRPA1's ability to sense a wide array of chemical irritants, it acts as a chemosensor for the luminal environment and together with intestinal odorant receptors modulates gastrointestinal functions such as epithelial permeability and electrogenic anion secretion(91).

1.2.3.5   Respiratory System

TRPA1 is highly expressed in most of the nonneuronal cell types forming the respiratory system. Experimental data are sparse with regards to the function of TRPA1 expression in nonneuronal respiratory tissue, as much of the research has been carried out on the role of TRPA1 expressed in sensory neuronal cells that innervate the respiratory tract. However, there is evidence that highlights a fundamental role for TRPA1 expressed in nonneuronal cells in normal airway function with it becoming increasingly important for acquired disease(92,93). In cultured TRPA1 expressing human lung fibroblasts (CCD19-Lu) and alveolar epithelial cell line (A549), it was shown that selective activation of TRPA1 promoted the release of the chemokine IL-8. Upon pretreatment of a selective TRPA1 antagonist this response was diminished. These data show a potential role for TRPA1 in modulating the release of an important chemokine in airways inflammation.

1.2.3.6 Skin

It has been found that TRPA1 is expressed in nonneuronal cells types such as human keratinocytes, fibroblasts and melanocytes. TRPA1 has been shown to play a role in the expression of proinflammatory cytokines(94).

1.2.3.7 Dental Pulp

TRPA1 in expressed highly in the dental pulp fibroblasts of human teeth. It has been considered to act a thermoreceptor as it has been shown that TRPA1 is activated by noxious cold temperatures (below 17°C)(95). It is also believed to be involved in pain associated with mechanotransduction. A high proportion of pulpal afferent nerves express TRPA1 and for these reasons TRPA1 is a potential target for treatments of dental sensitivity.

1.2.4 Physiological functions of TRPA1

TRPA1 is expressed throughout the human body in many different tissues. TRPA1 is activated by several different pathways such as; electrophilic chemicals (including ROS and RNS), noxious cold, mechano-activation and Ca^{2+} dependent modulation. As a result of widespread expression and several vastly different stimuli, it is no surprise that TRPA1 has several important functions in the body. These functions include sensory functions such as sensing harmful exogenous chemical irritants, activating the release of inflammatory mediators, evoking mechanical hypersensitivity upon inflammation and thermoregulation.

1.2.4.1 Sensory Functions

1.2.4.1.1 Inflammation

TRPA1s involvement in inflammation was first shown in studies using allylisothiocyanate (AITC) to induce the release of substance P (SP) and CGRP which had the effect of promoting thermal and mechanical hypersensitivity via the release of inflammatory mediators(96). At the time it was unknown through what mechanism AITC elicited this response. Since then it has been shown in studies that when TRPA1 is blocked or the channel is removed through genetic knockout the inflammatory effects of AITC were significantly decreased(97–99).

Not only does TRPA1 have a role in instigating an inflammatory response but it may also be playing a crucial role in hypersensitivity that occurs during inflammation. It has been found that TRPA1 is activated by inflammatory mediators. Reactive oxygen species (ROS) are released by cells in response to tissue damage which can cause lipid peroxidation to produce species such as 4-hydroxynonenal (4-HNE) and 4-oxononenal (4-ONE) that have been found to directly activate TRPA1(100,101). Prostaglandins are produced at the site of inflammation and can mediate inflammatory responses and sensitization. One such prostaglandin derivative 15d-PGJ$_2$ has been found to activate TRPA1(100–103). TRPA1 can also be sensitised indirectly during inflammation through interaction with G protein-coupled receptors (GPCRs). Tissue damage can cause the production of bradykinin (BK) which can activate BK$_2$R GPCRs in TRPA1 expressing nociceptors which through Phospholipase C can modulate TRPA1 to promote sensitization to thermal, mechanical and chemical stimuli(98,104,105).

1.2.4.1.2   In the Respiratory System

The vast array of, both exogenous and endogenous, chemical stimuli suggests that TRPA1 may play a role as a chemosensor. It has been shown that TRPA1 expressed in primary sensory neurons that innervate the airways provides an early warning of potential damage from exogenous chemical irritants to the respiratory tract.

The respiratory tract allows the passage of air to the alveoli and as a result is the first contact point for any airborne irritants and noxious chemicals. The primary afferent sensory neurons that innervate the airways have been found to be activated by potentially damaging agents. In order to protect the airways from damage, protective reflex responses can be activated such as coughing, sneezing, bronchoconstriction and a decrease in respiratory rate. In order for these responses to occur the irritant chemicals must be detected by chemosensors. It is believed that TRPA1 is a chemosensor that covers a broad range of chemical irritants that can cause significant damage to the airways. In early chemical exposure studies in animals it was shown that reactive irritants cross-desensitized each other's ability to evoke a protective respiratory response(106). These results suggested that sensory neurons contained one single reactive receptor and once it has been saturated when exposed to one chemical irritant it becomes unresponsive to further exposure by a different irritant. Another view was that there were many different receptors

and cross-desensitization occurred through cellular signalling pathways(106,107). Since then it has been discovered that TRPA1, which is a chemosensor to a wide range of chemical irritants, is highly expressed throughout the cells that make up the airways and is expressed in many of the primary sensory neurons that innervate the airways(108).

The respiratory tract (from the nasal cavity to the bronchi) is heavily innervated with primary afferent C-fibres and A(δ)-fibers from the jugular ganglion, dorsal root ganglion, trigeminal ganglion and nodose ganglion. Activation of these neurons in the airways leads to the release of inflammatory neuropeptides such as SP and CGRP. SP and CGRP can induce bronchoconstriction, vasodilation, and recruitment of immune cells and modulation of the inflammatory response. These responses to airway irritants can result in respiratory responses such as cough, increased mucus secretion, and shallow breathing with the primary focus of reducing the exposure to harmful toxins(109).

The first line of defence against environmental irritants can be found in the nasal mucosa. The trigeminal chemosensory nerve endings that innervate the nasal mucosa, when excited, can cause irritation, pain and sneezing to occur(110). Neuropeptides such as SP and CGRP which are released by chemosensory TG neurons promote neurogenic inflammatory vasodilation and leakage, which causes the narrowing and potential obstruction of the nasal passages(111). It is known that a large percentage of TRPA1 expressing sensory neurons are peptidergic and release SP and CGRP, some of which are the trigeminal neurons that innervate the nasal mucosa(112).

1.2.4.1.3   TRPA1 induced Cough

Cough is a reflex response that helps to clear the respiratory tract of harmful chemical irritants, foreign particles and mucus. The cough reflex is a protective defence mechanism in normal healthy humans, however it is most commonly associated with inflammatory diseases of the respiratory system such as bronchitis, COPD and asthma.

The upper and lower respiratory tract are innervated by vagus neurons of the nodose ganglion and jugular ganglion. Activation of vagus afferent neurons has been seen to induce coughing in guinea pigs and humans. The induction of the cough reflex has been found to be caused by both mechanical and chemical stimuli(113,114).

It has long been established that another TRP channel, TRPV1 has a role in initiating the cough reflex. As there is evidence to show in both guinea pigs and humans that selective TRPV1 agonists, such as capsaicin, resiniferatoxin and citric acid, elicit robust tussive reponses(115,116). However, there are many other chemical irritants that can initiate cough that do not interact with TRPV1. TRPA1 is commonly coexpressed in sensory afferent neurons that innervate the lungs and in recent years experimental evidence has shown it to play an important role in the initiation of the cough reflex. Known TRPA1 agonists, AITC and cinnamaldehyde produce dose-dependent robust tussive responses in guinea pigs(77). The response to these TRPA1 agonists was diminished with pretreatment of TRP nonselective blockers ruthenium red, camphor and the TRPA1 selective antagonist HC-030031. In the same study acrolein and crotonaldehyde, which are TRPA1 agonists and are found in abundance in cigarette smoke, elicited a tussive response in guinea pigs; once again the effect was reduced by the use of HC-030031. Another study showed the partial inhibition of the tussive response caused by the inhalation of cigarette smoke by blocking TRPA1 with HC-030031(117). These results are reflected in humans which suggests that TRPA1 may be placed together with TRPV1 as a major mechanism for the initiation of the cough reflex(118).

1.2.4.2 Thermoregulation

The role of TRPA1 as a thermosensor has been strongly debated. The very first study to highlight TRPA1's involvement in thermoregulation showed that, in Chinese hamster ovary cells that expressed TRPA1, noxious cold elicited Ca^{2+} influx(69). These results were repeated in similar studies(119–122). However other studies observed no such response to noxious cold by TRPA1(60,96,123). The underlying cause of these conflicting results is due to difficulties in comparing results directly due to different experimental conditions and the use of clones from different species. An example of species differentiation can be seen in the function of TRPA1 in invertebrate and ancestral vertebrate species, such as fly, mosquito, frog, lizard and snake, as TRPA1 has been found to be heat sensitive in these species and has a role in infrared detection, rather than being cold sensitive as is thought to be the case in mammals(124–127). Recent results seem to confirm that in humans TRPA1 does not function as a thermosensor of noxious cold. Chen *et al.* have shown that rat and mouse TRPA1 is indeed sensitive to cold temperatures however human and rhesus monkey

TRPA1 is not sensitive. They found that a single residue variation caused the change in sensitivity between rodents and primates, this variation is found within the S5 transmembrane domain G878 in rodents with the corresponding residue in primates being V875(128).

1.2.5 TRPA1 activation

The agonist catalogue for TRPA1 spans a large diverse spectrum, which is mostly due to the diverse mechanisms of modulation that TRPA1 displays. Many of the chemical agonists have one common feature that is they all have an electrophilic functional group which can covalently modify cysteine residues in the N-terminus of TRPA1, chemicals such as ally isothiocyanate, acrolein, and cinnamaldehyde. There are many other chemicals that do not contain such reactive moieties, for example menthol and thymol, which are believed to interact with the channel via a classical ligand binding mechanism.

1.2.5.1 Activation via covalent modification of cysteine residues

TRPA1 is gated by a wide array of chemicals that structurally share no significant resemblance to each other. However, many TRPA1 agonists are similar with regards to their reactivity; the vast range of chemical TRPA1 activators contain some sort of electrophilic functional group that can interact with the side chains of cysteine, lysine and histidine amino acid residues. Indeed, in studies carried out by Hinman *et al.*(64)*.* and Macpherson *et al.*(63)*,* it was discovered that TRPA1 activators such as AITC and acrolein activated TRPA1 through an unusual interaction. Rather than the classic lock-and-key binding it was found that electrophilic, sulfhydryl reactive, functional groups of TRPA1 agonists reacted covalently with several cysteine residues to cause channel activation. Site-directed mutagenesis experiments by the same groups indicated several of the 31 cysteine residues in the N-terminus as being crucial to the activation of TRPA1. Hinman *et al*. showed C622, C642 and C666 located between the last ankyrin repeat and the S1 transmembrane domain were crucial. Meanwhile Macpherson *et al.* highlighted C415, C422 and C622. Modelling studies show that in the homotetrameric TRPA1 structure a cysteine binding pocket forms between two adjacent TRPA1 proteins, specifically C415 and C422 from one subunit and C622 from the adjacent subunit, which can form a ligand binding pocket. This may include the C642 which is located on a flexible loop close to the C622 residue. As for how the

covalent modification of these cysteine residues causes the knock on effect of channel gating can only be postulated at this point and no experimental data have provided a mechanism through which gating of the channel is achieved.

Upon the discovery of activation of TRPA1 via covalent modification by Hinman *et al.* and Macpherson *et al.* they also inferred that the reaction mechanism for this was through a conjugate addition route. However, a more recent study has shown that it is not as cut and dry as first believed. Sadofsky *et al.*(129) have shown that α,β-unsaturated aldehyde agonists, which have two electrophilic sites (one at the carbonyl carbon and the other at the β-carbon) and can potentially undergo conjugate and direct addition reactions with the thiol side chain of cysteine. Their results also show that molecules that can react in either conjugate or direct addition activate TRPA1 preferentially via the direct addition of the thiol group. Sadofsky *et al.* found that molecules only capable of conjugate addition showed no significant physiological response when exposed to TRPA1 expressed in HEK293 cells. Molecules that are capable of both conjugate and direct addition were shown to activate TRPA1 in a robust dose dependent reversible manner which leads to the hypothesis that reversible direct addition of the thiol group produces an unstable kinetic product is the preferred route of interaction with the cysteine residues of TRPA1.

1.2.5.2   Activation of TRPA1 via non-covalent modification

While the most prevalent form of TRPA1 activation is via a reversible covalent modification mechanism, TRPA1 has also been found to be modulated via non-covalent mechanisms. There is a growing number of different classes of non-covalent modulators of TRPA1. This section will give an overview of these classes.

Thymol and related alkylated phenols, such as carvacrol, have been found to activate TRPA1. Because they have no electrophilic functional groups, they are believed to activate via a non-covalent mechanism most likely through a ligand binding mechanism(130). It was reported that the steric hindrance to the phenol group and the lipophilicity of the compound played a role in the potency of activation. This theory has been supported by the results reported that show primary alcohols activate TRPA1 with the potency increasing with increasing carbon chain length(131). Derivatives of thymol have been shown to have diverse effects. The compounds tested contain a thymol moiety which is linked to another

phenyl ring, with different linker groups and substitutions on the phenyl rings altering the effect on TRPA1(132).

Similarly related to thymol, menthol, also known for its agonist effect on TRPM8, has been shown to have a bimodal effect on TRPA1(133)(134). Menthol has been observed to activate TRPA1 at a low concentration and inhibit the channel at higher concentrations, greater than 1mM. This effect is only true for human TRPA1; in mouse TRPA1 menthol was only found to inhibit TRPA1 at high concentrations(135). It has been reported that menthol activation of TRPA1 occurs through key amino acid residues found within the S5 membrane domain(55). Thymol and carvacrol activation were also found to occur through this binding pocket.

Another example of a species dependent agonist of TRPA1 is caffeine. Caffeine has been reported to activate mouse TRPA1 yet inhibit human TRPA1(136). The Met268Pro mutation of mouse TRPA1 was reported to reverse the effect of caffeine from agonist to inhibitor, and highlighting the Met268 residue as the site of interaction for caffeine(137).

Ligustilide has been shown to activate TRPA1(138). This may be through a covalent mechanism however it was observed that the aromatised derivative dehydroligustlide inhibits TRPA1. This indicates that the mechanism of activation of ligustilide may be through a non-covalent ligand binding mechanism. 3-ylidenepthalide derivatives based on ligustilide have also shown a variety of different TRPA1 modulatory properties(139).

Similar to the effect of menthol on human TRPA1, nicotine and closely derived chemicals have been shown to have a bimodal effect on TRPA1(140). It is believed that the topical application of nicotine, for example, as part of nicotine replacement therapies, causes irritation of the mucosa and skin due to TRPA1 activation. Yet at higher concentrations nicotine inhibits TRPA1(140).

A range of different drugs have been reported to modulate TRPA1. A group of fenamate NSAIDs, which include flufenamic acid, mefenamic acid, niflumic acid, ketoprofen, diclofenac and flurbiprofen, have been shown to activate TRPA1(141). These NSAIDs were found to reversibly activate TRPA1 and also desensitise the channel. In addition, anaesthetic agents have been reported to activate TRPA1 in a non-covalent manner. A closely related chemical to the fenamate NSAIDs which also has been reported to activate

TRPA1 is NPPB. NPPB, best known for being a chloride channel blocker, is a potent TRPA1 agonist(142). It was also reported that closely related derivatives of NPPB also activate TRPA1 but to a lesser extent. Propofol, a commonly used intravenous anaesthetic, elicits intense pain upon injection. It has been shown that TRPA1 activation may be the cause of this(143). General anaesthetics which depress the CNS have been reported to activate peripheral nociceptive neurons through the activation of TRPA1. The more pungent general anaesthetics such as isoflurane and desflurane were found to be more potent agonists of TRPA1 than less pungent general anaesthetics(144). As well as general anaesthetics, several local anaesthetics have been identified as TRPA1 agonists. Lidocaine, which inhibits voltage gated sodium channels, can activate TRPA1 in a concentration dependent manner(145). Lidocaine has also been observed to inhibit TRPA1, however this was more prevalent in rat TRPA1 than human TRPA1(145).

1.2.6   TRPA1 Antagonism

TRPA1 has been validated thoroughly as a therapeutic target in recent years for treatment of pain, itch and respiratory disorders(1,77,146–149). This has generated interest from several pharmaceutical companies, who are actively developing TRPA1 antagonists.

The first blockers of TRPA1 used as pharmacological tools were non-specific inhibitors such as ruthenium red, amiloride and gadolinium(149). The first specific potent TRPA1 antagonist that was identified was HC-030031, with an IC50 of ~4 µM(77). HC-030031 is a caffeine derivative that is linked through an amide bond to a phenyl ring (see Figure 7). Identified via high throughput screening by Hydra Biosciences and patented in 2007 it is the most widely used pharmacological tool in TRPA1 research. Other common specific TRPA1 antagonists used in research are oxime derivatives AP-18 and A96(see Figure 7)(104,150).
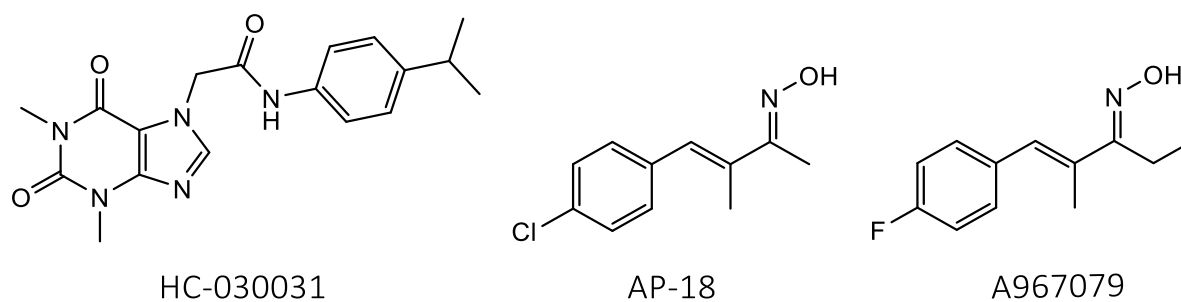
Figure 7 Chemical structures of common TRPA1 specific antagonists.

The current progress of research into the development of TRPA1 antagonists has been fully reviewed by Preti *et al.* (151). Four main pharmaceutical companies are actively pursuing the development of potent selective TRPA1 agonists. These are; Hydra Biosciences, Glenmark Pharmaceuticals, Janssen Pharmaceuticals and Hoffmann-La Roche. To date more than 40 patents have been filed for compounds that inhibit TRPA1 with IC50 potencies ranging from less than 25nM to low μM. The efforts of Hydra and Glenmark have focused on refining the HC-030031 structure, whereas Janssen and Hoffman-La Roche have filed patents for sulfonamide based structures. Common trends seem to be clear from the range of structures listed by Preti *et al.* (151). Bicyclic and tricyclic structures make up the majority of TRPA1 antagonists, with aromatic rings proving to be most prevalent. Secondly the linking of cyclic structures always contains a hydrogen bonding functional group, most commonly an amide or sulfonamide. Aryl halide groups appear heavily in the structures of the most potent TRPA1 antagonists that have been patented with fluoro aryl halide groups generally appearing to be the most prevalent.

Several of the patented TRPA1 antagonists have shown promise in *in vivo* studies and have been taken forward to clinical trials. The antagonist that has been progressed the furthest is GRC-17536 which is currently in phase 2a proof of concept study in patients with chronic cough. The structure for this antagonist has not been disclosed but is most likely a derivative of HC-030031.

The current efforts as mentioned previously have been focused on the refinement of the HC-030031 compound. Other than this only a handful of different drug leads have been reported or patented, which include the oximes AP-18 and A96 mentioned above. With the wide range of TRPA1 agonists that have been reported and the bimodal nature of many of

24

the non-covalent agonist, which indicates that there still remains a lot of potential for development of novel drug leads that target TRPA1.

1.3 Aims and hypothesis

As part of the literature review, it has been shown that TRPA1 is gaining popularity as a potential target for drug development to treat chronic pain and neuronal inflammatory conditions as well as chronic inflammatory respiratory conditions including cough. The activation of TRPA1 by reversible covalent modification has been studied in depth, and it has been established that most electrophile containing chemical compounds will activate TRPA1. It has also been shown that TRPA1 is activated by multiple different mechanisms and not much is known as to the mechanisms of non-covalent traditional ligand binding interactions. Several studies have been carried out that highlight potential key TRPA1 amino acid residues for certain agonist and antagonist interactions however in some cases these studies have contradicted one another.

TRPA1 has been shown to be modulated by many different non-covalent compounds, several key structural components have been hypothesised as being crucial to the binding of compounds to TRPA1. These include bicyclic and tricyclic aromatic structures, hydrogen bond donor and acceptor functional groups such as amide and sulfonamide groups and aryl halide groups.

Currently, drug development of TRPA1 antagonists has focused on the HC-030031 structure, which is based on a modulator of TRPA1 caffeine. It is my aim to identify novel TRPA1 modulators which are different to the core structures of TRPA1 antagonists being developed by pharmaceutical companies yet using the key structural components hypothesised as being crucial for ligand binding to TRPA1.

In chapter 3 the aim was to synthesise compounds based on the thymol and carvacrol structure, which are known TRPA1 agonists, and report the effects of any compounds that give a response in assay experiments.

In chapter 4 the aim was to report the effects of novel fenamic acid derivatives on TRPA1 and determine structural features that were key to the response.

In chapter 5 the objective was to report the effect of NDGA and M4N on TRPA1 and determine what structural features were key to their response on TRPA1. This was carried out by testing the effects of monocyclic derivatives of NDGA and M4N.

Using structure-activity relationship studies of several novel groups of compounds, the aim of this thesis is to further the understanding of non-covalent modulation of TRPA1 and outline structural features key to activation and inhibition of TRPA1. Also, it is the aim of this thesis to further understand the structure-activity relationship between NDGA/M4N and TRPA1. Through this research, I am hoping to aid drug development by identifying key structural features for TRPA1 modulation.

2 Materials and Methods

2.1 Synthesis

Commercial solvents and reagents were used without further purification unless stated otherwise. Chemical reagents were purchased from Sigma-Aldrich, Fluka, Acros, Lancaster, Alfa Aesar, TCI Europe, and Novabiochem at the highest grade of purity available, and were used as received, unless otherwise stated.

^{1}H and ^{13}C NMR spectra were recorded on JEOL Eclipse 400 and JEOL Lambda 400 spectrometers (operating at 400 MHz for ^{1}H and 100 MHz for ^{13}C). CDCl$_3$, and DMSO-D$_6$, were used as solvents. Chemical shifts (δ) are reported in parts per million (ppm), referenced to either CHCl$_3$ (^{1}H, 7.26 ppm; ^{13}C, 77.16 ppm) or DMSO (^{1}H, 2.50 ppm; ^{13}C, 39.52 ppm). Coupling constants (J) are recorded in Hz and significant multiplicities described by singlet (s), doublet (d), triplet (t), quadruplet (q), broad (br), multiplet (m), or doublet of doublets (dd).

Elemental and GC-MS analysis was carried out by the Chemistry department's analytical services group.

2.1.1 Synthesis of amide and ester-linked thymol derivatives

2.1.1.1 Amide Method

3.7 mmol of 2-isopropylaniline, 4.3 mmol of triethylamine and a catalytic amount of DMAP was dissolved in 15 ml of DCM. The solution was then stirred, and 4.1 mmol of the desired acyl chloride was slowly added. The solution was stirred at room temperature for 2 hours. The solution was diluted with 15 ml DCM and washed with 10 ml water, 10 ml saturated NaHCO$_3$(aq) and 10 ml saturated NaCl(aq) three times. The washed DCM solution was then dried over MgSO$_4$, then the DCM solvent was evaporated off to yield the crude product. The crude product was then purified via recrystallisation from a 10 ml 50:50 mix of ethanol and water. The crystallised product was then dried in a vacuum desiccator.

2.1.1.2   *Ester Method*

3.7 mmol of 2-isopropylphenol, 4.3 mmol of triethylamine and a catalytic amount of DMAP was dissolved in 15 ml of DCM. The solution was then stirred, and 4.1 mmol of the desired acyl chloride was slowly added. The solution was stirred at room temperature for 2 hours. The solution was diluted with 15 ml DCM and washed with 10 ml water, 10 ml saturated $NaHCO_3$(aq) and 10 ml saturated NaCl(aq) three times. The washed DCM solution was then dried over $MgSO_4$, then the DCM solvent was evaporated off to yield the crude product. The crude product was then purified via recrystallisation from a 10 ml 50:50 mix of ethanol and water. The crystallised product was then dried in a vacuum desiccator.

2.1.2   Synthesis of thymol and carvacrol acetamide linked derivatives

The methods used to synthesis the ojk06 and ojk07 groups of compounds is detailed below.

2.1.2.1   *Synthesis of 2-(5-isopropyl-2-methylphenoxy)acetic acid.*

To a solution of 39 mmol of carvacrol (5.83 g) and 47 mmol of chloroacetic acid (1.2 mol equiv.) (4.46g) in 100 ml of dH_2O, 117 mmol of NaOH (3 mol equiv.) (4.67 g) in 100 ml dH_2O was added slowly. The solution was heated to 110 ^{o}C and left for 12 hours. Throughout the reaction the pH was monitored and if a drop in pH was recorded pellets of NaOH were added to maintain the basic environment. Upon completion, the solution was allowed to cool, and any unreacted carvacrol was removed via extraction with 20 ml diethyl ether, three times. The aqueous layer was acidified with concentrated HCl and the resulting precipitate was collected, and an extraction using 15 ml diethyl ether was carried out three times to extract leftover protonated product. The extracts were combined with the precipitate and the solution was diluted. The organic solvent was then washed with 15 ml dH_2O, 15 ml sat. NaCl(aq) and 15 ml sat. $NaHCO_3$(aq). The organic layer was then dried over $MgSO_4$. The diethyl ether was then evaporated off to yield a solid product which was then dried in a vacuum desiccator overnight.

2.1.2.2   *Synthesis of 2-(2-isopropyl-5-methylphenoxy)acetic acid.*

To a solution of 43 mmol of thymol (6.48 g) and 52 mmol of chloroacetic acid (1.2 mol equiv.) (4.91 g), in 100 ml of dH_2O, 129 mmol of NaOH (3 mol equiv.) (5.16 g) in 100 ml dH_2O, was added slowly. The solution was heated to 110^oC and left for 12 hours. Throughout the reaction the pH was monitored and if a drop in pH was recorded pellets of NaOH were added to maintain the basic environment. Upon completion, the solution was allowed to cool, and any unreacted carvacrol was removed via extraction with 15 ml diethyl ether three times. The aqueous layer was acidified with concentrated HCl and the resulting precipitate was collected, and an extraction using 15 ml diethyl ether was carried out three times to extract leftover protonated product. The extracts were combined with the precipitate and the solution was diluted. The organic solvent was then washed with 15 ml dH_2O, 15 ml sat. NaCl(aq) and 15 ml sat. $NaHCO_3$(aq). The organic layer was then dried over $MgSO_4$. The diethyl ether was then evaporated off to yield a solid product which was then dried in a vacuum desiccator overnight.

2.1.2.3   *Synthesis of acetamide linked derivatives.*

To a solution of 1.4 mmol of the relevant phenoxyacetic acid intermediate (0.30 g) in 15 ml DCM 1.1mol equiv. of the relevant amide (1.586 mmol) and 1.2 mol equiv. of EDC (1.734 mmol) was added slowly. The reaction was left at room temperature for 18 hours. The reaction solution was then diluted with 15 ml DCM and washed with 10 ml dH_2O, 10 ml sat. NaCl(aq) and 10 ml sat. $NaHCO_3$(aq). The organic layer was then dried using $MgSO_4$ and the solvent was evaporated off leaving a solid precipitate. The precipitate was then recrystallized in a 10 ml 50:50 mix of EtOH and H_2O to yield the purified solid which was then left to dry in a vacuum desiccator.

2.1.3   Synthesis of fenamic acid derivatives

The SE and SLE compounds assayed in chapter 4 have been synthesised previously and all methods, materials and results can be found in Jiang *et al.* (152).

2.2 Calcium Signalling Assay

In order to determine the effect on TRPA1, a calcium signalling assay has been developed

in order to determine the influx of calcium into cells expressing TRPA1 which can be related to the effect of the test compounds on TRPA1.

Compounds which have been tested using this assay method have either been synthesised as part of this piece of research, previously synthesised in-house at University of Hull, or purchased and used without further purification from Sigma Aldrich. The ojk01, ojk06 and ojk07 compounds have been synthesised as part of this research and details of synthesis and characterisation can be found in section 3. The SE and SLE compounds used in section 4 have been synthesised previously by the University of Hull Chemistry Department details of the synthesis and characterisation have been published by Jiang *et al.*(152). The NSAIDs tested in section 4, and all of the compounds tested in section 5 have been purchased and used without further purification from Sigma Aldrich; details of characterisation and purity can be found at www.sigmaaldrich.com.

2.2.1   Culture and Maintenance

Pre-developed, according to the protocol as stated in Sadofsky *et al.* (153), stable human TRPA1 expressing HEK293 cell lines were passaged every 48 hours at a ratio of 1:3. They were harvested by pouring off the media and rinsed in PBS before lifting and transferring to a new flask in supplemented Dulbecco's modified Eagle's media and G418 and grown to 80-90 % confluence in a 5 % carbon dioxide 37°C incubator.

2.2.2   Preparation of assay media

Transfected TRPA1 HEK293 cells were grown to 80-90 % confluent growth in a T25 flask and harvested. Cells were washed with PBS, lifted and centrifuged for 4 minutes at 1500 rpm. The supernatant was subsequently discarded, and the cell pellet was broken up. The cells were incubated in supplemented media, 0.25 mM sulfinpyrazone, and 12.5 µg Fluo-3 AM for 30 minutes at room temperature on an orbital shaker. Then the cells were centrifuged again with 5 ml PBS for 4 minutes at 1500 rpm. The supernatant was discarded and the cells resuspended in 2 ml of calcium assay buffer (20 mM HEPES, 3 mM KCl, 150 mM NaCl, 10 mM glucose and 1.5 mM $CaCl_2$). A 100 µl aliquot of the cell suspension was added to 1x1 cm, 2 ml cuvettes, containing 1.9 ml calcium assay buffer and a magnetic flea under constant agitation.

2.2.3   Controls

Both positive and negative controls were used to substantiate the anticipated effect of TRPA1 channels. DMSO, used as a vehicle control, demonstrated that it played no involvement in cell activity in response to test compounds. Cinnamaldehyde, at a concentration of 30 µM (the calculated EC50 concentration) was used to demonstrate the presence of TRPA1 channels because it is a known agonist and therefore is expected to have a specific effect; see Figure 8 for a full concentration effect curve for cinnamadehyde on TRPA1-HEK293 cells. A further control to monitor the decline in cell function during assay is calcium ionophore (CaI)(A23187); used at a concentration of 100 µM; it is assumed to function at 100 % of the cells' capacity by chelation of calcium into the cell to increase the intracellular calcium concentration. HC-030031, a selective and potent TRPA1 antagonist, was used when using the TRPA1-HEK293 cell lines to determine whether the agonist response of the test compounds was via a TRPA1 mechanism, see Figure 9 for a full concentration effect curve for the inhibitory effect of HC-030031 on the activation of TRPA1-HEK293 cells by cinnamaldehyde. A concentration of 30 µM was used as this fully inhibits the effect of 30 µM cinnamaldehyde (EC50 concentration).
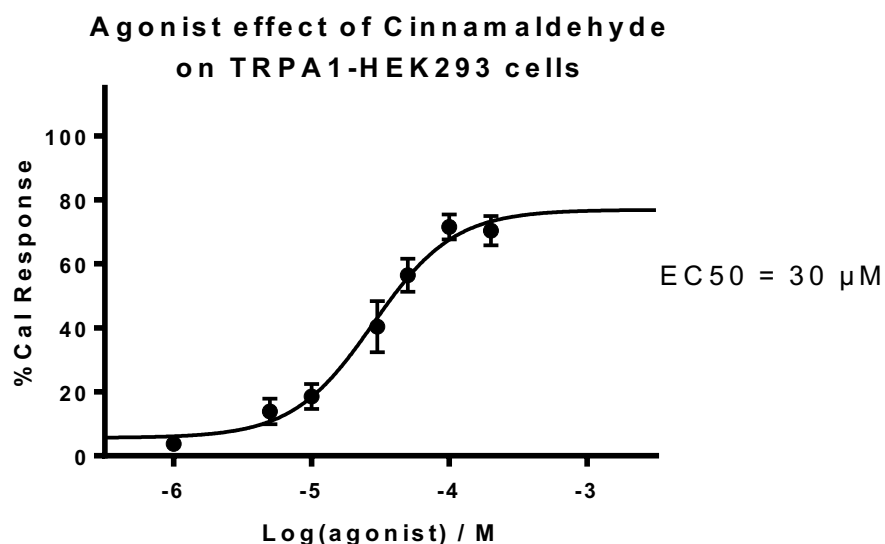
Figure 8 Agonist concentration effect curve for cinnamaldehyde on TRPA1-HEK293 cells. Data points are means±SEM of N = 3 experiments

Cinnamaldehyde, the agonist control for the TRPA1-HEK293 cell calcium signalling assay has been tested using the agonist calcium signalling method. The resulting concentration

effect curve can be seen in Figure 8 above. A concentration dependent increase in intracellular calcium was observed; this response was inhibited fully by the TRPA1 specific inhibitor HC-030031. Therefore, this response can be attributed to the gating of TRPA1 channels. Cinnamaldehyde was tested over the concentration range of 1 to 200 µM; over this range a typical sigmoidal response was observed. The first significant response was observed at 5 µM with a mean %CaI response of 14. The maximum response was observed at the 100 µM concentration point with a mean %CaI response of 72. A maximum plateau can be observed between the 50 and 100 µM concentration points, this maximum response observed at 100 µM is confirmed by the response observed at the 200 µM which was 71 %CaI. Non-linear regression analysis using the variable slope model was carried out which calculated and EC50 value of 30 µM.
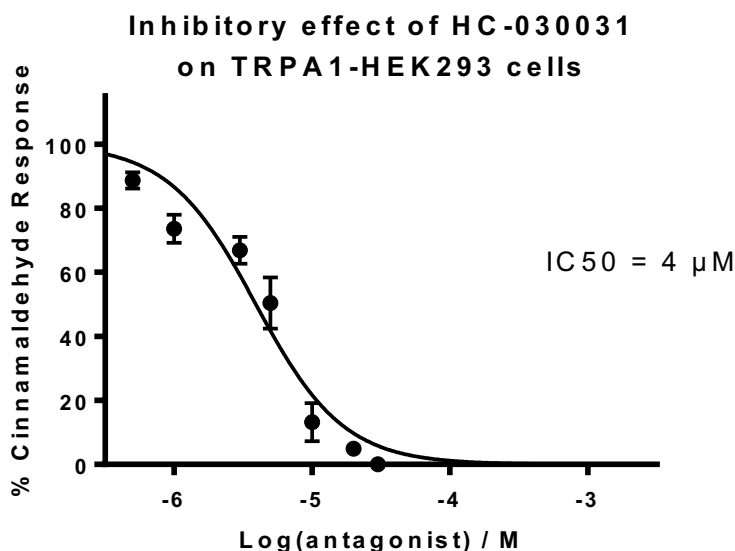
Figure 9 Antagonist concentration effect curves for HC-030031 on TRPA1-HEK293 cells. Data points are means±SEM of N=3 experiments

HC-030031, the antagonist control has been assayed using the antagonist calcium signalling assay to assess the compounds effect on TRPA1-HEK293 cells. The resulting concentration effect curve can be seen in Figure 9. A concentration dependent decrease in the response of 30 µM of cinnamaldehyde (EC50 concentration of cinnamaldehyde) was observed with increasing concentration of pre-dosed HC-030031. HC-030031 was tested over the concentration range of 1-30 µM over this range a typical reversed sigmoidal curve was observed. The first decrease in the cinnamaldehyde response was observed at 1 µM with a decrease in cinnamaldehyde response of 12 %. Complete reduction of the cinnamaldehyde

response occurred at the 30 μM concentration point. The best fit non-linear regression analysis model was the normalised variable slope model which has an R^2 value of 0.9059, the calculated IC50 value for this model is 4 μM.
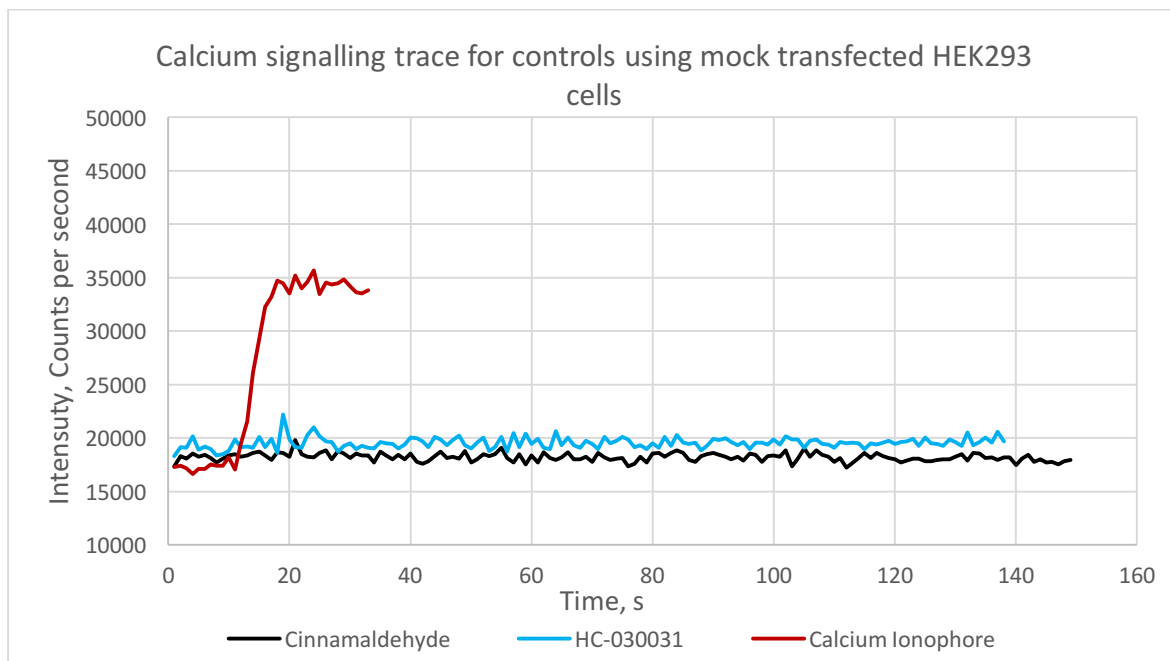
Figure 10 Calcium signalling trace of controls using mock transfected HEK293 cells.

Both cinnamaldhyde and HC-030031 showed no response at concentrations of 200 and 30 μM when assayed using mock transfected HEK293 cells (see Figure 10). It can be deemed that the response observed using the TRPA1-HEK293 cells are TRPA1 specific.

2.2.4   Agonist Assay

To the cuvettes containing the cell suspension; prepared as per section 2.2.2; a concentrated solution of the test compound is added using a volume of approximately 6 μl to attain the desired final cuvette concentration. Intensity changes induced by agonistic properties of the experimental compounds were measured with an excitation wavelength of 506nm and emission at 526nm with a fluorospectrometer and software Felix-GX, and responses were recorded until plateau or their peak. A difference from the baseline to the peak height is measured and the final result is reported as a percentage of the response observed for CaI (%CaI), see Figure 11. Each concentration point was tested in duplicate in each experiment, to determine the precision of the results, and averaged to give the result for that experiment. The experiment was then repeated a minimum of three times and the

result from each experiment was then averaged to give a final result and the standard error of the mean calculated and used to represent the error bars in the concentration effect curve.
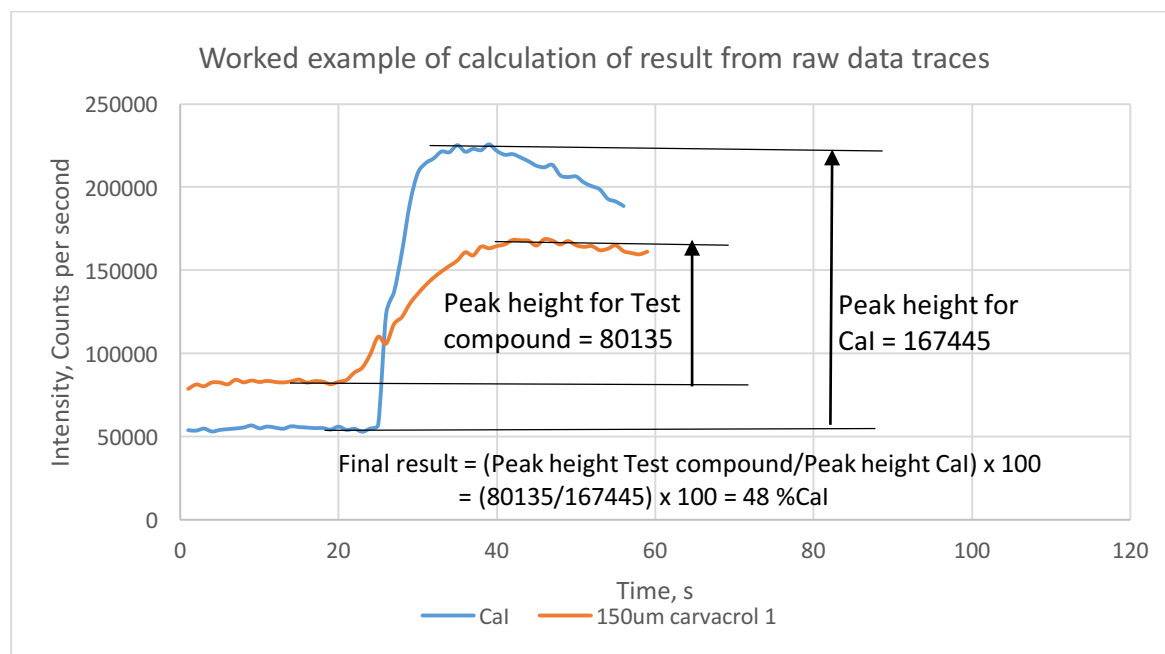
Figure 11 Calcium signalling raw data traces for test compound and CaI. Worked example of agonist result calculation.

2.2.5 Antagonist Assay

To the cuvettes containing the cell suspension; prepared as per section 2.2.2; a concentrated solution of the test compound is added using a volume of approximately 6 µl to attain the desired final cuvette concentration. The cuvettes with the cell suspension and test compound were then left to incubate for 10 minutes. After incubation the fluorescence of the suspension was recorded as outlined in section 2.2.4. Addition of 30 µM cinnamaldehyde (EC50 concentration) was then carried out. Antagonistic and desensitising effects of the experimental compounds were tested by incubation of the cell suspension for 10 minutes before assay and the subsequent addition of the EC50 concentration of the channel agonist, 30 µM cinnamaldehyde for TRPA1, 100 µM WS-5 for TRPM8. The responses of both uninhibited cinnamaldehyde and inhibited cinnamaldehyde were measured as a percentage of the peak effect of CaI (A23187), as per section 2.2.4. The result of the inhibited cinnamaldehyde response was then used to calculate a final result by converting it into a percentage of the uninhibited cinnamaldehyde response, see Figure 12

34

for a worked example of the results calculation. The uninhibited agonist response is the average response of the three agonist controls carried out at the beginning, middle, and end of the experiment. Each concentration point was tested in duplicate in each experiment, to determine the precision of the results, and averaged to give the result for that experiment. The experiment was then repeated a minimum of three times and the result from each experiment was then averaged to give a final result and the standard error of the mean calculated and used to represent the error bars in the concentration effect curve.
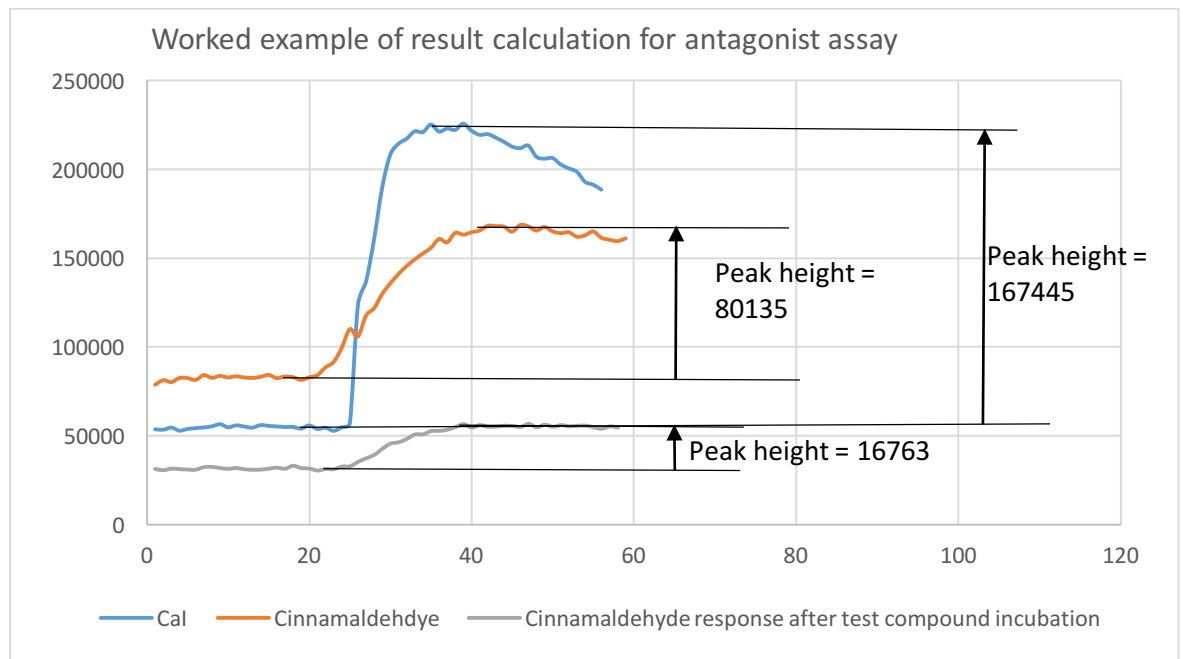
$$\%CaI\ result\ for\ test\ compound = \left(\frac{peak\ response}{peak\ response\ of\ CaI}\right) \times 100 = \left(\frac{16763}{167445}\right) \times 100 = 10$$

$$\%CaI\ result\ for\ cinnamaldehyde = \left(\frac{peak\ response}{peak\ response\ of\ CaI}\right) \times 100$$

$$= \left(\frac{80135}{167445}\right) \times 100 = 48$$

$$Final\ result = \left(\frac{\%CaI\ response\ test\ compound}{\%CaI\ response\ cinnamaldehyde}\right) \times 100 = \left(\frac{10}{48}\right) \times 100$$

$$= 21\ \%\ Cinnamaldehyde$$

Figure 12 Calcium signalling traces for CaI, Cinnamaldhyde and Test compound. Worked example of antagonist result calculation.

2.2.6   TRPM8 Calcium signalling assay method

The TRPM8 calcium signalling assay was carried out in exactly the same way as described above with the following differences:

- A TRPM8 expressing HEK298 cell line was cultured in the same way and used in the assay as described above.
- The agonist control used was WS-5 at a concentration of 100 μM

2.2.7   Data analysis

Raw data from each repeat of the calcium signalling assays was entered into GraphPad Prism 6. The responses were averaged and plotted on a $\log_{10}$(concentration/M) versus % Calcium Ionophore response (for the agonist assay results) or % Cinnamaldehyde response (for the antagonist assay results). Non-linear regression analysis was then carried out on the resulting graph to calculate a concentration effect curve, two models of analysis was carried out and the best curve was determined. For the agonist assays the two models that were carried out are:

- Log(agonist) vs. response – Variable Slope (four parameters); this model determines the top and bottom plateau and determines a Hill slope which best fits the data points and uses the following calculation:
  - Y=Bottom + (Top-Bottom)/(1+10^((LogEC50-X)*HillSlope))
- Log(agonist) vs. normalised to maximum cinnamaldehyde response – Variable slope; this model assumes a bottom plateau of zero and a top plateau of 72 %CaI response as this is the maximum response observed for cinnamaldehyde on TRPA1-HEK293 cells in my system. The model then determines a Hill slope to best fit the data points. This model uses the following calculation:
  - Y=72/(1+10^((LogEC50-X)*HillSlope))

For the antagonist assays the two models used are as follows:

- Log(inhibitor) vs. response – Variable Slope (four parameters); this model determines the top and bottom plateau and determines a Hill slope which best fits the data points and uses the following calculation:
  - Y=Bottom + (Top-Bottom)/(1+10^((LogIC50-X)*HillSlope))

- Log(inhibitor) vs. normalised response – Variable slope; this model assumes a bottom plateau of zero and a top plateau of 100 %Cinnamaldehyde response. The model then determines a Hill slope to best fit the data points. This model uses the following calculation:
  - Y=100/(1+10^((LogIC50-X)*HillSlope))

2.2.7.1 Definitions for data analysis

The results from the repeats of calcium signalling assays have been collected and presented as concentration effect graphs. The concentration effect graphs that have been produced have been reported and analysed in chapters 3, 4 and 5. The guidelines and definitions used in these chapters have been detailed below.

For the agonist assay, the concentration of the first observed response is defined as the first concentration point which has an average result of greater than 10 %CaI. For the antagonist assay, this is defined as the first concentration point which reduces the effect of the agonist by 10 %. Full inhibition is determined when a 90 % reduction of the agonist response is observed.

Determination whether an agonist response was a full agonist or a partial agonist was carried out by calculating the test compound's efficacy of response. The efficacy of response was calculated as a percentage of the maximum response of cinnamaldehyde, which was observed to occur at 100 μM with an average response of 72 %CaI, see section 2.2.3. An efficacy of below 85 % was deemed to be a partial agonist response and an efficacy above 85 % was deemed to be a full agonist response.

In the antagonist assay, compounds deemed to be full inhibitors were observed to fully inhibit the activation of TRPA1 by cinnamaldehyde, with full inhibition deemed to occur when the cinnamaldehyde response was reduced by 90 % or more.

In the following results sections (sections 3, 4 and 5) test compounds are referred to as agonist, antagonist and desensitisers. Below, in Figure 13, Figure 14 and Figure 15, are examples of the raw data traces from the calcium signalling assay method for an agonist, an antagonist and a desensitiser. An agonist is defined as a compound which increases intracellular calcium levels, presumably via channel activation, and after incubation does

37

not inhibit the response of the agonist control. An antagonist is defined as a compound which upon exposure to the cell suspension does not have an effect on intracellular calcium levels i.e. there is no channel activation. After an incubation period the response of the agonist control is diminished in a concentration dependent manner. A desensitiser is defined as a compound which exhibits an agonist response upon first exposure to the cell suspension and after incubation also inhibits the response of the agonist control in a concentration dependent manner.
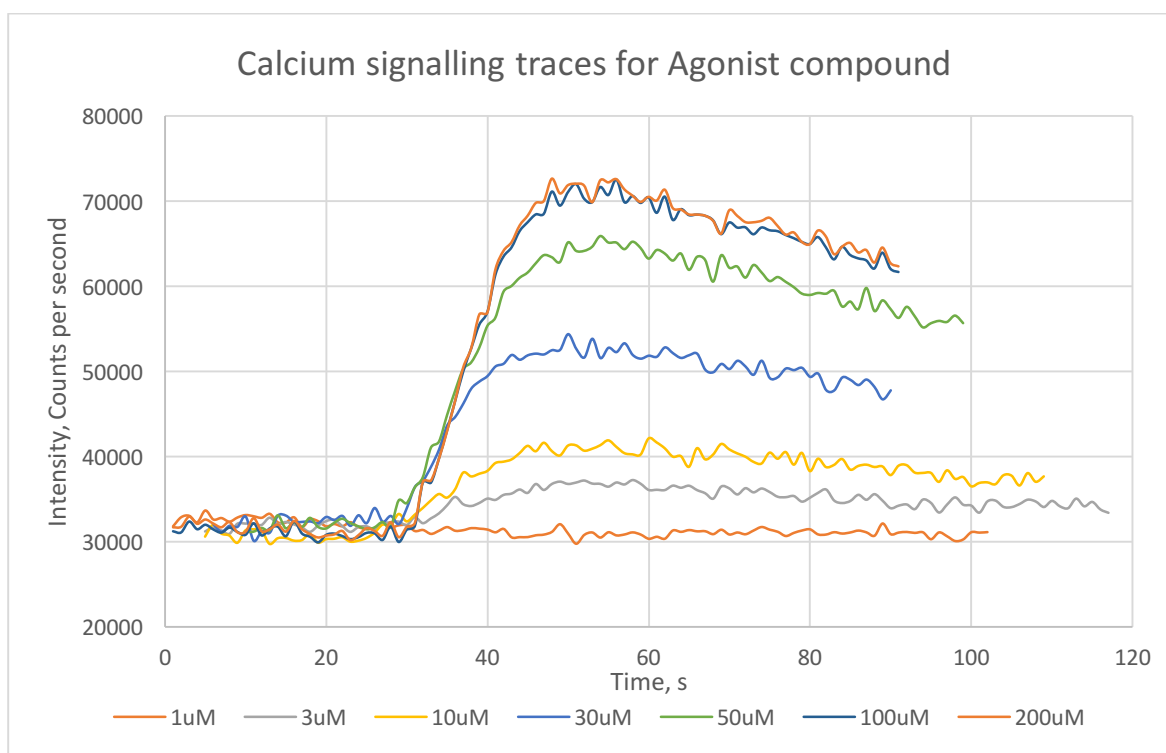
Figure 13 Raw data trace for an agonist compound

38
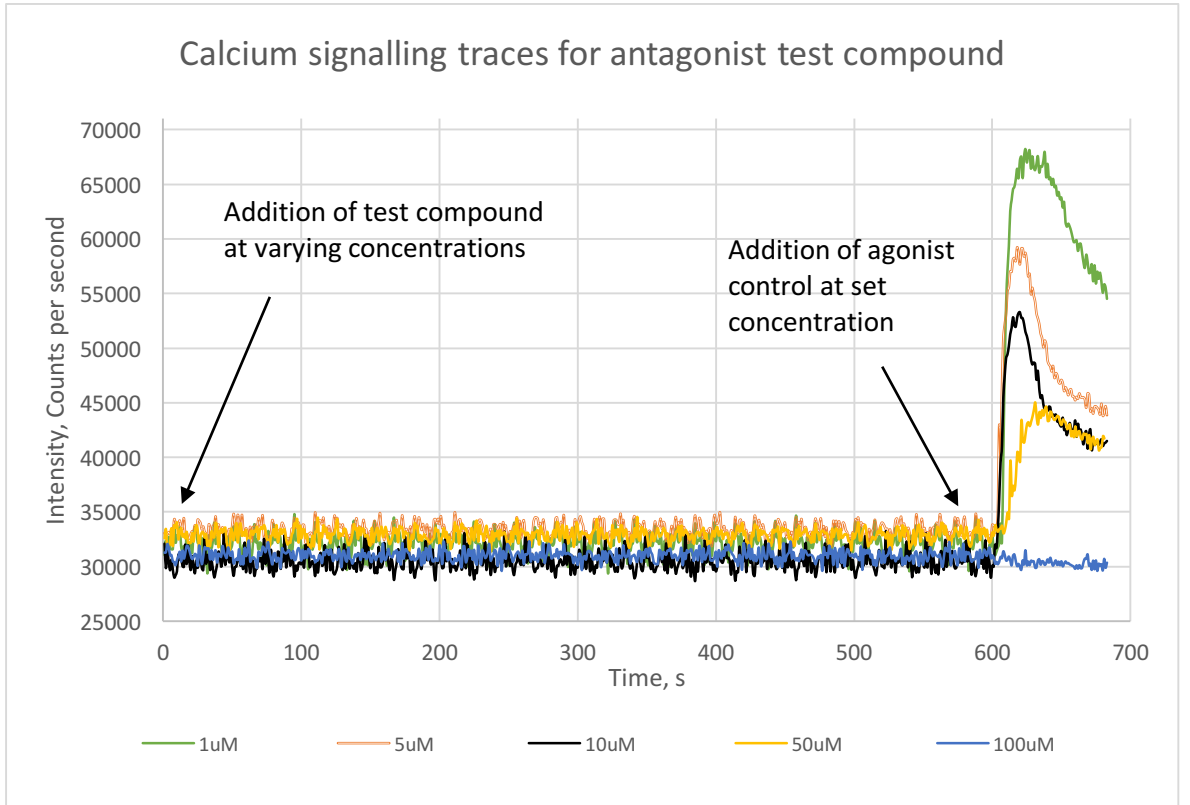
Figure 14 Raw data trace for an antagonist compound.
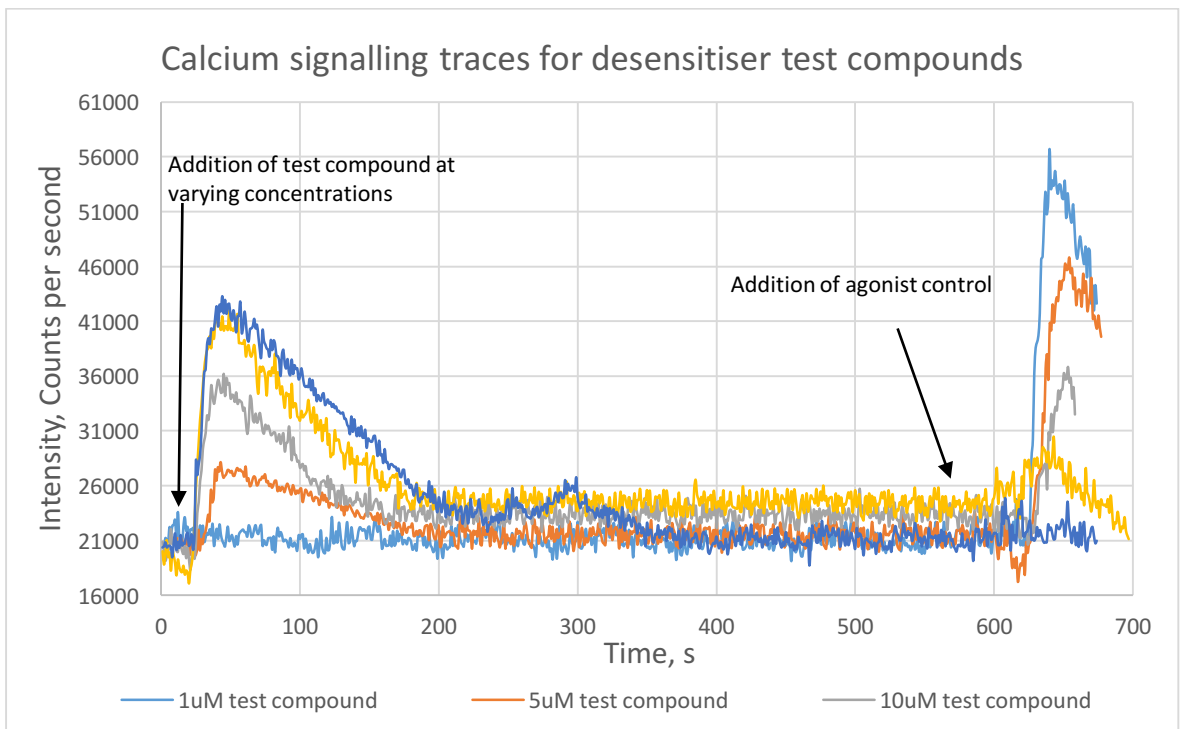
Figure 15 Raw data trace for a desensitiser compound.

3 Modulation of TRPA1 by synthesised novel derivatives of thymol and carvacrol

3.1 Introduction

Thymol and Carvacrol are both monoterpenes that have been shown to interact with TRPA1(130). Thymol and Carvacrol are naturally occurring phenolic monoterpene isomeric derivatives of p-cymene, with the molecular formula $C_{10}H_{14}O$. Thymol is the main component found in essential oils of thyme which is extracted from, most commonly, *Thymus vulgaris* (also known as common thyme) as well many other kinds of plants. Carvacrol is the main active component of oregano essential oils.

3.1.1   Essential oils

Essential oils are a complex mixture of volatile constituents biosynthesised by living organisms. Essential oils occur mainly in aromatic plants. They are liberated or extracted from organic matter by water, steam and dry distillation techniques. Essential oils, or their fractions and isolated constituents are utilised in flavour and fragrance, food, perfumery, cosmetics, fine chemicals and pharmaceuticals industries for a multitude of different purposes(154).

Terpenoid and non-terpenoid are the two main classes of essential oils; both thymol and carvacrol are of terpenoid origin. All of the compounds that make up essential oils are hydrocarbons and oxygenated derivatives of hydrocarbons; some may also contain nitrogen or sulfur groups. Monoterpenes, such as thymol and carvacrol, sesquiterpenes and even diterpenes are the most common constituents of essential oils.

Phenylpropanoids, fatty acids and their esters are also regularly encountered in essential oils although in smaller concentrations(154).

Non-terpenoid hydrocarbons found in essential oils such as short chain alcohols and aldehydes are formed by metabolic conversion or degradation of phospholipids and fatty acids(154).

Terpenes, or isoprenoids, are a class of naturally occurring chemicals formed by head-to-tail rearrangement of two or more isoprene molecules. To date, more than 30,000 terpenoids have been isolated from plants, microorganisms and animals(155). Monoterpenes are the most common type of terpene and are formed from two isoprene molecules. Thymol and carvacrol may be termed monoterpenic phenols. They are biosynthesised from γ-terpinene through p-cymene, see Figure 16 for details(156). Therefore, essential oils that contain thymol will always contain carvacrol and vice versa. They may also contain the biosynthetic intermediates such as terpinen-4-ol, cumin alcohol, p-cymen-8-ol as shown in Figure 16(156).
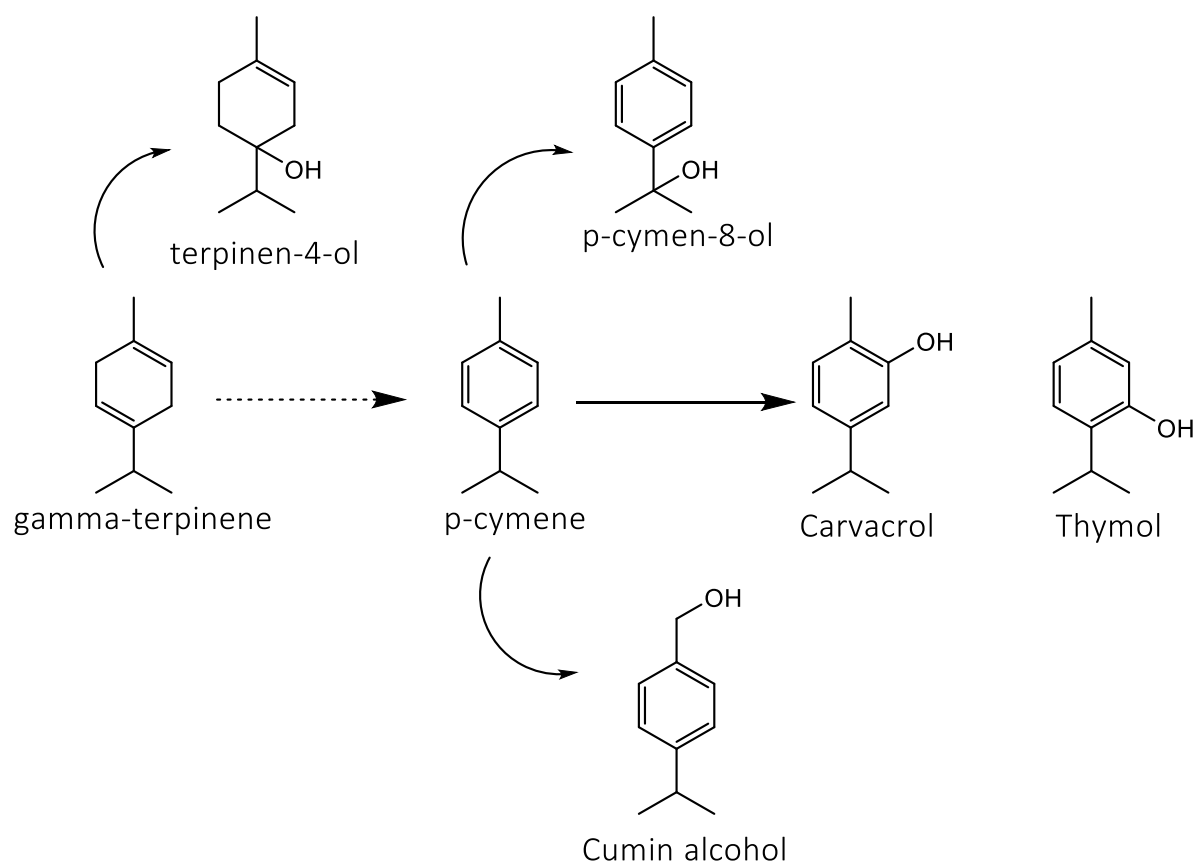
Figure 16 Biosynthesis of thymol and carvacrol(156)

3.1.2 Biological activities of thymol, carvacrol and their related essential oils

Oregano is a collective term referring to members of several genera, which include *Origanum, Thymbra, Thymus, Satureja* all belonging to the Limiacaeae family, that have the common feature of carvacrol being the main constituent of their essential oils(157). Thyme being the collective term referring to the same genera but all have thymol as the main constituent of their essential oils(158). Oregano and thyme essential oils are commonly used today to flavour and season food. They have been used throughout history, including recent times, to treat a variety of ailments. Hippocrates (500 BC) knew about the antiseptic properties of oregano and used it to treat stomach ache and respiratory diseases. Dioscorides (1st century AD) recommended drinking oregano tea with wine for snake bites as well as mixing oregano with honey to treat cold, cough and pneumonia. He also

42

recommended the used of thyme to treat asthma and loosen congestion in the throat and stomach.

Thymol and carvacrol and essential oils containing them have been shown to have a wide range of biological and pharmacological activity. They both tend to show the same biological and pharmacological properties with only slight variations between them such as potency and efficacy.

The antimicrobial activities of thymol and carvacrol have been well documented over the last 50 years. They have both been discovered to possess antibacterial and antifungal properties in *in vitro* studies(159–161). The mechanisms through which carvacrol and thymol act has been well documented and vary between microorganisms.

Both carvacrol and thymol have been shown to display antitumor activity. Carvacrol dose dependently decreased the number of cancer cells, total protein content and degeneration of cell morphology in a human non-small cell lung cancer cell line A549(162). Thymol was reported to have an anticancer effect against human gastric cancer cells via the inhibition of cell growth and the induction of apoptosis(163).

Carvacrol and thymol have both been shown to inhibit the formation of 3-nitrotyrosin and malondialdehyde. Their biosynthetic precursors p-cymene and γ-terpinene did not exhibit the same activity. This shows the importance of thymol and carvacrol in preventing the formation of toxic products by the action of reactive nitrogen species(164). An i*n vitro* study has shown that thymol has an antioxidant effect in a lipid system consisting of a purified fraction of triacylglycerols of lard and sunflower oil(165). Also, the essential oils with high thymol and carvacrol content have also been shown to have antioxidant properties(166,167).

Anti-inflammatory and antinociceptive activities of the essential oil of *L. gracilis,* which has a high content of thymol, were observed in an *in vivo* study. Carrageenan-induced oedema formation was reduced by the essential oil of *L. gracilis*. The carrageenan-induced leukocyte migration into the peritoneal cavity decreased with this essential oil(168). The same group also showed thymol to have an anti-inflammatory effect when it significantly decreased the oedema and the influx of leukocytes in wounded rodents, wounds showed high retraction rates and an improved granulation reaction when thymol was

administered(168). Carvacrol has shown a strong analgesic activity by inhibiting prostaglandin synthesis(169).

3.1.3 Biological activities of thymol and carvacrol derivatives

The above introduction has given a very brief overview of the research carried out on thymol, carvacrol and essential oils containing a high content of them. It highlights the wide variety of biological activity that these naturally occurring compounds have. It is no surprise then to find that thymol and carvacrol have been used as a basis for drug development, and that derivatives of them have been shown to have a wide range of biological activity.

Nagle *et al.* (170) synthesised a variety of thymol derivatives which showed good antioxidant activity, structure shown in Figure 17. The derivatives that showed good antioxidant activity also showed greater antimicrobial and antifungal properties than thymol, the parent molecule.
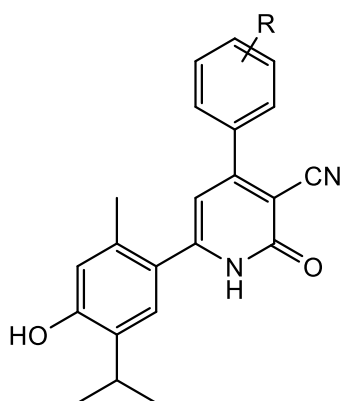
Figure 17 General structure of IV_{g-m} from Nagle *et al.* (170)

Huang *et al.*(171) showed that THPI is a potential reactive oxygen species scavenger and may prevent platelet aggregation (see Figure 18 for the structure of THPI).
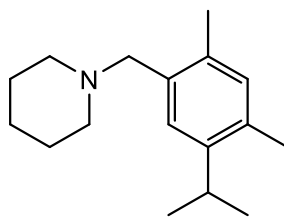
1-(5-isopropyl-2,4-dimethylbenzyl)piperidine

Figure 18 Chemical structure of THPI

2-(4*H*-1,2,4-triazole-3-ylthio)acetamide derivatives of thymol, compounds 18 and 19, see Figure 19, have been deemed to have an anticancer activity against PC-3, A549 and K-562 cells after antiproliferative effects were demonstrated(172).
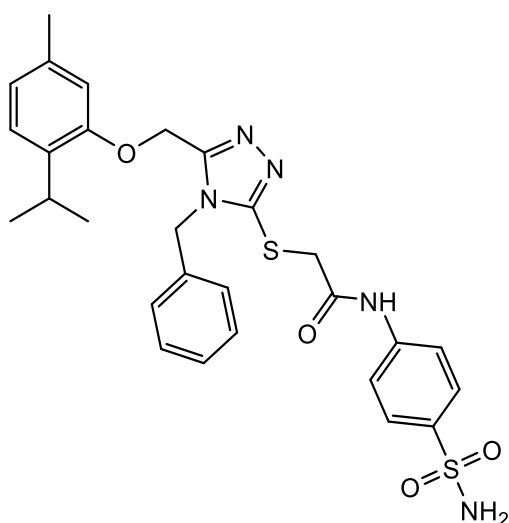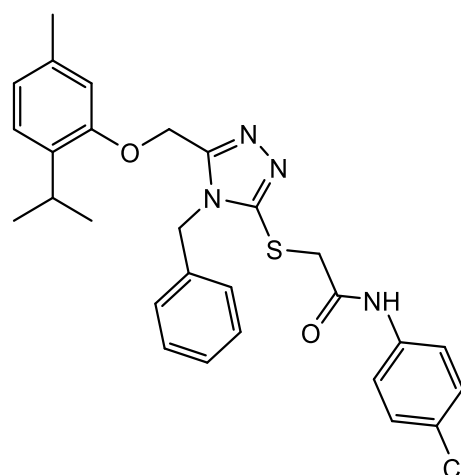
Compound 18   Compound 19

Figure 19 Chemical structure of compound 18 and 19 which have shown to have anticancer activity(172)

Antifungal activities of novel derivatives of thymol and carvacrol have been shown by Bound *et al.* (173). They found derivatives of thymol and carvacrol (general structure found in Figure 20) to be potent antifungal agents against *Aspergillus flavus, Aspergillus ochraceus, Fusarium oxysporum, Saccharomyces cerevisiae* and *Candida albicans*.
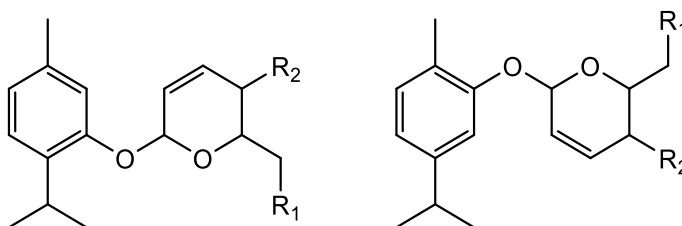
Figure 20 General structure of antifungal agents reported by Bound *et al.* (173).

To discover new effective and safe topical depigmenting agents alkoxy benzoates and alkoxy cinnamates of thymol (see Figure 21 for structures) were found to inhibit melanin synthesis in cultured melanocytes with the added benefit of having a low cytotoxicity(174).

R_1, R_2, R_3 = H, Me, Et, Pr, Bu

X= CO, $CH_2=CH_2CO$ (E)
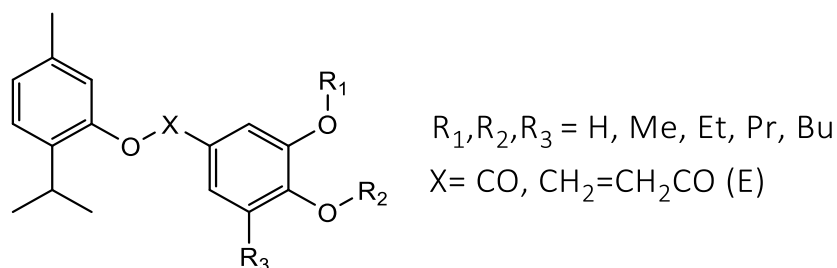
Figure 21 Structure of thymol esters which display depigmenting activity(174)

Thymol and carvacrol are also of interest due to studies that have shown them both to be agonists of TRPA1. Carvacrol was first discovered to activate TRPA1 by Xu *et al.* (175) they reported that carvacrol activated and then rapidly desensitised TRPA1. Thymol was later reported to activate TRPA1 which was followed by desensitisation(130). They also reported the results for related alkyl phenols and found that phenols with less bulky carbon substituents and lower logP values were less potent in general.

3.1.4   Aims and Objectives

As can be seen from this introduction the monoterpenes thymol and carvacrol have been shown to have a range of biological activity. Their essential oils have been used throughout history to treat all manner of ailments and now in modern times research has been carried out to enhance the natural activities of thymol and carvacrol by altering their chemical structure. It has been shown that TRPA1 is activated and then rapidly desensitised by thymol and carvacrol(130). It is my aim to enhance thymol and carvacrol's interactions with TRPA1. This will be carried out by synthesising derivatives of thymol and carvacrol and screening them for TRPA1 modulation. The results from this will provide useful information with regards to structure activity relationships. Two groups of compounds shall be synthesised. The first group, designated ojk01, has been designed based on TRPM8 modulators that are derivatives of menthol (see Figure 22)(176). The key structural points that shall be discussed are the substituents on the second phenyl ring, the length of the linker group (ojk0105 compared to ojk0107) and the effect of the missing methyl group on the first phenyl ring in comparison to thymol and carvacrol.
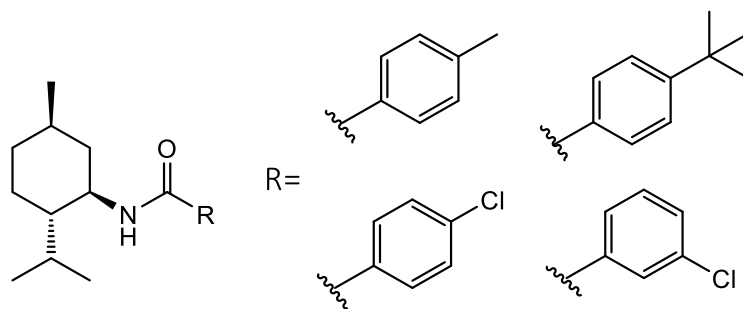
Figure 22 Structure of key menthlamine derivatives from Ortar *et al.* 2010(176)

TRPA1 and TRPM8 are closely related thermos-TRP channels regarding sequence homology and both interact with menthol. It has been shown that menthol, thymol and carvacrol all bind to TRPA1 through the same transmembrane 5 active site(55). Therefore, this was deemed to be a good starting point. The second group of compounds, the ojk06 and ojk07 compounds, has been designed to be similar to the TRPA1 antagonist HC-030031 which is a derivative of caffeine. Caffeine has been shown to modulate TRPA1; in mouse TRPA1 it is an agonist and in human TRPA1 it is an inhibitor(136).

HC-030031
IC50 = 4uM
Highlighted to signify the
core structural similarites to ojk0609
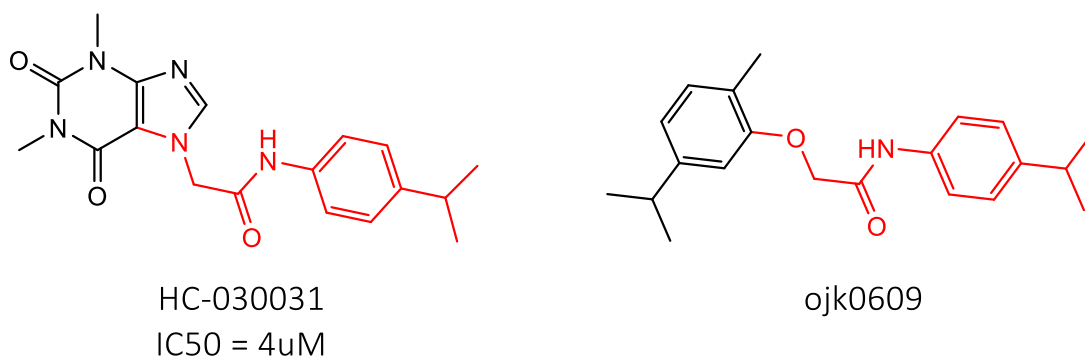
ojk0609

Figure 23 Chemical structure comparison of ojk0609 with TRPA1 antagonist HC-030031. The core structure of both compounds has been highlighted red.

The ojk06 and ojk07 compounds use carvacrol and thymol respectively as a starting base which was linked to another phenyl group via an acetamide linking group which is similar to the linking group in HC-030031(see Figure 23). The compounds were then screened for TRPA1 modulation, and any structure-activity relationships were discussed. The key structure activity relationship points that shall be discussed are the effect of the

thymol/carvacrol moiety, and the effect of the substituent groups on the second phenyl ring. The general aim of this research was to widen the pool of TPRA1 active compounds which will help further the understanding of TRPA1 activation and inhibition which will aid the development of TRPA1 targeted drugs for pain, inflammation and chronic respiratory inflammatory diseases.

3.2 Results

In this section the results for the synthesis of the compounds synthesised and the calcium signalling assays have been described in detail.

All the compounds assayed have been tested against mock-transfected HEK293 cells, at the highest concentration used in the agonist and antagonist assays, to determine any effects that the compound has on HEK293 cells. There was no response observed in the mock-transfected HEK293 cells for all of the compounds assayed, therefore the responses observed in the TRP gene transfected HEK293 cells can be deemed to be via gene product of the plasmid the HEK293 cells have been transfected with (see Figure 24 for data traces of responses for selected test compounds from each of the three compound groups).
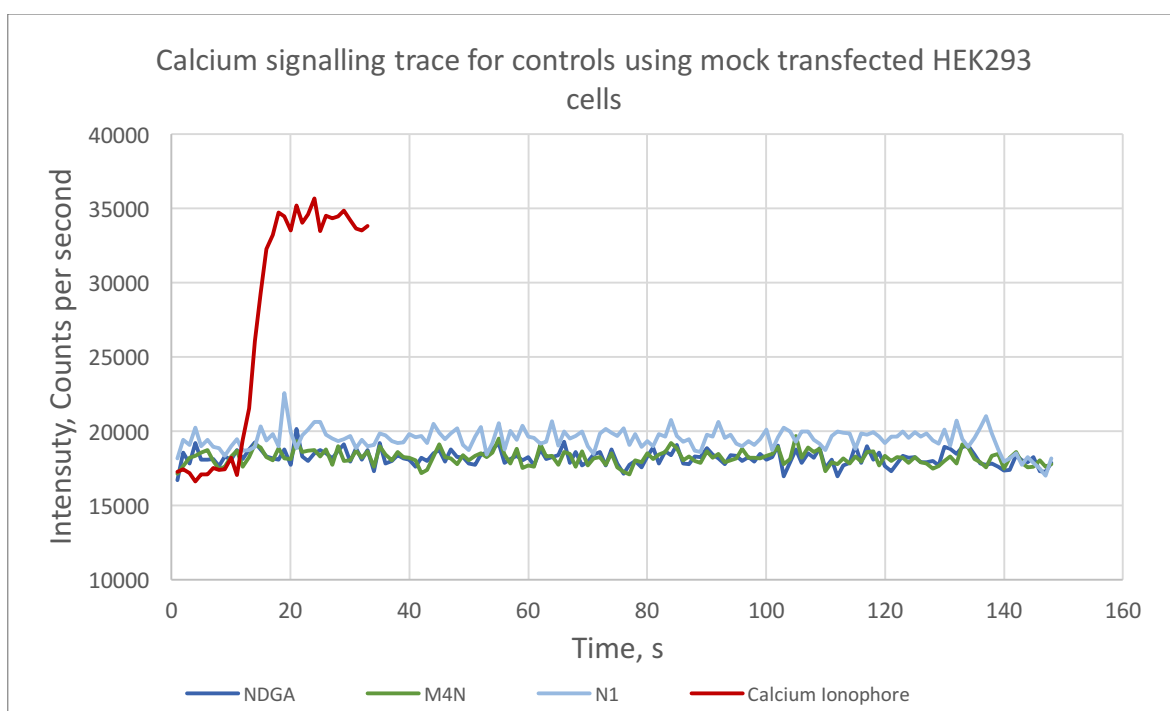
Figure 24 Raw data traces for a selection of test compounds on mock transfected HEK293 cells.

3.2.1 Issues with the method

3.2.1.1 Solubility of test compounds in the assay media

For some of the compounds tested a full concentration effect curve was not completed due to the insolubility of the test compound in the assay media at higher concentrations. Once the concentration of the test compound goes beyond the solubility limit, the undissolved

particles cause a disturbance in the trace recorded by the fluorescence spectrometer. This is due to the solid particles refracting the light into the detector. The effect of the undissolved material on the recorded trace line was instantaneous upon addition of the test compound and constant over time. Attempts were made to deduct the disruption from the test trace to generate a result which represented the response of the test compound on the TRPA1 protein. This was carried out by determining the increase observed by the undissolved material in blank assay media and deducting that value from the recorded result trace. However, after several attempts and refinement, it was determined that due to the small volumes involved and the variance in the disturbance of the replicates that this method increased the error of the final result by a significant margin that the results obtained would not be reliable.

Where the solubility of the test compound restricted the concentration range, the non-linear regression analysis of the incomplete concentration effect curve was used to predict the nature of the response beyond the solubility limit. The non-linear regression models were compared and the responses of similar compounds considered, and a prediction was made as to the nature of the response, in some cases, a clear trend was visible and others it was more difficult to make a reliable prediction.

3.2.2 Amide and ester derivatives of thymol (ojk01)

3.2.2.1 Synthesis
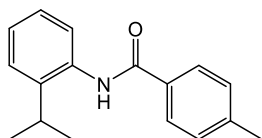
ojk0101
N-(2-isopropylphenyl)-4-methylbenzamide
Chemical Formula: $C_{17}H_{19}NO$
Molecular Weight: 253.35
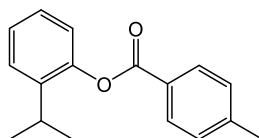
ojk0102
2-isopropylphenyl 4-methylbenzoate
Chemical Formula: $C_{17}H_{18}O_2$
Molecular Weight: 254.33
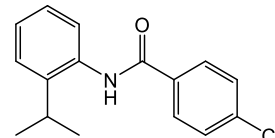
ojk0103
4-chloro-N-(2-isopropylphenyl)benzamide
Chemical Formula: $C_{16}H_{16}ClNO$
Molecular Weight: 273.76
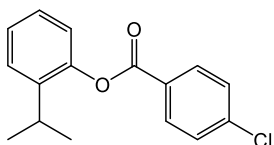
ojk0104
2-isopropylphenyl 4-chlorobenzoate
Chemical Formula: $C_{16}H_{15}ClO_2$
Molecular Weight: 274.74
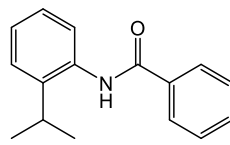
ojk0105
N-(2-isopropylphenyl)benzamide
Chemical Formula: $C_{16}H_{17}NO$
Molecular Weight: 239.32
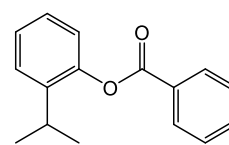
ojk0106
2-isopropylphenyl benzoate
Chemical Formula: $C_{16}H_{16}O_2$
Molecular Weight: 240.30
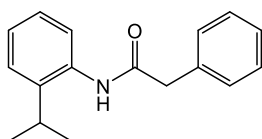
ojk0107
N-(2-isopropylphenyl)-2-phenylacetamide
Chemical Formula: $C_{17}H_{19}NO$
Molecular Weight: 253.35
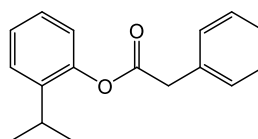
ojk0108
2-isopropylphenyl 2-phenylacetate
Chemical Formula: $C_{17}H_{18}O_2$
Molecular Weight: 254.33
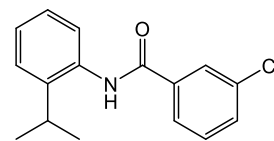
ojk0109
3-chloro-N-(2-isopropylphenyl)benzamide
Chemical Formula: $C_{16}H_{16}ClNO$
Molecular Weight: 273.76
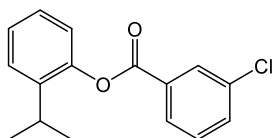
ojk0110
2-isopropylphenyl 3-chlorobenzoate
Chemical Formula: $C_{16}H_{15}ClO_2$
Molecular Weight: 274.74
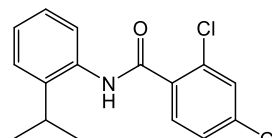
ojk0111
2,4-dichloro-N-(2-isopropylphenyl)benzamide
Chemical Formula: $C_{16}H_{15}Cl_2NO$
Molecular Weight: 308.20

Figure 25 Summary of ojk01 compounds

The ojk01 compounds containing an amide functional group in Figure 25 have been synthesised using the method described in section 2.1.1.1 and followed the reaction scheme in Figure 26. The ester compounds in Figure 25 have been synthesised using the method described in section 2.1.1.2 and followed the reaction scheme in Figure 26. The following will detail the results for the synthesis of the ojk01 compounds.
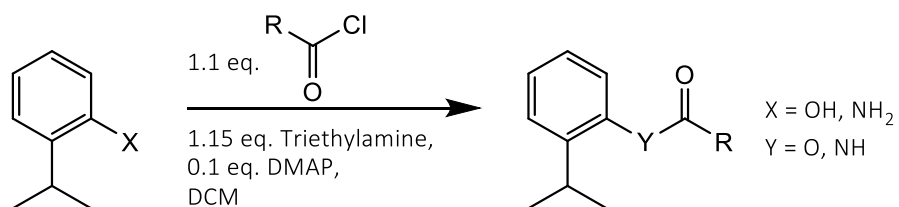
Figure 26 Reaction scheme for ojk01 amide derivatives

3.2.2.1.1   Ojk0101

Ojk0101 was synthesised successfully and positively characterised as the predicted structure. See Table 1 for details.
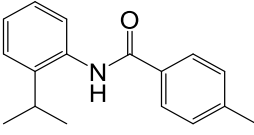
  ojk0101 Chemical Formula: $C_{17}H_{19}NO$ Molecular Weight: 253.35	N-(2-isopropylphenyl) 4-methylbenzamide
	%yield = 68
	^{1}H NMR (400 MHz, CHLOROFORM-*d*) δ ppm 1.29 (d, *J*=6.73 Hz, 6 H) 2.43 (s, 3 H) 3.10 (spt, *J*=6.80 Hz, 1 H) 7.18 - 7.26 (m, 2 H) 7.28 - 7.36 (m, 2 H) 7.69 - 7.88 (m, 4 H)
	^{13}C NMR (101 MHz, CHLOROFORM-*d*) δ ppm 21.77 (s, 1 C) 21.82 (s, 1 C) 23.29 (s, 1 C) 23.32 (s, 1 C) 28.49 (s, 1 C) 124.98 (s, 1 C) 125.93 (s, 1 C) 126.33 (s, 1 C) 126.80 (s, 1 C) 127.31 (s, 1 C) 127.37 (s, 1 C) 129.80 (s, 1 C) 132.43 (s, 1 C) 134.57 (s, 1 C) 140.69 (s, 1 C) 142.63 (s, 1 C) 166.20 (s, 1 C)
	Elemental Analysis (calculated): C, 80.60; H, 7.56; N, 5.53; O, 6.32
	Melting point = 156-158°C

Table 1 ojk0101 synthesis results

3.2.2.1.2 Ojk0102

Ojk0102 was synthesised successfully and positively characterised as the predicted structure. See Table 2 for details.
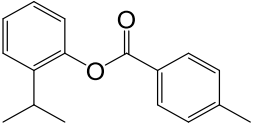
 ojk0102 Chemical Formula: $C_{17}H_{18}O_2$ Molecular Weight: 254.33	2-isopropylphenyl 4-methylbenzoate
	%yield = 40
	^{1}H NMR (400 MHz, CHLOROFORM-*d*) δ ppm 1.29 (d, *J*=6.88 Hz, 6 H) 2.47 (s, 3 H) 2.96 (spt, *J*=6.88 Hz, 1 H) 7.05 (d, *J*=8.13 Hz, 1 H) 7.08 (s, 1 H) 7.15 (d, *J*=7.82 Hz, 1 H) 7.30 - 7.39 (m, 3 H) 8.11 (d, *J*=8.13 Hz, 2 H)
	^{13}C NMR (101 MHz, CHLOROFORM-*d*) δ ppm 21.84 (s, 1 C) 21.93 (s, 1 C) 23.95 (s, 1 C) 34.09 (s, 1 C) 119.14 (s, 1 C) 119.77 (s, 1 C) 124.05 (s, 1 C) 127.07 (s, 1 C) 129.30 (s, 1 C) 129.35 (s, 1 C) 129.67 (s, 1 C) 130.29 (s, 1 C) 130.73 (s, 1 C) 144.40 (s, 1 C) 150.77 (s, 1 C) 151.17 (s, 1 C) 165.42 (s, 1 C)
	Elemental Analysis (calculated): C, 80.28; H, 7.13; O, 12.58
	Melting point = 120-122°C

Table 2 ojk0102 synthesis results

3.2.2.1.3 Ojk0103

Ojk0103 was synthesised successfully and positively characterised as the predicted structure. See Table 3 for details.
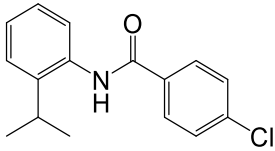
ojk0103 Chemical Formula: $C_{16}H_{16}ClNO$ Molecular Weight: 273.76	4-chloro-N-(2-isopropylphenyl)benzamide
	%yield = 58
	^{1}H NMR (400 MHz, CHLOROFORM-*d*) δ ppm 1.29 (d, *J*=6.88 Hz, 6 H) 3.10 (spt, *J*=6.83 Hz, 1 H) 7.22 - 7.29 (m, 2 H) 7.32 - 7.38 (m, 1 H) 7.47 (d, *J*=8.44 Hz, 2 H) 7.75 (br. s., 2 H) 7.82 (d, *J*=8.13 Hz, 2 H)
	^{13}C NMR (101 MHz, CHLOROFORM-*d*) δ ppm 23.02 (s, 2 C) 28.23 (s, 1 C) 124.94 (s, 1 C) 125.77 (s, 1 C) 126.48 (s, 1 C) 126.54 (s, 1 C) 128.50 (s, 1 C) 129.07 (s, 1 C) 133.29 (s, 1 C) 133.89 (s, 1 C) 138.08 (s, 1 C) 140.85 (s, 1 C)
	Elemental Analysis (calculated): C, 70.20; H, 5.89; Cl, 12.95; N, 5.12; O, 5.84
	Melting point = 205-206°C

Table 3 ojk0103 synthesis results

3.2.2.1.4 Ojk0104

Ojk0104 was synthesised successfully and positively characterised as the predicted structure. See Table 4 for details.
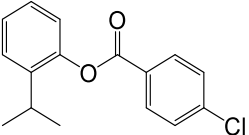
ojk0104 Chemical Formula: $C_{16}H_{15}ClO_2$ Molecular Weight: 274.74	2-isopropylphenyl 4-chlorobenzoate
	%yield = 58
	^{1}H NMR (400 MHz, CHLOROFORM-*d*) δ ppm 1.28 (d, *J*=6.94 Hz, 6 H) 2.96 (spt, *J*=6.87 Hz, 1 H) 6.99 - 7.11 (m, 2 H) 7.16 (d, *J*=7.75 Hz, 1 H) 7.33 - 7.40 (m, 1 H) 7.50 (d, *J*=8.57 Hz, 2 H) 8.15 (d, *J*=8.57 Hz, 2 H)
	^{13}C NMR (101 MHz, CHLOROFORM-*d*) δ ppm 23.86 (s, 1 C) 34.00 (s, 1 C) 118.89 (s, 1 C) 119.53 (s, 1 C) 124.26 (s, 1 C) 127.08 (s, 1 C) 128.17 (s, 1 C) 128.94 (s, 1 C) 129.31 (s, 1 C) 129.39 (s, 1 C) 131.54 (s, 1 C) 131.90 (s, 1 C) 140.06 (s, 1 C) 141.44 (s, 1 C) 150.82 (s, 1 C) 164.45 (s, 1 C)
	Elemental Analysis (calculated): C, 69.95; H, 5.50; Cl, 12.90; O, 11.65
	Melting point = 145-146°C

Table 4 ojk0104 synthesis results

3.2.2.1.5 Ojk0105

Ojk0105 was synthesised successfully and positively characterised as the predicted structure. See Table 5 for details.
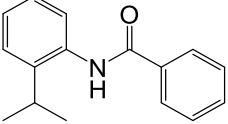
  ojk0105 *N*-(2-isopropylphenyl)benzamide Chemical Formula: $C_{16}H_{17}NO$ Molecular Weight: 239.32	N-(2-isopropylphenyl)benzamide
	%yield = 56
	^{1}H NMR (400 MHz, CHLOROFORM-*d*) δ ppm 1.29 (d, *J*=6.57 Hz, 6 H) 3.11 (spt, *J*=6.83 Hz, 1 H) 7.19 - 7.29 (m, 2 H) 7.30 - 7.37 (m, 1 H) 7.45 - 7.53 (m, 2 H) 7.53 - 7.60 (m, 1 H) 7.73 - 7.84 (m, 2 H) 7.88 (d, *J*=7.50 Hz, 2 H)
	^{13}C NMR (101 MHz, CHLOROFORM-*d*) δ ppm 23.13 (s, 2 C) 28.30 (s, 1 C) 124.88 (s, 1 C) 125.78 (s, 1 C) 126.30 (s, 1 C) 126.62 (s, 2 C) 127.14 (s, 2 C) 128.94 (s, 2 C) 131.91 (s, 1 C) 134.27 (s, 1 C) 135.11 (s, 1 C) 140.70 (s, 1 C)
	Elemental Analysis (calculated): C, 80.30; H, 7.16; N, 5.85; O, 6.69
	Melting point = 134-136°C

Table 5 ojk0105 synthesis results

3.2.2.1.6 Ojk0106

Ojk0106 was synthesised successfully and positively characterised as the predicted structure. See Table 6 for details.
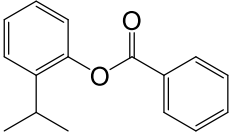
 ojk0106 Chemical Formula: $C_{16}H_{16}O_2$ Molecular Weight: 240.30	2-isopropylphenyl benzoate
	%yield = 36
	^{1}H NMR (400 MHz, CHLOROFORM-*d*) δ ppm 1.28 (d, *J*=6.94 Hz, 6 H) 2.96 (spt, *J*=6.97 Hz, 1 H) 6.99 - 7.13 (m, 2 H) 7.15 (d, *J*=7.75 Hz, 1 H) 7.36 (t, *J*=7.85 Hz, 1 H) 7.60 - 7.70 (m, 1 H) 8.22 (d, *J*=7.14 Hz, 2 H) 8.44 (d, *J*=6.53 Hz, 2 H)
	^{13}C NMR (101 MHz, CHLOROFORM-*d*) δ ppm 23.85 (s, 1 C) 33.98 (s, 1 C) 39.56 (s, 1 C) 106.38 (s, 1 C) 118.99 (s, 1 C) 119.62 (s, 1 C) 124.08 (s, 1 C) 128.12 (s, 1 C) 128.54 (s, 1 C) 129.25 (s, 1 C) 129.89 (s, 1 C) 130.15 (s, 1 C) 132.21 (s, 1 C) 133.51 (s, 1 C) 143.53 (s, 1 C)
	Elemental Analysis (calculated): C, 79.97; H, 6.71; O, 13.32
	Melting point = 134-136°C

Table 6 ojk0106 synthesis results

3.2.2.1.7 Ojk0107

Ojk0107 was synthesised successfully and positively characterised as the predicted structure. See Table 7 for details.
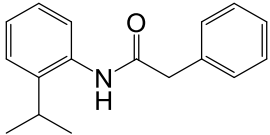
  ojk0107 Chemical Formula: $C_{17}H_{19}NO$ Molecular Weight: 253.35	N-(2-isopropylphenyl)-2-phenylacetamide
	%yield = 57
	^{1}H NMR (400 MHz, CHLOROFORM-*d*) δ ppm 1.01 (d, *J*=6.94 Hz, 6 H) 2.47 (spt, *J*=6.80 Hz, 1 H) 3.82 (s, 2 H) 6.97 (br. s., 1 H) 7.08 - 7.15 (m, 1 H) 7.16 - 7.23 (m, 2 H) 7.34 - 7.41 (m, 3 H) 7.42 - 7.50 (m, 2 H) 7.78 - 7.89 (m, 1 H)
	^{13}C NMR (101 MHz, CHLOROFORM-*d*) δ ppm 22.53 (s, 2 C) 27.86 (s, 1 C) 44.94 (s, 1 C) 123.27 (s, 2 C) 125.34 (s, 1 C) 125.57 (s, 1 C) 126.42 (s, 1 C) 127.88 (s, 2 C) 129.43 (s, 2 C) 129.74 (s, 2 C) 134.63 (s, 1 C) 139.00 (s, 1 C)
	Elemental Analysis (calculated): C, 80.60; H, 7.56; N, 5.53; O, 6.32
	Melting point = 122-123°C

Table 7 ojk0107 synthesis results

3.2.2.1.8   Ojk0108

Ojk0108 was synthesised successfully and positively characterised as the predicted structure. See Table 8 for details.
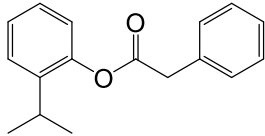
ojk0108 Chemical Formula: $C_{17}H_{18}O_2$ Molecular Weight: 254.33	2-isopropylphenyl 2-phenylacetate
	%yield = 46
	^{1}H NMR (400 MHz, CHLOROFORM-*d*) δ ppm 1.11 (d, *J*=7.06 Hz, 6 H) 2.27 (spt, *J*=6.93 Hz, 1 H) 3.62 (s, 2 H) 6.97 - 7.09 (m, 1 H) 7.11 - 7.19 (m, 2 H) 7.26 - 7.38 (m, 3 H) 7.39 - 7.40 (m, 2 H) 7.69 - 7.76 (m, 1 H)
	^{13}C NMR (101 MHz, CHLOROFORM-*d*) δ ppm 23.01 (s, 2 C) 27.92 (s, 1 C) 46.76 (s, 1 C) 124.27 (s, 2 C) 124.67 (s, 1 C) 124.98 (s, 1 C) 126.05 (s, 1 C) 128.65 (s, 2 C) 129.22 (s, 2 C) 129.46 (s, 2 C) 135.42 (s, 1 C) 156.45 (s, 1 C)
	Elemental Analysis (calculated): C, 80.28; H, 7.13; O, 12.58
	Melting point = 105-106°C

Table 8 ojk0108 synthesis results

3.2.2.1.9   Ojk0109

Ojk0109 was synthesised successfully and positively characterised as the predicted structure. See Table 9 for details.
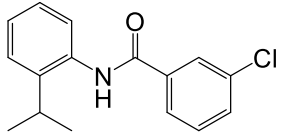
 ojk0109 Chemical Formula: $C_{16}H_{16}ClNO$ Molecular Weight: 273.76	3-chloro-N-(2-isopropylphenyl)benzamide
	%yield = 71
	^{1}H NMR (400 MHz, CHLOROFORM-*d*) δ ppm 1.30 (d, *J*=6.94 Hz, 6 H) 3.10 (spt, *J*=6.80 Hz, 1 H) 7.23 - 7.31 (m, 2 H) 7.33 - 7.39 (m, 1 H) 7.42 - 7.50 (m, 1 H) 7.55 (d, *J*=7.96 Hz, 1 H) 7.68 (br. s., 1 H) 7.75 (d, *J*=7.14 Hz, 2 H) 7.89 (s, 1 H)
	^{13}C NMR (101 MHz, CHLOROFORM-*d*) δ ppm 23.07 (s, 2 C) 28.25 (s, 1 C) 124.94 (s, 1 C) 125.00 (s, 1 C) 125.82 (s, 1 C) 126.60 (s, 2 C) 127.56 (s, 1 C) 130.16 (s, 1 C) 131.90 (s, 2 C) 133.75 (s, 1 C) 135.11 (s, 1 C) 136.76 (s, 1 C) 140.90 (s, 1 C)
	Elemental Analysis (calculated): C, 70.20; H, 5.89; Cl, 12.95; N, 5.12; O, 5.84
	Melting point = 196-198°C

Table 9 ojk0109 synthesis results

3.2.2.1.10 Ojk0110

Ojk0110 was synthesised successfully and positively characterised as the predicted structure. See Table 10 for details.
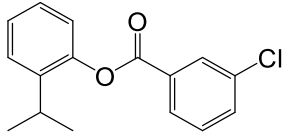
  ojk0110 Chemical Formula: $C_{16}H_{15}ClO_2$ Molecular Weight: 274.74	2-isopropylphenyl 3-chlorobenzoate
	%yield = 63
	^{1}H NMR (400 MHz, CHLOROFORM-*d*) δ ppm 1.29 (d, *J*=6.94 Hz, 6 H) 2.99 (spt, *J*=6.80 Hz, 1 H) 7.13 - 7.25 (m, 2 H) 7.28 - 7.34 (m, 1 H) 7.39 - 7.47 (m, 1 H) 7.60 (d, *J*=7.96 Hz, 1 H) 7.69 (d, *J*=7.14 Hz, 2 H) 7.83 (s, 1 H)
	^{13}C NMR (101 MHz, CHLOROFORM-*d*) δ ppm 22.95 (s, 2 C) 26.39 (s, 1 C) 124.65 (s, 1 C) 124.97 (s, 1 C) 125.76 (s, 1 C) 126.21 (s, 2 C) 127.18 (s, 1 C) 129.87 (s, 1 C) 131.64 (s, 2 C) 133.69 (s, 1 C) 135.27 (s, 1 C) 136.41 (s, 1 C) 139.76 (s, 1 C)
	Elemental Analysis (calculated): C, 69.95; H, 5.50; Cl, 12.90; O, 11.65
	Melting point = 164-165°C

Table 10 ojk0110 synthesis results

3.2.2.1.11 Ojk0111

Ojk0111 was synthesised successfully and positively characterised as the predicted structure. See Table 11 for details.

 ojk0111 Chemical Formula: $C_{16}H_{15}Cl_2NO$ Molecular Weight: 308.20	2,4-dichloro-N-(2-isopropylphenyl)benzamide
	%yield = 62
	^{1}H NMR (400 MHz, CHLOROFORM-*d*) δ ppm 1.28 (d, *J*=6.94 Hz, 6 H) 3.13 (spt, *J*=13.60 Hz, 1 H) 7.22 - 7.31 (m, 2 H) 7.33 - 7.38 (m, 1 H) 7.40 (dd, *J*=8.47, 1.73 Hz, 1 H) 7.51 (d, *J*=1.63 Hz, 1 H) 7.81 (d, *J*=8.36 Hz, 2 H) 7.85 (br. s., 1 H)
	^{13}C NMR (101 MHz, CHLOROFORM-*d*) δ ppm 23.18 (s, 2 C) 28.10 (s, 1 C) 124.91 (s, 1 C) 125.79 (s, 1 C) 126.55 (s, 1 C) 126.72 (s, 1 C) 127.84 (s, 1 C) 130.22 (s, 1 C) 131.29 (s, 1 C) 131.89 (s, 1 C) 133.47 (s, 1 C) 133.52 (s, 1 C) 137.27 (s, 1 C) 141.00 (s, 1 C) 163.94 (s, 1 C)
	Elemental Analysis (calculated): C, 62.35; H, 4.91; Cl, 23.00; N, 4.54; O, 5.19
	Melting point = 219-221°C

Table 11 ojk0111 synthesis results

3.2.2.2   *Calcium Signalling*

The compounds in Figure 25, have been assayed using the agonist and the antagonist calcium signalling assay methods on TRPA1-HEK293 cells, described in section 2.2. The only compounds that showed interaction with TRPA1-HEK293 cells were ojk0107, ojk0109 and ojk0111, which have been highlighted in boxes in Figure 25. All other compounds were assayed up to the limit of solubility of the test compound in the assay media (see section 3.2.1.1 for details on how low solubility of test compounds have been handled).

3.2.2.2.1   Ojk0107
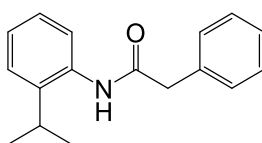
ojk0107
N-(2-isopropylphenyl)-2-phenylacetamide
Chemical Formula: $C_{17}H_{19}NO$
Molecular Weight: 253.35

Figure 27 Chemical structure of ojk0107

Agonist effect of ojk0107 on TRPA1-HEK293 cells

EC50 = 97 µM

Inhibitory effect of ojk0107 on TRPA1-HEK293 cells

IC50 = 81 µM
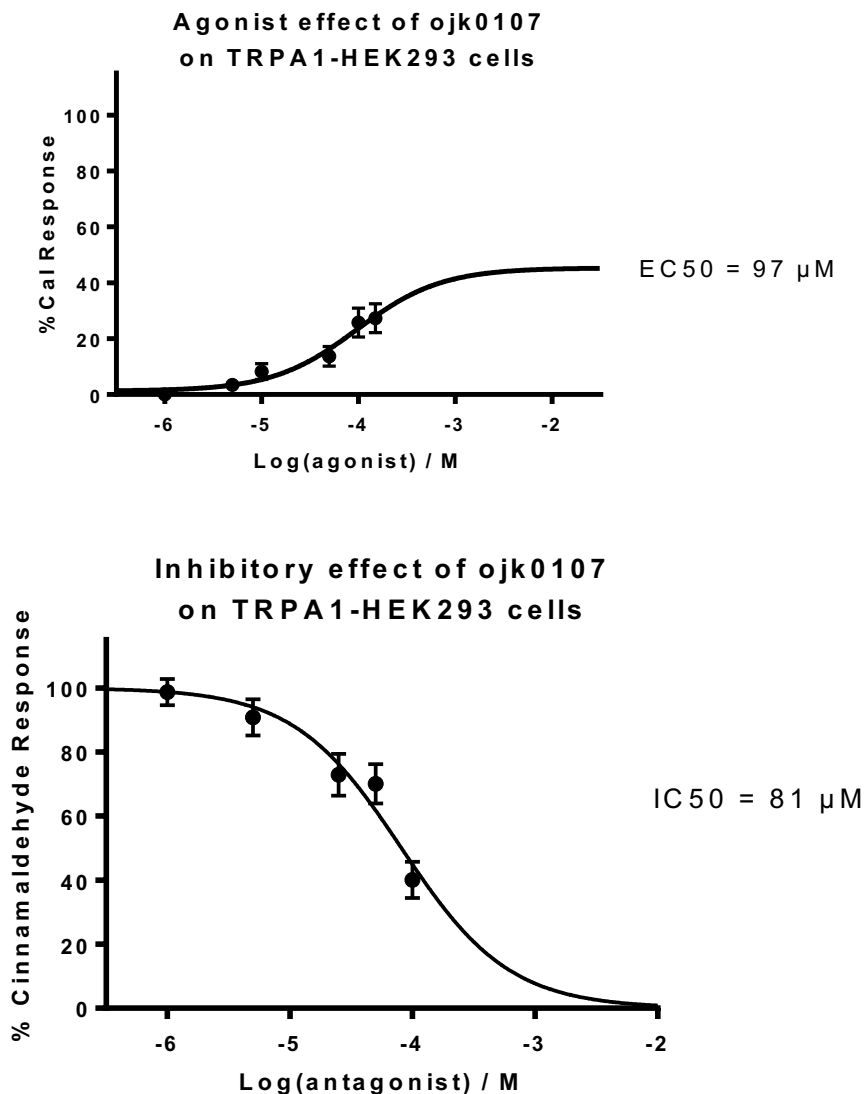
Figure 28 Agonist (above) and antagonist (below) concentration effect curves for ojk0107 on TRPA1-HEK293 cells. Data points are means±SEM of N = 3 experiments

Ojk0107 has been assayed using both the agonist and antagonist calcium signalling assays to assess the compound's effect on TRPA1-HEK293 cells. The resulting concentration effect curves can be seen in Figure 27 above.

In the agonist assay, a concentration dependent increase in intracellular calcium was observed, this response was fully inhibited by the TRPA1 specific inhibitor HC-030031. Therefore, this response can be attributed to the gating of TRPA1 channels. Ojk0107 was tested over the concentration range of 1 to 150 µM; over this range a complete sigmoidal response was not observed; higher concentration points have not been tested due to the maximum solubility of ojk0107 in the assay media being reached. However, non-linear

regression analysis was carried out using two different models in order to predict the nature of the response of the TRPA1-HEK293 cells to higher concentrations of ojk0107. Both models produced a good fit curve. The normalised variable slope model was normalised to the maximum response of cinnamaldehyde on TRPA1-HEK293 cells (which is 72%CaI) and assumes a 100 % response, the R^2 value of this model was calculated as 0.8439 which shows a good fit. The variable slope four parameter model has a better R^2 value, 0.8757. The models both show a good fit to the data points presented, with the variable slope four parameters model having an ever so slightly greater fit. However, this is not enough to discard the normalised variable slope model. With regards to calculated EC50 values, the normalised variable slope predicts an EC50 value of 306 μM with a 95 % CI of 181 μM to 518 μM. The variable slope four parameter model calculates an EC50 value of 97 μM with a 95 % CI of 24 μM to 393 μM. The 95 % confidence intervals for the EC50 values show a similar story to that of the R^2 values of the two models; the variable slope four parameter model has a slightly tighter 95 % CI than the normalised variable slope model. The better values for goodness of fit for the variable slope may be attributed to the shorter range of the predicted response. From the data and the non-linear regression analysis it is difficult to predict how ojk0107 interacts with TRPA1, it is not clear if ojk0107 is a full or partial agonist and whether its EC50 is 97 μM or 306 μM. However, what can be concluded is that ojk0107 shows an agonist response when exposed to TRPA1 which is more than that of many of the ojk01 compounds assayed and that the response whether it is a full or partial agonist is at a lower potency than that of ojk0109 and ojk0111 (results detailed on the following pages).

In the antagonist assay a concentration dependent decrease in the response of 30 μM of cinnamaldehyde (EC50 concentration of cinnamaldehyde) was observed with increasing concentration of pre-dosed ojk0107. Ojk0107 was tested over the concentration range of 1-100 μM. The first decrease in the cinnamaldehyde response was observed at 25 μM with a decrease in cinnamaldehyde response of 27%. The greatest reduction in the cinnamaldehyde response occurred at the 100 μM concentration point with a reduction of 60%. Higher concentration points for ojk0107 was not tested due to the insolubility of ojk0107 in the assay media at higher concentrations. Non-linear regression analysis was carried out to construct a curve of best fit. The model with the greatest fit to the data points

was the normalised variable slope model; with an R^2 value of 0.8157 this model assumes a full inhibitory response, all models used also predicted a full inhibition. The normalised variable slope model predicts an IC50 of 81 µM and full inhibition to occur at 639 µM.

From this analysis of the agonist and antagonist assays of ojk0107 on TRPA1-HEK293 cells, it can be determined that ojk0107 is an agonist of TRPA1, whether it is a full or partial response could not be determined. After the initial activation of TRPA1 by ojk0107 further activation by cinnamaldehyde via a desensitisation effect was observed.

3.2.2.2.2   Ojk0109
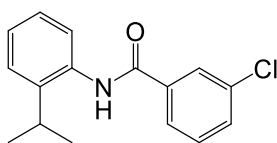
ojk0109

3-chloro-*N*-(2-isopropylphenyl)benzamide

Chemical Formula: $C_{16}H_{16}ClNO$

Molecular Weight: 273.76

Figure 29 Chemical structure of ojk0109

Agonist effect of ojk0109 on TRPA1-HEK293 cells

EC50 = 80 µM

Inhibitory effect of ojk0109 on TRPA1-HEK293 cells

IC50 = 38 µM
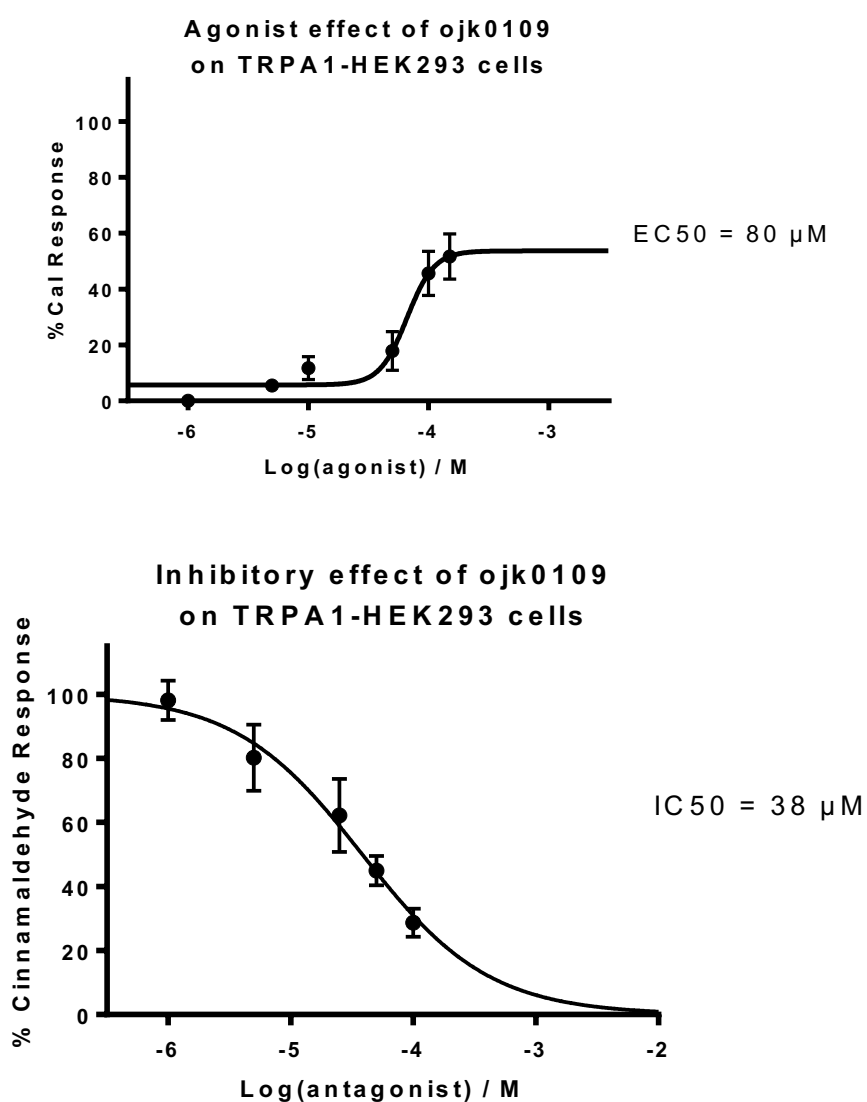
Figure 30 Agonist (above) and antagonist (below) concentration effect curves for ojk0109 on TRPA1-HEK293 cells. Data points are means±SEM of N = 3 experiments

Ojk0109 has been assayed using both the agonist and antagonist calcium signalling assays to assess the compound's effect on TRPA1-HEK293 cells. The resulting concentration effect curves can be seen in Figure 30 above.

In the agonist assay, a concentration dependent increase in intracellular calcium was observed. This response was inhibited fully by the TRPA1 specific inhibitor HC-030031. Therefore, this response can be attributed to the gating of TRPA1 channels. Ojk0109 was tested over the concentration range of 1 to 150 µM, over this range, a typical sigmoidal response was observed. The first significant response was observed at 50 µM with a mean %CaI response of 16. The maximum response was observed at the 150 µM concentration point with a mean %CaI response of 52. A maximum plateau was not observed within the data range tested. Higher concentrations have not been tested due to the limited solubility of ojk0109 in the assay media. Non-linear regression analysis was carried out using two different curve fit calculations the best fit was the variable Hill slope four parameter curve with an R^2 value of 0.8569, the normalised variable slope model showed a similar goodness of fit with an R^2 0.8215. These two models predict two different activity profiles for ojk0109 the normalised variable slope model predicts a full agonist, as is the nature of the model which fits the data to a full agonist response (i.e. the maximum response for cinnamaldehyde). This model predicts an EC50 value of 90 µM. The variable slope four parameter model predicts a partial agonist response, all be it with a high efficacy, with an EC50 value of 80 µM and an efficacy of 80 % with a maximum plateau predicted to occur at 204 µM. Both models show a good fit and very similar EC50 values and 95 % confidence intervals, and this indicates that the true response of ojk0109 is probably somewhere between these models but slightly favouring the variable slope four parameter model.

In the antagonist assay a concentration dependent decrease in the response of 30 µM of cinnamaldehyde (EC50 concentration of cinnamaldehyde) was observed with increasing concentration of pre-dosed ojk0109. Ojk0109 was tested over the concentration range of 1-100 µM. Over this range a partial typical reversed sigmoidal curve was observed. The first decrease in the cinnamaldehyde response was observed at 5 µM with a decrease in cinnamaldehyde response of 20 %. The greatest reduction in the cinnamaldehyde response occurred at the 100 µM concentration point with a reduction of 71%, although this cannot be deemed to be full inhibition further concentration points could not be tested due to the

insolubility of ojk0109 in the assay media at higher concentrations. However, using non-linear regression analysis the trend of the response at greater concentrations can be predicted. Two models were used to fit a curve to the data, of the models used the best fit was the normalised variable with an R^2 value of 0.8154, which shows a good level of fit. All models predicted a full inhibitory response, therefore using the normalised variable slope model, which assumes full inhibition, is justified. The normalised variable slope model gives an IC50 value of 38 µM with a full inhibition occurring at 535 µM.

From this analysis of the agonist and antagonist assays of ojk0109 on TRPA1-HEK293 cells, it can be determined that ojk0109 is a partial agonist of TRPA1, but very close to being considered a full agonist. After the initial activation of TRPA1 by ojk0109 further activation by cinnamaldehyde was inhibited fully via a desensitisation effect.

3.2.2.2.3   Ojk0111
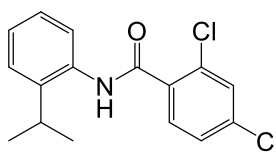
ojk0111

2,4-dichloro-*N*-(2-isopropylphenyl)benzamide

Chemical Formula: $C_{16}H_{15}Cl_2NO$

Molecular Weight: 308.20

Figure 31 Chemical structure of ojk0111

Agonist effect of ojk0111 on TRPA1-HEK293 cells

EC50 = 48 µM

Inhibitory effect of ojk0111 on TRPA1-HEK293 cells

IC50 = 23 µM

Figure 32 Agonist (above) and antagonist (below) concentration effect curves for ojk0111 on TRPA1-HEK293 cells. Data points are means±SEM of N = 3 experiments

Ojk0111 has been tested using both the agonist and antagonist calcium signalling assays to determine the compound's effect on TRPA1-HEK293 cells. The resulting concentration effect curves can be seen in Figure 32 above.

In the agonist assay, a concentration dependent increase in intracellular calcium was observed. This response was inhibited fully by the TRPA1 specific inhibitor HC-030031. Therefore, this response can be attributed to the gating of TRPA1 channels. Ojk0111 was tested over the concentration range of 1 to 150 µM, over this range, a typical sigmoidal response was observed. The first significant response was observed at 10 µM with a mean %CaI response of 14. The maximum response was observed at the 150 µM concentration point with a mean %CaI response of 60. A maximum plateau was not fully observed over the concentration range tested in order to predict the full concentration effect of ojk0111 on TRPA1-HEK293 cells. Two non-linear regression analysis models have been used to fit a curve to the data points. Of the two models, the best fit was the variable slope four parameter model which gave an R^2 value of 0.9198, the normalised variable slope model which assumes a maximum response to the same degree of cinnamaldehyde also showed a good fit with an R^2 value of 0.9169. The good fit of these two models and the trend observed over the test range strongly indicates a full agonist response for ojk0111. The efficacy for ojk0111 using the variable slope four parameter maximum predicted response is 105 % of the maximum response of cinnamaldehyde, and the calculated EC50 is 48 µM.

In the antagonist assay a concentration dependent decrease in the response of 30 µM of cinnamaldehyde (EC50 concentration of cinnamaldehyde) was observed with increasing concentration of pre-dosed ojk0111. Ojk0111 was tested over the concentration range of 1-100 µM. The first decrease in the cinnamaldehyde response was observed at 5 µM with a decrease in cinnamaldehyde response of 22 %. The greatest reduction in the cinnamaldehyde response occurred at the 100 µM concentration point with a reduction of 81; greater concentration points have not been tested due to the insolubility of ojk0111 in the assay media at higher concentrations. The data points collected trend towards a full inhibition, and this is confirmed by the non-linear regression analysis models used to fit a curve to the data points of which all of them predict full inhibition. The best fit model is the normalised variable slope model which has an R^2 value of 0.9390, the calculated IC50 value for this model is 23 µM with full inhibition predicted to occur at 231 µM.

From this analysis of the agonist and antagonist assays of ojk0111 on TRPA1-HEK293 cells, it can be determined that ojk0111 is a full agonist of TRPA1 which after the initial activation of TRPA1 inhibits further activation by cinnamaldehyde fully via a desensitisation effect.

3.2.3 Thymol and carvacrol acetamide linked derivatives (ojk06 and ojk07)

ojk0601
2-(5-isopropyl-2-methylphenoxy)-
N-(*p*-tolyl)acetamide
Chemical Formula: $C_{19}H_{23}NO_2$
Molecular Weight: 297.40

ojk0606
2-(5-isopropyl-2-methylphenoxy)-
N-(2-isopropylphenyl)acetamide
Chemical Formula: $C_{21}H_{27}NO_2$
Molecular Weight: 325.45

ojk0607
2-(5-isopropyl-2-methylphenoxy)-
N-(*o*-tolyl)acetamide
Chemical Formula: $C_{19}H_{23}NO_2$
Molecular Weight: 297.40

ojk0608
N-(4-chlorophenyl)-2-(5-isopropyl-2-
methylphenoxy)acetamide
Chemical Formula: $C_{18}H_{20}ClNO_2$
Molecular Weight: 317.81

ojk0609
2-(5-isopropyl-2-methylphenoxy)-
N-(4-isopropylphenyl)acetamide
Chemical Formula: $C_{21}H_{27}NO_2$
Molecular Weight: 325.45

ojk0703
2-(2-isopropyl-5-methylphenoxy)- *N*-(*p*-
tolyl)acetamide
Chemical Formula: $C_{19}H_{23}NO_2$
Molecular Weight: 297.40

ojk0705
2-(2-isopropyl-5-methylphenoxy)-
N-(2-isopropylphenyl)acetamide
Chemical Formula: $C_{21}H_{27}NO_2$
Molecular Weight: 325.45

ojk0706
2-(2-isopropyl-5-methylphenoxy)-
N-(*o*-tolyl)acetamide
Chemical Formula: $C_{19}H_{23}NO_2$
Molecular Weight: 297.40

ojk0707
N-(4-chlorophenyl)-2-(2-isopropyl-5-
methylphenoxy)acetamide
Chemical Formula: $C_{18}H_{20}ClNO_2$
Molecular Weight: 317.81

ojk0708
2-(2-isopropyl-5-methylphenoxy)-
N-(4-isopropylphenyl)acetamide
Chemical Formula: $C_{21}H_{27}NO_2$
Molecular Weight: 325.45

Figure 33 Chemical structures of ojk06 and ojk07 compounds

3.2.3.1   Synthesis
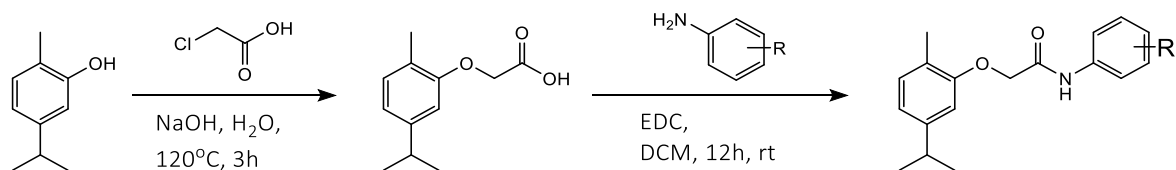
Figure 34 Reaction scheme for the synthesis of ojk06 and ojk07 compounds

The ojk06 and ojk07 compounds in Figure 33 have been synthesised using the method described in section 2.1.2 and followed the reaction scheme in Figure 34. The following will detail the results for the synthesis of the ojk06 and ojk07 compounds. All the compounds synthesised have been analysed by GC-MS and have been positively identified with no impurities observed above the limit of detection.

3.2.3.1.1   Ojk06

The following section reports the synthesis results for the five ojk06 compounds synthesised.

3.2.3.1.1.1   Ojk0601

Ojk0601 was synthesised successfully and positively characterised as the predicted structure. See Table *12 ojk0601 synthesis results* for details.
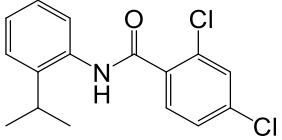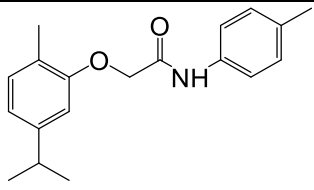
ojk0601 Chemical Formula: $C_{19}H_{23}NO_2$ Molecular Weight: 297.40	2-(5-isopropyl-2-methylphenoxy)-N-(p-tolyl)acetamide
	%yield = 57
	^{1}H NMR (400 MHz, CHLOROFORM-*d*) δ ppm 1.24 (d, *J*=7.14 Hz, 6 H) 2.33 (s, 3 H) 2.35 (s, 3 H) 2.88 (spt, *J*=6.90 Hz, 1 H) 4.63 (s, 2 H) 6.72 (d, *J*=1.63 Hz, 1 H) 6.86 (dd, *J*=7.55, 1.84 Hz, 1 H) 7.14 (dd, *J*=7.65, 0.71 Hz, 1 H) 7.17 (d, *J*=8.16 Hz, 2 H) 7.45 - 7.50 (m, 2 H) 8.32 (br. s., 1 H)
	^{13}C NMR (101 MHz, CHLOROFORM- *d*) δ ppm 23.96, 34.08, 39.66, 106.49, 119.09, 119.72, 124.18, 128.23, 128.65, 129.35, 129.80, 129.99, 130.25, 132.32, 133.61, 143.64, 150.83.
	Elemental Analysis Expected: C, 76.74; H, 7.80; N, 4.71; O, 10.76 Actual: C, 76.57; H, 8.06; N, 4.72

Table 12 ojk0601 synthesis results

3.2.3.1.1.2 Ojk0606

Ojk0606 was synthesised successfully and positively characterised as the predicted structure. See Table 13 *ojk0606 synthesis results* for details.
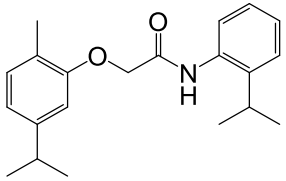
  ojk0606 Chemical Formula: $C_{21}H_{27}NO_2$ Molecular Weight: 325.45	2-(5-isopropyl-2-methylphenoxy)-N-(2-isopropylphenyl)acetamide
	%yield = 52
	^{1}H NMR (400 MHz, CHLOROFORM-*d*) δ ppm 1.24 (d, *J*=7.09 Hz, 6 H) 1.30 (d, *J*=7.06 Hz, 6 H) 2.35 (s, 3 H) 3.14 (spt, *J*=6.91 Hz, 1 H) 3.42 (spt, *J*=6.93 Hz, 1 H) 4.61 (s, 2 H) 6.72 (s, 1 H) 6.87 (d, *J*=7.75 Hz, 1 H) 7.20 – 7.32 (m, 4H) 7.96 (dd, *J*=7.93, 1.63 Hz, 1 H) 8.42 (br. s., 1 H)
	Elemental Analysis: Expected: C, 77.50; H, 8.36; N, 4.30; O, 9.83 Actual: C, 77.43; H, 8.44; N, 4.31

Table 13 ojk0606 synthesis results

3.2.3.1.1.3   Ojk0607

Ojk0607 was synthesised successfully and positively characterised as the predicted structure. See Table 14 *ojk0607 synthesis results* for details.
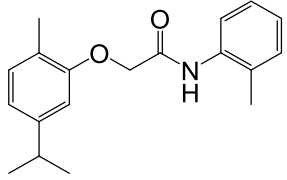
ojk0607 Chemical Formula: $C_{19}H_{23}NO_2$ Molecular Weight: 297.40	2-(5-isopropyl-2-methylphenoxy)-N-(o-tolyl)acetamide
	%yield = 61
	^{1}H NMR (400 MHz, CHLOROFORM-*d*) δ ppm 1.24 (d, *J*=7.09 Hz, 6 H) 1.33 (s, 3 H) 2.35 (s, 3 H) 3.14 (spt, *J*=6.91 Hz, 1 H) 3.42 (spt, *J*=6.93 Hz, 1 H) 4.61 (s, 2 H) 6.72 (s, 1 H) 6.87 (d, *J*=7.75 Hz, 1 H) 7.20 – 7.32 (m, 4H) 7.96 (dd, *J*=7.93, 1.63 Hz, 1 H) 8.42 (br. s., 1 H)
	Elemental Analysis: Expected: C, 76.74; H, 7.80; N, 4.71; O, 10.76 Actual: C, 76.61; H, 7.87; N, 4.78

Table 14 ojk0607 synthesis results

3.2.3.1.1.4 Ojk0608

Ojk0608 was synthesised successfully and positively characterised as the predicted structure. See Table 15 *ojk0608 synthesis results* for details.
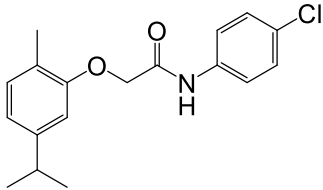
ojk0608 Chemical Formula: $C_{18}H_{20}ClNO_2$ Molecular Weight: 317.81	N-(4-chlorophenyl)-2-(5-isopropyl-2-methylphenoxy)acetamide
	%yield = 63
	^{1}H NMR (400 MHz, CHLOROFORM-*d*) δ ppm 1.24 (d, *J*=6.94 Hz, 6 H) 2.33 (s, 3 H) 2.89 (spt, *J*=6.90 Hz, 1 H) 4.63 (s, 2 H) 6.72 (s, 1 H) 6.87 (d, *J*=7.75 Hz, 1 H) 7.14 (d, *J*=7.75 Hz, 1 H) 7.34 (d, *J*=8.77 Hz, 2 H) 7.56 (d, *J*=8.77 Hz, 2 H) 8.38 (br. s., 1 H)
	Elemental Analysis: Expected: C, 68.03; H, 6.34; Cl, 11.15; N, 4.41; O, 10.07 Actual: C, 67.89; H, 6.43; N, 4.39

Table 15 ojk0608 synthesis results

3.2.3.1.1.5 Ojk0609

Ojk0609 was synthesised successfully and positively characterised as the predicted structure. See Table 16 *ojk0609 synthesis results* for details.
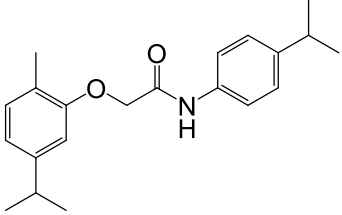
ojk0609 Chemical Formula: $C_{21}H_{27}NO_2$ Molecular Weight: 325.45	2-(5-isopropyl-2-methylphenoxy)-N-(4-isopropylphenyl)acetamide
	%yield = 67
	^{1}H NMR (400 MHz, CHLOROFORM-*d*) δ ppm 1.25 (dd, *J*=6.94, 2.86 Hz, 12 H) 2.33 (s, 3 H) 2.80 - 2.99 (m, 2 H) 4.63 (s, 2 H) 6.73 (s, 1 H) 6.86 (d, *J*=7.55 Hz, 1 H) 7.14 (d, *J*=7.75 Hz, 1 H) 7.23 (d, *J*=8.36 Hz, 2 H) 7.50 (d, *J*=8.36 Hz, 2 H) 8.32 (br. s., 1 H)
	Elemental Analysis: Expected: C, 77.50; H, 8.36; N, 4.30; O, 9.83 Actual: C, 77.77; H, 8.58; N, 4.12

Table 16 ojk0609 synthesis results

3.2.3.1.2 Ojk07

The following section reports the synthesis results for the five ojk06 compounds synthesised.

3.2.3.1.2.1 Ojk0703

Ojk0703 was synthesised successfully and positively characterised as the predicted structure. See Table 17 *ojk0703 synthesis results* for details.
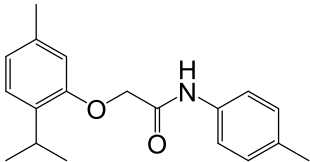
ojk0703 Chemical Formula: $C_{19}H_{23}NO_2$ Molecular Weight: 297.40	2-(2-isopropyl-5-methylphenoxy)-N-(p-tolyl)acetamide
	%yield = 58
	^{1}H NMR (400 MHz, CHLOROFORM-d) δ ppm 1.24 (d, J=7.02 Hz, 6 H) 2.36 (s, 3 H) 2.39 (s, 3 H) 2.98 (spt, J=6.86 Hz, 1 H) 4.63 (s, 2 H) 6.72 (d, J=1.67 Hz, 1 H) 6.88 (dd, J=7.43, 1.97 Hz, 1 H) 7.16 (dd, J=7.64, 0.71 Hz, 1 H) 7.19 (d, J=8.13 Hz, 2 H) 7.48 - 7.53 (m, 2 H) 8.34 (br. s., 1 H)
	Elemental Analysis: Expected: C, 76.74; H, 7.80; N, 4.71; O, 10.76 Actual: C, 76.56; H, 7.92; N, 4.71

Table 17 ojk0703 synthesis results

3.2.3.1.2.2 Ojk0705

Ojk0705 was synthesised successfully and positively characterised as the predicted structure. See Table 18 for details.
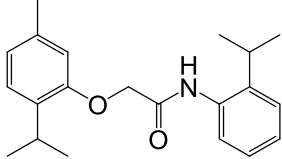
  ojk0705 Chemical Formula: $C_{21}H_{27}NO_2$ Molecular Weight: 325.45	2-(2-isopropyl-5-methylphenoxy)-N-(2-isopropylphenyl)acetamide
	%yield = 42
	^{1}H NMR (400 MHz, CHLOROFORM-d) δ ppm 1.24 (d, J=6.94 Hz, 6 H) 1.29 (d, J=6.94 Hz, 6 H) 2.35 (s, 3 H) 3.00 (spt, J=6.80 Hz, 1 H) 3.38 (spt, J=6.90 Hz, 1 H) 4.70 (s, 2 H) 6.72 (s, 1 H) 6.88 (d, J=7.75 Hz, 1 H) 7.21 – 7.33 (m, 4H) 7.98 (dd, J=7.96, 1.63 Hz, 1 H) 8.38 (br. s., 1 H)
	^{13}C NMR (101 MHz, CHLOROFORM-d) δ ppm 21.24 (s, 1 C) 21.28 (s, 1 C) 22.91 (s, 1 C) 22.94 (s, 1 C) 26.71 (s, 1 C) 27.85 (s, 1 C) 67.76 (s, 1 C) 112.69 (s, 1 C) 113.00 (s, 1 C) 122.94 (s, 1 C) 123.52 (s, 1 C) 125.55 (s, 1 C) 125.94 (s, 1 C) 126.27 (s, 1 C) 126.52 (s, 1 C) 133.17 (s, 1 C) 133.61 (s, 1 C) 137.02 (s, 1 C) 139.21 (s, 1 C) 153.81 (s, 1 C) 166.73 (s, 1 C)
	Elemental Analysis: Expected: C, 77.50; H, 8.36; N, 4.30; O, 9.83 Actual: C, 77.32; H, 8.51; N, 4.41

Table 18 ojk0705 synthesis results

3.2.3.1.2.3   Ojk0706

Ojk0706 was synthesised successfully and positively characterised as the predicted structure. See Table 19 for details.
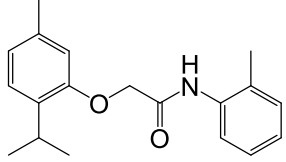
 ojk0706 Chemical Formula: $C_{19}H_{23}NO_2$ Molecular Weight: 297.40	2-(2-isopropyl-5-methylphenoxy)-N-(o-tolyl)acetamide
	%yield = 59
	^{1}H NMR (400 MHz, CHLOROFORM-*d*) δ ppm 1.29 (d, *J*=6.87 Hz, 6 H), 1.33 (s, 3 H) 2.34 (s, 3 H) 3.29 (spt, *J*=6.87 Hz, 1 H) 4.79 (s, 2 H) 6.81 (s, 1 H) 6.92 (d, *J*=7.79 Hz, 1 H) 7.15 – 7.37 (m, 4H) 8.01 (dd, *J*=7.90, 1.58 Hz, 1 H) 8.28 (br. s., 1 H)
	Elemental Analysis: Expected: C, 76.74; H, 7.80; N, 4.71; O, 10.76 Actual: C, 76.61; H, 7.99; N, 4.59

Table 19 ojk0706 synthesis results

3.2.3.1.2.4 Ojk0707

Ojk0707 was synthesised successfully and positively characterised as the predicted structure. See Table 20 for details.
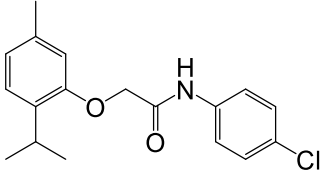
ojk0707 Chemical Formula: $C_{18}H_{20}ClNO_2$ Molecular Weight: 317.81	N-(4-chlorophenyl)-2-(2-isopropyl-5-methylphenoxy)acetamide
	%yield = 61
	^{1}H NMR (400 MHz, CHLOROFORM-d) δ ppm 1.32 (d, J=6.94 Hz, 6 H) 2.34 (s, 3 H) 3.33 (spt, J=6.87 Hz, 1 H) 4.62 (s, 2 H) 6.68 (s, 1 H) 6.88 (d, J=7.75 Hz, 1 H) 7.18 (d, J=7.75 Hz, 1 H) 7.34 (d, J=8.77 Hz, 2 H) 7.55 (d, J=8.98 Hz, 2 H) 8.35 (br. s., 1 H)
	Elemental Analysis: Expected: C, 68.03; H, 6.34; Cl, 11.15; N, 4.41; O, 10.07 Actual: C, 67.76; H, 6.57; N, 4.63

Table 20 ojk0707 synthesis results

3.2.3.1.2.5 Ojk0708

Ojk0708 was synthesised successfully and positively characterised as the predicted structure. See Table 21 for details.
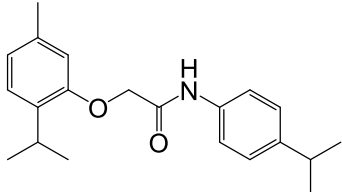
ojk0708 Chemical Formula: $C_{21}H_{27}NO_2$ Molecular Weight: 325.45	2-(2-isopropyl-5-methylphenoxy)-N-(4-isopropylphenyl)acetamide
	%yield = 65
	^{1}H NMR (400 MHz, CHLOROFORM-d) δ ppm 1.25 (d, J=6.94 Hz, 6 H) 1.31 (d, J=6.94 Hz, 6 H) 2.34 (s, 3 H) 2.91 (spt, J=6.80 Hz, 1 H) 3.34 (spt, J=6.90 Hz, 1 H) 4.62 (s, 2 H) 6.69 (s, 1 H) 6.86 (d, J=7.75 Hz, 1 H) 7.17 (d, J=7.75 Hz, 1 H) 7.24 (d, J=8.36 Hz, 2 H) 7.50 (d, J=8.57 Hz, 2 H) 8.30 (br. s., 1 H)
	Elemental Analysis: Expected: C, 77.50; H, 8.36; N, 4.30; O, 9.83 Actual: C, 77.42; H, 8.54; N, 4.33

Table 21 ojk0708 synthesis results

3.2.3.2   Calcium Signalling

3.2.3.2.1   Ojk06

3.2.3.2.1.1   Ojk0601

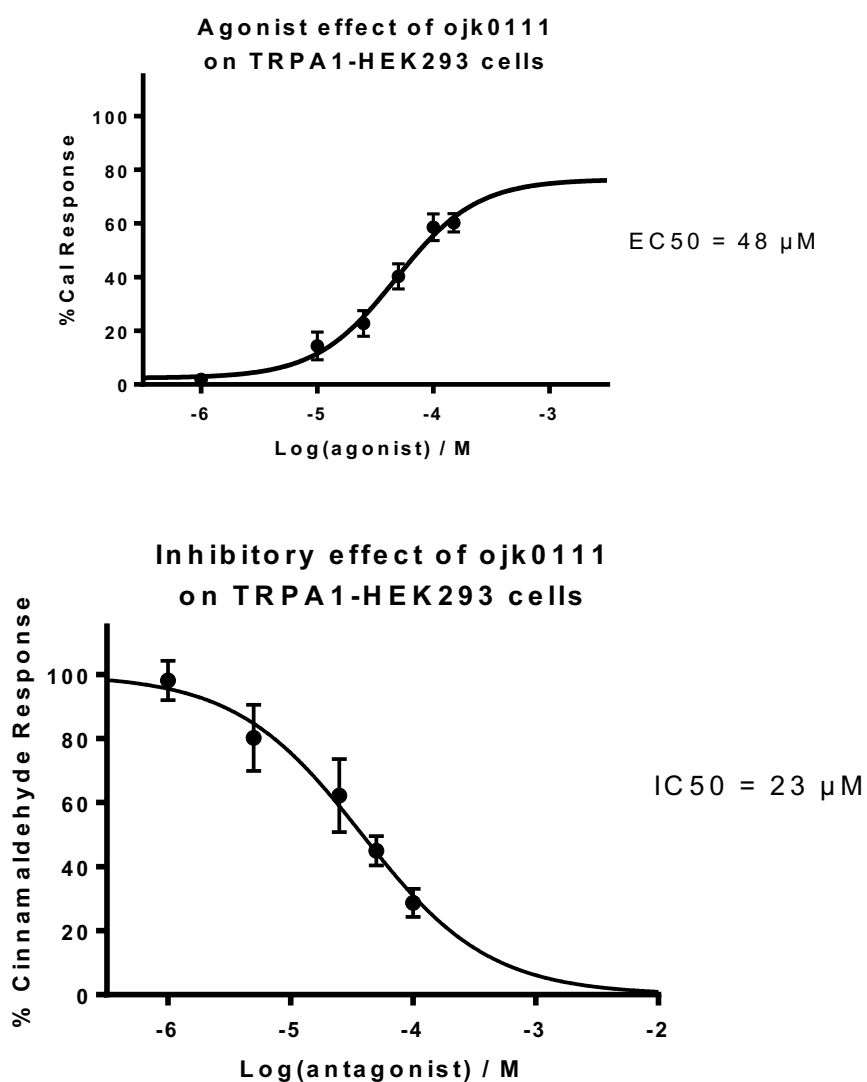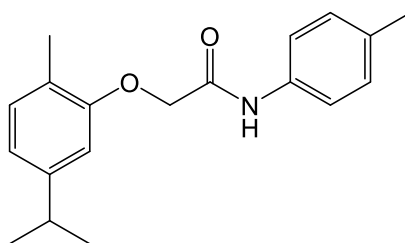ojk0601

Figure 35 Chemical structure of ojk0601

Figure 36 Agonist (above) and antagonist (below) concentration effect curves for ojk0601 on TRPA1-HEK293 cells. Data points are means±SEM of N = 3 experiments

85

Ojk0601 has been assayed using both the agonist and antagonist calcium signalling assays to assess the compound's effect on TRPA1-HEK293 cells. The resulting concentration effect curves can be seen in Figure 36 above.

In the agonist assay, a concentration dependent increase in intracellular calcium was observed; this response was inhibited fully by the TRPA1 specific inhibitor HC-030031. Therefore, this response can be attributed to the gating of TRPA1 channels. Ojk0601 was tested over the concentration range of 1 to 200 µM; over this range a typical sigmoidal response was observed. The first significant response was observed at 5 µM with a mean %CaI response of 16. The maximum response was observed at the 100 µM concentration point with a mean %CaI response of 70.2. A maximum plateau can be observed between the 50 and 100 µM concentration points, this maximum response observed at 100 µM is confirmed by the response observed at the 200 µM which was 70%CaI. Non-linear regression analysis was carried out using two different models, both models produced curves which were very similar, the best fit curve constructed using the variable slope four parameter model which has an R^2 value of 0.9392 which can be considered a very good fit, the other model showed comparable R^2 values. The best fit curve, variable slope four parameter curve, predicts the maximum response to occur between the 100 and 200 µM concentration points with an efficacy of 99.2 % of the maximum response observed for cinnamaldehyde. The best fit curve calculates an EC50 value of 15 µM.

In the antagonist assay a concentration dependent decrease in the response of 30 µM of cinnamaldehyde (EC50 concentration of cinnamaldehyde) was observed with increasing concentration of pre-dosed Ojk0601. Ojk0601 was tested over the concentration range of 1-100 µM over this range a typical reversed sigmoidal curve was observed. The first decrease in the cinnamaldehyde response was observed at 5 µM with a decrease in cinnamaldehyde response of 18 %. The greatest reduction in the cinnamaldehyde response occurred at the 100 µM concentration point with a reduction of 95 %, which is deemed to be full inhibition of the cinnamaldehyde response. The best fit non-linear regression analysis model was the normalised variable slope model which has an R^2 value of 0.9691, the calculated IC50 value for this model is 12 µM.

From this analysis of the agonist and antagonist assays of ojk0601 on TRPA1-HEK293 cells, it can be determined that ojk0601 is a full agonist of TRPA1 which after the initial activation of TRPA1 inhibits further activation by cinnamaldehyde fully via a desensitisation effect.

3.2.3.2.1.2 Ojk0606

ojk0606

Figure 37 Chemical structure of ojk0606

Agonist effect of ojk0606 on TRPA1-HEK293 cells

EC50 = 35 μM

Inhibitory effect of ojk0606 on TRPA1-HEK293 cells

IC50 = 7 μM

Figure 38 Agonist (above) and antagonist (below) concentration effect curves for ojk0606 on TRPA1-HEK293 cells. Data points are means±SEM of N = 3 experiments

Ojk0606 has been assayed using both the agonist and antagonist calcium signalling assays to assess the compound's effect on TRPA1-HEK293 cells. The resulting concentration effect curves can be seen in Figure 38 above.

In the agonist assay, a concentration dependent increase in intracellular calcium was observed. This response was inhibited fully by the TRPA1 specific inhibitor HC-030031. Therefore, this response can be attributed to the gating of TRPA1 channels. Ojk0606 was tested over the concentration range of 1 to 200 μM, over this range, a typical sigmoidal response was observed. The first significant response was observed at 30 μM with a mean %CaI response of 20. The maximum response was observed at the 100 μM concentration

point with a mean %CaI response of 45. A maximum plateau can be observed to form between the 50 and 100 µM concentration points with the plateau being confirmed at the 200 µM concentration point.

Non-linear regression analysis was carried out using two different curve fit calculations the best fit was the variable Hill slope four parameter curve with an R^2 value of 0.8576, the models which assumed a full agonist response showed a poor fit to the data points. Therefore, the agonist response of ojk0606 on TRPA1-HEK293 cells can be considered to be a partial agonist response. The efficacy of the maximum response of ojk0606 has been calculated to be 62% of the maximum cinnamaldehyde response. From the best fit curve, an EC50 value of 35 µM has been determined.

In the antagonist assay a concentration dependent decrease in the response of 30 µM of cinnamaldehyde (EC50 concentration of cinnamaldehyde) was observed with increasing concentration of pre-dosed ojk0606. Ojk0606 was tested over the concentration range of 1-100 µM over this range a typical reversed sigmoidal curve was observed. The first decrease in the cinnamaldehyde response was observed at 5 µM with a decrease in cinnamaldehyde response of 43 %. The greatest reduction in the cinnamaldehyde response occurred at the 100 µM concentration point with a reduction of 96 %, which is deemed to be full inhibition of the cinnamaldehyde response. This full inhibition could not be confirmed at greater concentrations due to the insolubility of ojk0606 in the assay media at higher concentrations. However, the data trend heavily towards full inhibition at concentrations of 100 µM and above. The best fit non-linear regression analysis model was the normalised variable slope model which has an R^2 value of 0.9465, the calculated IC50 value for this model is 7 µM.

From this analysis of the agonist and antagonist assays of ojk0606 on TRPA1-HEK293 cells, it can be determined that ojk0606 is a partial agonist of TRPA1 which after the initial activation of TRPA1 inhibits further activation fully via a desensitisation effect. It was also found that ojk0606 inhibits TRPM8 in a concentration dependent manner. See section 3.2.4 for a full description of these results.

3.2.3.2.1.3 Ojk0607
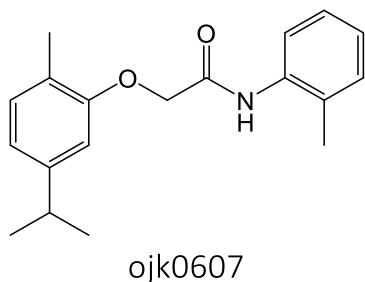
ojk0607

Figure 39 Chemical structure of ojk0607

**Agonist effect of ojk0607
on TRPA1-HEK293 cells**

EC50 = 29 µM

**Inhibitory effect of ojk0607
on TRPA1-HEK293 cells**

IC50 = 37 µM

Figure 40 Agonist (above) and antagonist (below) concentration effect curves for ojk0607 on TRPA1-HEK293 cells. Data points are means±SEM of N = 3 experiments

Ojk0607 has been assayed using both the agonist and antagonist calcium signalling assays to assess the compound's effect on TRPA1-HEK293 cells. The resulting concentration effect curves can be seen in Figure 40 above.

In the agonist assay, a concentration dependent increase in intracellular calcium was observed. This response was inhibited fully by the TRPA1 specific inhibitor HC-030031. Therefore, this response can be attributed to the gating of TRPA1 channels. Ojk0607 was tested over the concentration range of 1 to 200 μM, over this range, a typical sigmoidal response was observed. The first significant response was observed at 30 μM with a mean %CaI response of 31. The maximum response was observed at the 200 μM concentration point with a mean %CaI response of 56. A maximum plateau can be observed to form between the 100 and 200 μM concentration points. However, this plateau cannot be fully confirmed as testing above 200 μM was not possible due to the insolubility of Ojk0607 in the assay media.

Non-linear regression analysis was carried out using two different curve fit calculations the best fit was the variable Hill slope four parameter curve with an R^2 value of 0.9457, the models which assumed a full agonist response showed a poor fit to the data points. Therefore, the agonist response of ojk0607 on TRPA1 can be considered to be a partial agonist response. The efficacy of ojk0607 has been calculated using the response observed at the 200 μM concentration point as the best fit curve, using the variable slope four parameter model, predicts the maximum response to be the same of that observed at the 200 μM concentration point. The efficacy of ojk0607 has therefore been calculated to be 72% of the maximum response by cinnamaldehyde on TRPA1-HEK293 cells. The EC50 has been calculated to be 29 μM for ojk0607.

In the antagonist assay a concentration dependent decrease in the response of 30 μM of cinnamaldehyde (EC50 concentration of cinnamaldehyde) was observed with increasing concentration of pre-dosed Ojk0607. Ojk0607 was tested over the concentration range of 1-150 μM. The first decrease in the cinnamaldehyde response was observed at 10 μM with a decrease in cinnamaldehyde response of 35%. The greatest reduction in the cinnamaldehyde response occurred at the 150 μM concentration point with a reduction of 69 %. Greater concentration points have not been tested in order to reach a maximum response due to the insolubility of ojk0607 in the assay media at higher concentrations. In order to predict the nature of the inhibitory response of ojk0607 on the activation of TRPA1 by cinnamaldehyde two different non-linear regression models have been used to fit a curve to the data points. Of the curves constructed the best fit used the variable slope four

parameter model which gave an R^2 value of 0.9087, this model predicts a partial inhibitory response with ojk0607 reaching its maximum inhibitory effect at 316 μM where it reduces the cinnamaldehyde response by 73 %. The calculated IC50 of this model is 14 μM. The second best fit curve uses the normalised variable slope model which has an R^2 value of 0.8723, this curve shows a similar fit to the variable slope four parameter curve. The normalised variable slope curve assumes full inhibition, and therefore calculates different values for IC50 and the predicted concentration of the plateau point, which are 37 μM and 504 μM respectively. It is difficult to separate the two models as both show a good fit to the data points, with the variable slope four parameters curve displaying a better R^2 value. However, other compounds in this library have shown a full inhibitory response. Therefore, it is not unreasonable to assume that ojk0607 follows this trend.

From this analysis of the agonist and antagonist assays of Ojk0607 on TRPA1-HEK293 cells, it can be determined that Ojk0607 is a partial agonist of TRPA1 which after the initial activation of TRPA1 inhibits further activation via a desensitisation effect and it is inconclusive if this response is a full inhibitory response or a partial inhibitory response.

3.2.3.2.1.4 Ojk0608
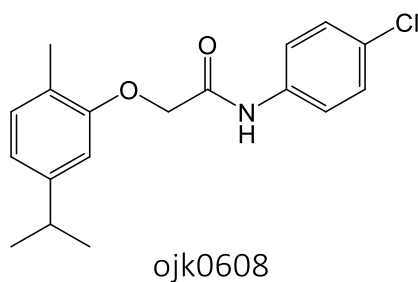
ojk0608

Figure 41 Chemical structure of ojk0608

EC50 = 32 µM

IC50 = 5 µM

Figure 42 Agonist (above) and antagonist (below) concentration effect curves for ojk0608 on TRPA1-HEK293 cells. Data points are means±SEM of N = 3 experiments

Ojk0608 has been assayed using both the agonist and antagonist calcium signalling assays to assess the compound's effect on TRPA1-HEK293 cells. The resulting concentration effect curves can be seen in Figure 42 above.

In the agonist assay, a concentration dependent increase in intracellular calcium was observed. This response was inhibited fully by the TRPA1 specific inhibitor HC-030031. Therefore, this response can be attributed to the gating of TRPA1 channels. Ojk0608 was tested over the concentration range of 1 to 200 μM, over this range, a typical sigmoidal response was observed. The first significant response was observed at 5 μM with a mean %CaI response of 12 %. The maximum response was observed at the 100 μM concentration point with a mean %CaI response of 57%. A maximum plateau can be observed to form between the 50 and 100 μM concentration points with the plateau being confirmed at the 200 μM concentration point. Non-linear regression analysis was carried out using two different curve fit calculations the best fit was the variable Hill slope four parameter curve with an R^2 value of 0.8228. This model predicts a strong partial agonist response, with an efficacy of 79 % of the maximum cinnamaldehyde response and an EC50 value of 32 μM.

In the antagonist assay a concentration dependent decrease in the response of 30 μM of cinnamaldehyde (EC50 concentration of cinnamaldehyde) was observed with increasing concentration of pre-dosed Ojk0608. Ojk0608 was tested over the concentration range of 0.5-50 μM over this range a typical reversed sigmoidal curve was observed. The first decrease in the cinnamaldehyde response was observed at 1 μM with a decrease in cinnamaldehyde response of 15 %. The greatest reduction in the cinnamaldehyde response occurred at the 20 μM concentration point with a reduction of 96%, which is deemed to be full inhibition of the cinnamaldehyde response. This full inhibition was confirmed at the 50 μM concentration point. The best fit non-linear regression analysis model was the normalised variable slope model which has an R^2 value of 0.9509, the calculated IC50 value for this model is 5 μM.

From this analysis of the agonist and antagonist assays of Ojk0608 on TRPA1-HEK293 cells, it can be determined that Ojk0608 is a partial agonist of TRPA1, which after the initial activation of TRPA1 inhibits further activation fully via a desensitisation effect.

3.2.3.2.1.5 Ojk0609
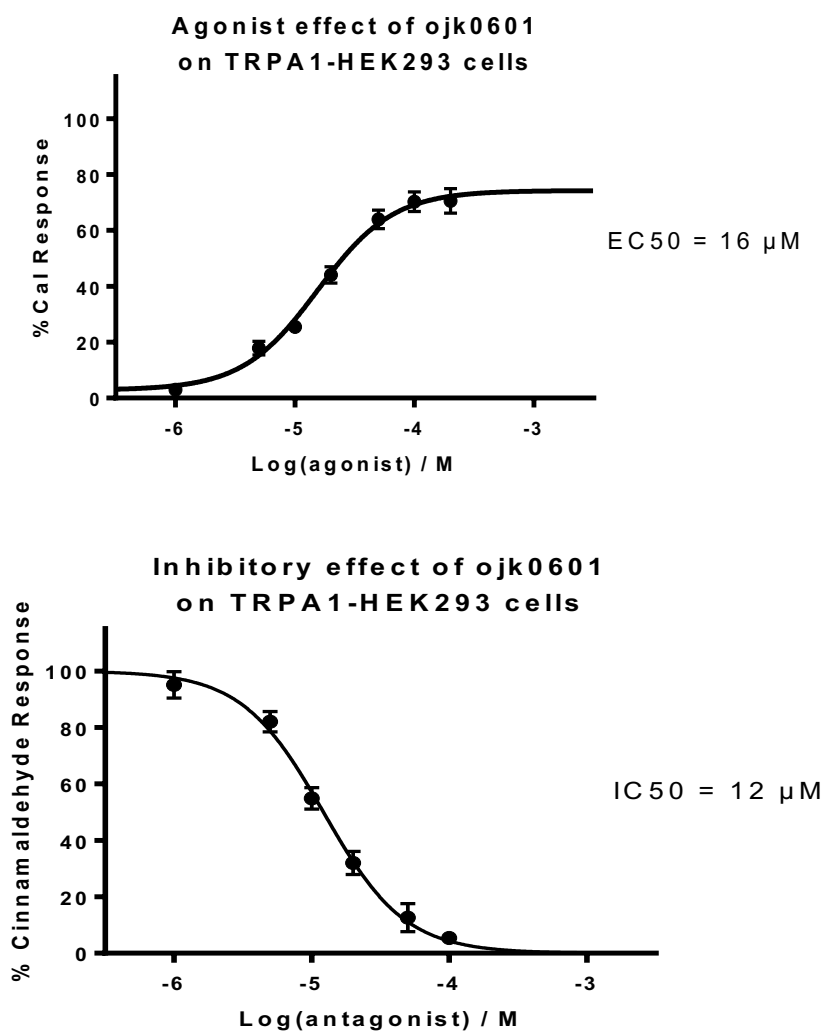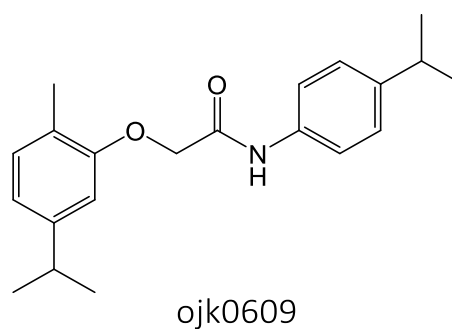

ojk0609

Figure 43 Chemical structure of ojk0609

Figure 44 Agonist (above) and antagonist (below) concentration effect curves for ojk0609 on TRPA1-HEK293 cells. Data points are means±SEM of N = 3 experiments
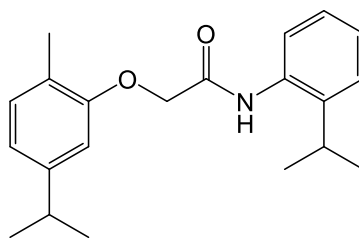
Ojk0609 has been assayed using both the agonist and antagonist calcium signalling assays to assess the compound's effect on TRPA1-HEK293 cells. The resulting concentration effect curves can be seen in Figure 44 above.

In the agonist assay, a concentration dependent increase in intracellular calcium was observed. This response was inhibited fully by the TRPA1 specific inhibitor HC-030031. Therefore, this response can be attributed to the gating of TRPA1 channels. Ojk0609 was tested over the concentration range of 1 to 200 µM, over this range, a typical sigmoidal response was observed. The first significant response was observed at 30 µM with a mean %CaI response of 12. The maximum response was observed at the 100 µM concentration point with a mean %CaI response of 31. A maximum plateau can be observed between the 50 and 100 µM concentration points, with the maximum response plateau being confirmed at the 200 µM concentration point.

Non-linear regression analysis was carried out using two different curve fit calculations the best fit was the variable Hill slope four parameter curve with an R^2 value of 0.8400. This curve predicts a partial agonist response which reflects what has been observed from the data points collected, this is confirmed by the models which assume a full agonist response show a very poor goodness of fit. The best fit curve calculates an EC50 of 36 µM and an efficacy of 42 % of the maximum cinnamaldehyde response.

In the antagonist assay a concentration dependent decrease in the response of 30 µM of cinnamaldehyde (EC50 concentration of cinnamaldehyde) was observed with increasing concentration of pre-dosed Ojk0609. Ojk0609 was tested over the concentration range of 0.5-50 µM over this range a typical reversed sigmoidal curve was observed. The first decrease in the cinnamaldehyde response was observed at 1 µM with a decrease in cinnamaldehyde response of 15%. The greatest reduction in the cinnamaldehyde response occurred at the 50 µM concentration point with a reduction of 93%, which is deemed to be full inhibition of the cinnamaldehyde response. The best fit non-linear regression analysis model was the normalised variable slope model which has an R^2 value of 0.8848, the calculated IC50 value for this model is 5 µM.

From this analysis of the agonist and antagonist assays of Ojk0609 on TRPA1-HEK293 cells, it can be determined that Ojk0609 is a partial agonist of TRPA1 which after the initial activation of TRPA1 inhibits further activation fully via a desensitisation effect.

3.2.3.2.2   Ojk07

3.2.3.2.2.1   Ojk0703

ojk0703

Figure 45 Chemical structure of ojk0703

Agonist effect of ojk0703 on TRPA1-HEK293 cells

EC50 = 6 µM

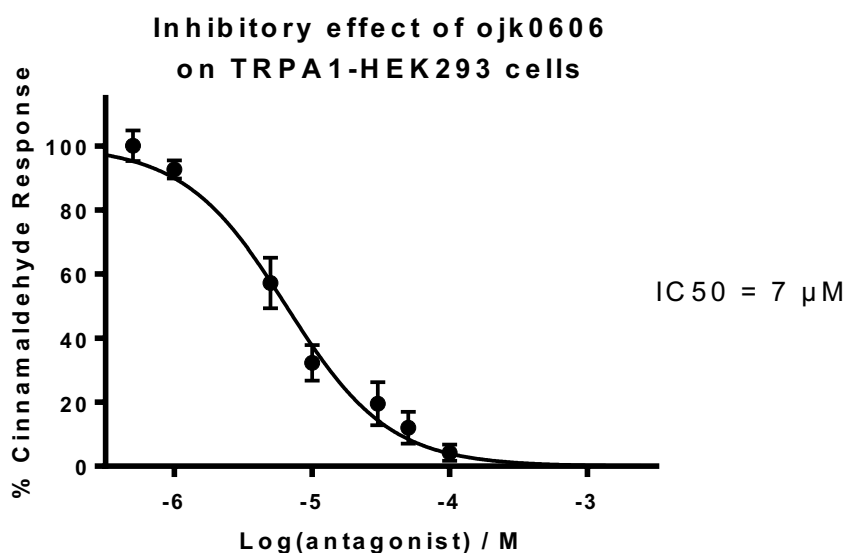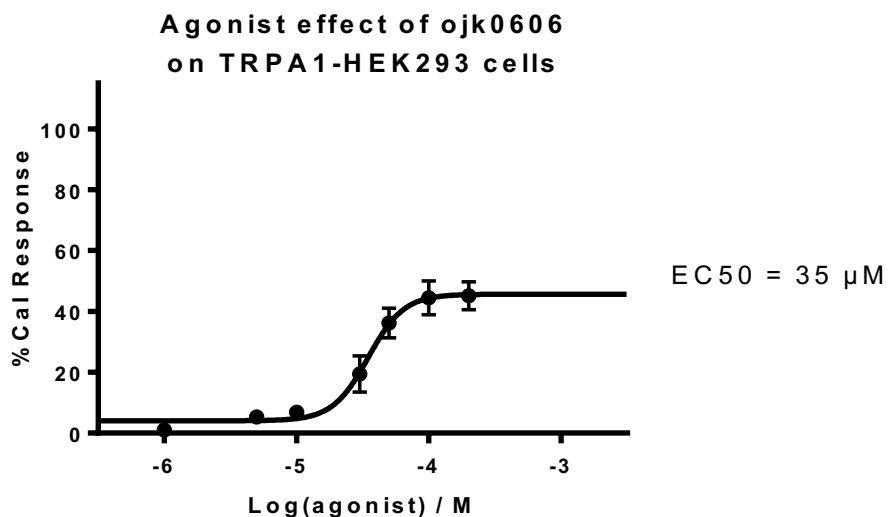**Inhibitory effect of ojk0703 on TRPA1-HEK293 cells**

IC50 = 23 µM

Figure 46 Agonist (above) and antagonist (below) concentration effect curves for ojk0703 on TRPA1-HEK293 cells. Data points are means±SEM of N = 3 experiments

Ojk0703 has been assayed using both the agonist and antagonist calcium signalling assays to assess the compound's effect on TRPA1-HEK293 cells. The resulting concentration effect curves can be seen in Figure 46 above.

In the agonist assay, a concentration dependent increase in intracellular calcium was observed. This response was inhibited fully by the TRPA1 specific inhibitor HC-030031. Therefore, this response can be attributed to the gating of TRPA1 channels. Ojk0703 was tested over the concentration range of 1 to 100 µM, over this range, a typical sigmoidal response was observed. The first significant response was observed at 5 µM with a mean %CaI response of 30. The maximum response was observed at the 100 µM concentration

point with a mean %CaI response of 69. A maximum plateau can be observed to form between the 20 and 50 µM concentration points, with the maximum plateau being confirmed at the 100 µM concentration point.

Non-linear regression analysis was carried out using two different curve fit calculations the best fit was the variable Hill slope four parameter curve with an R^2 value of 0.9221, the normalised variable slope model showed a similar goodness of fit with an R^2 0.9169. The normalised variable slope model assumes a full agonist response and displays a very good fit to the data, therefore, a full agonist response can be assumed, this is confirmed by the variable slope four parameter model which does not assume a full agonist response but shows an almost identical curve to the normalised variable slope curve. The best fit curve, the variable slope four parameter curve, calculates an EC50 of 6 µM and an efficacy of 95 % of the maximum cinnamaldehyde response.

In the antagonist assay a concentration dependent decrease in the response of 30 µM of cinnamaldehyde (EC50 concentration of cinnamaldehyde) was observed with increasing concentration of pre-dosed Ojk0703. Ojk0703 was tested over the concentration range of 1-100 µM over this range a typical reversed sigmoidal curve was observed. The first decrease in the cinnamaldehyde response was observed at 10 µM with a decrease in cinnamaldehyde response of 23.2 %. The greatest reduction in the cinnamaldehyde response occurred at the 100 µM concentration point with a reduction of 86%, which cannot be deemed to be full inhibition, further testing at greater concentrations were not carried out due to the insolubility of ojk0703 in the assay media at higher concentrations. Non-linear regression analysis was carried out using two different models, all of which predict full inhibition and show a good standard of fit, therefore, it can be predicted with confidence that Ojk0703 inhibits the activation of TRPA1 by cinnamaldehyde fully. The best fit curve was produced using the normalised variable slope model with an R^2 value of 0.9556 which predicts full inhibition to occur beyond 120 µM and calculates an IC50 of 23 µM.

From this analysis of the agonist and antagonist assays of Ojk0703 on TRPA1-HEK293 cells, it can be determined that Ojk0703 is a full agonist of TRPA1 which after the initial activation of TRPA1 inhibits further activation fully via a desensitisation effect.

3.2.3.2.2.2 Ojk0705
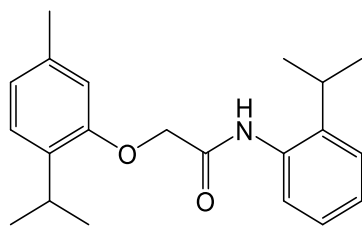
ojk0705

Figure 47 Chemical structure of ojk0705

**A g o n i s t   e f f e c t   o f   o j k 0 7 0 5
o n   T R P A 1 - H E K 2 9 3   c e l l s**

EC50 = 27 µM

**I n h i b i t o r y   e f f e c t   o f   o j k 0 7 0 5
o n   T R P A 1 - H E K 2 9 3   c e l l s**
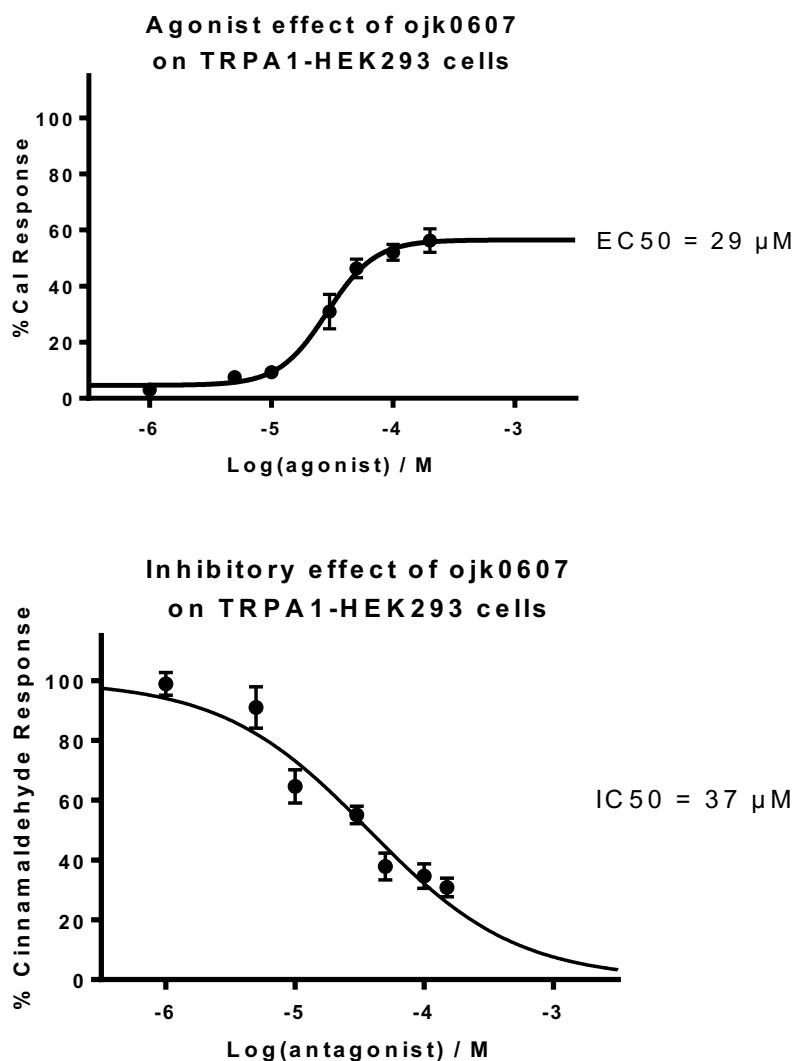
IC50 = 16 µM
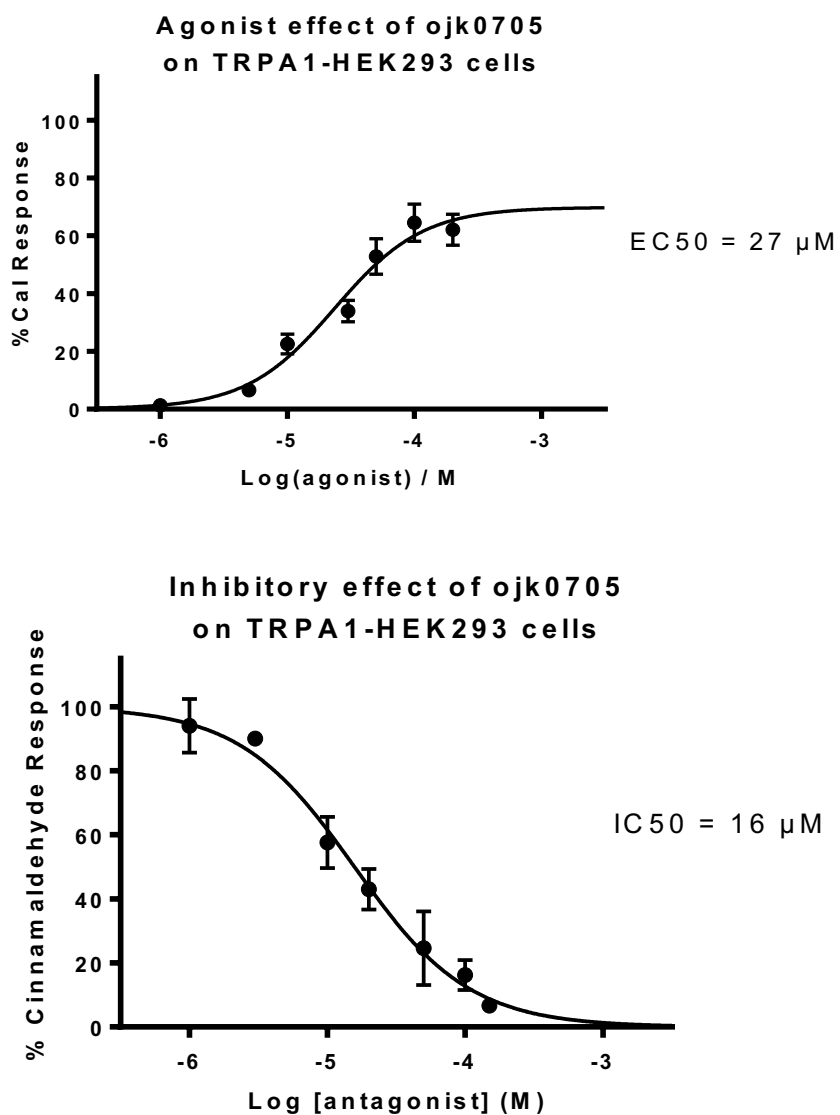
Figure 48 Agonist (above) and antagonist (below) concentration effect curves for ojk0705 on TRPA1-HEK293 cells. Data points are means±SEM of N = 3 experiments

Ojk0705 has been assayed using both the agonist and antagonist calcium signalling assays to assess the compound's effect on TRPA1-HEK293 cells. The resulting concentration effect curves can be seen in Figure 48 above.

In the agonist assay, a concentration dependent increase in intracellular calcium was observed. This response was inhibited fully by the TRPA1 specific inhibitor HC-030031. Therefore, this response can be attributed to the gating of TRPA1 channels. Ojk0705 was tested over the concentration range of 1 to 200 µM, over this range, a typical sigmoidal response was observed. The first significant response was observed at 10 µM with a mean %CaI response of 23. The maximum response was observed at the 100 µM concentration point with a mean %CaI response of 65. A maximum plateau can be seen to form between the 50 µM and the 100 µM with the plateau being confirmed by the 200 µM concentration point. However, the curve of best fit disagrees with this, and a maximum plateau is predicted occur at 230 µM and beyond.

Non-linear regression analysis was carried out using two different curve fit calculations the best fit was the variable Hill slope four parameter curve with an R^2 value of 0.8800. This curve predicts a full agonist response for ojk0705 and the goodness of fit for the normalised variable slope model which assumes a full agonist shows a good fit as well with an R^2 value of 0.8783 confirms this. The best fit curve calculates an EC50 value of 27 µM and an efficacy of 96 %.

In the antagonist assay a concentration dependent decrease in the response of 30 µM of cinnamaldehyde (EC50 concentration of cinnamaldehyde) was observed with increasing concentration of pre-dosed ojk0705. Ojk0705 was tested over the concentration range of 1-150 µM over this range a typical reversed sigmoidal curve was observed. The first decrease in the cinnamaldehyde response was observed at 10 µM with a decrease in cinnamaldehyde response of 42 %. The greatest reduction in the cinnamaldehyde response occurred at the 150 µM concentration point with a reduction of 93%, which is deemed to be full inhibition of the cinnamaldehyde response. This full inhibition could not be confirmed at greater concentrations due to the insolubility of ojk0705 in the assay media at higher concentrations. The best fit non-linear regression analysis model was the normalised variable slope model which has an R^2 value of 0.9078, the calculated IC50 value for this model is 16 µM.

From this analysis of the agonist and antagonist assays of ojk0705 on TRPA1-HEK293 cells, it can be determined that ojk0705 is a full agonist of TRPA1 which after the initial activation of TRPA1 inhibits further activation fully via a desensitisation effect.

3.2.3.2.2.3   Ojk0706
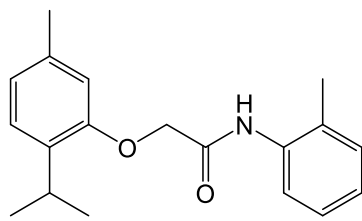
ojk0706

Figure 49 Chemical structure of ojk0706

**Agonist effect of ojk0706
on TRPA1-HEK293 cells**

EC50 = 18 µM

**Inhibitory effect of ojk0706
on TRPA1-HEK293 cells**

IC50 = 21 µM

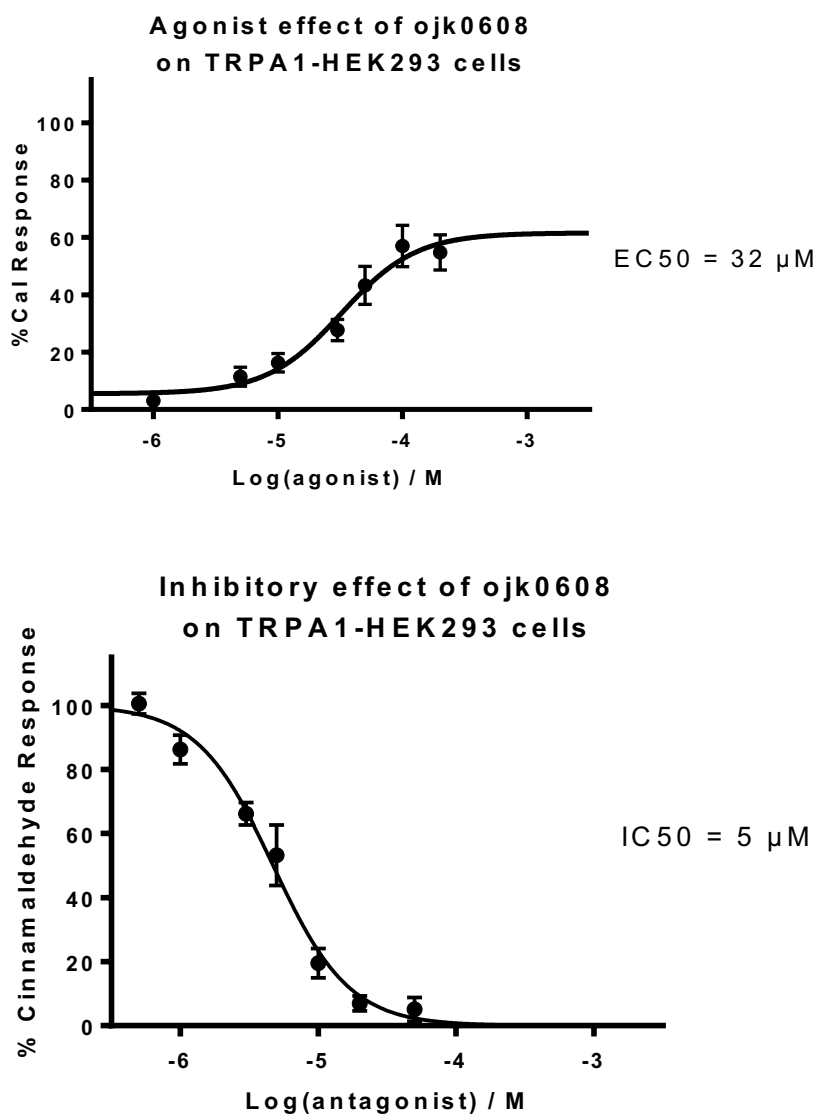*Figure 50* Agonist (above) and antagonist (below) concentration effect curves for ojk0706 on TRPA1-HEK293 cells. Data points are means±SEM of N = 3 experiments

Ojk0706 has been assayed using both the agonist and antagonist calcium signalling assays to assess the compound's effect on TRPA1-HEK293 cells. The resulting concentration effect curves can be seen in Figure 50 above.

In the agonist assay, a concentration dependent increase in intracellular calcium was observed. This response was inhibited fully by the TRPA1 specific inhibitor HC-030031. Therefore, this response can be attributed to the gating of TRPA1 channels. Ojk0706 was tested over the concentration range of 1 to 130 µM, over this range, a typical sigmoidal response was observed. The first significant response was observed at 10 µM with a mean %Cal response of 22. The maximum response was observed at the 130 µM concentration point with a mean %Cal response of 74. A maximum plateau can be observed to form

between the 50 and 100 µM concentration points with the plateau reaching its maximum at the 130 µM concentration point.

Non-linear regression analysis was carried out using two different curve fit calculations the best fit was the variable Hill slope four parameter curve with an R^2 value of 0.7916, the R^2 value for this curve is not as good as the R^2 values seen for the other compounds seen in this section, section 3.2.3.2.2, this is possibly due to the spread of the data points between repeats as the curve looks to fit the average data points well, however even though this R^2 value is lower than the others in this section the fit can be still be deemed to be good for the purposes of this study. The curve calculates an EC50 of 18 µM and an efficacy of 102 % of the maximum cinnamaldehyde response.

In the antagonist assay a concentration dependent decrease in the response of 30 µM of cinnamaldehyde (EC50 concentration of cinnamaldehyde) was observed with increasing concentration of pre-dosed Ojk0706. Ojk0706 was tested over the concentration range of 1-130 µM over this range a typical reversed sigmoidal curve was observed. The first decrease in the cinnamaldehyde response was observed at 10 µM with a decrease in cinnamaldehyde response of 35 %. The greatest reduction in the cinnamaldehyde response occurred at the 130 µM concentration point with a reduction of 94 %, which is deemed to be full inhibition of the cinnamaldehyde response. This full inhibition could not be confirmed at greater concentrations due to the insolubility of Ojk0706 in the assay media at higher concentrations. However, the data trends heavily towards full inhibition at concentrations of 130 µM and above. The best fit non-linear regression analysis model was the normalised variable slope model which has an R^2 value of 0.8688, the calculated IC50 value for this model is 21 µM.

From this analysis of the agonist and antagonist assays of Ojk0706 on TRPA1-HEK293 cells, it can be determined that Ojk0706 is a full agonist of TRPA1 which after the initial activation of TRPA1 inhibits further activation fully via a desensitisation effect.

3.2.3.2.2.4 Ojk0707
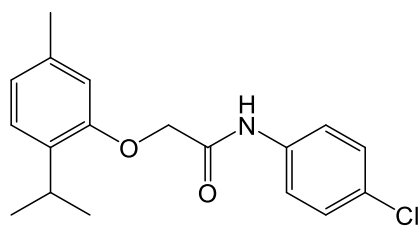
ojk0707

Figure 51 Chemical structure of ojk0707

Agonist effect of ojk0707 on TRPA1-HEK293 cells

EC50 = 32 µM

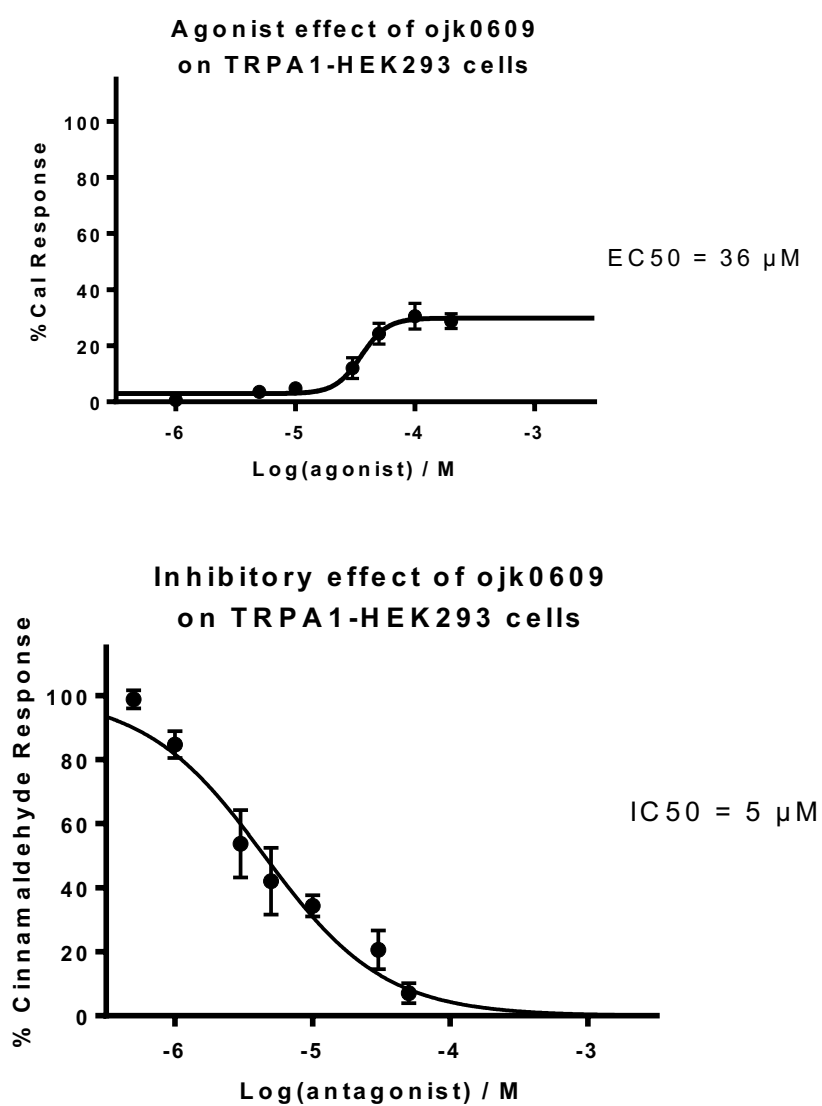**Inhibitory effect of ojk0707 on TRPA1-HEK293 cells**

IC50 = 6 µM
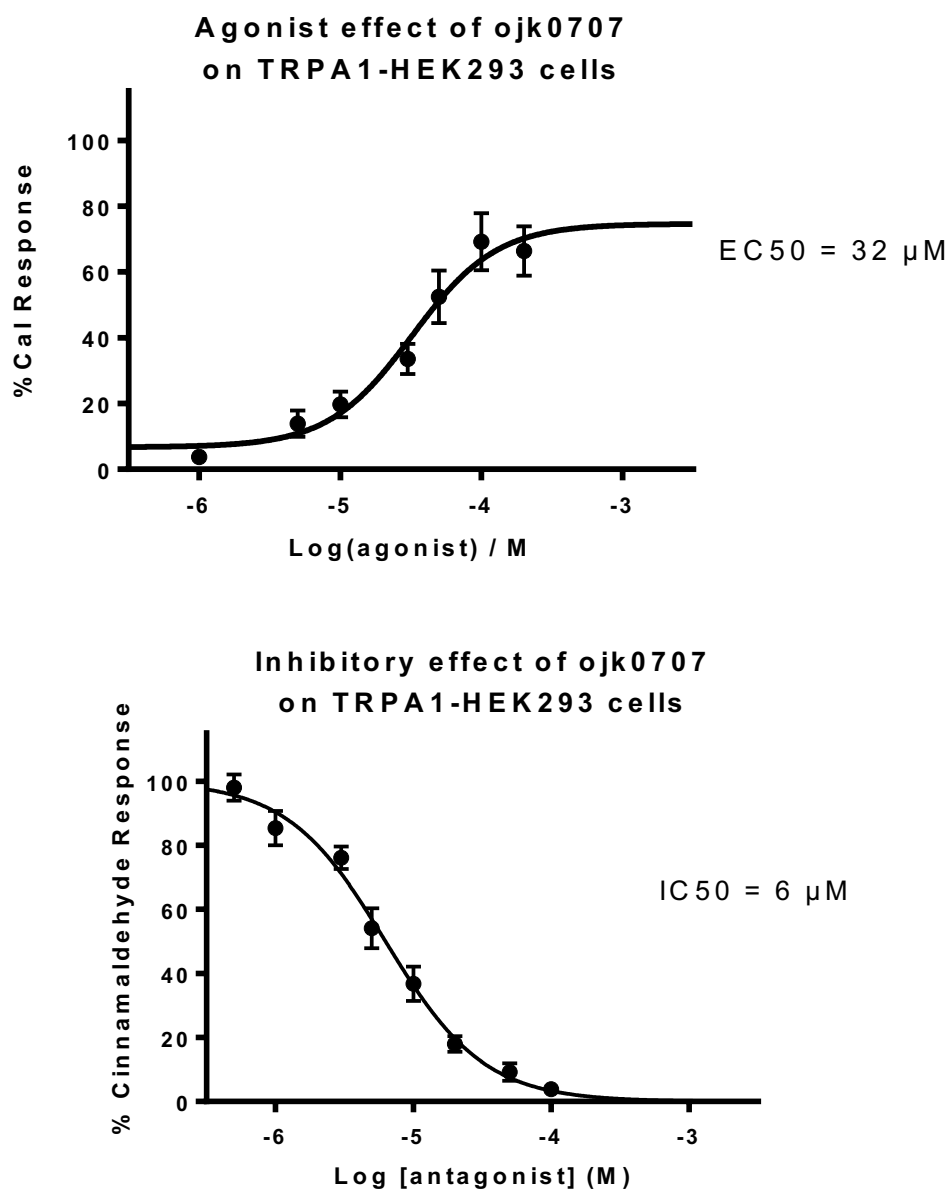
Figure 52 Agonist (above) and antagonist (below) concentration effect curves for ojk0707 on TRPA1-HEK293 cells. Data points are means±SEM of N = 3 experiments

Ojk0707 has been assayed using both the agonist and antagonist calcium signalling assays to assess the compound's effect on TRPA1-HEK293 cells. The resulting concentration effect curves can be seen in Figure 52 above.

In the agonist assay, a concentration dependent increase in intracellular calcium was observed. This response was inhibited fully by the TRPA1 specific inhibitor HC-030031. Therefore, this response can be attributed to the gating of TRPA1 channels. Ojk0707 was tested over the concentration range of 1 to 200 µM, over this range, a typical sigmoidal response was observed. The first significant response was observed at 5 µM with a mean %CaI response of 14. The maximum response was observed at the 100 µM concentration point with a mean %CaI response of 69.2. A maximum plateau can be observed to form between the 50 and 100 µM concentration points with the maximum plateau being confirmed at the 200 µM concentration point.

Non-linear regression analysis was carried out using two different curve fit calculations the best fit was the variable Hill slope four parameter curve with an R^2 value of 0.8229. This model predicts a full agonist response which reflects what the data collected shows, from the curve an EC50 value of 32 µM and an efficacy of 96 % of the maximum cinnamaldehyde response has been calculated.

In the antagonist assay a concentration dependent decrease in the response of 30 µM of cinnamaldehyde (EC50 concentration of cinnamaldehyde) was observed with increasing concentration of pre-dosed Ojk0707. Ojk0707 was tested over the concentration range of 0.5-100 µM over this range a typical reversed sigmoidal curve was observed. The first decrease in the cinnamaldehyde response was observed at 1 µM with a decrease in cinnamaldehyde response of 15 %. The greatest reduction in the cinnamaldehyde response occurred at the 100 µM concentration point with a reduction of 96%, which is deemed to be full inhibition of the cinnamaldehyde response. Full inhibition was first observed at the 50 µM point with a reduction in the cinnamaldehyde response of 92 %. The best fit non-linear regression analysis model was the normalised variable slope model which has an R^2 value of 0.9629, the calculated IC50 value for this model is 6 µM.

From this analysis of the agonist and antagonist assays of Ojk0707 on TRPA1-HEK293 cells, it can be determined that Ojk0707 is a full agonist of TRPA1 which after the initial activation of TRPA1 inhibits further activation fully via a desensitisation effect.

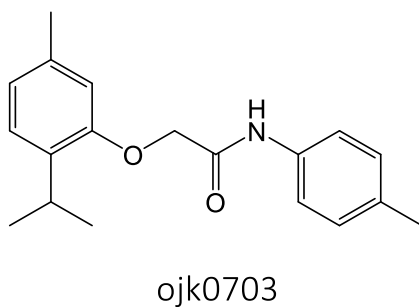### 3.2.3.2.2.5   Ojk0708
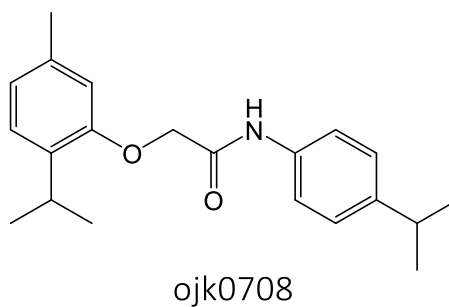
ojk0708

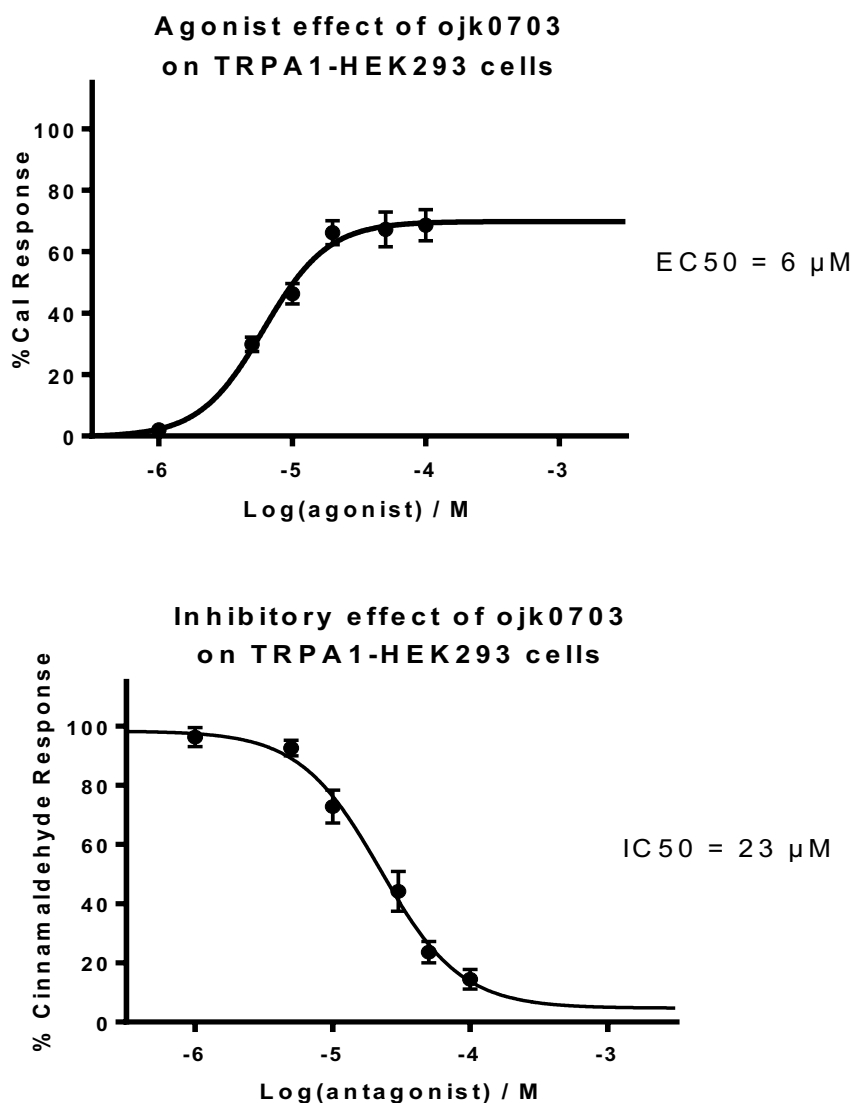*Figure 53* Chemical structure of ojk0708
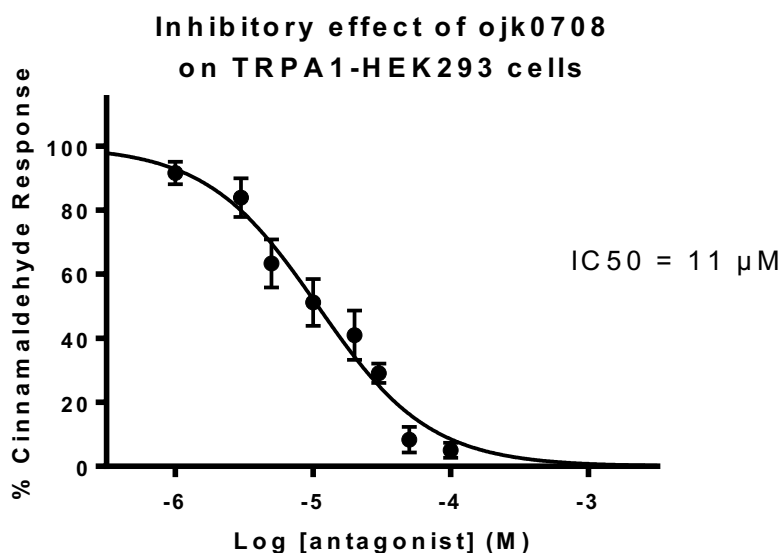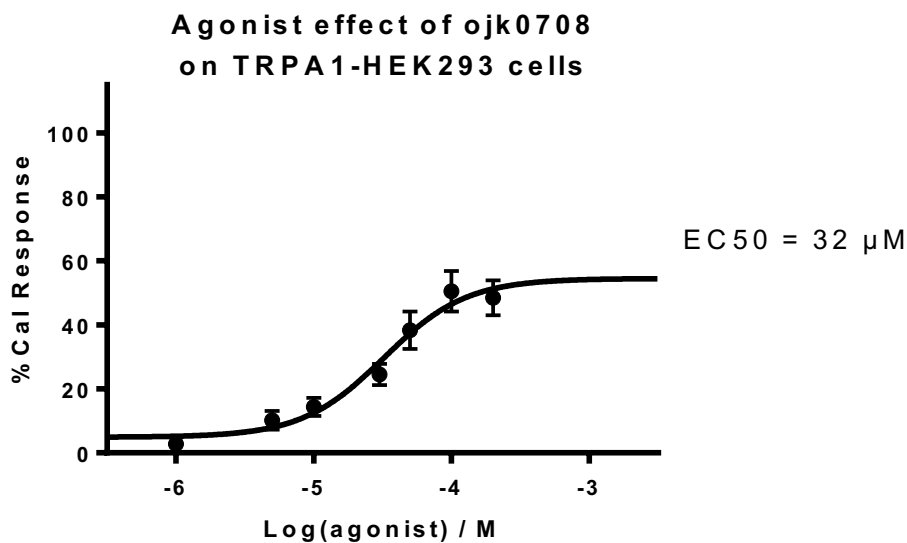
Figure 54 Agonist (above) and antagonist (below) concentration effect curves for ojk0708 on TRPA1-HEK293 cells. Data points are means±SEM of N = 3 experiments

Ojk0708 has been assayed using both the agonist and antagonist calcium signalling assays to assess the compound's effect on TRPA1-HEK293 cells. The resulting concentration effect curves can be seen in Figure 54 above.

In the agonist assay, a concentration dependent increase in intracellular calcium was observed. This response was inhibited fully by the TRPA1 specific inhibitor HC-030031. Therefore, this response can be attributed to the gating of TRPA1 channels. Ojk0708 was tested over the concentration range of 1 to 200 µM, over this range, a typical sigmoidal response was observed. The first significant response was observed at 10 µM with a mean

%CaI response of 14. The maximum response was observed at the 100 μM concentration point with a mean %CaI response of 51. A maximum plateau can be observed to form between the 50 and 100 μM concentration points with the plateau being confirmed at the 200 μM concentration point, greater concentrations could not be tested as testing above 200 μM was not possible due to the insolubility of Ojk0708 in the assay media at higher concentrations.

Non-linear regression analysis was carried out using two different curve fit calculations the best fit was the variable Hill slope four parameter curve with an R^2 value of 0.8227, this model predicts a partial agonist response which reflects what has been observed by the data. However, the normalised variable slope model has a similar goodness of fit with an R^2 value of 0.8130, this model assumes a full agonist response, without further testing at a higher concentration the nature of the full response of Ojk0708 cannot be fully confirmed. A partial agonist response has been seen with other compounds in this library so a partial agonist response for Ojk0708 does fit the trend observed. Therefore, with reasonable confidence, it can be determined that Ojk0708 acts as a partial agonist of TRPA1 with an EC50 of 32 μM and an efficacy of 70 % of the maximum cinnamaldehyde response were the maximum plateau occurs at concentrations greater than 189 μM.

In the antagonist assay a concentration dependent decrease in the response of 30 μM of cinnamaldehyde (EC50 concentration of cinnamaldehyde) was observed with increasing concentration of pre-dosed Ojk0708. Ojk0708 was tested over the concentration range of 0.5-100 μM over this range a typical reversed sigmoidal curve was observed. The first decrease in the cinnamaldehyde response was observed at 3 μM with a decrease in cinnamaldehyde response of 16%. The greatest reduction in the cinnamaldehyde response occurred at the 100 μM concentration point with a reduction of 95%, which is deemed to be full inhibition of the cinnamaldehyde response. Full inhibition was first observed at the 50 μM concentration point with a reduction of 93 %. The best fit non-linear regression analysis model was the normalised variable slope model which has an R^2 value of 0.9045, the calculated IC50 value for this model is 11 μM.

From this analysis of the agonist and antagonist assays of Ojk0708 on TRPA1-HEK293 cells, it can be determined that Ojk0708 is a partial agonist of TRPA1 which after the initial activation of TRPA1 inhibits further activation fully via a desensitisation effect.

3.2.4   Screening of active compounds on TRPM8-HEK293 cells

All of the TRPA1 active compounds from the ojk01, ojk06 and ojk07 groups have been screened for activity with TRPM8-HEK293 cells. The agonist and antagonist calcium signalling methods from section 2.2 were used with the exception that TRPM8-HEK293 cells were used alongside the relevant agonist controls (WS-5). Each compound was assayed at 10 and 100 µM in both the agonist and antagonist assay methods. All of the compounds except ojk0606 showed no modulation of TRPM8. This indicates that the compounds assayed do not interact with anything else expressed in the HEK293 cells due to the only difference between the two cell lines is the expression of TRPM8 rather than TRPA1. These results also imply a degree of selectivity however further work is required to fully determine specificity.

As previously mentioned ojk0606 gave a hit in the TRPM8 screening. It was found to inhibit the response of the known specific TRPM8 agonist WS-5. There was no agonist response observed for ojk0606 in TRPM8-HEK293 cells. A full concentration effect assay was then carried out to fully determine the inhibitory response of ojk0606 on the activation of TRPM8 by WS-5, the results can be seen in Figure 55.

Ojk0606 was tested over a concentration range of 1-100 µM. A decrease in the response of 100 µM of WS-5, a potent specific agonist of TRPM8, was observed with increasing concentration of pre-dosed ojk0606(177). A complete concentration effect curve was not completed due to the insolubility of ojk0606 in the assay medium above 100 µM. Over the concentration range tested, 1 to 100 µM, a typical sigmoidal curve was observed which heavily trended towards a full sigmoidal response. The first decrease in the WS-5 response was observed at the 10 µM concentration point with a 31% reduction in the WS-5 agonist response. The greatest reduction was observed at 100 µM concentration point, the maximum concentration tested, with a reduction of 77% of the WS-5 agonist response. Full inhibition was not observed due to solubility issues mentioned previously, however, non-linear regression analysis of the data points collected trends towards full inhibition of TRPM8 by ojk0606 heavily. The best fit curve was the normalised variable response curve with an R^2 value of 0.8359, this model does assume full inhibition and the good fit gives a

good indication that ojk0606 fully inhibits TRPM8 at higher concentrations. This prediction of full inhibition is backed up by the variable slope four parameter curve which does not assume full inhibition but predicts it with a similar goodness of fit to the normalised variable slope model. The best fit curve calculates an IC50 of 29 µM for the inhibition of TRPM8 by ojk0606.

Inhibitory effect of ojk0606 on TRPM8-HEK293 cells

IC50 = 29 µM

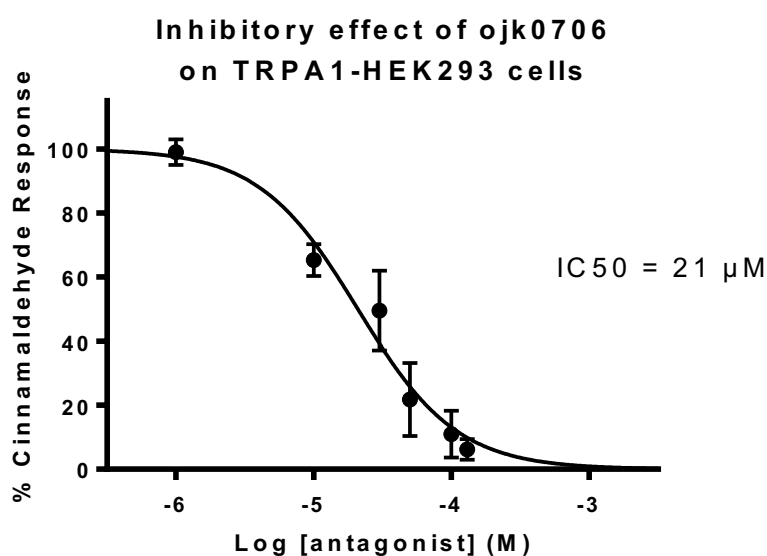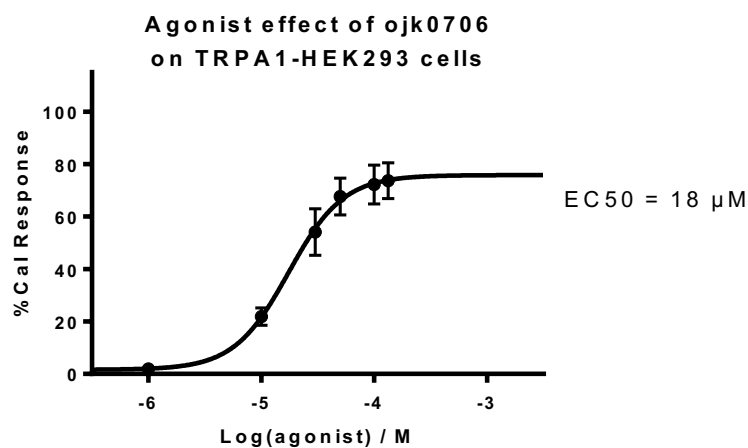Calcium signalling traces for ojk0606 antagonist on TRPM8-HEK293 cells repeat 1
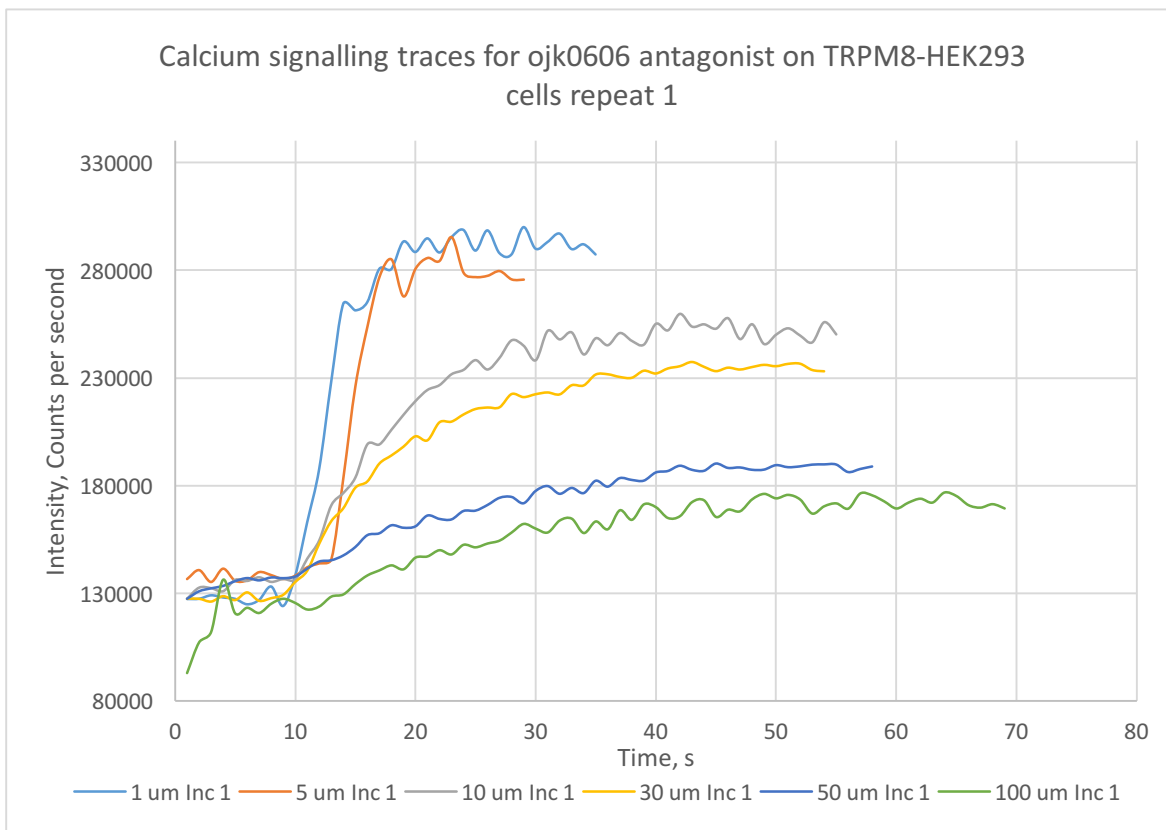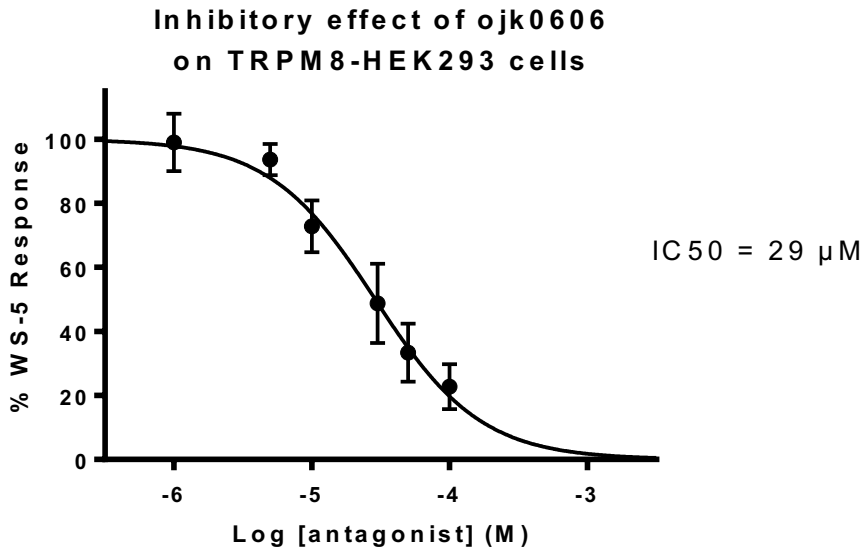
Figure 55 Above: Antagonist concentration effect curve for ojk0606 on TRPM8-HEK293 cells. Data points are means±SEM of N = 3 experiments Below: Raw data traces for repeat 1 of ojk0606 antagonist assay on TRPM8-HEK293 cells

3.3 Discussion

The results for the synthesis and calcium signalling assay of the ojk01, ojk06 and ojk07 compounds reported in section 3.2 shall be discussed in the following sections in detail.

3.3.1   Calcium signalling assay method

The calcium signalling assay method, detailed in section 2.2, has been used to monitor the effects of the test compounds on TRPA1-HEK293 cells with regards to intracellular calcium concentrations. Cinnamaldehyde (agonist control) and HC-030031 (antagonist control) were chosen as controls due to their widespread use in TRPA1 research as potent and selective TRPA1 modulators. Both controls have been fully assayed using the calcium signalling assay to determine their effect on TRPA1-HEK293 cells. Both controls used have also been tested on mock transfected HEK293 cells at the highest concentration they would be used at on TRPA1-HEK293 cells. Both the controls showed no effect on intracellular calcium levels in the mock transfected cells and can therefore be deemed selective to TRPA1 in my calcium signalling assay method.

With regards to the discussion below it must be noted that the assay method used only measures the functional effects of the test compounds on ion channel activity and not the physical interactions between the test compounds and ion channels. Steps have been taken to determine if the responses observed are due to the effects of the test compound on the ion channel such as testing the compounds on mock transfected HEK293 cells. While it is entirely feasible that the test compounds modulate the ion channels via direct binding, it must also be considered that other indirect mechanisms may be the cause of the compounds effect on the ion channels. Differentiation between direct and indirect modulation cannot be distinguished based on recording intracellular calcium levels alone.

3.3.2 Amide and ester derivatives of thymol (ojk01)

This section will discuss the results reported in section 1.1.1 which contain

3.3.2.1 Synthesis of ojk01 derivatives

3.3.2.1.1 Amide derivatives

2-isopropylaniline was coupled to several aromatic compounds via a 4-dimethylaminopyrodine (DMAP) catalysed acylation reaction. The general structure of the compounds that were produced can be seen below in Figure 56.
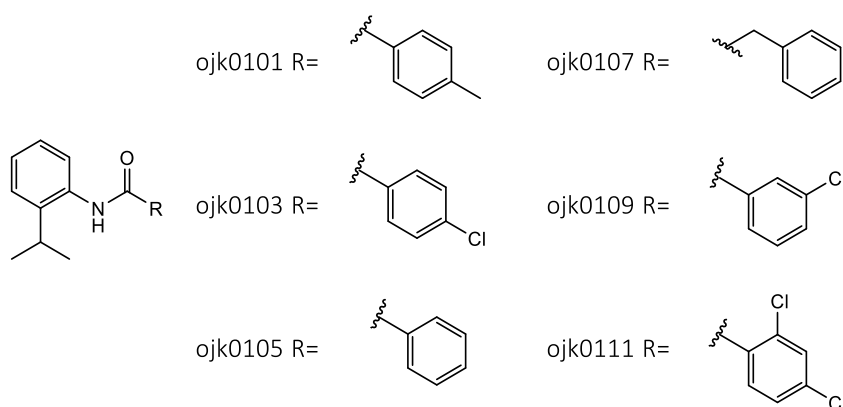
Figure 56 General structure of ojk01 amide derivatives

The analogues chosen were based on common substituents found in TRP modulators and from the groups which proved to be the most successful TRPM8 antagonists when coupled to menthylamine see Figure 57(176).
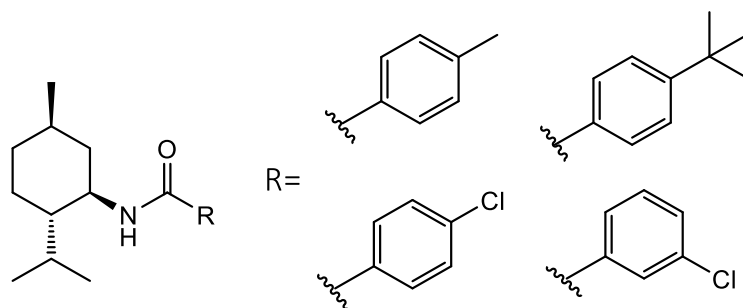
Figure 57 Structure of key menthlamine derivatives from Ortar *et al.* 2010(176)
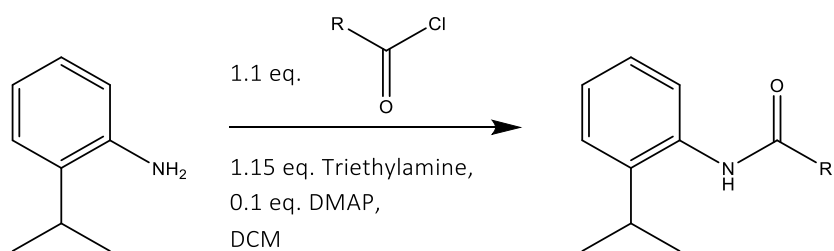
Figure 58 Reaction scheme for ojk01 amide derivatives

The reaction scheme can be seen in Figure 58. Considering the prevalence of DMAP catalysed reactions, there is a lack of understanding with regards to the underlying mechanism even in the simplest of DMAP catalysed reactions. The currently accepted mechanism, seen in Figure 59, occurs in the following order; DMAP reacts with the acyl chloride to form an acylpyridinium cation, this reaction is in equilibrium. The amine or alcohol then reacts with the acylated catalyst to produce the amide or ester product and the protonated, and therefore deactivated catalyst. The final step is the regeneration of the catalyst via deprotonation by triethylamine.
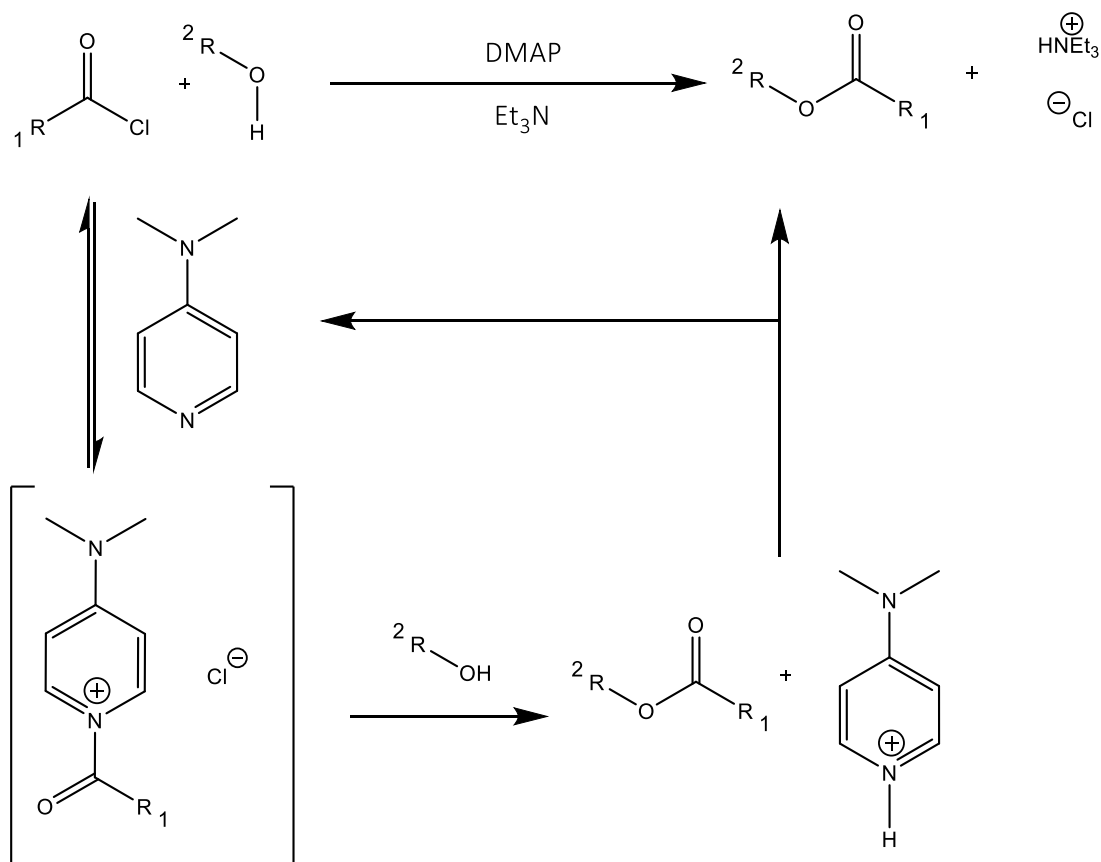
Figure 59 Generally accepted reaction scheme for DMAP catalysed cross linking reactions

DMAP is a particularly good catalyst for these types of reactions, especially compared to pyridine which could also be used. However, the reaction would have to take place in pyridine solution. This is because of the amino group which reinforces the nucleophilic nature of the nitrogen atom in the ring. The effect of the amino group is shown in Figure 60.
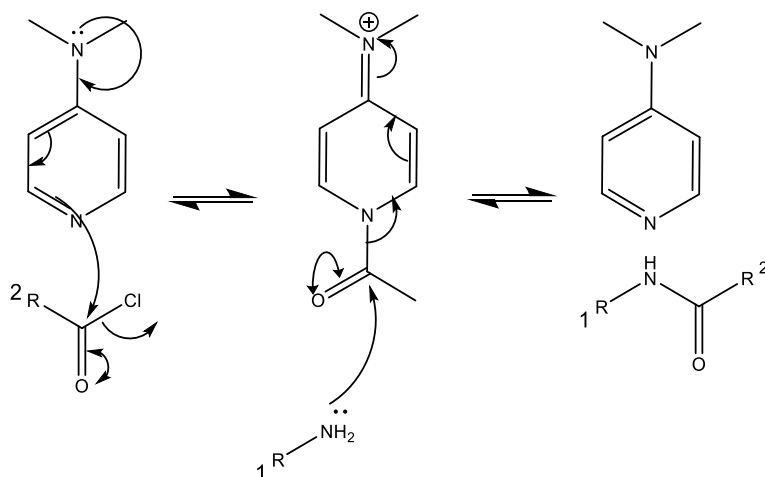
Figure 60 Reaction mechanism for DMAP in cross linking reactions

The percentage yields of the crude products were very similar, and all were about 90 %, the yields obtained were as expected. The reaction was a fairly clean reaction as all the unwanted by-products were removed in the aqueous work up. The recrystallisation yields were lower on average by 20 %, which is most likely due to poor technique.

The six analogues that were prepared all reacted in the same manner. When the acyl chloride was added an exothermic reaction took place, the colour of the solution turned from an almost clear solution to an orange colour. For a couple of the reactions, a small amount of white fumes was given off. This was probably HCl that had formed as it forms white fumes upon contact with atmospheric humidity. When the DCM was evaporated off the crude product, in all cases, was a light orange and white solid. The final crystallised products were all white crystals.

The ^{1}H and ^{13}C NMR spectra were taken for each compound (see section 3.2.2), after analysis and interpretation they were all positively characterised. The ^{1}H NMR was difficult to interpret the signals from the aromatic hydrogens due to the slow rotation of the C-N of the amide bond at room temperature. In addition to this, the melting points were determined. Elemental analysis was not carried out due to time constraints.

A range of 2-isopropylaniline amide derivatives was prepared and characterised successfully. The reaction can be deemed successful on a 0.5g scale.

3.3.2.1.2   Ester derivatives

Ester derivatives of 2-isopropylphenol were prepared via a DMAP catalysed acylation reaction in the same manner as the amide derivatives prepared in section 3.2.2. The general structure of the compounds produced can be seen in Figure 61.
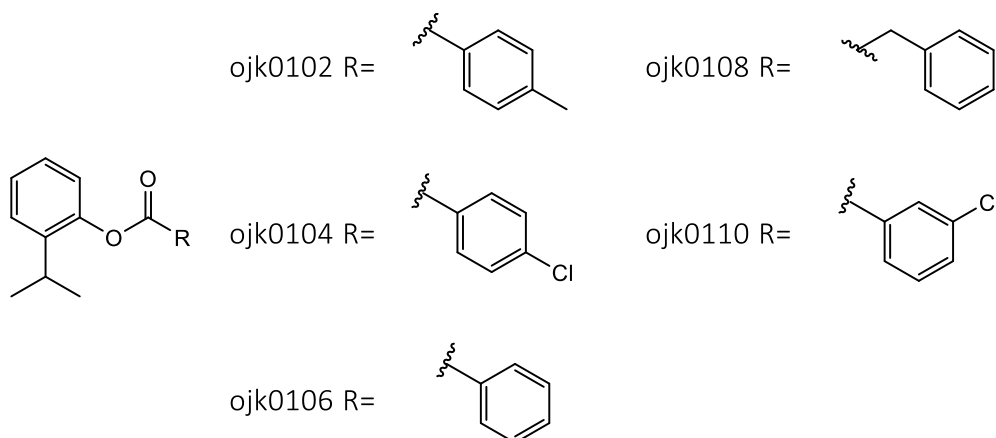
Figure 61 General structure of ojk01 ester derivatives

The reaction conditions are exactly the same as the acylation of 2-isopropylamine, except the starting material was 2-isopropylphenol.
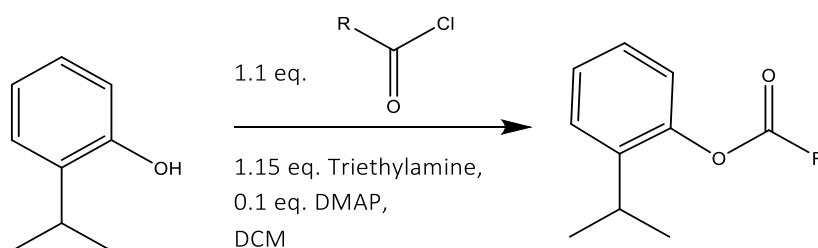
Figure 62 Reaction scheme of ojk01 ester derivatives

The crude product %yields for each reaction were all high. The %yields after recrystallisation was quite low, especially when compared to the %yields from the 2-isopropylaniline derivatives.

The reaction between the alcohol and the acyl chlorides was an exothermic reaction, which produced a change in the solution from clear to a slight yellow tinge. As with the amine acylation, there were white fumes given off. When the DCM was evaporated off a clear light yellow oil was left, this was the case for all the reactions.

117

Recrystallisation using EtOH/H_2O was unsuccessful for ojk0104, as when the solution was cooled the product was separated from the EtOH/H_2O solution as a separate liquid layer. The product was then recovered by diluting the mixture with DCM and using molecular sieves to dry the solution. The EtOH and DCM were then evaporated off. The recrystallisation was then repeated using MeOH/H_2O which was cooled to approximately -15°C which yielded the final product.

Several 2-isopropylphenol ester derivatives were prepared and characterised successfully; the recrystallisation proved to be difficult and resulted in poor purified %yields.

3.3.2.2   Calcium signalling results discussion

The ojk01 library consists of an isopropylphenyl group linked to a substituted phenyl ring via an amide or an ester functional group from the 2-position. The differences in compounds synthesised arise in the substitutions of the linked phenyl ring except for ojk0107 and ojk0108 which have an extra carbon atom between the linking group and the phenyl ring. All the compounds in the ojk01 library have been screened for modulation of TRPA1 expressed in HEK293 cells using the agonist and antagonist calcium signalling assays described in section 2.2. From this screening, three compounds were found to have an effect on TRPA1, highlighted green in Figure 25 these were ojk0107, ojk0109 and ojk0111, these compounds then were assayed over their effective concentration range in order to develop a concentration effect curve for both their agonist and inhibitory effects. From the results of the screening and the subsequent detailed assays for ojk0107, 09 and 11 several trends with regards to structure activity relationship between this library of compounds and TRPA1 have emerged and will be discussed below.

ojk0107
Partial agonist of TRPA1
and inhibited TRPA1

ojk0108
No modulation of TRPA1 observed

ojk0109
Partial agonist of TRPA1
and inhibited TRPA1

ojk0110
No modulation of TRPA1 observed
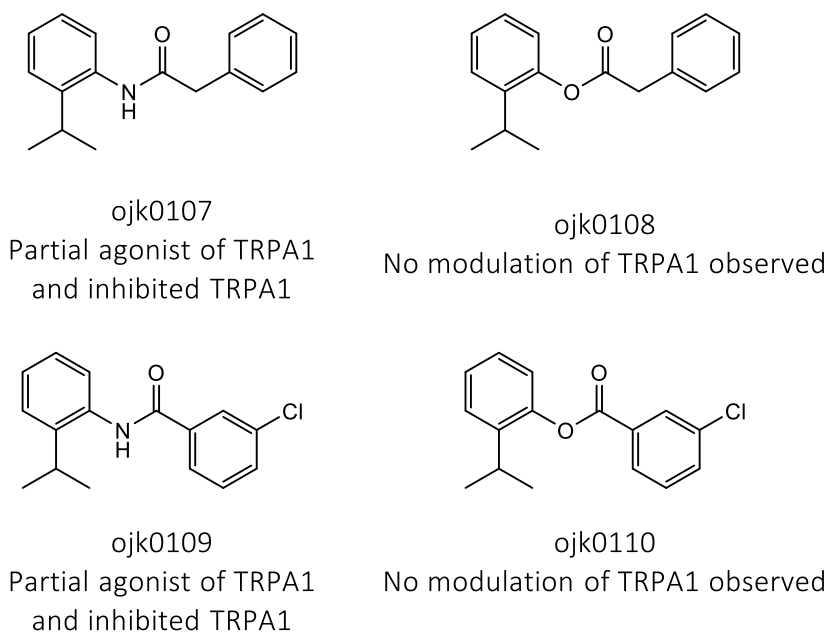
Figure 63 Comparison of amide and ester derivatives of ojk01 chemical structures.

One of the first trends observed was for the compounds which were found to have an effect on TRPA1 all linked the two phenyl groups with an amide groups, and their ester analogs did not show any effect, at least not at the concentration range tested which was limited by insolubility of the test compound in the assay media at higher concentrations. See

section 3.2.1.1 for details. See Figure 63 for the structures of the active amides and the non-active esters. This trend was only observed for ojk0107 and ojk0109 and their ester counterparts as the other amides did not show any activity towards TRPA1. It can be determined that while the substitution on the second phenyl ring is of importance with regards to TRPA1 interaction the nature of the linking group has an effect on the interaction with TRPA1. The reason for the difference in activity between the amides and esters is possibly due to the differences in polarity of the two functional groups, the amide being more polar and capable of forming hydrogen bonds and the ester group being the least polar and is not able of forming hydrogen bonds. Another possible reason for the ester compounds not showing any modulation of TRPA1 may be due to the compounds being hydrolysed by non-specific esterases upon penetrating the plasma membrane, in a similar way to how the calcium indicator Fluo-3AM is broken down. However, hydrolysis of the ester compounds would affect the antagonist assay more than the agonist assay due to the incubation time of the compounds in the antagonist assay. This trend is apparent in chapter 4 (discussed in section 4.3.1) were the amine linked compounds FFA, MFA and DFC displayed modulation of TRPA1 while ketoprofen, a ketone linked compound showed significantly lower interaction with TRPA1, see Figure 64 for structures. This may be due to in part to the ability of the amine linking group to form hydrogen bonds and the ketone linking group not being able to form hydrogen bonds. The ability to form hydrogen bonds via a polar amide linking group may be a significant factor in the modulation of TRPA1 by the ojk06 and ojk07 compounds which will be discussed in section 3.3.3.
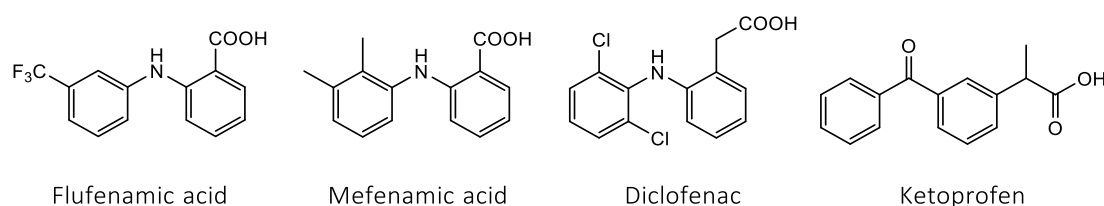
Figure 64 Chemical structures of fenamic acid related NSAIDs that have been reported to activate TRPA1(141).

Another trend to be observed was that of the chain length as there was a distinct difference between the interaction with TRPA1 between ojk0105 and ojk0107. From the structures in Figure 65, it can be seen that ojk0107 has a carbon atom between the amide linking group and the second phenyl ring whereas ojk0105 has a direct amide link between the two phenyl rings. From the results, seen in section 1.1.1.1, ojk0105 does not show any

modulation of TRPA1 whereas ojk0107 shows a partial agonist response and a trend towards full inhibition of cinnamaldehyde activation of TRPA1. As previously mentioned the only difference between these two compounds is the extra carbon atom in the linker between the two phenyl groups in ojk0107, this slight change in structure allows ojk0107 to have a greater interaction with TRPA1.

ojk0105
No modulation of TRPA1 observed

ojk0107
Partial agonist of TRPA1, also inhibited TRPA1
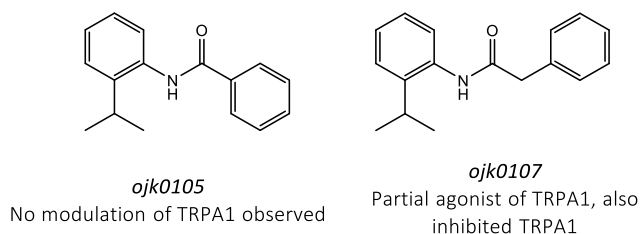
Figure 65 Chemical structures of ojk0105 and ojk0107

This trend can be taken one step further when, for example, ojk0703 is considered, see Figure 66 for structures. Ojk0703 has an extra atom in the chain linking the two phenyl rings, which is in the form of the ether group when compared to ojk0107. Comparing the TRPA1 assay results, see Figure 67 for comparison graph, of the three compounds in Figure 66 a trend is observed with increasing linking group chain length an increase in the efficacy and potency occurs. Ojk0703, which has the longest linker group, has the greatest efficacy and potency followed by ojk0107, which has the second longest linker group, and then ojk0105 which has the shortest linker group and has not shown any interaction with TRPA1 over the concentrations tested. When including ojk0703 in this trend the other structural differences must be considered and what effect they may have on its interaction with TRPA1, these structural differences include the extra methyl groups on both the phenyl rings, the orientation of the amide group with regards to the isopropyl group and lastly the extra atom in the linking group is an oxygen atom and not a carbon atom like in ojk0107.

ojk0703
Full agonist of TRPA1
and inhibited TRPA1

ojk0107
Partial agonist of TRPA1
and inhibited TRPA1

ojk0105
No modulation of
TRPA1 observed
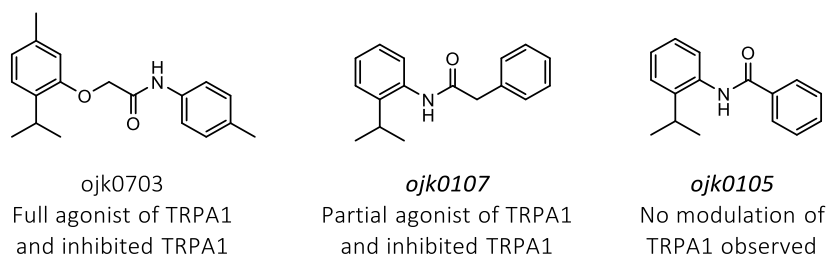
Figure 66 Chemical structure comparison of ojk0703, ojk0107 and ojk0105

The effect of increasing linker group length on the activation of TRPA1-HEK293 cells
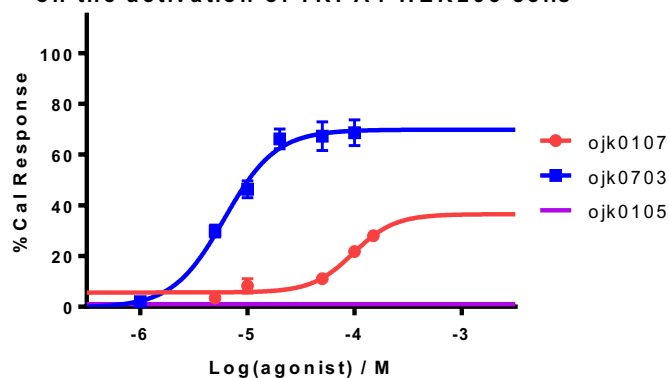
The effect of increasing linker group length on the inhibition of TRPA1-HEK293 cells
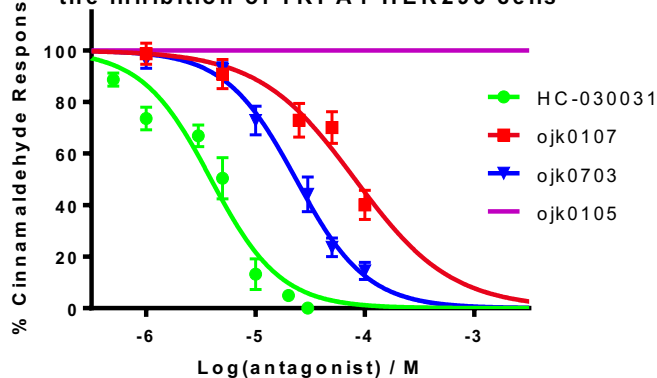
Figure 67 Comparison of concentration effect curves for ojk0105, ojk0107and ojk0109 on TRPA1-HEK293 cells. Data points are means±SEM of N = 3 experiments

NPB
5-nitro-2-(phenylamino)benzoicacid
EC50 = 14uM

NPEB
5-nitro-2-(phenethylamino)benzoicacid
EC50 = 6uM

NPPB
5-nitro-2-((3-phenylpropyl)amino)benzoic acid
EC50 = 0.37uM
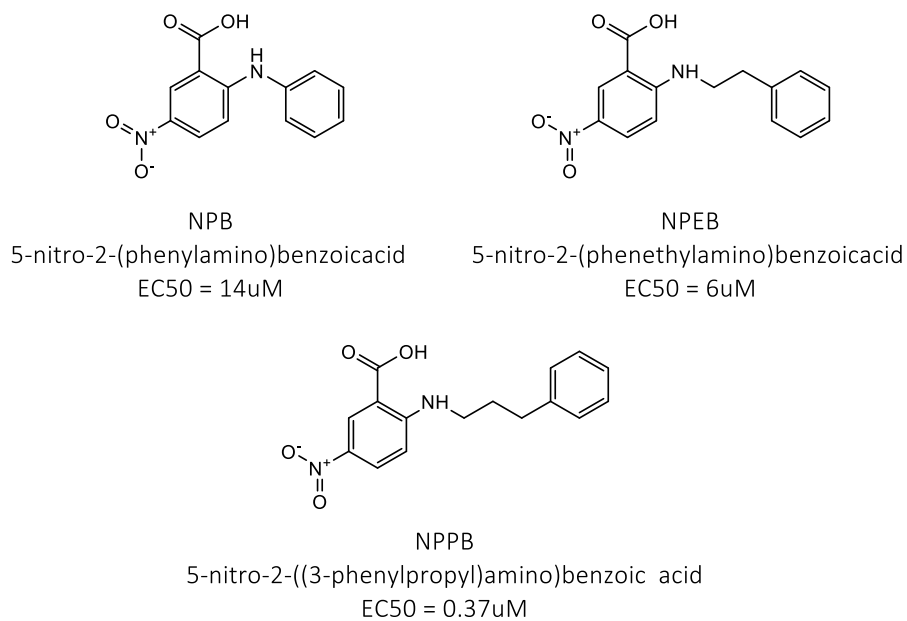
Figure 68 Chemical structures of TRPA1 agonist NPB, NPEB and NPPB.

The effect of the other structural differences between ojk0703 and the ojk01 compounds on the interaction with TRPA1 cannot be fully determined however the trend described in this section has also been seen with regards to NPPB by Liu *et al.* (142), when they reported that NPPB showed an increased potency with regards to TRPA1 activation over analogues of NPPB with shorter linking groups, see Figure 68 for details. Liu *et al.* report that NPPB shows no antagonist properties towards TRPA1, therefore, the trend observed for the agonist potency for NPPB, NPEB and NPB was not investigated with regards to inhibition of TRPA1. However, ojk0105, ojk0107 and ojk0703 have all been assayed using the antagonist assay, and the same trend was observed in the agonist assays. This inhibitory trend shows that as the linking group increases in length the potency of the inhibition of TRPA1 increases.

HC-030031
Ring 1, linking group, Ring 2

ojk0703
Ring 1, linking group, Ring 2

ojk0107
Ring 1, linking group, Ring 2

ojk0105
Ring 1, linking group, Ring 2
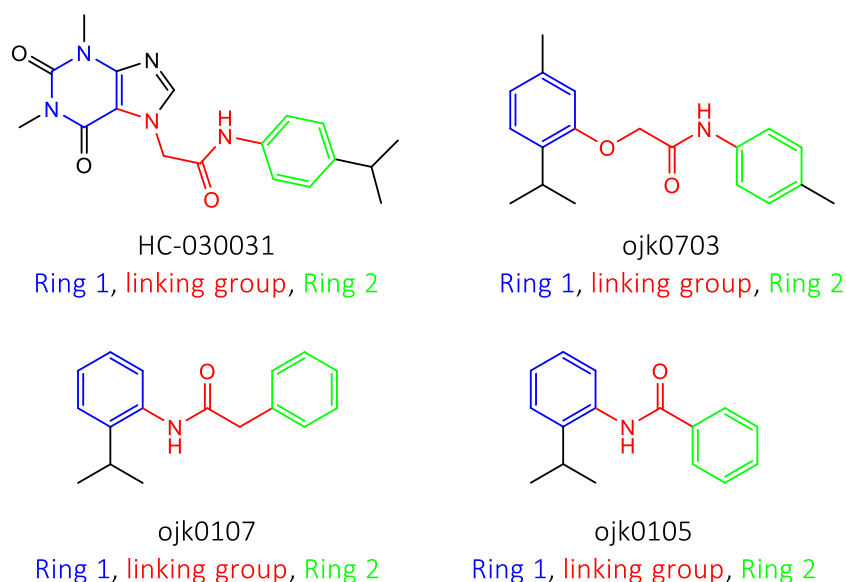
Figure 69 Chemical structure comparison of HC-030031, ojk0703, ojk0107 and ojk0105. First ring structure highlighted in blue, linking group highlighted in red (part of the imidazole ring of HC-030031 has been included), the second ring has been highlighted in green.

Compound	Linking group length	IC50, uM
HC-030031	5 atoms	4
Ojk0703	5 atoms	23
Ojk0107	3 atoms	81
Ojk0105	2 atoms	Inhibition not observed

Table 22 Linking group length and IC50 values of compounds shown in Figure 37

HC-030031 is a potent specific TRPA1 antagonist, it has a similar structure to the ojk01, ojk06 and ojk07 compounds as in it contains two ring structures that are linked through an amide group(99). Figure 69 shows the structures of HC-030031, ojk0703, ojk0107 and ojk0105 and highlights three groups, the red group highlights the linking group. As can be seen in Figure 69 HC-030031 and ojk0703 have a 5 atom length linking group, ojk0107 has a 3 atom length linking group and ojk0105 has a 2 atom length linking group, the trend for the IC50 values for each of the compounds follows the linking group length with the longest linking group having the most potent inhibitory response. However, it appears that the site(s) of interaction on the TRPA1 protein that HC-030031, ojk0703, ojk0107 interact with seem to favour longer compounds, this trend is backed up in part by Liu *et al.* (142)*.* with what they reported for NPPB, NPEB and NPB.

ojk0105
No modulation of TRPA1 observed

ojk0103
No modulation of TRPA1 observed

ojk0109
Partial agonist of TRPA1 and inhibited TRPA1

ojk0111
Full agonist of TRPA1 and inhibited TRPA1
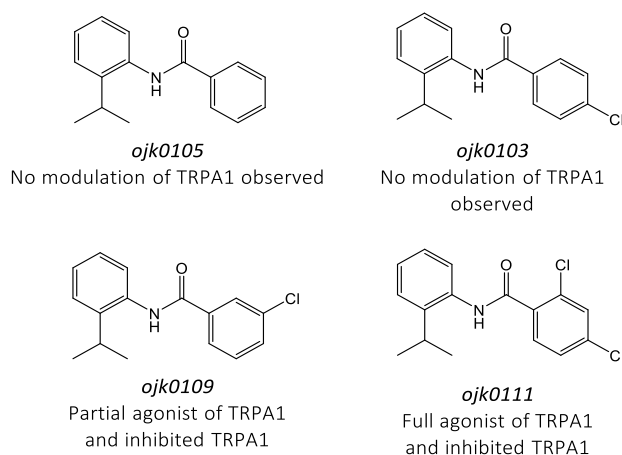
Figure 70 Chemical structures and modulation of TRPA1 of ojk01 chloro derivatives and ojk0105
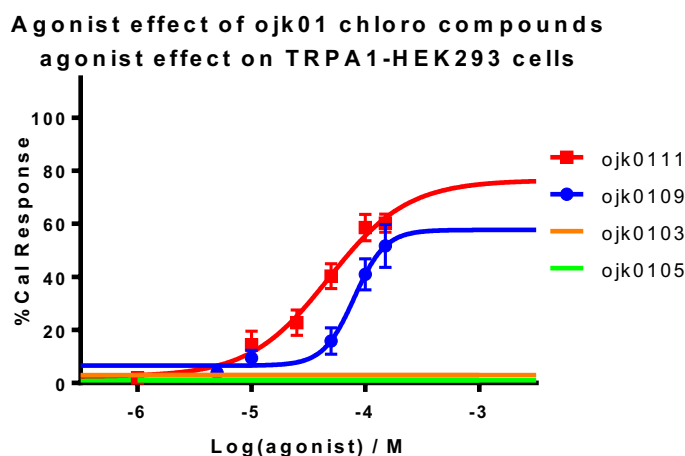
Figure 71 Comparison of concentration effect curves for ojk0103, ojk0105, ojk0107and ojk0109 on TRPA1-HEK293 cells. Data points are means±SEM of N = 3 experiments

124

The next trend observed in the assay results from the ojk01 library is the effect of chlorine groups on the second phenyl ring. From Figure 70, the structures for ojk0105, ojk0103, ojk0109 and ojk0111 can be seen as well as a general description of their respective interactions with TRPA1 that have been described in full in results section 3.2.2. Ojk0105 shows no interaction with TRPA1 neither does ojk0103 which has a p-chloro group. Interestingly ojk0109, which has an m-chloro group interacts with TRPA1 with activation and inhibition being observed. Finally, ojk0111, which has a 2,4-dichlorophenyl structure interacts with TRPA1 as a full agonist and in an inhibitory capacity. Unfortunately, the o-chloro derivative was not synthesised and tested due to the availability of reagents and time restraints. The data suggests that the position of the chloro group on the second phenyl ring has a significant effect on the interaction with TRPA1. Therefore, it can be assumed that chloro group may be vital to the binding between TRPA1 and ojk0109/ojk0111 and that the para position places the chloro group just far enough away from the site of interaction for ojk0103 to have an effect on TRPA1. With regards to ojk0111, a question arises in the form of does the p-chloro group contribute to the response observed? So is the p-chloro group synergising with the o-chloro group to produce a potent response or is the o-chloro group solely responsible for the response? The answers to these questions can only be postulated without knowing the response of the ortho monochloride analogue, which as previously mentioned has not been tested due to time restraints. From the results of this series of compounds, it can be determined that the ortho and meta positions are key for the binding of the chloro derivatives in the ojk01 compound library.

Also, it must be noted the importance of the linking amide group over the ester group as all of the ester derivatives of the compounds shown in Figure 63 showed no response in the calcium signalling assays. This revelation reveals a potential mechanism through which the active ojk01 compounds interact with TRPA1. An amide bond is capable of forming H-bonds whereas an ester group cannot; it may be that the H-bonding of the amide bond is crucial to the modulation of TRPA1 and that the two phenyl rings anchor the amide bond in place for binding. It may be the case that the substitutions on the second methyl ring have an electronic effect on the amide bond allowing greater binding with TRPA1. Using this theory, the responses observed for the chloro derivatives can be made sense of with

regards to the closeness of the chloro group to the amide group, for example, the p-chloro derivative shows no response, and this is due to the distance of the chloro group from the amide bond, and therefore the electronic effect on the amide group from the chloro group is relatively weak. Next is ojk0109 where the chloro group is a bit closer to the amide group and therefore its electronic effect on the amide group is slightly greater than in ojk0103 which is reflected in a greater response being observed. Finally, is ojk0111 which has a chloro group as close as is possible to the amide group in the ortho position which can have the greatest electronic effect on the amide group which is reflected in ojk0111 having the most potent response of the series.

The ojk01 compounds have shown a range of activity towards TRPA1 and when screened against TRPM8 showed no activity. Compounds similar in structure have been synthesised and assayed against TRPA1 and TRPM8 by Ortar *et al.* (132). The reported results show some similarities as well as some key differences to the results reported in section 3.2.2, the following section will discuss the two sets of results with regards to key similarities and key differences.

The first key difference is that Ortar *et al.*(178) tested against the rat variant of TRPA1, TRPM8 and TRPV3 whereas I tested against the human variant of TRPA1 and TRPM8. TRPA1 is remarkable in the sense that its most distinctive feature i.e. activation by covalent modification by reactive electrophiles, is highly conserved throughout ~500 million years of animal evolution yet other functions and interactions of TRPA1 differentiate between species drastically(57). The differences of TRPA1 between species has been somewhat of a stumbling block in terms of drug development as rodent studies, which the pharmaceutical industry relies heavily upon are not suitable as it has been reported in several studies and reviewed by Chen and Kym (179), that TRPA1 species differences even in species which are deemed to be fairly similar, e.g. rats and humans, show very different functionalities. Menthol has been shown to be an activator of mouse TRPA1 at low concentrations, and a blocker at high concentrations, whereas in human TRPA1 menthol only acts as an activator and in non-mammalian TRPA1 menthol has no effect at all(55). Caffeine is another example as it has been reported to activate mouse TRPA1 yet inhibit activation in human TRPA1(136). The potent and selective human TRPA1 inhibitor A967079 (A96) also displays differences in activity between species as reported by Nakatsuka *et al*. (180) in which they

detailed how A96 was a human TRPA1 antagonist yet showed no effect on western clawed frog TRPA1. In this study, they utilised this difference to identify two amino acid residues which were crucial to A96's inhibitory action. These were serine-873 and threonine-874 in human TRPA1 which when mutated to reflect western clawed frog TRPA1, A96 showed no inhibitory effect. As can be seen, the interactions between TRPA1 and agonists and inhibitors vary dependent on the species of TRPA1 but in Nakatsuka *et al.*'s case, it has been shown that examining species differentiation can reveal a great deal. So with this in mind there is one key difference between the results reported in section 3.2.2 and Ortar *et al.* results this is that the ojk01 ester compounds tested showed no modulation of human TRPA1 and certain amides displayed both activation and inhibition of human TRPA1. Whereas, Ortar *et al.* reported that the ester compounds in their library were more potent agonists and inhibitors than their amide counterparts in rat TRPA1. As previously mentioned the amide linking group of the ojk01 compounds may be vital to the binding to TRPA1 due to its ability to H-bond. Whereas, the ojk01 ester derivatives displayed no activity in human TRPA1 assays. Therefore, comparing my results with Ortar *et al.* suggests the binding site in human TRPA1 may contain amino acid residues capable of hydrogen bonding but in rat TRPA1 the amino acid residue binds better with an ester functional group. Another point to note with regards to the comparison of results is that Ortar *et al.* (132) reported that thymol in their system was a weak rat TRPA1 activator with an EC50 = ~287 µM, which in comparison to other literature values reported ranging from 6 to 127 µM(130) and my value of 58 µM this could be due to species differences in TRPA1 but may also highlight issues with regards to Ortar *et al*'s(132) methods or the cell line that has been used for their assay.

Another difference in between Ortar *et al.* and the results shown in section 3.2.2 is that the series of compounds synthesised by Ortar *et al.* all have a p-cymene base structure whereas the ojk01 compounds series all have a 2-isopropylphenyl base structure. The addition of the extra methyl para to the isopropyl group in the first ring may aid in the binding to TRPA1 and is potentially a reason why many of the ojk01 compounds showed no interaction with TRPA1. On the other hand, the heightened interaction with TRPA1 due to the extra methyl may be due to an increase in lipophilicity allowing it to penetrate the

plasma membrane and therefore increasing the intracellular concentration of the assay compound.

Increasing linking group length
Increasing potency of response

5b	5d	5f
TRPA1 efficacy 59.3%	TRPA1 efficacy 212.3%	TRPA1 efficacy 93.4%
TRPA1 EC50 11.3uM	TRPA1 EC50 6.5uM	TRPA1 EC50 0.8uM
TRPA1 IC50 17.9uM	TRPA1 IC50 3.9uM	TRPA1 IC50 1.4uM
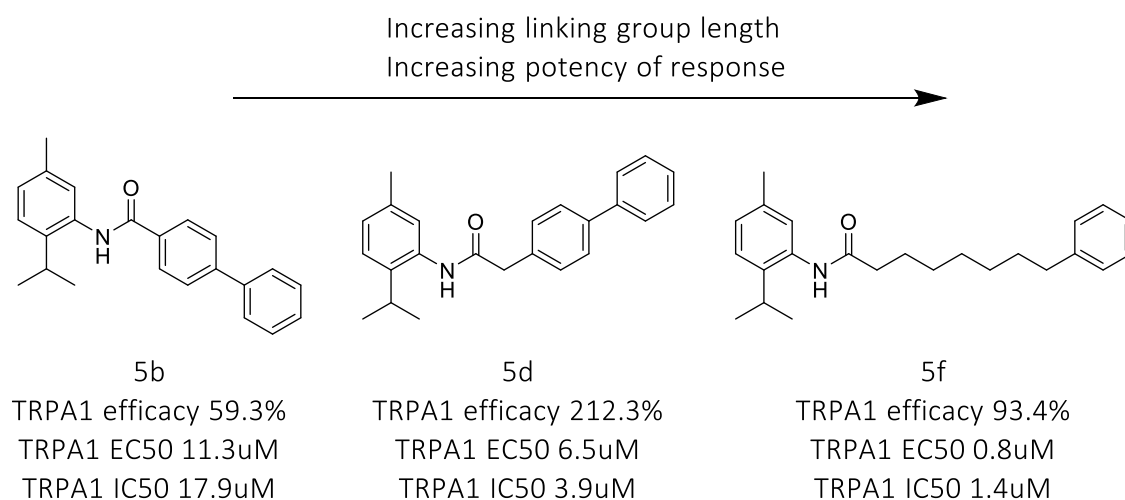
Figure 72 TRPA1 active compounds from Ortar *et al.* 2012(132) ordered from left to right increasing in linking group length. Efficacy calculated as percent of AITC (100 µM), IC50 against effect of AITC (100 µM)

The amide derivatives which Ortar *et al.* assayed showed a similar trend to what has been reported in this section. An increase in chain length between phenyl rings shows an increase in the potency of response observed. Ortar *et al.* reported assay results for three compounds (shown in Figure 72) the potency of the agonist and inhibitory response can be seen to increase with increasing chain length between the p-cymene ring and second phenyl ring. This trend comes with some considerations. Firstly, the extra phenyl group for 5b and 5d must be taken into account. Secondly, 5f has a seven carbon long chain between the amide group and the phenyl ring which is a massive increase in the chain length compared to the ojk01, ojk0703, 5b and 5d. Therefore, the results of Ortar *et al*., the NPPB assay results by Liu *et al*. (142)and the results reported in this chapter all suggest that an increasing chain length between two phenyl rings results in an increasing potency of interaction with TRPA1.

3.3.3 Thymol and carvacrol acetamide linked derivatives (ojk06 and ojk07)

The results reported in section 3.2.3 with regards to the synthesis and calcium signalling assay results shall be discussed in detail in the following sections.

3.3.3.1 Synthesis of ojk06 and ojk07 derivatives results discussion
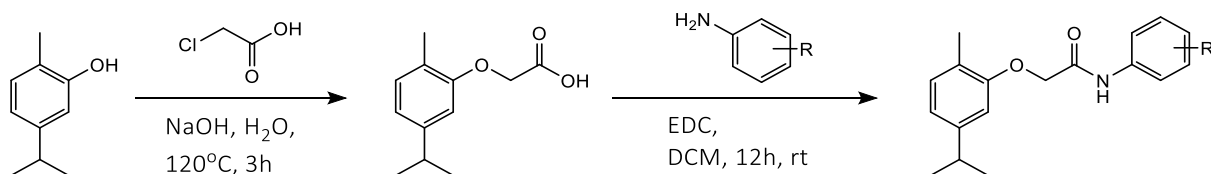
Figure 73 Reaction scheme for the synthesis of ojk06 and ojk07 compounds

The ojk06 and ojk07 acetamide compounds were prepared in a two-step reaction, summarised above in Figure 73. The first step was an S_N2 type reaction in which the alkylated phenol (carvacrol for ojk06 and thymol for ojk07) was coupled to chloroacetic acid to form the phenoxyacetic acid intermediate. The intermediate was then purified using a standard aqueous workup which produced an off-white powder. The intermediate was then coupled to the aniline derivative of choice using the carbodiimide crosslinker ethyl-(N',N'-dimethylamino)propylcarbodiimide hydrochloride (EDC). As can be seen in Figure 74 EDC reacts with the carboxylic acid group to form an active O-acylisourea intermediate that is displaced by a nucleophilic attack from the amine group. The aniline derivative and the phenoxyacetic acid intermediate form an amide bond and an EDC by-product is released as a water soluble urea derivative.

The method used to synthesise the ojk06 and ojk07 compounds was a suitable method which produced pure products at decent yields. There was no effect on the synthesis results due to the different phenol starting materials or due to the different aniline derivatives used in step 2. The only real difficulty with this method was in removing the thymol and carvacrol starting materials in step 1 which was overcome by repeating the extraction process. The carbodiimide crosslinker reaction proved to be a successful method and allowed for an easy purification.
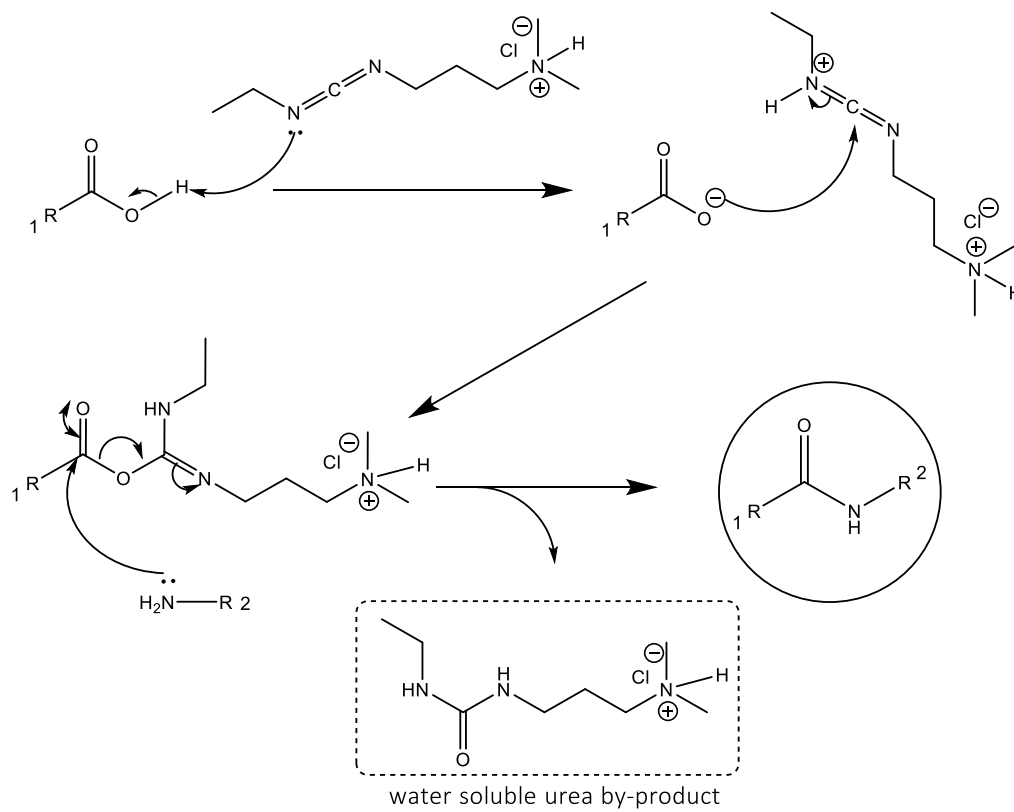
Figure 74 Carbodiimide crosslinking reaction mechanism

3.3.3.2 Calcium signalling results discussion
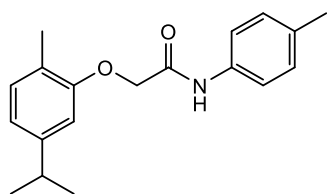
ojk0601
Efficacy = 99.2%
EC50 = 15.5uM
IC50 = 12.2uM
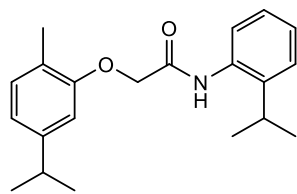
ojk0606
Efficacy = 61.5%
EC50 = 34.8uM
IC50 = 6.5uM
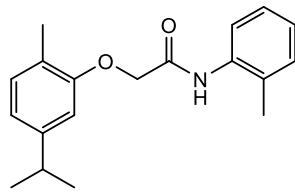
ojk0607
Efficacy = 72.0%
EC50 = 28.6uM
IC50 = 37.3uM*
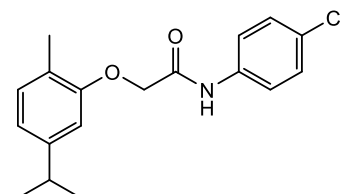
ojk0608
Efficacy = 78.8%
EC50 = 32.3uM
IC50 = 4.7uM
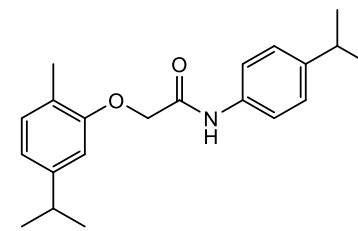
ojk0609
Efficacy = 42.2%
EC50 = 35.5uM
IC50 = 4.5uM
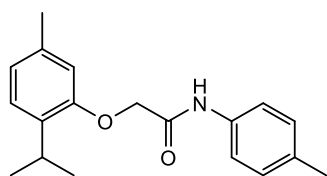
ojk0703
Efficacy = 94.8%
EC50 = 6.1uM
IC50 = 23.4uM
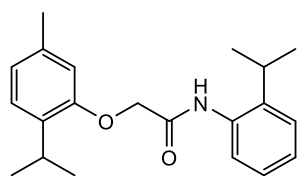
ojk0705
Efficacy = 96.4%
EC50 = 26.7uM
IC50 = 15.7uM
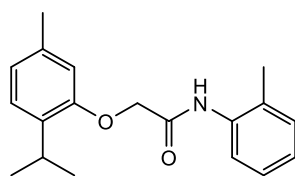
ojk0706
Efficacy = 102.7%
EC50 = 17.5uM
IC50 = 20.9uM
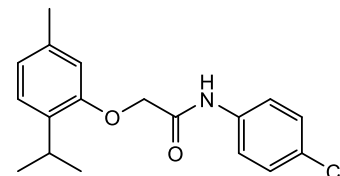
ojk0707
Efficacy = 95.6%
EC50 = 32.4uM
IC50 = 6.3uM
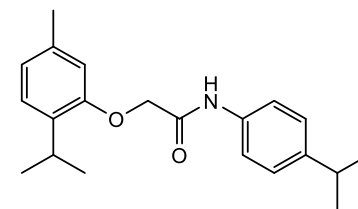
ojk0708
Efficacy = 69.8%
EC50 = 32.3uM
IC50 = 10.8uM

*This assumes full inhibition
All results are from calcium signaling assays using TRPA1 transfected HEK293 cells
Efficacy calculated as a percentage of the maximum response of cinnamaldehyde

Figure 75 Chemical structures, TRPA1 efficacies, EC50 and IC50 values of ojk06 and ojk07 compounds.

In Figure 75, the structures and results from the calcium signalling assays can be seen for both the ojk06 and ojk07 compound libraries. Each of the compounds from these libraries gave a significant response in each of the agonist and antagonist assays against TRPA1-HEK293 cells all the responses observed had a greater potency than for their parent compound; for ojk06 this is carvacrol and for ojk07 this is thymol. The efficacy of activation, however, is a different story for the ojk06 library as only ojk0601 (efficacy 99.2 %) had a greater efficacy than the carvacrol (efficacy 90 %) parent compound. The ojk07 library only ojk0708 (efficacy 70 %) had an efficacy lower than the thymol (efficacy 91%) parent compound. As mentioned in section 3.3.2, the responses observed for all the ojk06 and ojk07 compounds are assumed to be via direct interaction with the TRPA1 protein. The following sections, section 3.3.3.3 through to section 3.3.3.5 will go on to discuss the trends observed with regards to structure and theorise how these compounds bind with TRPA1 to produce both the activation responses and inhibitor responses observed. Firstly, the trends observed within each library shall be discussed. Then a comparison of the ojk06 and ojk07 libraries shall be carried out and the effect of the position of the linking group will be discussed in detail.

3.3.3.3   Ojk06 discussion

The ojk06 library comprises 5 compounds based on carvacrol which has been linked via the phenol group to another phenyl group, with the linking group taking the form of an acetamide functional group. The 5 derivatives differ due to the substituents on the second phenyl ring see Figure 76 for the general structure of the ojk06 compounds. This section compares the results obtained for the ojk06 library.
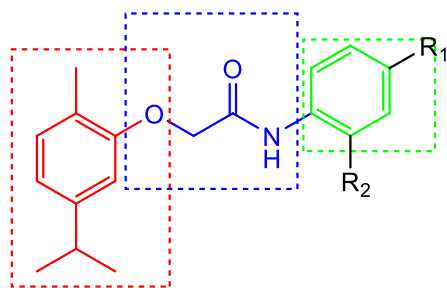
General structure of ojk06
red = carvacrol moeity
blue = acetamide linking group
green = second phenyl ring

Figure 76 General structure of ojk06 compounds

3.3.3.3.1   Ojk06 ortho position comparison

Two of the compounds assayed have substituents in the ortho position. One has an o-methyl group, ojk0607, and the other has an o-isopropyl group, ojk0606. Comparison graphs for concentration effect curves from both the agonist and antagonist calcium signalling assays can be seen in Figure 77. As can be seen, the methyl derivative, ojk0607, shows greater efficacy (72% compared to the 62 % reported for ojk0606). The greater agonist response for ojk0606 with regards to efficacy is reflected by the potency as the methyl derivative, ojk0607, is more potent with an EC50 = 29 μM compared to the isopropyl derivative which has an EC50 = 35 μM. The activation of TRPA1 by these two compounds is fairly similar with not much difference in efficacy and potency however it is clear that ojk0607, the o-methyl derivative, is a better agonist. From this, it can be said that the isopropyl group due to its greater steric effect slightly blocks the binding mechanism. The results from the agonist assay of ojk0606 and ojk0607 may lead to the thinking that the effect of an alkyl substituent in the ortho position of the second ring does not have a great effect on the activation of TRPA1 by the generic ojk06 structure.
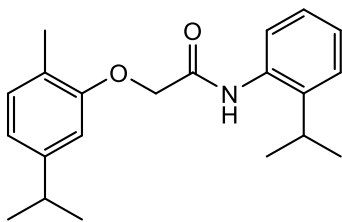
ojk0606
Efficacy = 61.5%
EC50 = 34.8uM
IC50 = 6.5uM
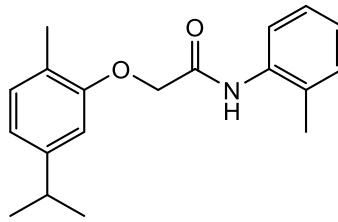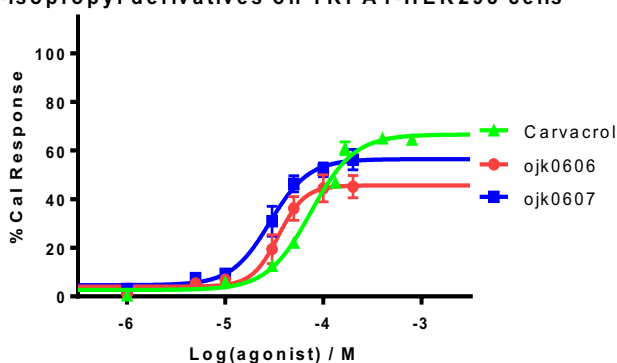
ojk0607
Efficacy = 72.0%
EC50 = 28.6uM
IC50 = 37.3uM*
*Value assumes full inhibition
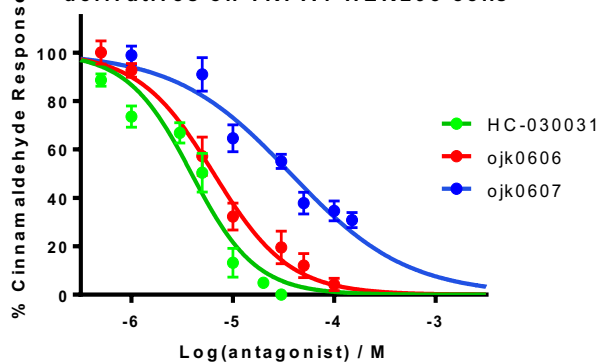
Figure 77 Above: Comparison of assay results for ojk0606 and ojk0607. Below: Comparison of concentration effect curves for ojk0606 and ojk0607 on TRPA1-HEK293 cells. Data points are means±SEM of N = 3 experiments

The results from the antagonist assay tells a slightly different story as from the comparison graph and the IC50 values that are shown in Figure 77 it can be seen that the o-isopropyl derivative, ojk0606 is a much more potent inhibitor of TRPA1 with an IC50 = 7 μM compared to the o-methyl derivative, ojk0607, which has an IC50 = 37 μM. It must also be noted that ojk0607 is the weakest inhibitor of the ojk06 and ojk07 compounds.

To conclude this comparison, the o-methyl derivative is a more potent and efficacious TRPA1 agonist, yet the o-isopropyl derivative is the more potent TRPA1 inhibitor. The difference between the activation profiles shows that there is not much difference between the two derivatives which highlights that the alkyl groups in the ortho position of the second phenyl ring do not have a great effect on the activation. On the other hand, the difference between the inhibitory profiles shows that alkyl substituents in the ortho position of the second phenyl ring have a drastic effect on TRPA1 inhibition. This possibly indicates to the activation and inhibition by these compounds occurring at different sites along the TRPA1 protein.

3.3.3.3.2 Ojk06 alkyl para comparison

ojk0601
Efficacy = 99.2%
EC50 = 15.5uM
IC50 = 12.2uM

ojk0609
Efficacy = 42.2%
EC50 = 35.5uM
IC50 = 4.5uM

Figure 78 Above: Comparison of assay results of ojk0601 and ojk0609. Below: Comparison of concentration effect curves for ojk0601 and ojk0609 on TRPA1-HEK293 cells. Data points are means±SEM of N = 3 experiments

Ojk0601 and ojk0609 both have alkyl substituents in the para position of the second phenyl ring, ojk0601 has a methyl group, and ojk0609 has an isopropyl group, structures can be seen Figure 78. The comparison graphs for both their agonist and antagonist concentration effect curve can be seen in Figure 78. It can be seen that similarly to the comparison of ojk0606 and ojk0607 the methyl derivative, ojk0601, is a more potent and efficacious

agonist of TRPA1 than the isopropyl derivative, ojk0609. Whereas, the isopropyl derivative, ojk0609, is a more potent inhibitor than the methyl derivative, ojk0601. This trend could be put down to the differences in lipophilicity with the activation site of TRPA1 favouring the less lipophilic methyl derivatives and the inhibition site of TRPA1 favouring the more lipophilic isopropyl derivatives. Alternatively, this could be due to steric factors and that a larger, bulkier group is more beneficial binding to the inhibitor site and vice versa for the activation site of TRPA1. With this comparison, it can be seen that the difference in agonist profiles are greater than that of the ortho derivatives in section 3.3.3.3.1, yet the difference in the inhibitor profiles of the para derivatives are lesser than that of the ortho derivatives. This leads to the idea that alkyl derivatives in the para position have more of an effect on how the compounds activate TRPA1 than in the ortho derivatives and that alkyl derivatives in the ortho position have a greater effect on how the compounds inhibit TRPA1 than in the para position.

3.3.3.3.3   Ojk06 chloro derivative
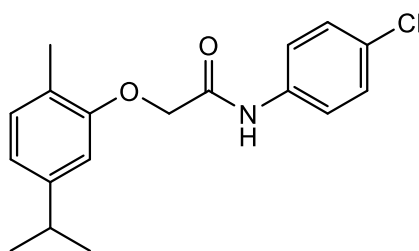
ojk0608
Efficacy = 78.8%
EC50 = 32.3uM
IC50 = 4.7uM

Figure 79 Assay results for ojk0608

One of the compounds in the ojk06 library has a p-chloro group on the second phenyl group, the structure of this compound, ojk0608 can be seen in Figure 79. When compared to the other two other ojk06 compounds with groups in the para position an assessment of the effectiveness of the chloro group can be made with regards to activation and inhibition of TRPA1, comparison graphs for both the agonist and antagonist concentration effect curves can be seen in Figure 80. As can be seen from Figure 80 the chloro derivative, ojk0608, fits right in the middle with regards to efficacy and potency of its agonist response when compared to the other ojk06 para derivatives. In the antagonist assay, the potency

of inhibition was only slightly less than that for the p-isopropyl derivative, ojk0609. The chloro group in terms of size is only slightly bigger than the methyl group and if there is any steric hindrance from the group in the para position as suggested in section 3.3.3.3.2 then the agonist response for the chloro derivative, ojk0608 would be slightly less than that observed for ojk0601, which is exactly what has been observed however this trend cannot be truly confirmed without testing derivatives with much more varying sizes of groups in the para position.

Figure 80 Comparison of concentration effect curves for ojk0601, ojk0608 and ojk0609 on TRPA1-HEK293 cells. Data points are means±SEM of N = 3 experiments

This assessment does not take into account the electronic effects of the chloro group which has an inductive electron withdrawing effect whereas the methyl and isopropyl groups have an inductive electron donating effect. If the electronic effects of the substituent groups had a substantial effect on the activation of TRPA1 and steric effects had a very little effect then ojk0608, chloro derivative, would either be the greatest agonist or the weakest

138

agonist of TRPA1 out of the three dependent on the how they interact. However, this is not the case, and ojk0608's agonist response fits somewhere between the small methyl group and the larger isopropyl group. Also, as previously mentioned in section 3.3.3.3, the lipophilicity of the compounds may affect the activation of TRPA1 as was discussed by Lee *et al.*(130) with regards to the activation of TRPA1 by alkylated phenols. This seems not to be the case with regards to the para derivatives of ojk06 as the chloro derivative which is a lot less lipophilic than both the methyl and the isopropyl derivatives and is more potent than the isopropyl and less potent than the methyl.

Dismissing the electronic effects and the lipophilicity of these compounds in order to place confidence in the hypothesis that the greater the steric effects of the para substituent the lower the activation of TRPA1 will be. This disregards any synergy between the properties of ojk0608 which, place it just behind ojk0601 in terms of activation efficacy and potency of TRPA1. Without further testing of different derivatives which disprove or confirm this hypothesis no conclusion can be drawn.

The results of the antagonist assay, however, pose a slightly different question in that they do not conform to the steric effect trend discussed above which as previously suggested in section 3.3.3.3.2. This may be due to the compounds interacting with a different site in order to inhibit TRPA1. This different site may be more receptive to the inductive electron withdrawing effects of the chloro derivative as it is almost as potent as ojk0609 with regards to its antagonist effect. Alternatively, it may be that ojk0608 inhibits by an alternative site altogether, for example, A96 and AP-18 have been shown to inhibit TRPA1 via the TM5 menthol activation site(180), the same activation site as carvacrol and thymol which ojk06 and ojk07 compounds are based on. The structure of these antagonists can be seen in Figure 81(181). As can be seen from the structures of A96 and AP-18 they both contain an aryl halide moiety similar to that of ojk0608. HC-030031 does not inhibit via interaction the TM5 menthol site as reported by Xiao *et al.* (55), but may bind to the same site as caffeine in human TRPA1(137). This has so far not been reported, but it is reasonable to assume as HC-030031 is based on the caffeine structure. The ojk06 compounds may interact with the same site as caffeine and potentially HC-030031 given the similarities in structure and ojk0608 with its chloro group may inhibit at the same site and also be able to interact with TRPA1 via the same binding site as A96 and AP-18.
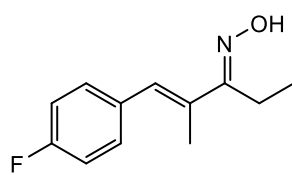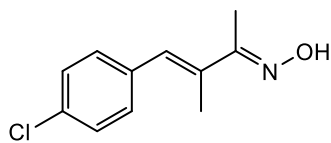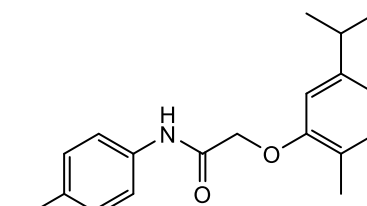
Figure 81 Comparison of ojk0608 with specific potent TRPA1 antagonists A96 and AP18(104,182)

3.3.3.3.4 Comparison of ojk06 methyl derivatives

So far the effects of different substituents in the same position on the second phenyl ring has been discussed, and similar trends have been observed between the ortho and para positions with the substituents in the para position proving to have a more drastic effect on the activation potential of TRPA1. In this section the differences between the same substituent group in different ring positions will be assessed firstly the methyl derivatives shall be compared followed by the isopropyl derivatives.
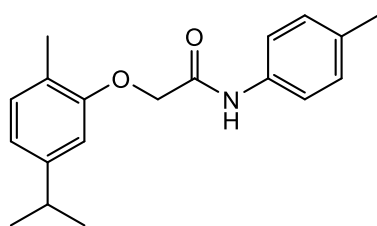
ojk0601

| Efficacy = 99.2% |
| EC50 = 15.5uM |
| IC50 = 12.2uM |
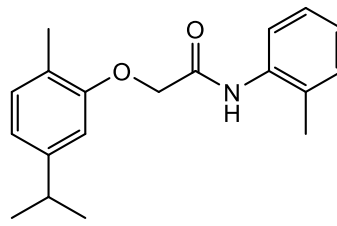
ojk0607

Efficacy = 72.0%

EC50 = 28.6uM

IC50 = 37.3uM*

*Value assumes full inhibition
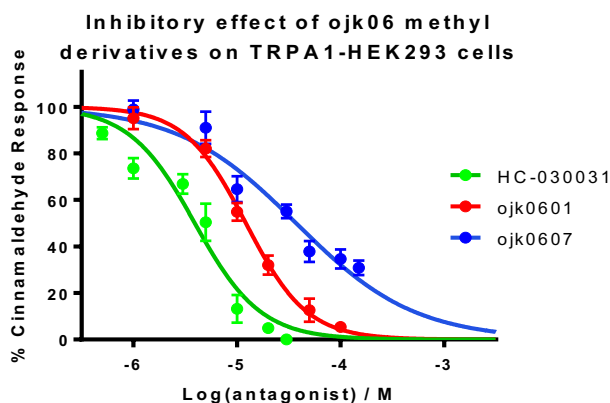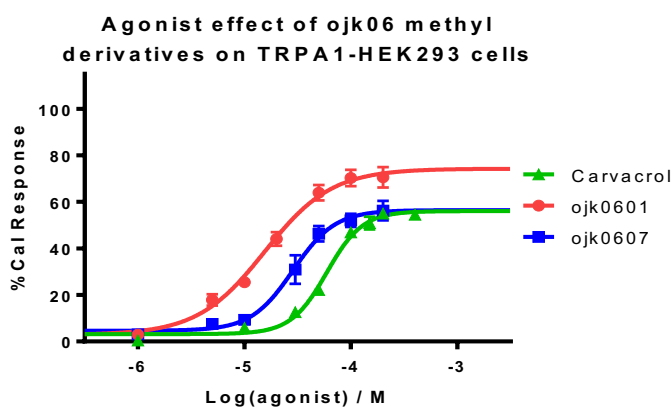
Figure 82 Above: Comparison of assay results of ojk0601 and ojk0607. Below: Comparison of concentration effect curves for ojk0601 and ojk0607 on TRPA1-HEK293 cells. Data points are means±SEM of N = 3 experiments

The two methyl derivatives ojk0601, p-methyl, and ojk0607, o-methyl, have been compared in Figure 82. From this comparison, it can be seen that the para derivative is a more potent and efficacious TRPA1 agonist and a more potent inhibitor than the ortho derivative. The effect of the position of the methyl group does not completely negate any of the modulation properties of the compound with regards to TRPA1 however it does affect the magnitude of modulation. It can only be postulated to the reason why this is the

141

case at the moment, it may be the case that the o-methyl group sterically hinders the hydrogen bonding of the amide group which is key to the binding of the compound or it may be that the p-methyl group is in a better position to bind to a key part if the binding site. With regards to electronic effects, both groups are inductive electron donating groups and any potential effect on the amide bond will be similar except that the o-methyl group will have a stronger effect due to the closer proximity.

3.3.3.3.5 Comparison of ojk06 isopropyl derivatives

ojk0606
Efficacy = 61.5%
EC50 = 34.8uM
IC50 = 6.5uM

ojk0609
Efficacy = 42.2%
EC50 = 35.5uM
IC50 = 4.5uM
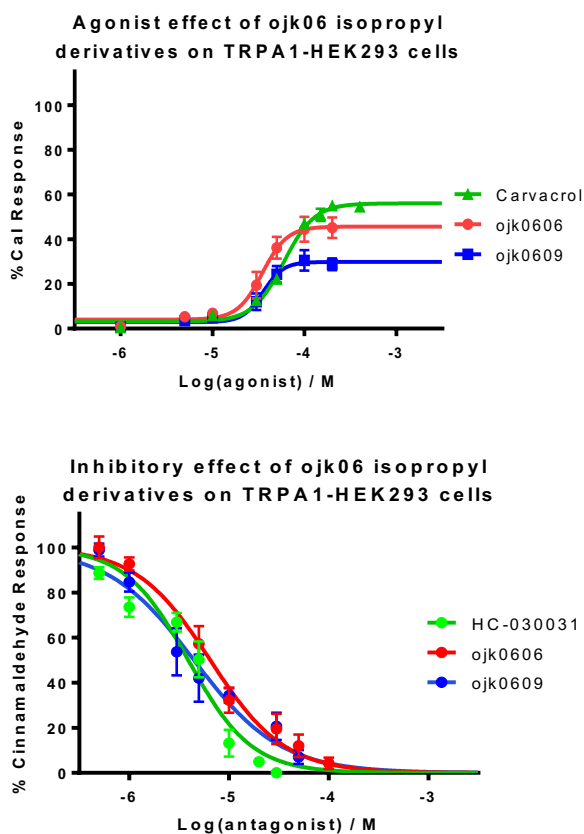
Figure 83 Above: Comparison of assay results of ojk0606 and ojk0609. Below: Comparison of concentration effect curves for ojk0606 and ojk0609 on TRPA1-HEK293 cells. Data points are means±SEM of N = 3 experiments

The results from ojk0606, o-isopropyl derivative, ojk0609, p-isopropyl derivative, are compared in Figure 83. Both compounds show very similar agonist and antagonist potencies and only differ significantly with regards to the efficacy of the agonist response with the ortho derivative having the greater efficacy. The differences of the methyl derivatives, discussed in section 3.3.3.3.4, show a more substantial differences in responses

143

which could be due steric and electronic effects based on ring position, if this is the case then the responses observed for the isopropyl derivatives would be much more pronounced as the steric and electronic effects would be greater, yet this is not the case. It must be stated that both ojk0606 and ojk0609 have the highest EC50 values and lowest efficacies of the ojk06 and ojk07 compounds, this could be due to the general bulkiness of the isopropyl group which is having a negative effect on the agonist response rather than ring position. With regards to the antagonist results it appears that the isopropyl group has an impact on the binding of the compound and that the para position allows for slightly greater binding, with ojk0609 being the most potent TRPA1 inhibitor out of the ojk06 and ojk07 compounds and is only slightly less potent than HC-030031 which in my system has a calculated IC50 of 4 µM. When the structures of the ojk06 isopropyl derivative are compared it can be seen that they share similarities to the HC-030031 structure see Figure 84. They both share the same isopropyl phenyl ring structure which is linked to another ring structure via an alkyl amide linking group. The difference between the ojk0609 and that of HC-030031 is the ring structure; ojk0609 has a 2-methyl-5-isopropyl phenyl ring and HC-030031 has a purine ring structure. The similarities between these two compounds may be the determining factor of the TRPA1 inhibition. This further backs up the possibility that the ojk06 compounds inhibit TRPA1 via the same binding site as HC-030031, potentially through the caffeine binding site reported by Nagatomo *et al.*(137).

HC-030031
IC50 = 4uM
Highlighted to signify the
core structural similarites to ojk0609

ojk0609
Efficacy = 42%
EC50 = 36uM
IC50 = 5uM
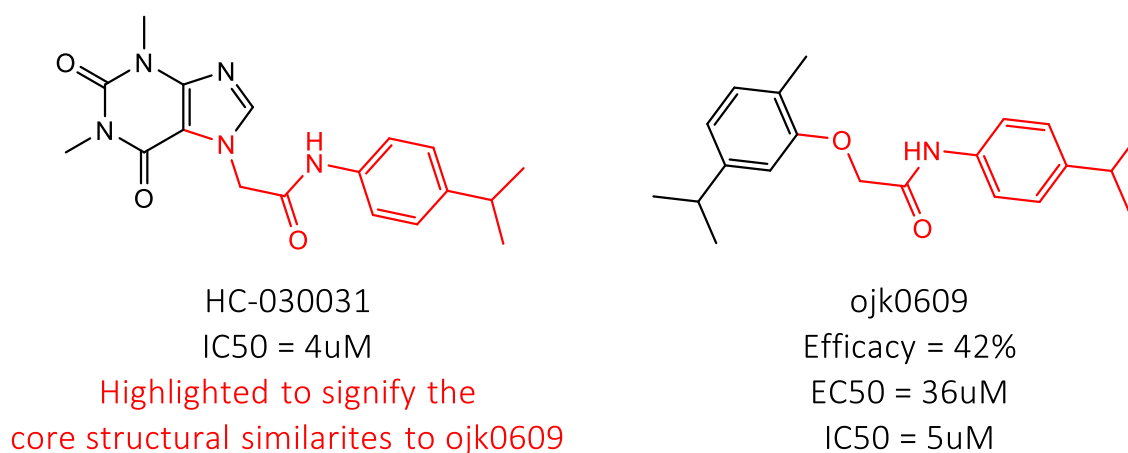
Figure 84 Chemical structure comparison of ojk0609 with TRPA1 antagonist HC-030031. The core structure of both compounds has been highlighted red.

3.3.3.4   Ojk07 discussion

The ojk07 library comprises 5 compounds based on thymol which has been linked via the phenol group to another phenyl group, with the linking group taking the form of an acetamide functional group. The 5 derivatives differ due to the substituents on the second phenyl ring see Figure 85 for the general structure of the ojk07 compounds. This section now compares the results obtained for the ojk07 library.
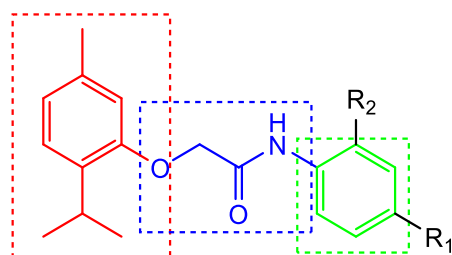
ojk0703 R_1 = Me, R_2 = H
ojk0705 R_1 = H, R_2 = i-Pr
ojk0706 R_1 = H, R_2 = Me
ojk0707 R_1 = Cl, R_2 = H
ojk0708 R_1 = i-Pr, R_2 = H

General structure of ojk07
red = thymol moeity
blue = acetamide linking group
green = second phenyl ring

Figure 85 General structure of ojk07 compounds

3.3.3.4.1 Ojk07 ortho comparison

ojk0705
Efficacy = 96.4%
EC50 = 26.7uM
IC50 = 15.7uM

ojk0706
Efficacy = 102.7%
EC50 = 17.5uM
IC50 = 20.9uM

Agonist effect of ojk07 o-methyl and o-isopropyl derivatives on TRPA1-HEK293 cells

Inhibitory effect of ojk07 o-methyl and o-isopropyl derivatives on TRPA1-HEK293 cells
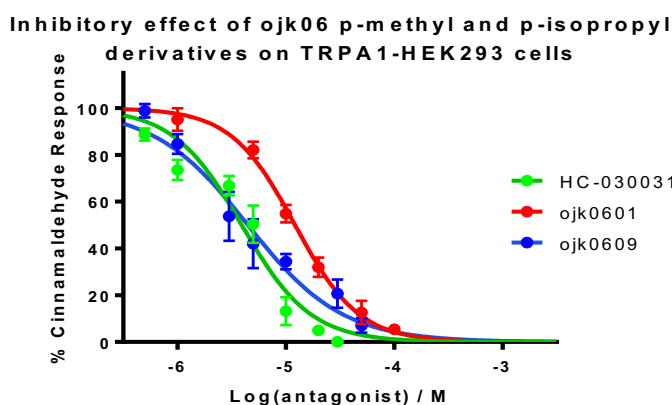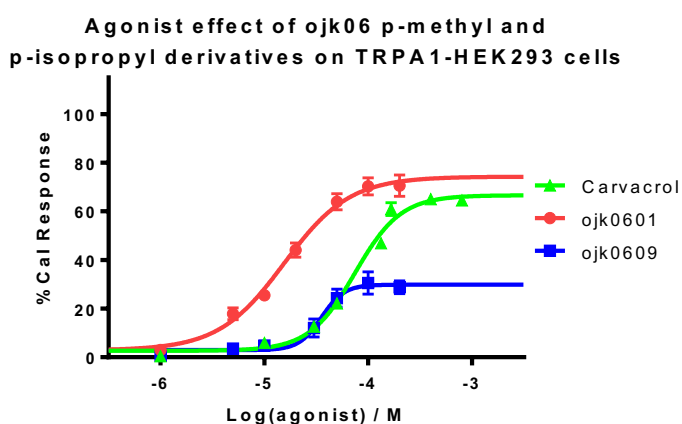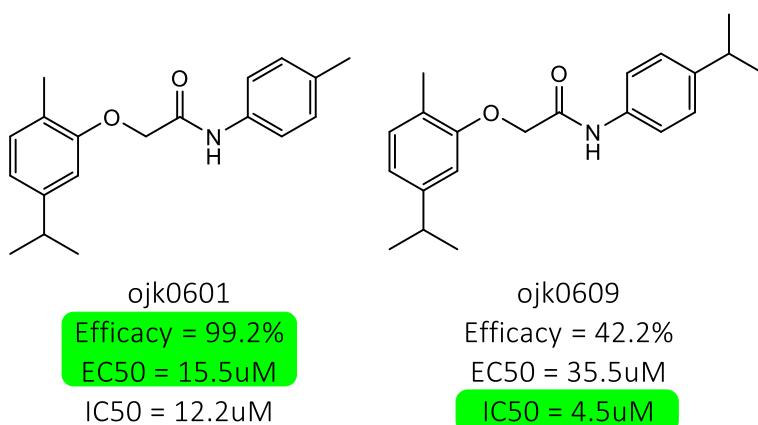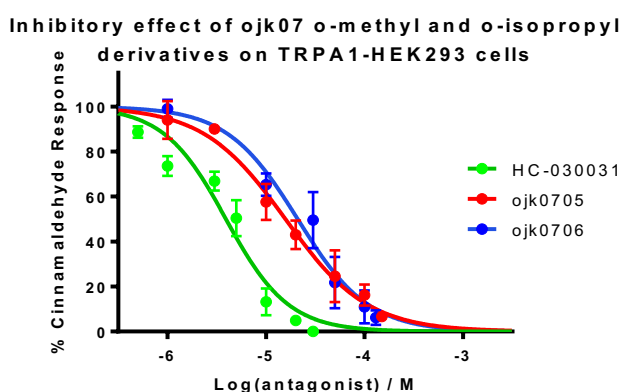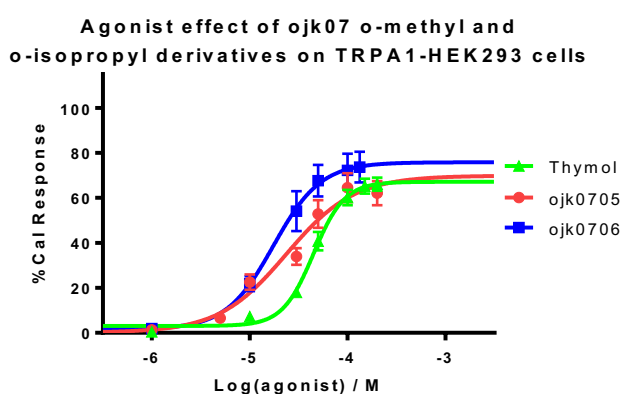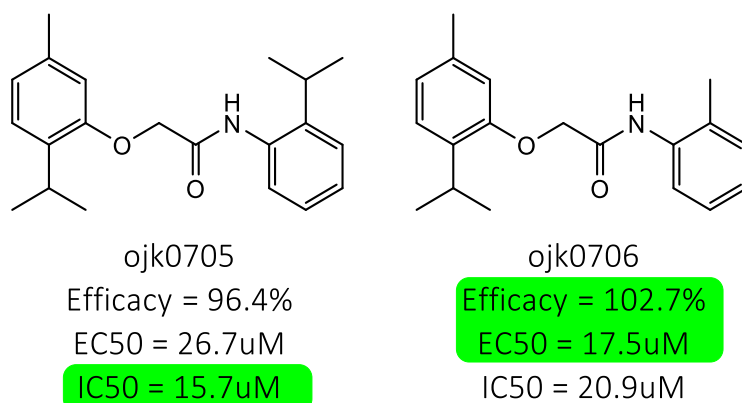
Figure 86 Above: Comparison of assay results of ojk0705 and ojk0706. Below: Comparison of concentration effect curves for ojk0705 and ojk0706 on TRPA1-HEK293 cells. Data points are means±SEM of N = 3 experiments

The comparison of the ojk07 ortho derivatives in Figure 86 shows a similar story to the comparison of the same ojk06 derivatives in that the o-methyl derivative, ojk0706, is the more potent TRPA1 agonist and the o-isopropyl derivative, ojk0705 is the more potent TRPA1 inhibitor. The efficacy of both compounds are very similar with the more potent agonist ojk0706, methyl derivative, being slightly greater. The difference in the agonist potency is greater than that observed for the ojk06 compounds and the difference in the

146

potency of inhibition is much lesser than that observed for the ojk06 compounds, this is possibly due to ojk07 compounds in general being more potent agonists and ojk06 compounds being the more potent inhibitors this will be discussed in greater detail in section 3.3.3.5. Overall the trend observed for the ojk06 compounds is observed for the ojk07 compounds with regards to the ortho ring position derivatives with slight differences which are most likely due to the orientation of the second ring based on the linking group.

3.3.3.4.2 Ojk07 para alkyl comparison
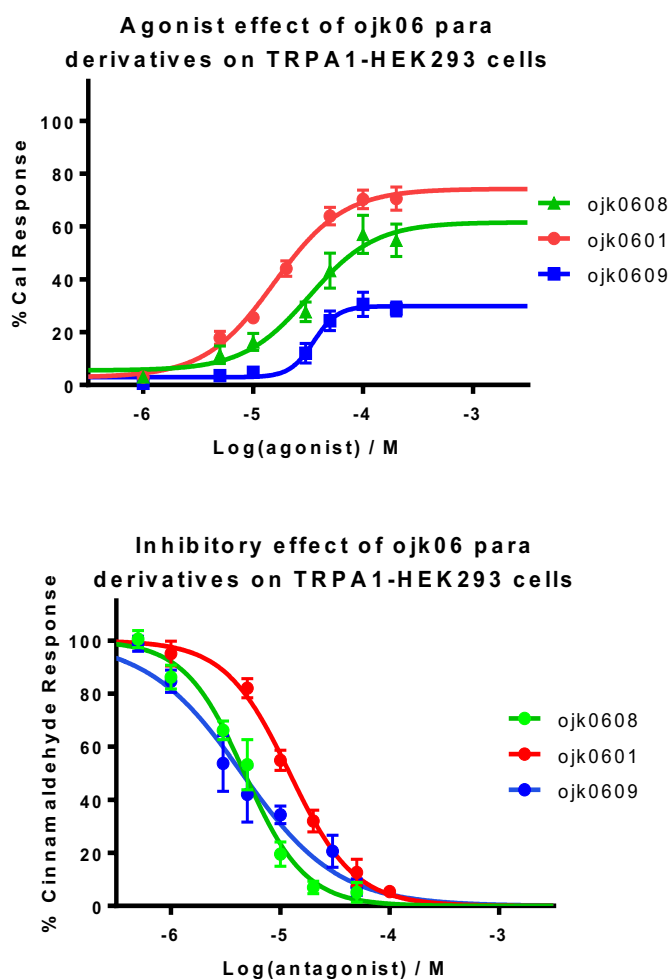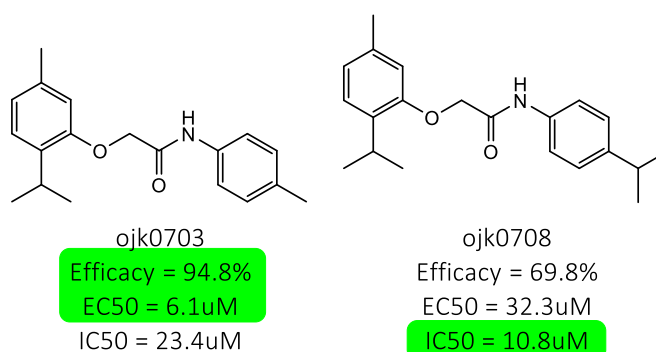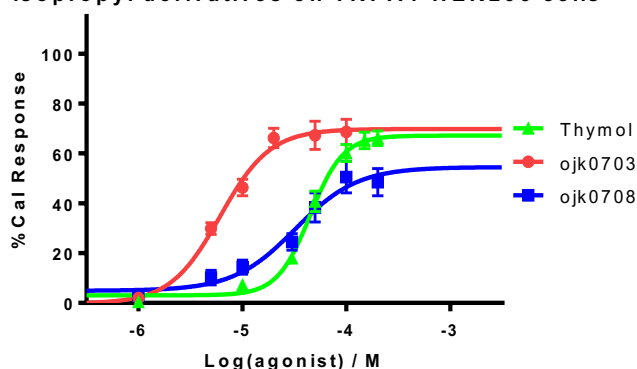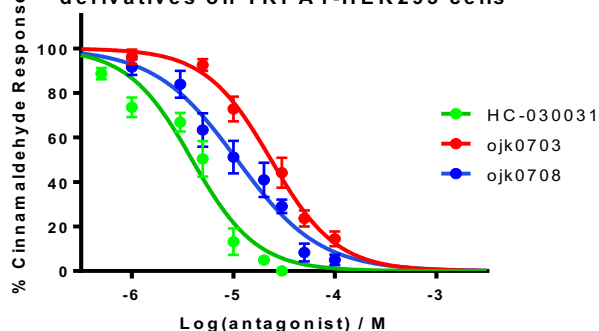

Figure 87 Above: Comparison of assay results of ojk0703 and ojk0708. Below: Comparison of concentration effect curves for ojk0703 and ojk0708 on TRPA1-HEK293 cells. Data points are means±SEM of N = 3 experiments

The comparison of the ojk07 alkyl para derivatives can be seen in Figure 87. The same trend appears for these compounds as shown for their ojk06 counterparts. The p-methyl derivative, ojk0703, is a more potent and efficacious TRPA1 agonist than the isopropyl derivative, ojk0708, and the isopropyl derivative is a more potent TRPA1 inhibitor. The potency of the p-isopropyl derivative, ojk0708, is a lot lower than the p-methyl, ojk0703, and is similar to that of its ojk06 counterpart ojk0609. This shows that the p-isopropyl group lowers the potency of these compounds by a substantial amount even in the more agonist favourable thymol configuration. The exact reason for this cannot be fully confirmed, but the most likely reason is due to the increased size of the isopropyl group over the methyl group.

With regards to the results from the antagonist assay, it can be seen that the p-isopropyl derivative, ojk0708, is a more potent inhibitor of TRPA1 than the p-methyl derivative, ojk0703. These results are in line with what was observed for the ortho derivatives of ojk07 i.e. the o-isopropyl derivative of ok07 was a more potent inhibitor of TRPA1 than the o-methyl derivative. Likewise, this also fits with the observations for the ojk06 compounds, see section 3.3.3.3. These results show that isopropyl group of the second phenyl ring has a beneficial effect on the inhibition of TRPA1 regardless of ring position. Also, the results show that the isopropyl group of the second phenyl ring has a negative effect on the agonist properties of both the ojk06 and ojk07 compounds with the group in the para position having the greatest effect.

3.3.3.4.3   Ojk07 p-chloro comparison
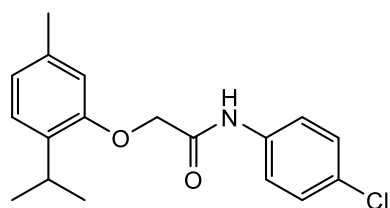
ojk0707
Efficacy = 95.6%
EC50 = 32.4uM
IC50 = 6.3uM

Figure 88 Assay results for ojk0707.

148

The ojk07 p-chloro derivative, ojk0707, is fairly similar in its potency of activation of TRPA1 to ojk0708, the p-isopropyl derivative, but has a greater efficacy than ojk0703, p-methyl derivative. With regards to its full agonist profile of TRPA1, ojk0707 falls somewhere between ojk0703 and ojk0708 as can be seen by the concentration effect comparison graph in Figure 89. This shares some similarities to what was observed with the ojk06 compounds.
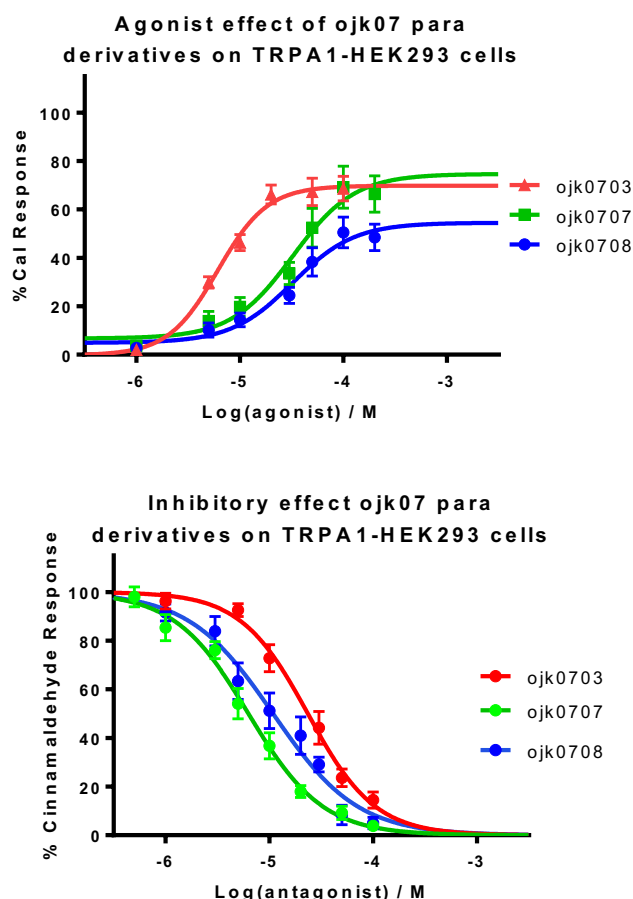
Figure 89 Comparison of concentration effect curves for ojk0703, ojk0707 and ojk0708 on TRPA1-HEK293 cells. Data points are means±SEM of N = 3 experiments

The antagonist assay results show that ojk0707 has the greatest potency of inhibition of TRPA1 out of all the ojk07 compounds. It was suggested in section 3.3.3.3.3 that the p-chloro derivative ojk0608 may inhibit TRPA1 via a different binding site due to its similarities to A96 and AP-18 and this may be the case for ojk0707. The difference in IC50 values between the ojk07 para derivatives does suggest that ojk0707 inhibits via a different binding site. The alternate binding site for the chloro derivatives will be discussed further in section 3.3.3.5. Alternatively, the differences may be due to the differences in the electronic effect of the substituent group as the methyl group has the lowest inductive

electron donating effect, the isopropyl has a greater inductive electron donating effect, and the chloro group has a strong inductive electron withdrawing effect. The strength and type of electronic effect may reflect the potency of the inhibition observed with a strong electron withdrawing group having the strongest inhibitory effect, this has been observed and discussed further in chapter 4.

3.3.3.4.4 Ojk07 methyl ring position comparison

ojk0703
Efficacy = 94.8%
EC50 = 6.1uM
IC50 = 23.4uM

ojk0706
Efficacy = 102.7%
EC50 = 17.5uM
IC50 = 20.9uM
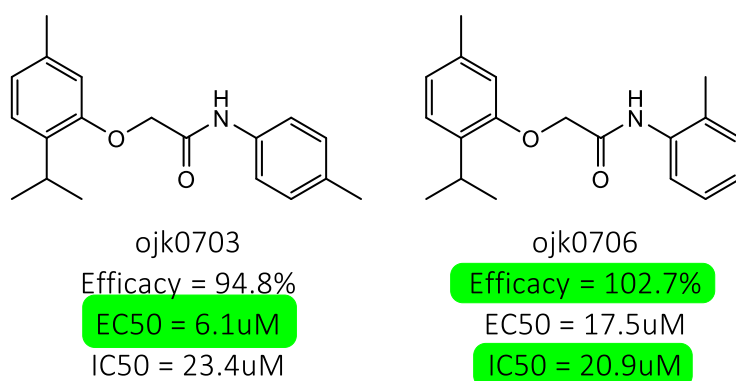
Figure 90 Comparison of assay results of ojk0703 and ojk0706.

When the results for ojk0703, p-methyl derivative, and ojk0706, o-methyl derivative, are compared there is not much difference in the two sets of results except for the EC50 values. Ojk0703 is a much more potent agonist than ojk0706 which shows that the position of the methyl group does have a significant effect on how the compound binds to the TRPA1 protein. This trend was also observed for the ojk06 compounds in section 3.3.3.3.4 although the responses of the ojk06 compounds were not as potent, a similar difference in EC50 values was apparent. The ojk0706 compound has a slightly more potent antagonist response. However, the IC50 values are fairly similar and taking into account the error in the results it can be determined that the position of the methyl group has no effect on the inhibitory mechanism. This was not the case for the ojk06 methyl derivatives were a significant difference in IC50 values was observed, this suggests that the orientation of the linking group affects the interactions of the second phenyl ring, therefore, the methyl groups for the ojk07 do not have an effect on the binding. The orientation of the linking group will be discussed further in section 3.3.3.5. The differences between the comparisons of the methyl derivatives from the ojk06 group and the ojk07 group also suggest that activation of TRPA1 and the inhibition of TRPA1 by these compounds occurs at different binding sites.

Agonist effect of ojk07 methyl derivatives on TRPA1-HEK293 cells

Inhibitory effect ojk07 methyl derivatives on TRPA1-HEK293 cells
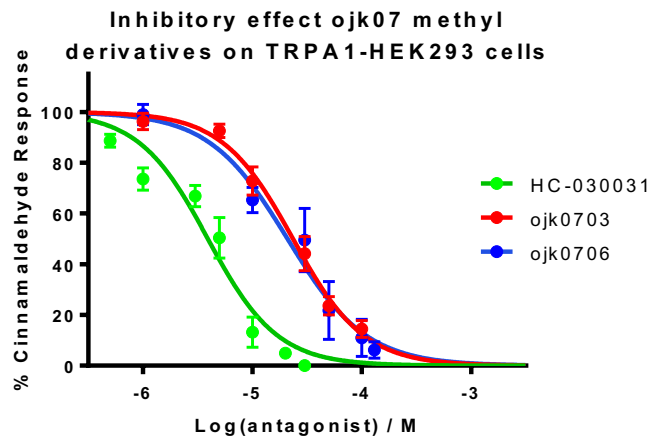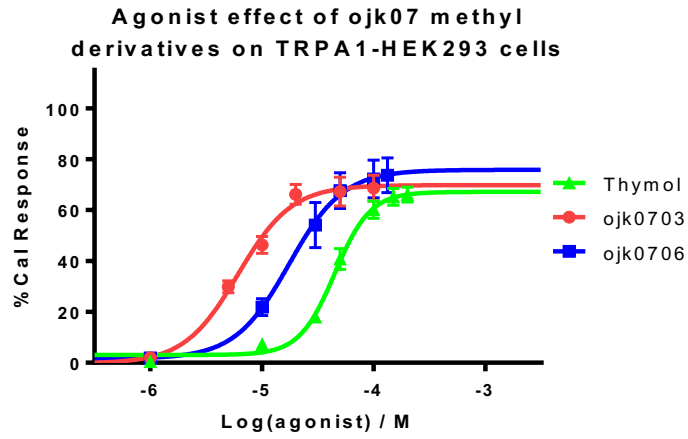
Figure 91 Comparison of concentration effect curves for ojk0703 and ojk0706 on TRPA1-HEK293 cells. Data points are means±SEM of N = 3 experiments

3.3.3.4.5 Ojk07 isopropyl ring position comparison

ojk0705
Efficacy = 96.4%
EC50 = 26.7uM
IC50 = 15.7uM

ojk0708
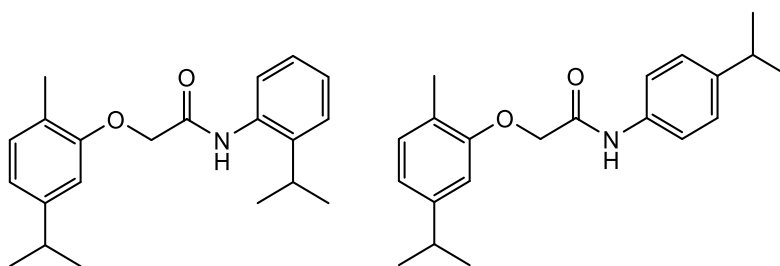Efficacy = 69.8%
EC50 = 32.3uM
IC50 = 10.8uM
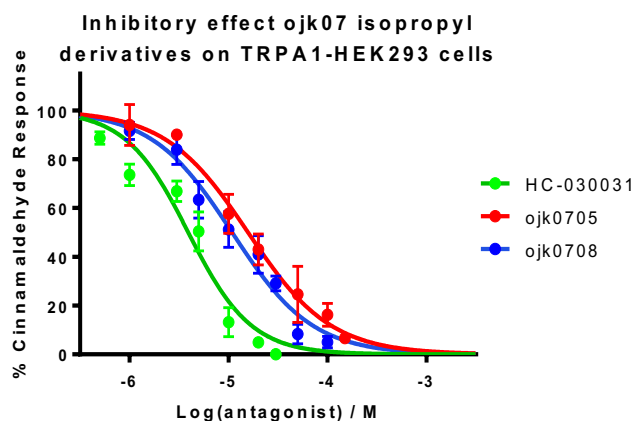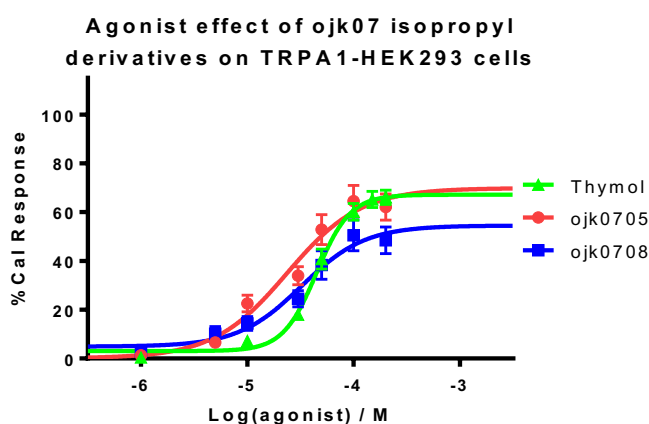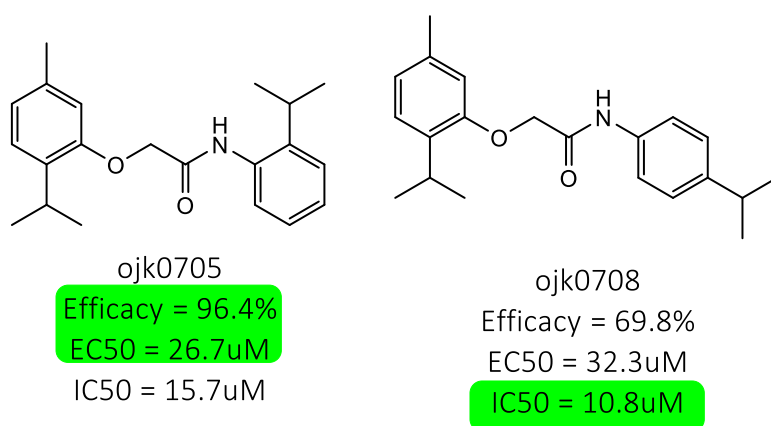
Figure 92 Above: Comparison of assay results of ojk0705 and ojk0708. Below: Comparison of concentration effect curves for ojk0705 and ojk0708 on TRPA1-HEK293 cells. Data points are means±SEM of N = 3 experiments

The isopropyl derivatives of the ojk07 group have been compared in Figure 92. The ortho derivative is a slightly more potent agonist and has a higher efficacy than the para derivative. However, the para derivative is a more potent inhibitor of TRPA1 than the ortho derivative. The differences in the responses of the two compounds show that the position

of the isopropyl group on the second phenyl ring has a slight effect on the way it interacts with the TRPA1 protein. Although the effect of the methyl group position produced a bigger difference in the potency of the agonist response, but there is a bigger difference in efficacy observed for the isopropyl derivatives. This suggests that the methyl group may be important to the binding of the compound, whereas the isopropyl group affects the affinity of the compound to the receptor site and therefore the efficacy of the compound. When comparing the differences of the isopropyl derivatives of the ojk07 group to the ojk06 group, similar trends were observed except the differences in responses for the ojk06 isopropyl derivatives were not as great.

3.3.3.5   Ojk06 vs. ojk07

In section 3.3.3.3 and section 3.3.3.4 the compounds of ojk06 and ojk07 groups were compared to each other. In this section, the two groups of compounds will be compared against one another, in order to determine the effect of the position of the linking acetamide group on the modulation of TRPA1. Comparison graphs for each of the derivatives can be seen in Figure 94. Generally, the ojk07 compounds, which are based on thymol, are greater agonists of TRPA1 than the ojk06 compounds, which are based on carvacrol, and that ojk06, are more potent inhibitors of TRPA1 than ojk07, thymol based. This follows the trend observed for the thymol and carvacrol assays carried out in chapter 5 which saw thymol being the greater agonist and carvacrol the greater inhibitor of TRPA1. These data suggest that the phenol or the ether group of thymol/carvacrol and ojk06/ojk07 respectively are important to influence how the compounds bind to the TRPA1 receptor. The reason for the differing responses may be due to the proximity of the phenol/ether group to the isopropyl group. In the thymol based compounds, the phenol/ether group is close to the isopropyl compared to the carvacrol based compounds where it is further away. Being closer to the isopropyl group may be beneficial to activation and have a negative effect on inhibition.

The differences between the two groups may lay in the lowest energy conformation of the compounds due to the position of the linking groups. It may be the case that the ojk07 compounds, due to the proximity of the isopropyl group on the first ring, have a more planar structure and that the ojk06 compounds show a more angled structure with regards to how the two phenyl rings align. The structures of the linking groups and how they align

to the two phenyl groups may be the reason why there is a difference between the two groups with regards to activation and inhibition. The complex calculations required to give an indication to the lowest energy conformations for these compounds is out of the scope of this research.

The responses observed for the two chloro derivatives, ojk0608 and ojk0707, show very similar inhibitory responses which disagree with the general trends observed; this may be due to the TRPA1 binding site that these two molecules interact with. As previously mentioned in section 3.3.3.3.3 the structure of the chloro derivatives closely matches that of known TRPA1 antagonists A96 and AP-18 which have been shown to act through the TM5 menthol binding site(55). This further backs up the idea proposed in section 3.3.3.3.3 that these compounds act through a different binding site to the rest of the ojk06 and ojk07 compounds.
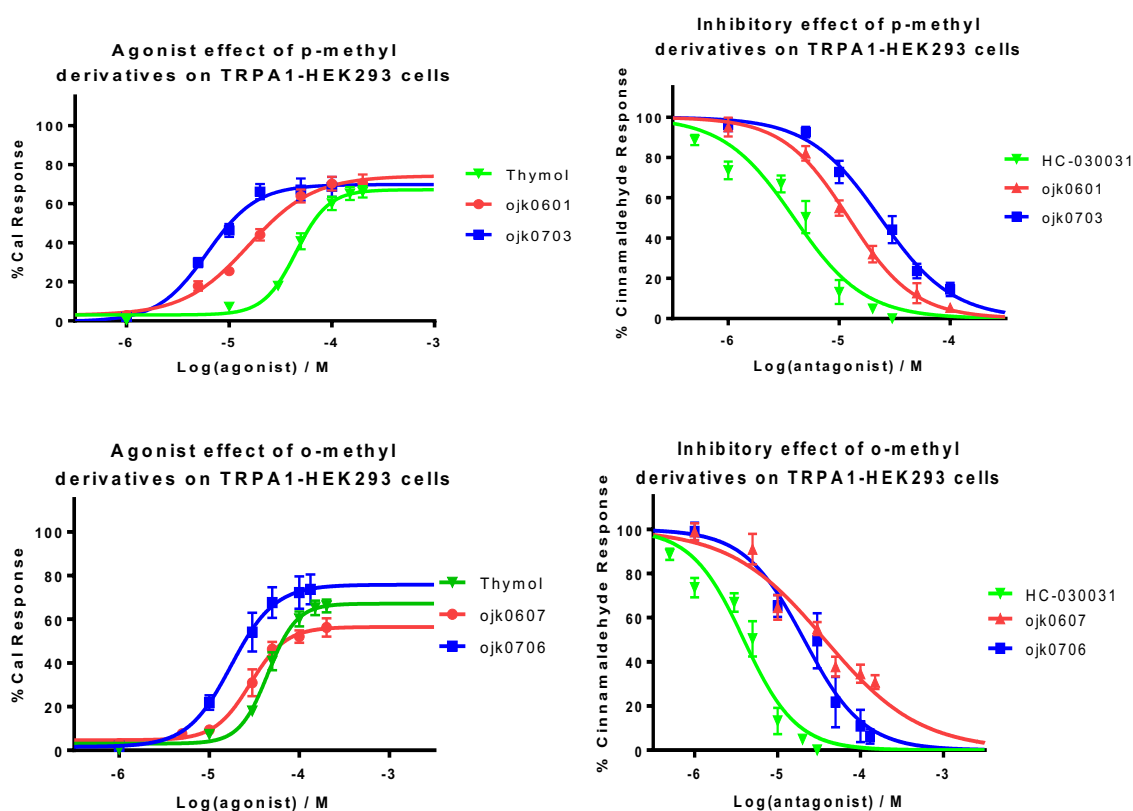
Figure 93 Comparison of concentration effect curves for ojk06 and their ojk07 counterparts on TRPA1-HEK293 cells. Data points are means±SEM of N = 3 experiments
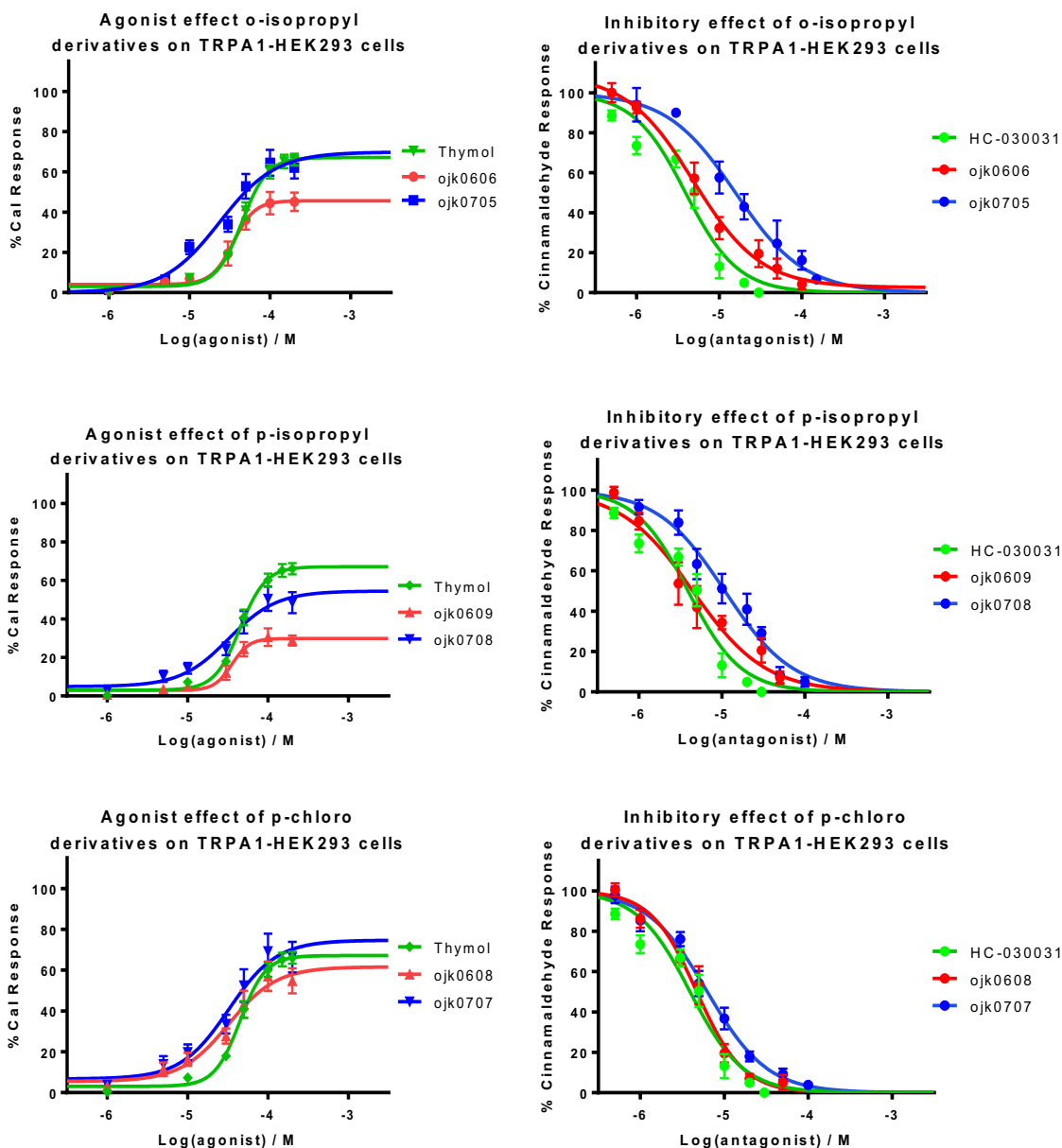
Figure 94 Comparison of concentration effect curves for ojk06 and their ojk07 counterparts on TRPA1-HEK293 cells. Data points are means±SEM of N = 3 experiments

3.3.3.5.1   TRPM8 Modulation

All of the ojk01, ojk06 and ojk07 compounds were screened for modulation of TRPM8-HEK293 cells using the same calcium signalling assay as for the TRPA1-HEK293 cells. The only hit was for ojk0606 which was found to inhibit TRPM8 channels. The results of the screening indicate that the effects of these compounds on TRPA1 are selective to TRPA1 over TRPM8. This is a significant finding because TRPM8 is similar in structure and function

and both share common modulators such as menthol and thymol, the parent compound for many of this series.

A full concentration effect curve was then constructed, and ojk0606 was found to fully inhibit the agonist effect of WS-5 on TRPM8 with an IC50 value of 29 µM. The potency of ojk0606 is slightly higher than known TRPM8 antagonists BCTC, thio-BCTC and capsazepine (IC50 = 0.8, 4 and 18 µM respectively)(183). Further work is required to determine the key structural features that allow for the inhibition of TRPM8 by ojk0606.

3.3.4   Summary and Conclusion

To conclude this chapter an array of novel compounds, based on the TRPA1 agonist's thymol and carvacrol, have been synthesised using two different pathways. They have then been assayed for interaction with the ion channel, TRPA1, expressed in HEK293 cells. The synthesis pathways used to produce the compounds in this chapter are based on simple reactions that when utilised in a certain order produced novel compounds, the routes used are simple and produced products of high yield and purity. The compounds synthesised have been assayed in three different cell systems; TRPA1-HEK239 cells, TRPM8-HEK293 cells and mock transfected-HEK293 cells. All compounds showed no response in the mock transfected-HEK293 cells which determined the responses observed in the TRPA1 and TRPM8 systems are through the TRPA1 and TRPM8 protein. In the TRPM8-HEK293 cells, only ojk0606 was found to inhibit the activation of TRPM8 by WS-5 all of the other compounds from the ojk01, ojk06 and ojk07 groups showed no activity with regards to TRPM8, this determines that the responses observed in the TRPA1-HEK293 cells are via TRPA1. The results using the TRPA1-HEK293 cell system showed a more varied array of results. Of the ojk01 group, only three compounds showed any modulation of TRPA1 these were ojk0107, ojk0109 and ojk0111 all three displayed activation and desensitisation of TRPA1. From the analysis of the results obtained from the ojk01 compounds it was seen that the linking group was important to the binding of the compounds to the TRPA1 receptor sites as the ester compounds showed no modulation whatsoever while all the active compounds had amide linking groups. Ojk0109 and ojk0111 were both chloro derivatives and the position of the chloro group on the second phenyl ring proved to have an influence over the gating of TRPA1. Also, the length of the linking group was speculated
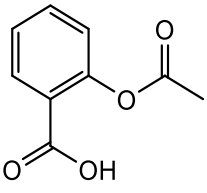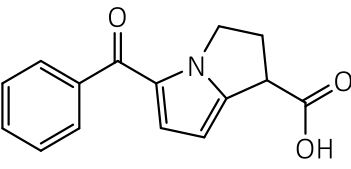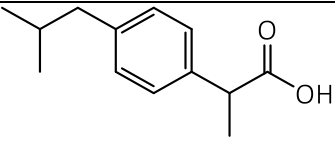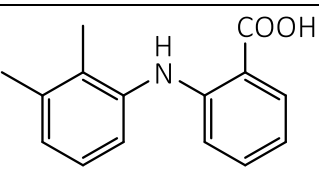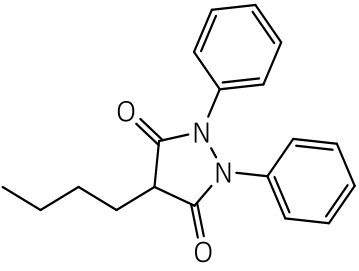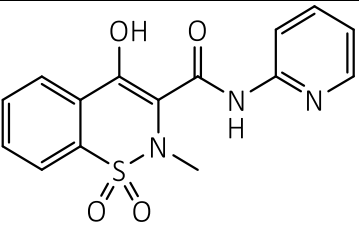
to have an effect on the potency of activation and inhibition. The ojk06 and ojk07 compounds were all TRPA1 agonists which then desensitised any further activation. A detailed structure-activity relationship study was carried out and identified key structural features which had an effect on the potency and efficacy of the TRPA1 interaction. The results from this research have met the aims as it has highlighted certain key points to be considered for future TRPA1 drug development.

4 The effect of fenamic acid derivatives on TRPA1

4.1 Introduction

Non-steroidal anti-inflammatory drugs (NSAIDs) are one of the most frequently prescribed classes of drugs around the world. NSAIDs are recognised as having very effective anti-inflammatory, antipyretic and pain relieving effects. Usage of NSAIDs can date back 3,500 years since the discovery of the pain relieving, soothing effect of bark from the willow tree(184). Salicylic acid, the extract from willow bark responsible for its therapeutic effects, was altered to acetylsalicylic acid, marketed by Bayer AG in 1897 as Aspirin, which it is commonly referred to today. It wasn't until 1959 when another drug was synthesised with similar therapeutic properties as aspirin. This was ibuprofen discovered by John Nicholson from the Boots Company. Ibuprofen was the first non-aspirin NSAID brought to market. Since then NSAIDSs have proved to be a successful treatment for mild pain relief, as today there are approximately 50 other non-aspirin NSAIDs available to patients. Together NSAIDS are the most commonly prescribed drug worldwide(185).

NSAIDs are commonly prescribed for mild to moderate pain relief in inflammatory diseases such as rheumatoid arthritis. NSAIDs as a class of drug can be subdivided into 7 main groups see Table 23. As diverse as NSAIDs appear to be, with differing pharmacokinetic and pharmacodynamics properties, they all share the same mode of action. They all inhibit cyclooxegenase enzymes, blocking prostaglandin production producing the analgesic, antipyretic and anti-inflammatory therapeutic effect but at the risk of gastric bleeding(186).

Group Name	Representative chemical structure	Brand Name examples
Salicylates	Aspirin	Aspirin, Diflunisal, Salsalate
Arylalkanoic acids	Ketorolac	Diclofenac, Indomethacin, Tolmetin
2-arylpropionic acids (profens)	Ibuprofen	Ibuprofen, Naproxen, Ketoprofen, Flurbiprofen
N-arylanthranilic acids or fenamic acids	Mefenamic acid	Flufenamic acid. Mefanamic acid, Meclofenamic acid
Pyrazolidine derivatives	Phenylbutazone	Phenylbutazone
Oxicams	Piroxicam	Piroxicam, Meloxicam, Droxicam
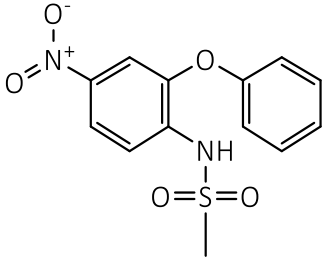
Sulfonanilides		Nimesulide
	Nimesulide	

Table 23 7 classes of NSAIDs

Of these seven groups of NSAIDs one in particular, the fenamic acids, have shown varied activity on ion channels. Mefanamic and Flufenamic acid (MFA and FFA respectively) were first found to have therapeutic effects similar to ibuprofen and aspirin in the early 1960s by Winder *et al*.(187,188). Since then many other derivatives of fenamic acid have been found to act upon COX enzymes in the same way to produce a similar therapeutic effect; a selection can be seen in Figure 95. Fenamic acids, despite lower effectiveness compared to other NSAIDs, have been commonly used to treat pain and inflammation associated with musculoskeletal and joint disorders with local application. Oral use of fenamic acids was discontinued in the 1980s due to the variability of absorption(189). With these drawbacks and the fact that fenamic acids still showed similar side effects to other NSAIDs, their use was somewhat limited.
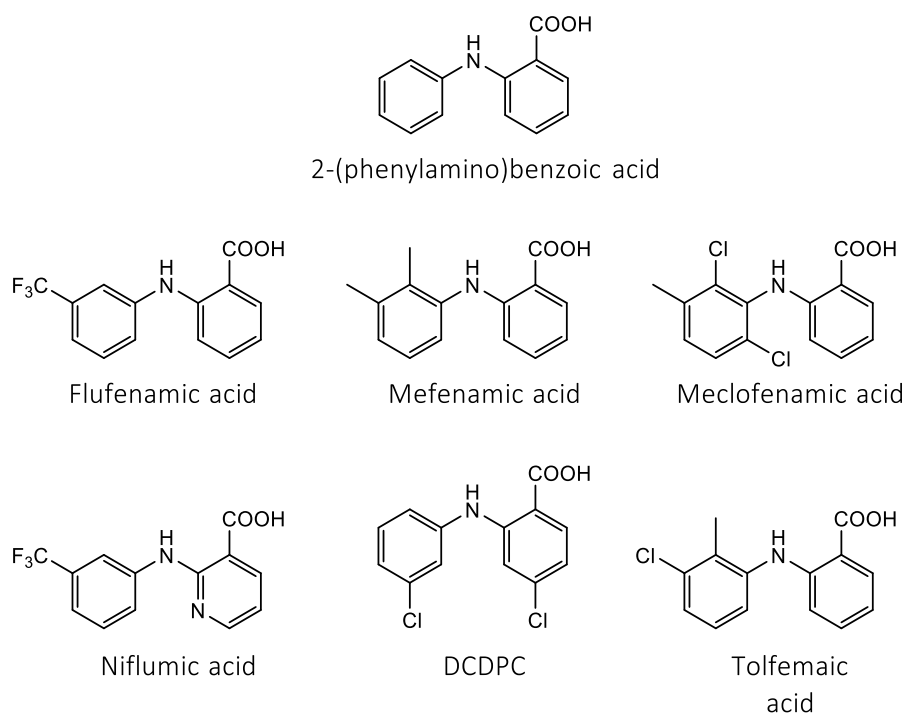
Figure 95 Selection of marketed NSAIDs based on the fenamic acid structure

Interest in fenamic acid, with flufenamic acid leading the way, has been regenerated due to the discovery that fenamic acid compounds have an effect on calcium and sodium uptake in lymphoid cells suggesting interactions with ion channel proteins(190). In the last 15 years, the identities of these channels have been discovered; so far these include Cl^-, Na^+, K^+ and non-selective cation channels. The effect that fenamic acids have on this broad spectrum of channels varies depending on which derivative is used and is very much based on chemical properties of the derivative as to whether it acts as an agonist or inhibitor with regards to a certain ion channel.

Flufenamic acid has been the most frequently studied with regards to the effect of fenamic acids on ion channel proteins. It seems when other fenamic acids have been studied such as niflumic acid and mefenamic acid, flufenamic acid tends to have a more potent effect. The following is a discussion of the effects that FFA has on different TRP channels.

FFA was found to activate an alpha-adrenoreceptor-activated and Ca^{2+}-permeable non-selective cation channel in rabbit portal vein smooth muscle(191). The identity of the channel responsible was later found to be TRPC6; when expressed in HEK293 cells FFA concentrations of 100 μM doubled the amplitude of the current prior to exposure to FFA(192). The activation effect of FFA on TRPC6 has been replicated and studied in more detail by Foster *et al*. who showed that intracellular calcium increases in TRPC6-HEK293 expression systems was due to direct interaction with FFA, and mutations in the TRPC6 protein abolished the effect caused by FFA(193). They also showed Niflumic acid (NFA) had no observable effect on TRPC6-HEK293 cells indicating a very specific interaction between FFA and TRPC6. Interestingly another report has shown FFA to have an inhibitory effect on TRPC6 with an IC50 value of 17 μM when expressed in HEK293 cells(194). The contradictory results presented by these two studies show that more research is necessary to fully elucidate the nature of FFA interaction with the TRPC6 channel. One possible explanation is the formation of heterotetramers that can form between TRPC6 and TRPC3/TRPC7 as FFA has been shown to inhibit both TRPC3 and TRPC7. Inoue *et al.* have shown that 100 μM FFA inhibits TRPC3 and TRPC7 by 60 and 90 % respectively(192). It has also been shown that FFA inhibits TRPC3-like currents from rabbit ear arterial myocytes(195).

TRPC3/6/7 form one subdivision of the TRPC family due to their sequence similarity, another subdivision can be formed due to sequence similarity, this family is TRPC1/4/5.

TRPC5 was first found to interact with FFA by Lee *et al.*(196). They found that 100 µM FFA reduced TRPC5 current by 92 %. More recently FFA and other fenamic acid derivatives were found to inhibit TRPC4 and 5. It was also shown that one derivative did not inhibit but activated the channel. This was the 2-(2'-methoxy-5'methylphenyl)aminobenzoic acid derivative (see Figure 96 for the structure)(152).
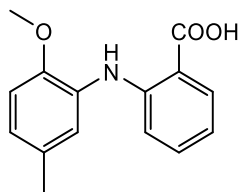
2-((2-methoxy-5-methylphenyl)amino)benzoic acid

Figure 96 TRPC4/5 inhibitor

TRPM2 has been found to be the most abundant TRP channel in the brain and indicated to play a role in cell death caused by oxidative stress(197). It has been shown by several groups that fenamic acids inhibit TRPM2, with FFA being the most potent inhibitor tested, followed by NFA and then MFA. FFA has been found to inhibit TRPM2 (expressed in HEK293 cells) activation by 90 % at dose concentrations of 50 µM and at 200 µM (197,198). It is of interest to note that extracellular acidification enhances the inhibitory effect of FFA and other fenamic acids. This effect can be potentially explained by the effect a decrease in pH has on the acidic group of the fenamic acids allowing them to diffuse across the cell membrane more readily, therefore increasing intracellular concentration and greater interaction between the channel and fenamic acid. Another explanation has been put forth that acidic pH modifies the TRPM2 channel in such a way that is favourable towards interaction with fenamic acids(197). More recently the same interactions have been observed by Klose *et al.* who reported an IC50 of 155 µM for TRPM2 inhibition by FFA. In addition it was reported that TRPM3 was also inhibited by fenamic acids with FFA reported to have an IC50 of 33 µM; both TRPM2 and M3 were expressed in HEK293 cells(194).

TRPM4 and TRPM5 do not conduct Ca^{2+} but instead are activated by internal Ca^{2+}. Despite their similarities with regards to Ca^{2+} interaction TRPM4 and 5 have vastly different functions in the body. TRPM4 is associated with insulin secretion, immune response, neural blast discharge in breathing related neurons and cardiac dysfunctions(199). TRPM5 on the other hand has a role to play in taste receptor cells(200). FFA has been found to inhibit both

channels. It is TRPM4 that is of most interest due to the potency of the inhibition that FFA has on the channel not just in heterologous expression systems such as HEK293 cells (IC50 = 2.8 μM) but also in native tissue, such as rat cardiomyocytes. TRPM4 has been inhibited by FFA with a calculated IC50 value of 6 μM(201). These IC50 values are significantly lower than those found for TRPM5. The IC50 for FFA in TRPM5-HEK293 cells is 25 μM, tenfold higher than that for TRPM4(202). The high potency of FFA on TRPM4 may lend its self to being a useful pharmacological tool in the study of TRPM4 channels. Interestingly the plasma concentrations of FFA, ranging from 4-12 μM after application, are sufficiently high to have an effect on TRPM4, which is ubiquitously expressed(203). The effect of FFA on TRPM4 may explain some of the physiological effects caused by FFA.

TRPM7 and M8 have been reported to interact with FFA. It has been reported by three separate groups in three different cell lines, rat brain microglia, human breast cancer cell line MCF-7 and in mouse renal tubule, that 100 μM of FFA reduces TRPM7-like currents by 50 %. However, it must be noted that no direct interaction between TRPM7 and FFA has been reported(204–206). Hu *et al.* have reported the partial inhibition of TRPM8 heterologously expressed in Xenopus oocytes by 100 μM of FFA(141)*.

It has been reported that concentrations of 100 μM FFA inhibit TRPV1 by 57-75 % when heterologously expressed in *Xenopus* oocytes. The same report shows TRPV3 inhibition by FFA at 100 μM by 57-67 % when expressed in *Xenopus* oocyte(141). The mechanosensitive TRPV4 channel expressed in HEK293 cells was found to be inhibited by common fenamic acids with FFA proving to be the most potent followed by NFA and then MFA. FFA was found to inhibit TRPV4 with an IC50 of 41 μM(194).

The effect of fenamic acids on TRP channels has shown a trend of inhibition with TRPC6 being the exception. TRPA1 is also another exception, as it has been reported that a variety of different fenamic acids and other NSAIDs activate TRPA1. FFA and NFA both stand out as being the most potent TRPA1 agonists with EC50 values of 24 μM and 28 μM respectively for TRPA1 expressed in WI-38 fibroblast. FFA and NFA are slightly more potent than MFA which has been reported to have an EC50 value of 61 μM in the same system. FFA was also shown to activate TRPA1 in HEK293 cells with an EC50 value of 57 μM. FFA and NFA were found to be the most potent agonists of TRPA1 when tested alongside other common NSAIDs, see Table 24 for a summary of results(141). TRPA1 is believed to be

163

thermosensitive and be activated by noxious cold temperatures (below 17°C). It is of interest to note that a study has shown that warming from 23 to 39°C prevents TRPA1 activation by FFA at a concentration of 300 μM(207).

NSAID compounds	EC50 (μM) in TRPA1 expressing WI-38 cells
FFA	24±3
NFA	28±3
MFA	61±5
Nifedipine	157±8
Diclofenac	210±22
Flurbiprofen	342±6
Indomethacin	470±54
Ketoprofen	500±62
Controls compounds	
Ally isothiocyanate	50±5
Acrolein	85±9
Cinnamaldehyde	400±41

Table 24 Effect of common NSAIDs on TRPA1 as reported by Hu et al.(141)

4.1.1   Aims and hypothesis

So far fenamic acids (particularly FFA) have been shown to interact with a wide variety of TRP channels. It has also been shown that FFA is a strong activator of TRPA1 with an EC50 of 24 μM when expressed in WI-38 fibroblasts. Alongside FFA only NFA and MFA have been studied with regards to their effect on TRPA1. I aim to therefore expand on these initial results by assaying a series of ten fenamic acid derivatives on TRPA1 expressed in HEK293 cells in a structure activity relationship (SAR) study. It has been shown in TRPC4/5 that small changes in structure can drastically alter the functional effect a compound has on the TRPC4/5 as the 2-(2'-methoxy-5'methylphenyl) aminobenzoic acid was reported to stimulate TRPC4/5 instead of blocking activity as with other fenamic acids(152). It is therefore hypothesised that structural modification of the fenamic acid skeleton may directly alter the nature of interaction and/or the potency of interaction with TRPA1.

4.2 Results

In this section the results for the calcium signalling assays have been described in detail.

All the compounds assayed have been tested against mock-transfected HEK293 cells, at the highest concentration used in the agonist and antagonist assays, to determine any effects that the compound has on HEK293 cells. There was no response observed in the mock-transfected HEK293 cells for all of the compounds assayed. Therefore the responses observed in the TRP gene transfected HEK293 cells can be deemed to be via gene product of the plasmid the HEK293 cells have been transfected with (see Figure 97 for data traces of responses for selected test compounds from each of the three compound groups).
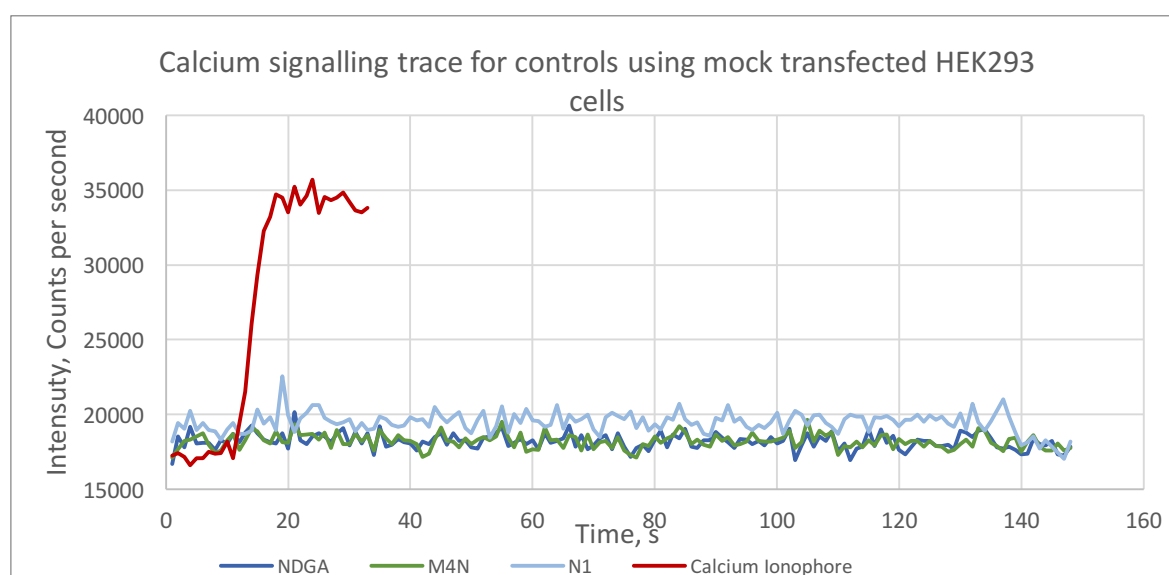
Figure 97 Raw data traces for a selection of test compounds on mock transfected HEK293 cells

4.2.1   Issues with the calcium signalling assay method

In section 3.2.1 any issues with the calcium signalling method and subsequent corrective actions have been explained.

4.2.2   Fenamic acid and associated NSAIDs

Fenamic acid

Flufenamic acid   Mefenamic acid   Diclofenac   Ketoprofen
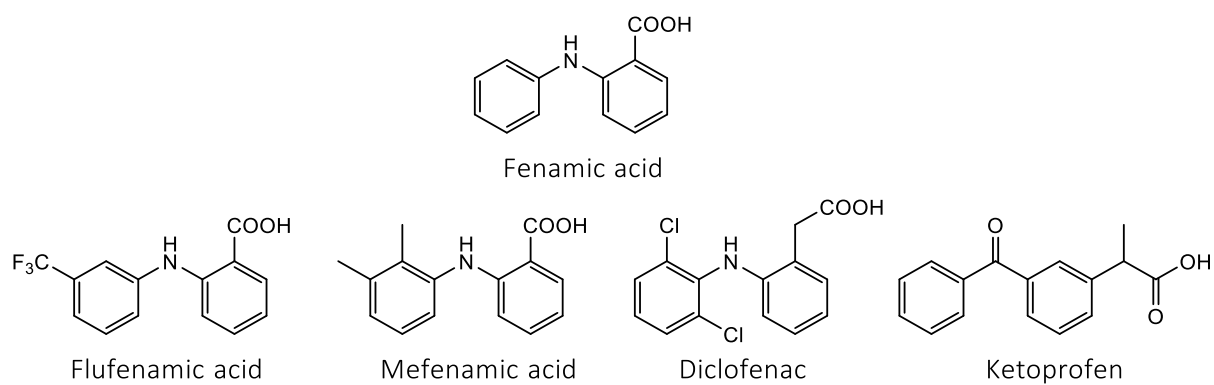
Figure 98 Chemical structures of fenamic acid and related NSAIDs

	EC50 / μM	Efficacy / % of full Cinnamaldehyde response	IC50 / μM
Fenamic acid	71.36	96	151.50
Flufenamic acid	24.04	107.3	7.86
Mefenamic acid	33.77	109.2	8.46
Diclofenac	60.97	63.1	13.87
Ketoprofen	111.20	44.0	ND

Table 25 Summary of fenamic acid NSAIDs response on TRPA1-HEK293 cells

Fenamic acid and fenamic acid based NSAIDs have been analysed in full for both agonist and antagonist response in calcium signalling assays using TRPA1 transfected HEK293 cells as per the method in section 2.2; their structures can be seen in Figure 98 above.
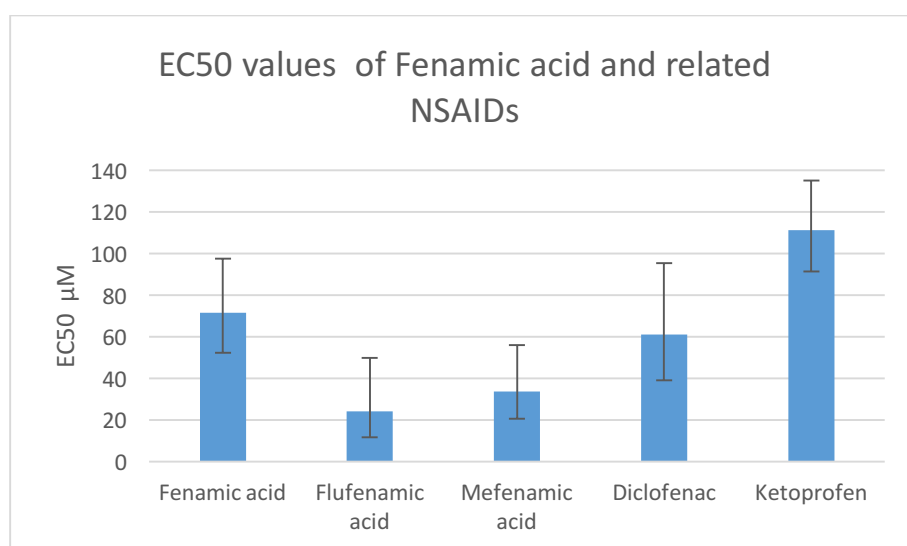
Figure 99 EC50 values calculated from agonist calcium signalling assay. Error bars represent 95 % Confidence interval of non-linear regression analysis
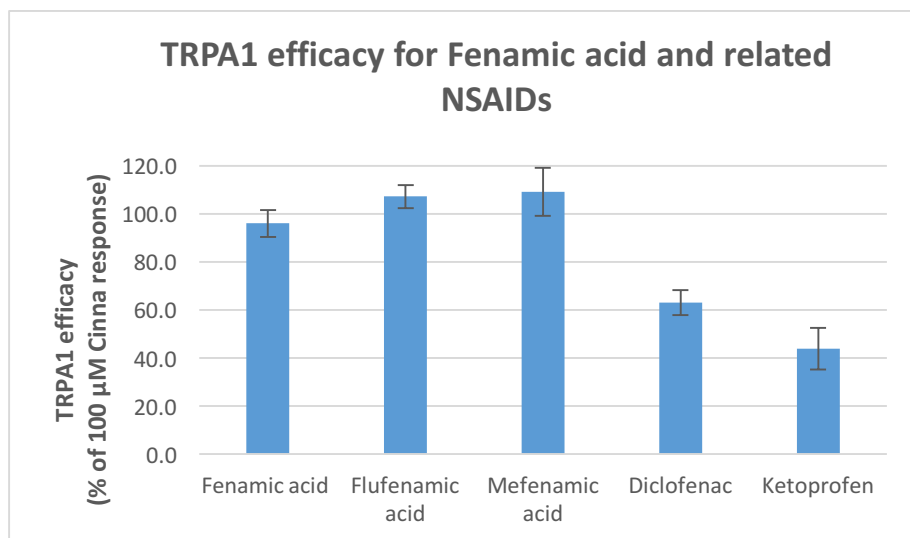
Figure 100 Efficacy of Fenamic acid and related NSAIDs on TRPA1-HEK293 cells compared to max response (100 µM) of the TRPA1 agonist Cinnamaldehyde

All 5 of the compounds have been assayed for their activation of TRPA1 in transfected HEK293 cells at a minimum of 6 concentration points ranging 1 µM to 300 µM (allowing for solubility) in triplicate. Each concentration was tested in duplicate for each replicate assay carried out. All 5 compounds showed a concentration dependent increase in intracellular calcium upon exposure to the assay compound which was fully inhibited by the TRPA1 specific antagonist HC-030031. Therefore it can be assumed that the increase in intracellular calcium is due to the activation and the subsequent gating of TRPA1 causing an influx of calcium into the cells. The EC50 values calculated for these compounds can be found in Figure 99 above. Flufenamic acid (FFA) was found to be the most potent agonist with a calculated EC50 value of 24 µM, and the least potent compound was Ketoprofen with an EC50 value of 111 µM.

4.2.2.1   Fenamic acid
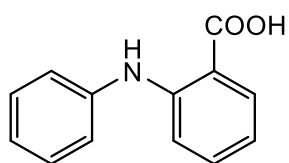
Fenamic acid

Figure 101 Chemical structure of fenamic acid

Agonist effect of Fenamic acid on TRPA1-HEK293 cells

EC50 = 71 μM
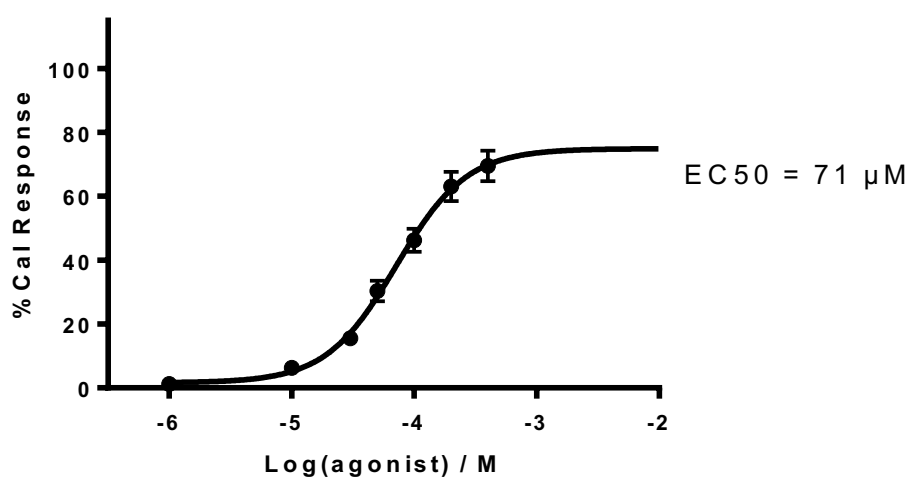
Inhibitory effect of Fenamic acid on TRPA1-HEK293 cells

IC50 = 151 μM
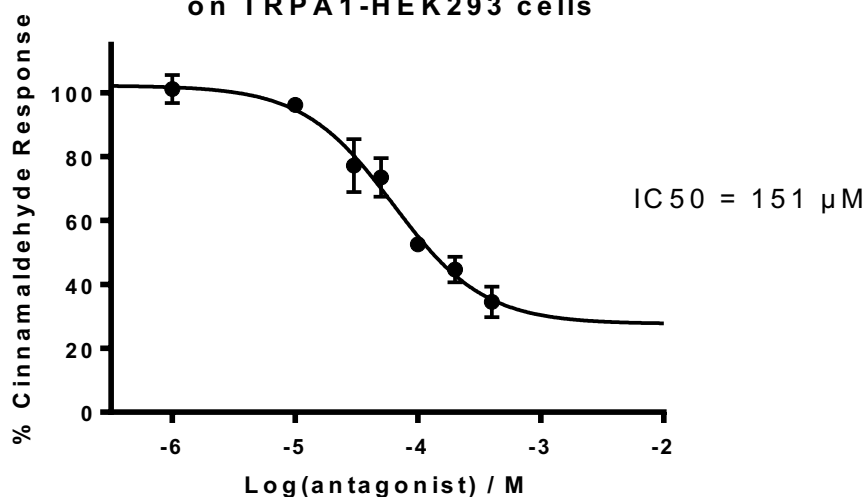
Figure 102 Agonist (above) and antagonist (below) concentration effect curves for Fenamic acid on TRPA1-HEK293 cells. Data points are means±SEM of N = 3 experiments

Fenamic acid, the parent structure for all the compounds analysed in this chapter has been assayed using both the agonist and antagonist calcium signalling assays, outlined in section 2.2 to assess the compound's effect on TRPA1-HEK293 cells. The resulting concentration effect curves can be seen in Figure 102.

In the agonist assay, a concentration dependent increase in intracellular calcium was observed. This response was inhibited fully by the TRPA1 specific inhibitor HC-030031; therefore this response can be attributed to the gating of TRPA1 channels. The agonist concentration effect shows an almost complete sigmoidal curve over the testing concentration range of 1 µM to 400 µM, testing at greater concentrations was not carried out due to the insolubility of fenamic acid in the test medium at higher concentrations causing light scattering to occur and affecting the fluorescent response. From the non-linear regression analysis, the best fit curve, the variable slope four parameter curve, indicates that the response at 400 µM is just at the plateau point. The calculated EC50 was 71 µM, with an initial response occurring at 10 µM and a maximum response of 70 %CaI occurring at 400 µM which is the assumed plateau point. The efficacy of fenamic acid has been calculated at 96 % of the maximum response of Cinnamaldehyde (100 µM). Therefore, fenamic acid can be deemed to be a full agonist of TRPA1.

In the antagonist assay a concentration dependent decrease in the response of 30 µM of cinnamaldehyde (EC50 concentration of cinnamaldehyde in my system) was observed with increasing concentration of pre-dosed fenamic acid. Fenamic acid was tested over the concentration range of 1 µM to 400 µM. Fenamic acid was not soluble in the assay media with concentrations greater than 400 µM therefore a response was not recorded. The first significant reduction in response to cinnamaldehyde occurred at the 30 µM concentration point when the response was reduced by 23 %. The maximum reduction in response to cinnamaldehyde occurred at 400 µM when the response was reduced by 65 %. Full inhibition was not observed over the concentration range tested. Whether fenamic acid inhibits TRPA1 fully or partially cannot be fully elucidated from the data presented, however non-linear regression analysis of the data points can fit a curve from which a prediction can be made. The first non-linear regression analysis assumes full inhibition. This is the normalised variable response curve, the curve has a good fit with an R^2 = 0.8962 this curve calculates an IC50 value of 151 µM. The second non-linear regression model, the

variable slope four parameter model, fits the curve to the data points with a variable Hill slope i.e. not fixed to -1.0 and doesn't assume full inhibition. This curve showed a greater degree of fit with an R^2 = 0.9107, however this is only a slightly better fit than the normalised model. The curve for this model predicts a partial agonist response with a predicted IC50 value of 63 µM. With the data presented it is difficult to conclude the full nature of the inhibitory response observed for fenamic acid.

From this analysis of the agonist and antagonist assays of fenamic acid on TRPA1-HEK293 cells, it can be determined that fenamic acid is a full agonist of TRPA1 which after the initial activation of TRPA1 inhibits further activation via a desensitisation effect. Fenamic acid is the parent compound to all the other compounds assayed in this chapter and provides a good basis of comparison for the calcium signalling results of the derivatives of fenamic acid to be analysed.

4.2.2.2   Flufenamic acid
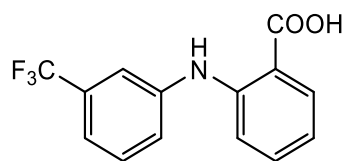
Flufenamic acid

Figure 103 Chemical structure of flufenamic acid

Agonist effect of Flufenamic acid on TRPA1-HEK293 cells

EC50 = 24 µM
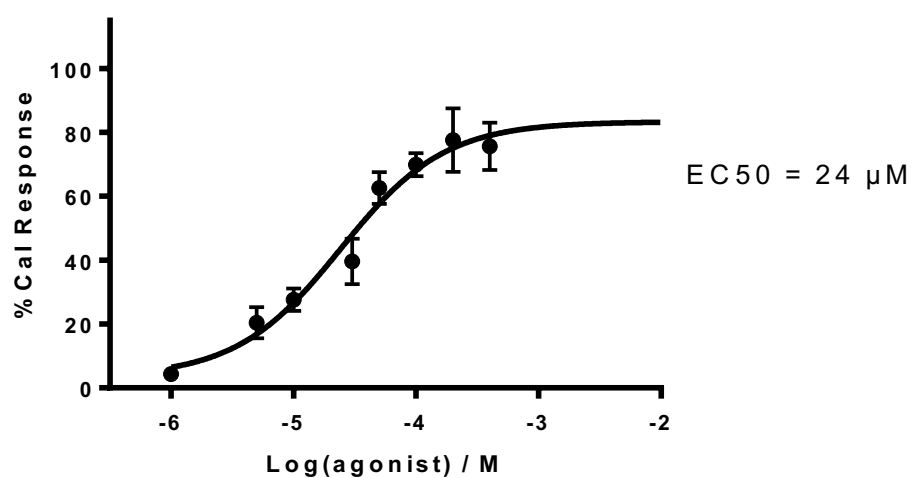
Inhibitory effect of Flufenamic acid on TRPA1-HEK293 cells

IC50 = 8 µM
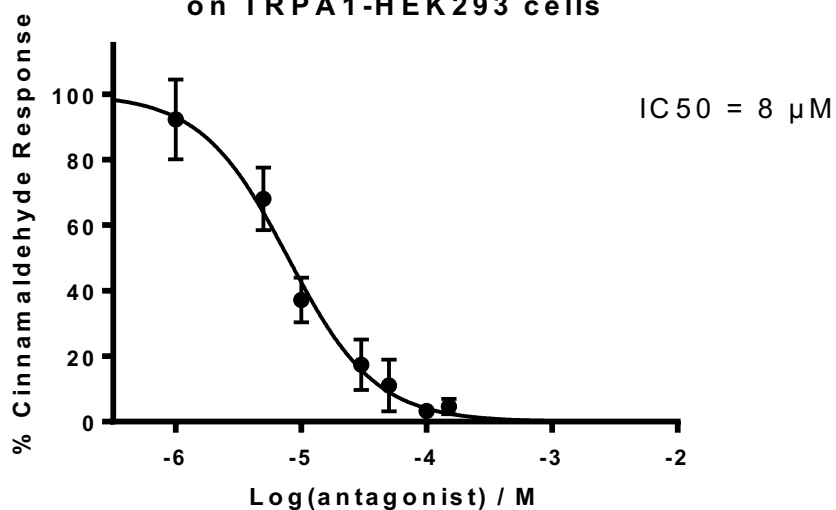
Figure 104 Agonist (above) and antagonist (below) concentration effect curves for Flufenamic acid on TRPA1-HEK293 cells. Data points are means±SEM of N = 3 experiments

Flufenamic acid (FFA) has been assayed using both the agonist and antagonist calcium signalling assays to assess the compound's effect on TRAP1-HEK293 cells; the resulting concentration effect curves can be seen in Figure 104 above. In the antagonist assay, a concentration dependent reduction in the cinnamaldehyde response was observed suggesting that FFA desensitised TRPA1 to further activation by cinnamaldehyde.

In the agonist assay a concentration dependent increase in intracellular calcium was observed, which was inhibited fully by the TRPA1 specific inhibitor HC-030031 therefore this response can be attributed to gating of TRPA1 channels. An increase in intracellular calcium corresponding to activation of the TRPA1 channel was first seen at the 5 µM concentration which gave a response of 20 %CaI. The response plateaued between the 50 µM and 100 µM concentration levels. The plateau was found to occur at 80 %CaI this maximum result gave FFA an efficacy of 107 % of the maximum response of cinnamaldehyde. Therefore FFA can be deemed a full agonist of TRPA1. Non-linear regression analysis was carried out with the variable slope four parameter model producing the best fit curve. This curve gave a calculated EC50 value of 24 µM.

The antagonist concentration effect shows a complete sigmoidal curve over the testing concentration range of 1 µM to 150 µM. The first significant reduction in response to cinnamaldehyde occurred at the 5 µM concentration point when the response was reduced by 32 % and the maximum reduction in response to cinnamaldehyde occurred at 100 µM when the response is reduced by 96 % which can be deemed to be full inhibition of TRPA1. Non-linear regression analysis was carried out and the best fit curve used the normalised variable slope model which calculated an IC50 of 8 µM.

4.2.2.3   Mefenamic acid
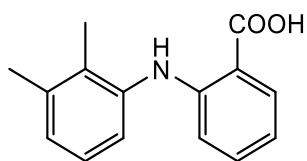
Mefenamic acid

Figure 105 Chemical structure of mefenamic acid

EC50 = 34 μM

IC50 = 10 μM
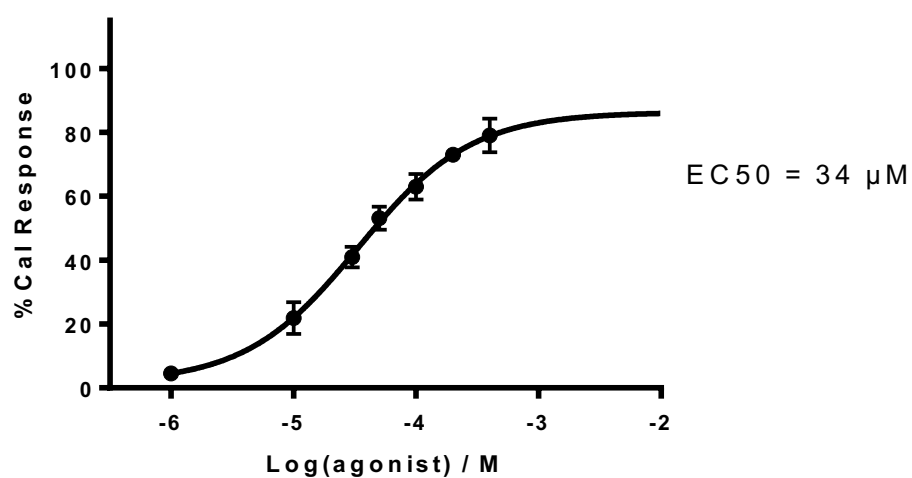
Figure 106 Agonist (above) and antagonist (below) concentration effect curves for Mefenamic acid on TRPA1-HEK293 cells. Data points are means±SEM of N = 3 experiments

Mefenamic acid (MFA) has been assayed using both the agonist and antagonist calcium signalling assays to assess the compound's effect on TRPA1-HEK293 cells. The resulting concentration effect curves can be seen in Figure 106 above.

In the agonist assay a concentration dependent increase in intracellular calcium was observed, which was inhibited fully by the TRPA1 specific inhibitor HC-030031 therefore this response can be attributed to gating of TRPA1 channels. MFA was assayed over the concentration range of 1 µM to 400 µM with a close to complete sigmoidal curve, concentrations above 400 µM could not be tested due to solubility issues. An increase in intracellular calcium corresponding to activation of the TRPA1 channel was first seen at 10 µM with a response of 22 %CaI. The maximum response was observed at the 400 µM concentration point with a response of 79 %CaI. Non-linear regression analysis was used with two different models being fit to the data points. The best fit curve was the variable slope four parameter curve which predicts a plateau to occur at concentrations just above 400 µM with an efficacy of 109 % of the maximum cinnamaldehyde response. The best fit curve also calculates an EC50 of 34 µM.

In the antagonist assay, a concentration dependent reduction in the cinnamaldehyde response was observed suggesting that MFA desensitised TRPA1 to further activation by cinnamaldehyde. The antagonist concentration effect shows a complete sigmoidal curve over the testing concentration range of 0.1 µM to 150 µM. The first significant reduction in response to cinnamaldehyde occurred at the 1 µM concentration point when the response was reduced by 21 % and the maximum reduction in response to cinnamaldehyde occurred at 150 µM when the response was reduced by 96 %, which is deemed to be full inhibition of TRPA1. MFA completely inhibits the agonist response of cinnamaldehyde on TRPA1. Non-linear regression analysis was used to determine the best fit curve, which was calculated using the normalised variable slope model. The best fit curve calculates an IC50 of 10 µM.
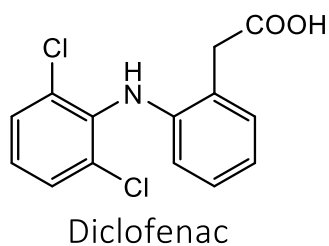
4.2.2.4   Diclofenac

Figure 107 Chemical structure of Diclofenac

Figure 108 Agonist (above) and antagonist (below) concentration effect curves for Diclofenac on TRPA1-HEK293 cells.
Data points are means±SEM of N = 3 experiments

Diclofenac (DFC) was assayed using both the agonist and antagonist calcium signalling assays to assess the compound's effect on TRAP1-HEK293 cells, the resulting concentration effect curves can be seen in Figure 108 above.

In the agonist assay a concentration dependent increase in intracellular calcium was observed, which was inhibited fully by the TRPA1 specific inhibitor HC-030031 therefore this response can be attributed to gating of TRPA1 channels.

DFC was assayed over the concentration range of 1 µM to 400 µM, over which a complete sigmoidal curve was observed. An increase in intracellular calcium corresponding to activation of the TRPA1 channel was first seen at the 30 µM concentration with a response of 11 %CaI. The maximum response was observed at the 200 µM concentration point with a response of 46 %CaI. The response can be seen to plateau between the 100 and 200 µM concentration points; this plateau corresponds to an efficacy of 63%. Non-linear regression analysis using the two models outlined in section 2.2.6 was carried out, the best fit curve was the variable slope four parameter curve. The best fit curve confirms that DFC is a partial agonist of TRPA1 and has also calculated an EC50 of 61 µM.

In the antagonist assay, a concentration dependent reduction in the cinnamaldehyde response was observed suggesting that DFC desensitised TRPA1 to further activation by cinnamaldehyde. The antagonist concentration effect shows a complete sigmoidal curve over the testing concentration range of 1 µM to 150 µM. The first significant reduction in response to cinnamaldehyde occurred at the 10 µM concentration point when the response was reduced by 44 % and the maximum reduction in response to cinnamaldehyde occurred at 150 µM when the response was reduced by 91 %, which is deemed to be complete inhibition of TRPA1. DFC completely inhibits the agonist response of cinnamaldehyde on TRPA1. Non-linear regression analysis was carried out, and the best fit curve was produced using the normalised variable slope model which calculated an IC50 of 11 µM.
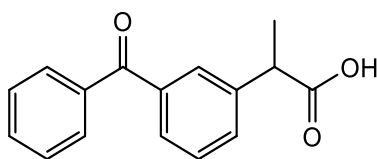
4.2.2.5   Ketoprofen

Ketoprofen

Figure 109 Ketoprofen
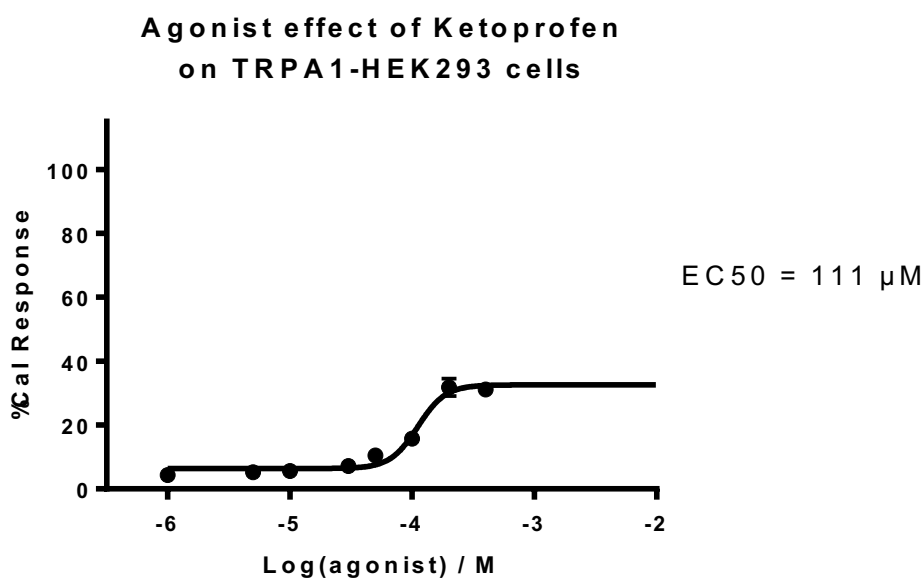
Figure 110 Agonist concentration effect curves for ketoprofen on TRPA1-HEK293 cells. Data points are means±SEM of N=3 experiments

Ketoprofen has been assayed using both the agonist and antagonist calcium signalling assays to assess the compound's effect on TRPA1-HEK293 cells; the resulting concentration effect curve can be seen in Figure 110 above.

In the agonist assay a concentration dependent increase in intracellular calcium was observed, which was inhibited fully by the TRPA1 specific inhibitor HC-030031 therefore this response can be attributed to gating of TRPA1 channels. Ketoprofen was assayed over the concentration range of 1 µM to 400 µM, over which a complete typical sigmoidal curve was observed. An increase in intracellular calcium corresponding to activation of the TRPA1 channel was first seen at the 50 µM concentration point with a response of 10%Cal. The response then plateaued between the 100 and 200 µM concentration points. The maximum response observed was at the 200 µM concentration point with a response of

32 %CaI. This maximum response corresponds to an efficacy of 44%, therefore indicating that ketoprofen acts as a partial agonist of TRPA1. Non-linear regression analysis was carried out, and the best fit curve was produced using the variable slope four parameter model which calculated an EC50 of 111 µM.

In the antagonist assay, no inhibition of the activation of TRPA1 by cinnamaldehyde was detected. When assayed using the antagonist calcium signalling assay ketoprofen showed no inhibition of the activation of TRPA1 by cinnamaldehyde up to a concentration of 400 µM, concentrations greater than this could not be tested due to issues with solubility.

4.2.3   Preliminary Screening
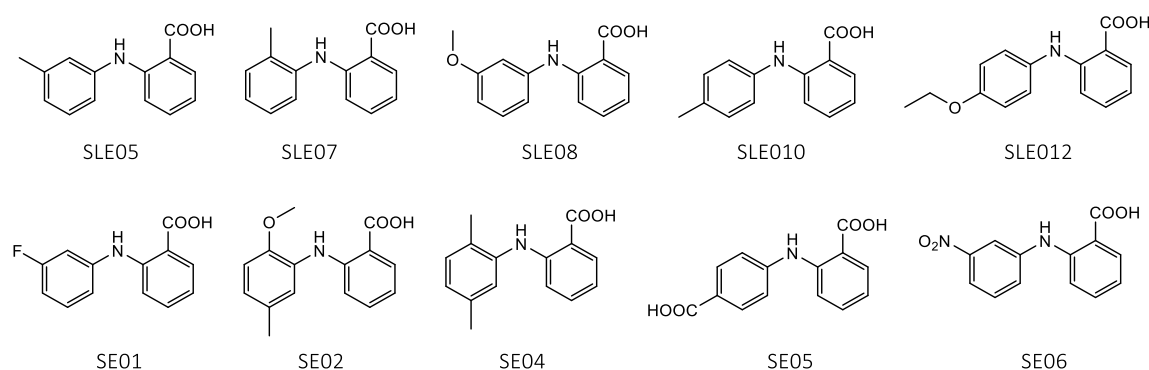
Figure 111 Chemical structure of synthesised fenamic acid derivatives

A preliminary screen was carried out on all of the in-house synthesised fenamic acid derivatives seen in Figure 111. The compounds screened have previously been screened for TRPC4/5 modulation and details on the synthesis can be found within the published article by Jiang *et al.* (152)*.* The preliminary screening comprised of each compound being tested at a 50 µM concentration level in both agonist and antagonist calcium signalling assays on TRPA1 transfected HEK293 cells. Any compounds that showed any kind of significant response were taken forward to be assayed in full. For the agonist assay, a significant response was deemed to be an increase in intracellular calcium equal or greater than 10 % of the calcium ionophore response. For the antagonist assay, a significant response was deemed to be a decrease in cinnamaldehyde response by equal or greater than 10 %.

	Average Agonist Response at 50 µM %Cal	SEM	Average Antagonist Response at 50 µM %Cinna Response	SEM
SLE05	15	4.0	ND	-
SLE07	11	3.9	ND	-
SLE08	35	2.7	ND	-
SLE10	30	2.2	ND	-
SLE12	16	4.1	ND	-
SE01	ND	-	18	8.9
SE02	ND	-	51	22.2
SE04	62	6.0	54	19.2
SE05	ND	-	59	23.1
SE06	ND	-	70	13.1

Table 26 Preliminary Screening results table. ND: Response Not Detected

The calcium signalling preliminary screening was carried out as per the method in section 2.2 each compound was tested in triplicate, in both agonist and antagonist assays, an average response was calculated and reported in Table 26. Of the ten derivatives tested 6 gave a positive hit as a potential agonist these were; SLE05, SLE07, SLE08, SLE10, SLE12 and SE04 the structures of these derivatives can be seen in Figure 111. The antagonist assay gave positive hits for 5 of the ten derivatives these were SE01, SE02, SE04, SE05 and SE06. Of the five antagonist hits only one derivative gave a hit in the agonist assay this being SE04. The other four potential antagonists did not show a positive response in the agonist preliminary screen.

4.2.4 Calcium signalling results for synthesised fenamic acid derivatives

From the preliminary screening in section 4.2.3 the following derivatives: SLE05, SLE07, SLE08, SLE10, SLE12 and SE04 were selected to be assayed over a range of concentrations using the agonist calcium signalling method. The following derivatives: SE01, SE02, SE04, SE05 and SE06 were selected to be assayed over a range of concentrations using the antagonist calcium signalling method.

181

4.2.4.1   SLE05
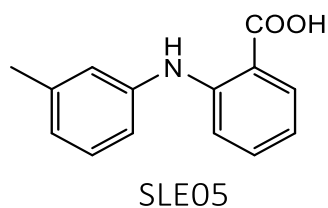
SLE05

Figure 112 Chemical structure of SLE05

Figure 113 Agonist concentration effect curves for SLE05 on TRPA1-HEK293 cells. Data points are means±SEM of N = 3 experiments

From the preliminary screening SLE05 displayed potential agonist properties towards TRPA1. Figure 113 above shows the result of a full concentration effect profile carried out using the agonist calcium signalling assay method, detailed in section 2.2, with TRPA1-HEK293 cells.

In the agonist assay, a concentration dependent increase in intracellular calcium was observed. This response was inhibited fully by the TRPA1 specific inhibitor HC-030031 therefore this response can be attributed to the gating of TRPA1 channels. SLE05 was tested over the concentration range of 1 µM to 300 µM; over this range a partial sigmoidal response was observed. Greater concentrations could not be tested due to solubility issues, and therefore a full concentration effect curve could not be constructed. The first significant response was observed at the 10 µM concentration point with a response of 12 %Cal. The maximum response was observed at 300 µM with a response of 34 %Cal. The

concentration effect curve does not reach a maximum plateau within the concentration range assayed and therefore an accurate determination of the TRPA1 agonist characteristics cannot be made. However, non-linear regression analysis was carried out using the two models described in section 2.2.6. The best fit curve was produced using the variable slope four parameter model. The curve predicts a partial agonist response for SLE05 with an efficacy of 55 %. The curve also calculates an EC50 of 77 μM.

4.2.4.2   SLE07
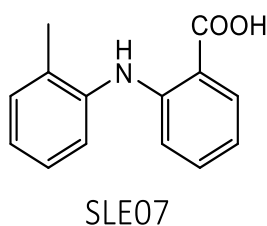
SLE07

Figure 114 Chemical structure of SLE07

Figure 115 Agonist concentration effect curve for SLE07 on TRPA1-HEK293 cells. Data points are means±SEM of N = 3 experiments

From the preliminary screening SLE07 displayed potential agonist properties towards TRPA1. Figure 115 above shows the result of a full concentration effect profile carried out using the agonist calcium signalling assay method, detailed in section 2.2 with TRPA1-HEK293 cells.

In the agonist assay a concentration dependent increase in intracellular calcium was observed. This response was inhibited fully by the TRPA1 specific inhibitor HC-030031 therefore this response can be attributed to the gating of TRPA1 channels. SLE07 was tested over the concentration range of 1 µM to 300 µM, over this range a partial sigmoidal curve was observed, further testing at higher concentrations was not possible due to the insolubility of SLE07 in the assay media at higher concentrations.

The first significant response was observed at the 100 µM concentration point with a response of 19 %Cal. The maximum response was observed at 300 µM with a response of 27 %Cal, the concentration effect curve does not reach a maximum plateau within the concentration range assayed and therefore an accurate determination of the TRPA1 agonist characteristics cannot be fully made. However, predictions can be made by fitting a curve to the data points of the two non-linear regression models the variable slope four parameter model produced the best fitting curve. The best fit curve predicts a partial agonists response for SLE07 with TRPA1, with an efficacy of 44 % of the maximum cinnamaldehyde response (100 µM). The curve also calculates an EC50 of 93 µM.

4.2.4.3   SLE08

Figure 116 Chemical structure for SLE08

From the preliminary screening SLE08 displayed potential agonist properties towards TRPA1. Figure 117 above shows the result of a full concentration effect profile carried out using the agonist calcium signalling assay method, detailed in section 2.2, with TRPA1-HEK293 cells.

In the agonist assay a concentration dependent increase in intracellular calcium was observed. This response was inhibited fully by the TRPA1 specific inhibitor HC-030031 therefore this response can be attributed to the gating of TRPA1 channels. SLE05 was tested over the concentration range of 1 µM to 300 µM, over this range an almost complete sigmoidal curve was observed, testing at greater concentrations was not possible due to the insolubility of SLE08 in the assay media at higher concentrations.

The first significant response was observed at the 3 µM concentration point with a response of 19 %CaI. The maximum response was observed at 300 µM with a response of 66 %CaI. Non-linear regression analysis was carried out using the two models described in section 2.2.6. The best fit curve was produced using the variable slope four parameter model. The curve agrees that at the 300 µM concentration point a maximum plateau does form. This gives SLE08 an efficacy value of 91 % of the maximum cinnamaldehyde response as this efficacy is close to the maximum cinnamaldehyde response it can be deemed that SLE08 is a full agonist of TRPA1. The curve calculates an EC50 of 36 µM.

4.2.4.4   SLE10
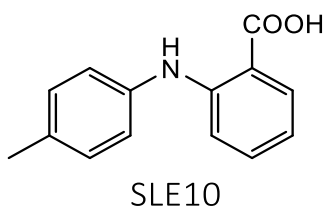
Figure 118 Chemical structure for SLE010
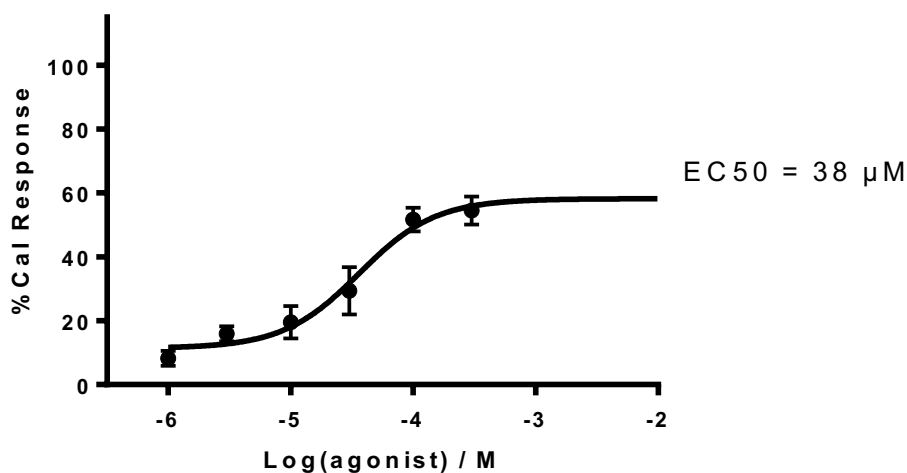
Figure 119 Agonist concentration effect curve for SLE010 on TRPA1-HEK293 cells. Data points are means±SEM of N = 3 experiments

From the preliminary screening SLE10 displayed potential agonist properties towards TRPA1. Figure 119 above shows the result of a full concentration effect profile carried out using the agonist calcium signalling assay method, detailed in section 2.2, with TRPA1-HEK293 cells.

In the agonist assay a concentration dependent increase in intracellular calcium was observed. This response was inhibited fully by the TRPA1 specific inhibitor HC-030031 therefore this response can be attributed to the gating of TRPA1 channels. SLE010 was tested over the concentration range of 1 µM to 300 µM, over this range an almost complete sigmoidal response was observed, greater concentrations were not tested due to the insolubility of SLE010 in the assay media at higher concentrations. The first significant response was observed at the 3 µM concentration point with a response of 16 %Cal. The maximum response was observed at 300 µM with a response of 54 %Cal. Non-linear regression analysis was carried out using the two models, the best fit curve was produced using the variable slope four parameter model. This model predicts a partial agonist response which plateaus just after the 300 µM concentration point with an efficacy of 75 % of the maximum cinnamaldehyde response. The curve also calculates an EC50 of 38 µM.

4.2.4.5   SLE12
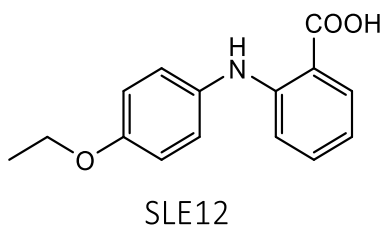
Figure 120 Chemical structure for SLE012
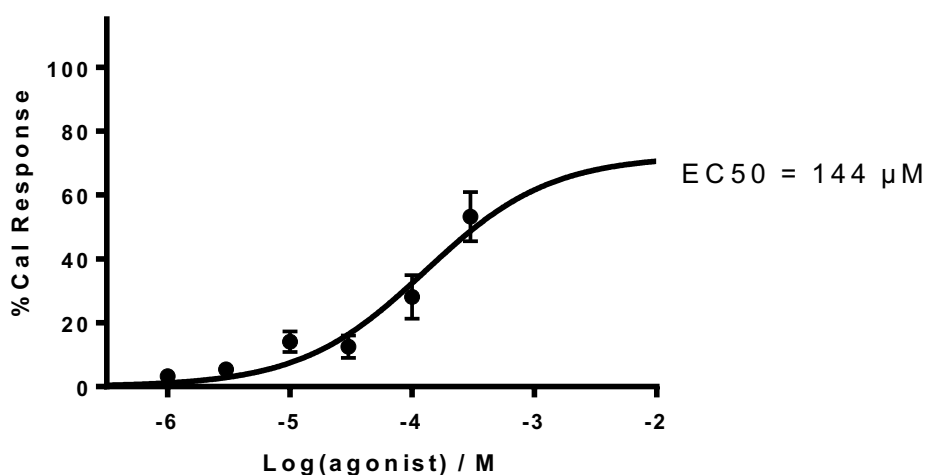
Figure 121Agonist concentration effect curve for SLE012 on TRPA1-HEK293 cells. Data points are means±SEM of N = 3 experiments

From the preliminary screening SLE12 displayed potential agonist properties towards TRPA1. The Figure 121 above shows the result of a full concentration effect profile carried out using the agonist calcium signalling assay method, detailed in section 2.2, with TRPA1-HEK293 cells.

In the agonist assay a concentration dependent increase in intracellular calcium was observed. This response was inhibited fully by the TRPA1 specific inhibitor HC-030031 therefore this response can be attributed to the gating of TRPA1 channels. SLE12 was tested over the concentration range of 1 µM to 300 µM, over this range a full typical sigmoidal concentration response curve was not observed. Greater concentrations could not be tested due to the insolubility of SLE12 in the assay media at higher concentrations.

The first significant response was observed at the 10 μM concentration point with a response of 14 %CaI. The maximum response was observed at 300 μM with a response of 53%CaI, the concentration effect curve does not reach a maximum plateau within the concentration range assayed and therefore an accurate determination of the TRPA1 agonist characteristics cannot be made. However, non-linear regression analysis has been carried out in order to give an indication as to the full effect of SLE12 on TRPA1. Of the two models used, described in section 2.2.6, the best fit curve was produced using the normalised variable slope model with an R^2 value of 0.8172 which can be deemed a good degree of fit and therefore reliable. Using this model fits the bottom and top of the curve to 0 and 72%CaI respectively, which reflects a full agonist response in my system by cinnamaldehyde activation of TRPA1. From the data points it is clear that SLE12 will have a close to full agonist response as a minimum. The other model used, the variable slope four parameter model, has not produced a reliable curve as the equations have not defined a value for the top of the curve within in the calcium ionophore response. Therefore, the exact efficacy of SLE12 cannot be predicted, however due to the goodness of fit for the normalised variable slope curve and the trend of the data up to 300 μM, it can be predicted, with confidence that SLE12 is a full agonist of TRPA1. The best fit curve calculates an EC50 value of 144 μM.

4.2.4.6   SE01
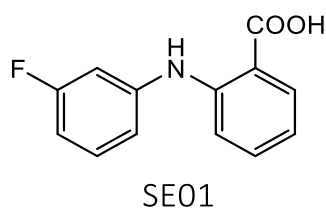
SE01

Figure 122 Chemical structure for SE01

Inhibitory effect of SE01 on TRPA1-HEK293 cells

IC50 = 13 µM
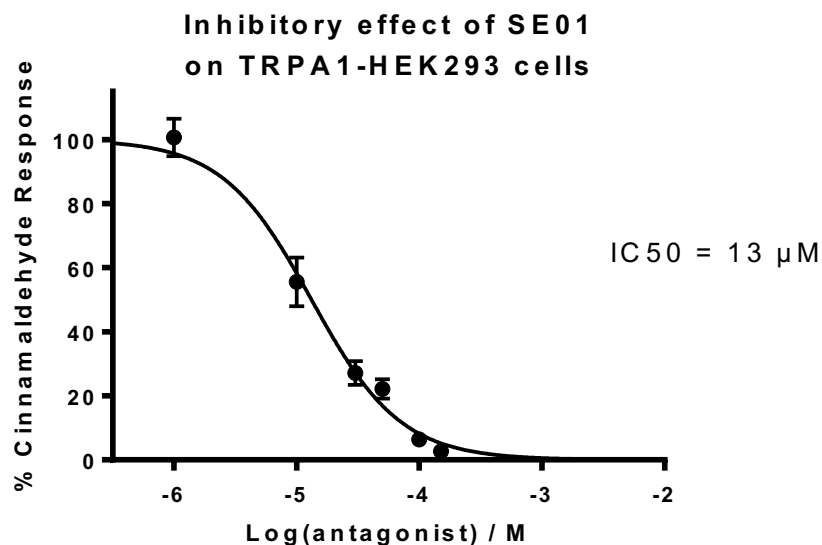
Figure 123 Antagonist concentration effect curve for SE01 on TRPA1-HEK293 cells. Data points are means±SEM of N = 3 experiments

From the preliminary screening SE01 displayed potential antagonist properties in relation to TRPA1. The Figure 123 above shows the result of a full concentration effect profile carried out using the antagonist calcium signalling assay method, detailed in section 2.2, with TRPA1-HEK293 cells.

In the antagonist assay a concentration dependent decrease in the response of 30 µM of cinnamaldehyde (EC50 concentration of cinnamaldehyde) was observed with increasing concentration of pre-dosed SE01. SE01 was tested over the concentration range of 1-150 µM over this range a typical reversed sigmoidal curve was observed. The first decrease in the cinnamaldehyde response was observed at 10 µM with a decrease in cinnamaldehyde response of 45%. The greatest reduction in the cinnamaldehyde response occurred at the 150 µM concentration point with a reduction of 97 %, which is deemed to be full inhibition of the cinnamaldehyde response. The best fit non-linear regression analysis model was the normalised variable slope model which has an R^2 value of 0.9570, the calculated IC50 value for this model is 13 µM.

4.2.4.7   SE02
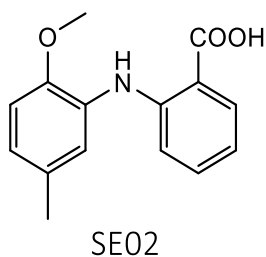
SE02

Figure 124 Chemical structure for SE02

Inhibitory effect of SE02 on TRPA1-HEK293 cells

IC50 = ND
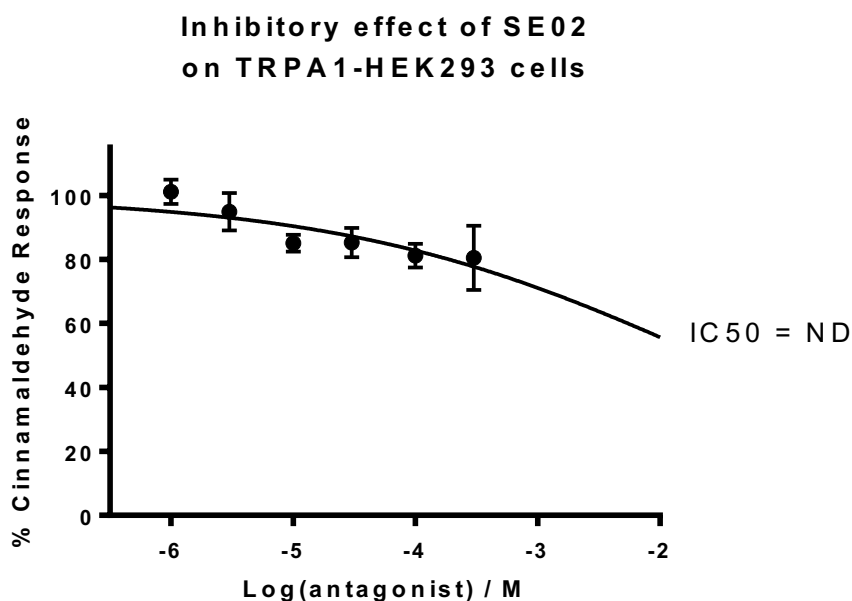
Figure 125 Antagonist concentration effect curve for SE02 on TRPA1-HEK293 cells. Data points are means±SEM of N = 3 experiments

From the preliminary screening SE02 displayed potential antagonist properties in relation to TRPA1. The Figure 125 above shows the result of a full concentration effect profile carried out using the antagonist calcium signalling assay method, detailed in section 2.2, with TRPA1-HEK293 cells.

SE02 was tested over the range of 1 µM to 300 µM, over this range the response of 30 µM of cinnamaldehyde (EC50 concentration of cinnamaldehyde) slightly decreased with increasing concentration of pre-dosed SE02. The response observed is a very weak inhibitory response with the maximum reduction observed at the 300 µM concentration point with a reduction in the cinnamaldehyde response of 20 %. The inhibitory response of

SE02 at greater concentrations could not be carried out due to the poor solubility of SE02 in the assay media. SE02 may inhibit TRPA1 fully but at high millimolar concentration levels.

4.2.4.8   SE04
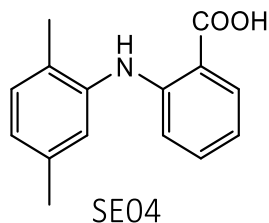
Figure 126 Chemical structure for SE04
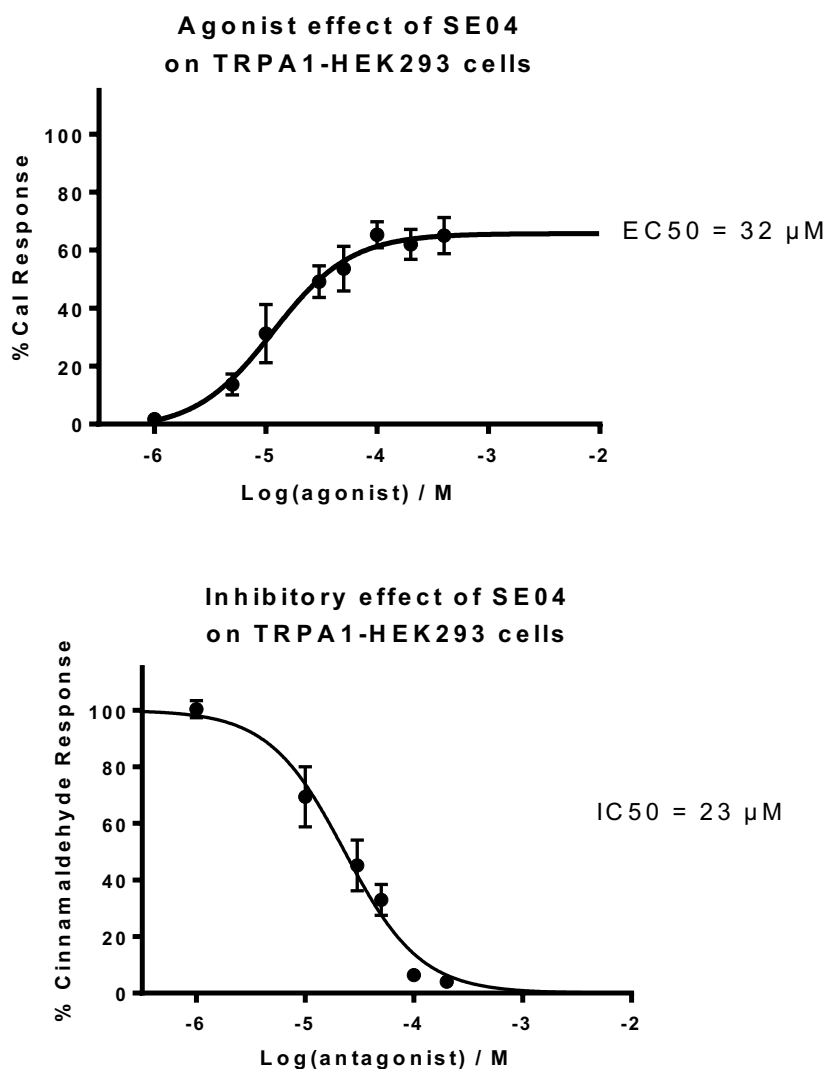
Figure 127 Agonist (above) and antagonist (below) concentration effect curves for SE04 on TRPA1-HEK293 cells. Data points are means±SEM of N = 3 experiments

From the preliminary screening SE04 displayed potential for both agonist and antagonist properties in relation to TRPA1. The Figure 127 above shows the result of a full concentration effect profile carried out using the agonist and antagonist calcium signalling assay method, detailed in section 2.2, with TRPA1-HEK293 cells.

In the agonist assay a concentration dependent increase in intracellular calcium was observed. This response was inhibited fully by the TRPA1 specific inhibitor HC-030031 therefore this response can be attributed to the gating of TRPA1 channels. SE04 was tested over the concentration range of 1 µM to 400 µM, over this range a full sigmoidal response was observed.

The first significant response is observed at 5 µM with a response of 14 %CaI. The response plateaued between 50 µM and 100 µM with the maximum response being observed at 100 µM with a response of 65 %CaI, this maximum response was 90% of the maximum response observed for cinnamaldehyde suggesting that SE04 acts as a full agonist of TRPA1. Non-linear regression analysis was carried out using the two models described in section 2.2.6. The best fit curve was produced using the variable slope four parameter model which had an R^2 value of 0.8708. This curve displays a maximum plateau which agrees with the calculated efficacy from the data points and also calculates an EC50 value of 12 µM.

The antagonist assay for SE04 was carried out over a concentration range of 1-200 µM, over which a full concentration effect curve was constructed. SE04 decreased the activation response of cinnamaldehyde on TRPA1-HEK293 cells in a concentration dependent manner. The first significant reduction was observed at the 10 µM concentration point with a reduction in the cinnamaldehyde response of 31 %. The cinnamaldehyde response was completely inhibited at the 100 µM response with a total reduction of 94 %. Non-linear regression analysis was carried out, using the models described in section 2.2.6, to fit a curve to the data points. The best fit curve was carried out using the normalised response variable slope model which has an R^2 value of 0.9189 and gave a calculated IC50 of 23 µM.

4.2.4.9   SE05

SE05

**Inhibitory effect of SE05
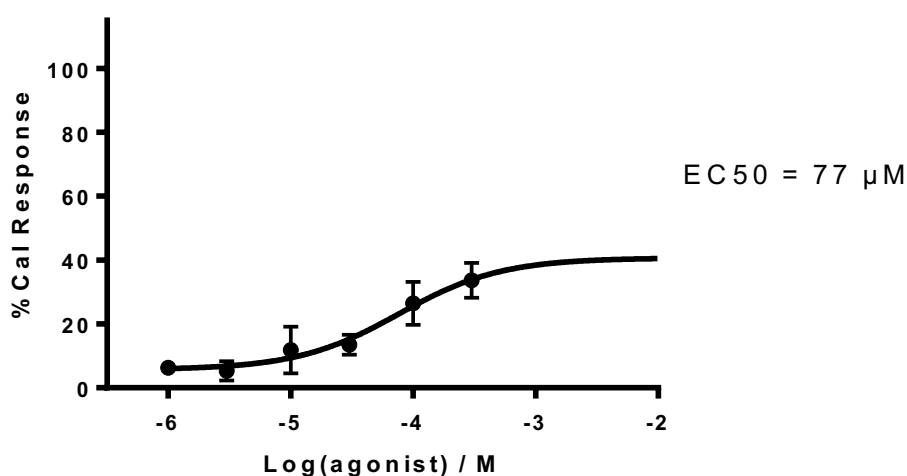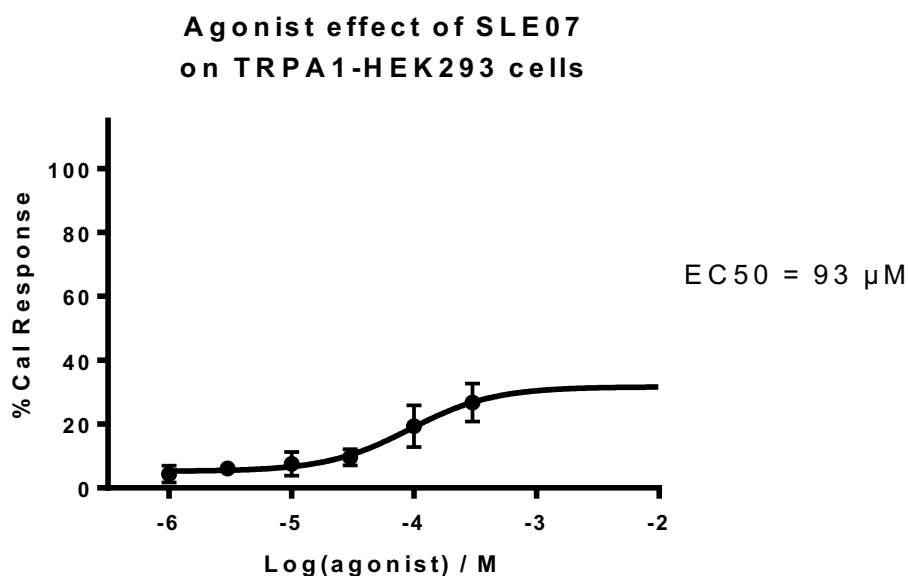on TRPA1-HEK293 cells**

IC50 = ND
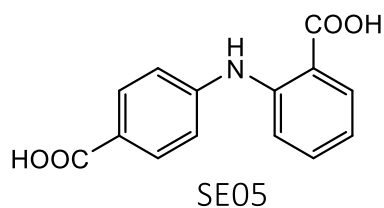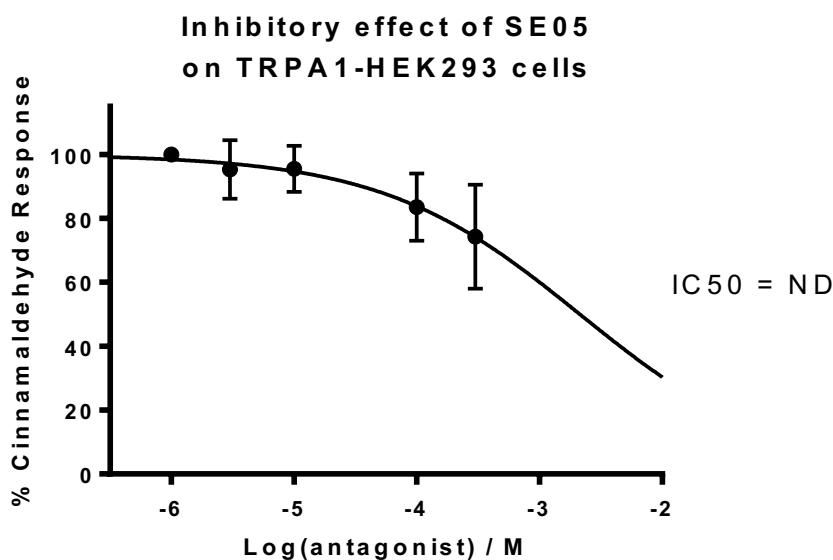
Figure 129 Antagonist concentration effect curve for SE05 on TRPA1-HEK293 cells. Data points are means±SEM of N = 3 experiments

From the preliminary screening SE05 displayed potential antagonist properties in relation to TRPA1. The Figure 129 above shows the result of a full concentration effect profile carried out using the antagonist calcium signalling assay method, detailed in section 2.2, with TRPA1-HEK293 cells.

In the antagonist assay a concentration dependent decrease in the response of 30 μM of cinnamaldehyde (EC50 concentration of cinnamaldehyde) was observed with increasing concentration of pre-dosed SE05. SE05 was tested over the concentration range of 1-300 μM. Over this range SE05 had a small inhibitory response on the activation of TRPA1 by cinnamaldehyde, a full concentration curve was not completed as greater concentrations could not be tested due to the insolubility of SE05 in the assay media at higher concentrations. The first significant reduction in the cinnamaldehyde response was observed at 100 μM with a reduction of 17 %. The maximum reduction was observed at

the 300 µM concentration point when the cinnamaldehyde response was reduced by 25 %. From the data, it is unclear as to how SE05 may inhibit TRPA1 at higher concentrations. Non-linear regression analysis was carried out, however both models used showed a poor fit to the data.
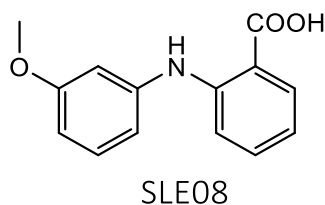
4.2.4.10   SE06
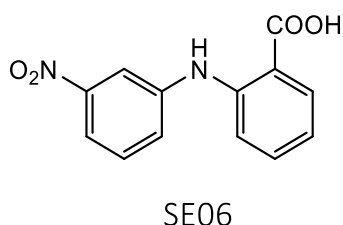
SE06

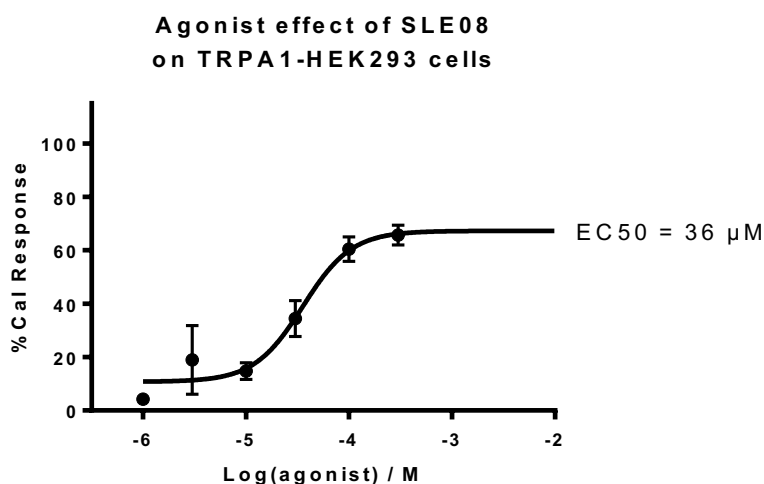*Figure 130 Chemical structure for SE06*
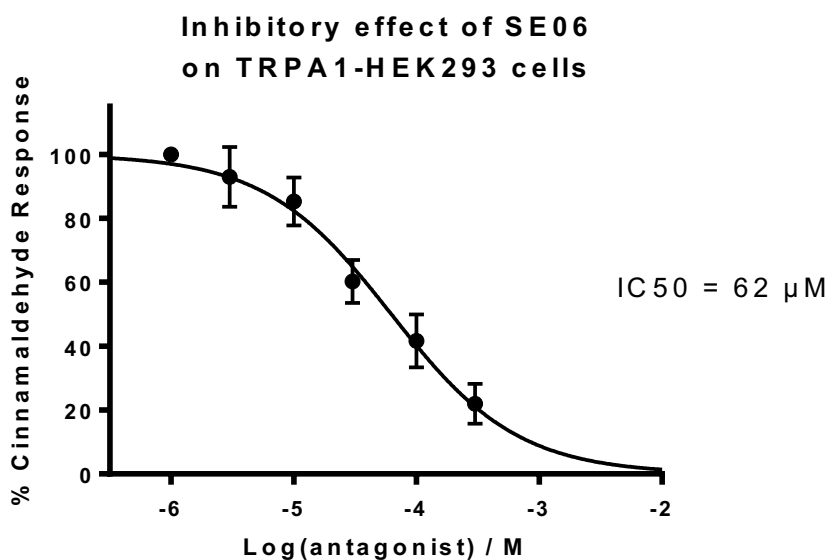
Figure 131 Antagonist concentration effect curve for SE06 on TRPA1-HEK293 cells. Data points are means±SEM of N = 3 experiments

From the preliminary screening SE06 displayed potential antagonist properties in relation to TRPA1. The Figure 131 above shows the result of a full concentration effect profile carried out using the antagonist calcium signalling assay method, detailed in section 2.2, with TRPA1-HEK293 cells.

In the antagonist assay a concentration dependent decrease in the response of 30 µM of cinnamaldehyde (EC50 concentration of cinnamaldehyde) was observed with increasing concentration of pre-dosed SE06. SE06 was tested over the concentration range of 1-

300 μM over this range an almost complete sigmoidal concentration effect curve was observed. Greater concentrations could not be tested due to the insolubility of SE06 in the assay media at higher concentrations.

The first reduction in the cinnamaldehyde response was observed at the 10 μM concentration point with a 15 % reduction in the cinnamaldehyde response. The maximum reduction in the cinnamaldehyde response was observed at the 300 μM concentration point with a reduction of 78 %.

 Non-linear regression analysis has been carried out using the two models described in section 2.2.6 in order to predict the nature of SE06's inhibitory response at greater concentrations than those tested. Both curves fit the data to the same degree both with R^2 values of 0.83, the variable slope four parameter curve predicts full inhibition which matches with a visual assessment of the data points. Therefore it can be deemed that SE06 inhibits TRPA1 activation by cinnamaldehyde fully. The calculated IC50 from the normalised curve variable slope model is 62 μM.

4.3 Discussion

The results reported in section 4.2 shall be discussed in this section and any structure activity relationships shall also be explored.

4.3.1 Fenamic acid and related NSAIDs
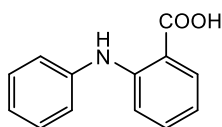
Fenamic acid
EC50 = 71uM
Efficacy = 96%
IC50 = 151uM
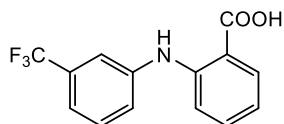
Flufenamic acid
EC50 = 24uM
Efficacy = 107%
IC50 = 8uM
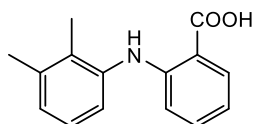
Mefenamic acid
EC50 = 34uM
Efficacy = 109%
IC50 = 10uM
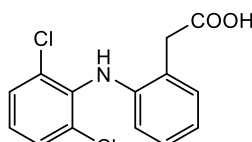
Diclofenac
EC50 = 61uM
Efficacy = 63%
IC50 = 11uM
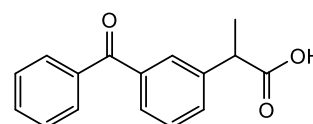
Ketoprofen
EC50 = 111uM
Efficacy = 44%
IC50 = ND

Figure 132 Chemical structures and summary of assay results of fenamic acid and related NSAIDs
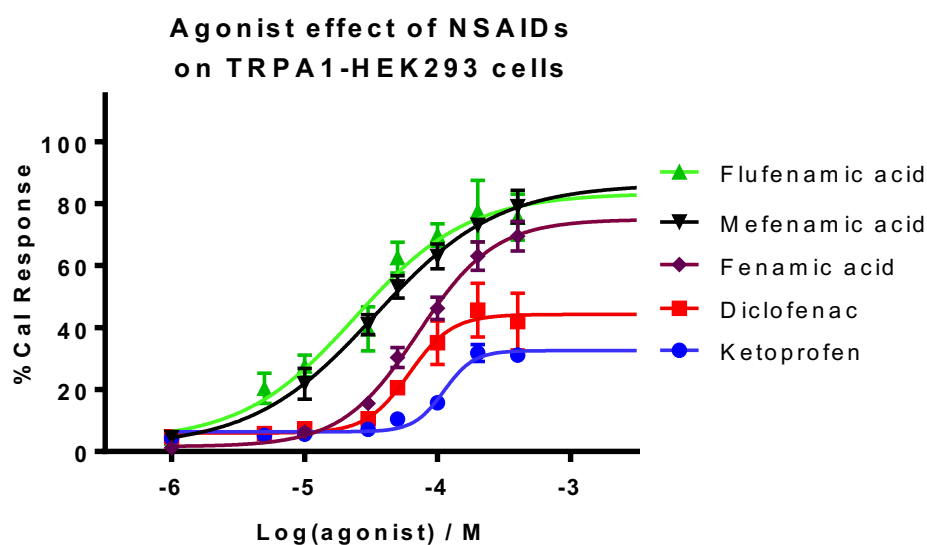
Figure 133 Comparison of agonist concentration effect curves for fenamic acid based NSAIDs on TRPA1-HEK293 cells. Data points are means±SEM of N = 3 experiments
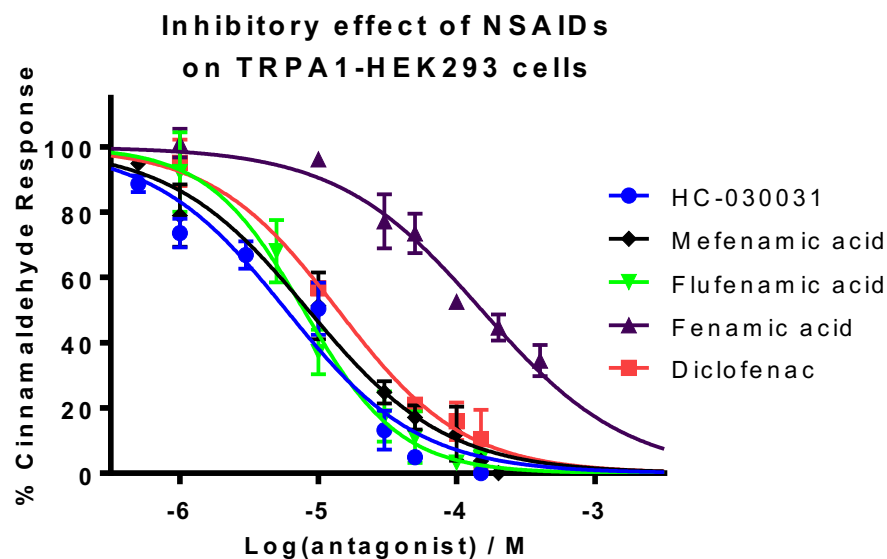
Figure 134 Comparison of antagonist concentration effect curves for fenamic acid based NSAIDs on TRPA1-HEK293 cells. Data points are means±SEM of N = 3 experiments

As can be seen in section 4.2.2, a selection of fenamate NSAIDs have been assayed using the agonist and antagonist calcium signalling methods (see section 2.2). Alongside the NSAIDs, fenamic acid, the parent molecule for these NSAIDs has also been assayed. The comparison graphs for their respective agonist and antagonist concentration effect curves on TRPA1-HEK293 cells can be seen in Figure 133 and Figure 134. What can immediately be seen is the range in efficacy and potency of their agonist responses. The results from the antagonist tell a different story as FFA, MFA and DFC all display a similar antagonist response, which is much greater than their parent molecule fenamic acid.

Compounds	EC50 (μM) on TRPA1 expressing WI-38 fibroblasts(141)	EC50 (μM) on TRPA1-HEK293 cells from results section 4.2.2
Flufenamic acid	24	24
Mefenamic acid	61	34
Diclofenac	210	61
Ketoprofen	>500	111

Table 27 Comparison table for EC50 values from Hu et al. 2010(141) and reported results from section4.2.2

Firstly, the results reported must be compared to that of Hu *et al.*(141) who first reported the activation of TRPA1 by fenamate NSAIDs. They reported that FFA, MFA, DFC and Ketoprofen activated human and rat TRPA1 expressed in a variety of different systems in a

concentration dependent manner. They reported EC50 values of FFA, MFA, DFC and ketoprofen for endogenously expressed human TRPA1 in WI-38 fibroblasts, which can be seen in Table 27. They also reported the EC50 of FFA for human TRPA1 transfected HEK293 cells, which was 57 μM. The only comparison between the two TRPA1 systems is the response for FFA. In the HEK293 system FFA's potency was more than double that recorded in the WI-38 fibroblast system. The results that I have reported in section 4.2.2 can be seen in Table 27. When compared to the results reported by Hu *et al.*(141) it can be seen that my results follow a similar trend with regards to the order of potency. The EC50 for FFA in my TRPA1-HEK293 cells is slightly more potent than that reported by Hu *et al.*(141) in TRPA1-HEK293 cells. There seems to be no significant difference between my TRPA1-HEK293 system and that of Hu *et al.* as the EC50 values for FFA do not differ by a significant margin. However, it seems that TRPA1 in my system is slightly more sensitive to the agonist effect of DFC and ketoprofen as there seems to be a significant difference in EC50 values between my system and the TRPA1 WI-38 fibroblast system of Hu *et al.*(141), the reason for this is unclear as there is no significant difference in the results obtained for FFA and MFA.

My results confirm the validity of the results reported by Hu *et al.*(141) and in doing so validate my assay method as a reliable system to determine the effects of chemical compounds on human TRPA1.

From the agonist and antagonist results for the four NSAIDs and fenamic acid several key points can be made with regards to their structure activity relationship with TRPA1. The importance of the N-phenylanthranilic acid structure to the activation of TRPA1 is clear as fenamic acid, FFA, MFA, all show a full and potent agonist response, whereas ketoprofen shows a partial agonist response with a low potency. Ketoprofen and fenamic acid differ in structure a fair amount as can be seen from Figure 132. One of the key differences being the functional group of the linker between the two phenyl groups. Fenamic acid has an amine group linking the two rings which is capable of hydrogen bonding as both an acceptor and a donor whereas ketoprofen has a ketone linker group which is only a hydrogen bond acceptor. It may be that the greater versatility of hydrogen bonding of the amine group allows for a greater interaction with TRPA1 resulting in a more potent and efficacious response. It must also be noted that the ketone group of ketoprofen can also

react with nucleophiles and it maybe that ketoprofen covalently binds to TRPA1 cysteine residues causing channel gating. This was discussed with regards to the amide and ester linker groups for the ojk01 compounds in chapter 3, with a similar trend being observed in that the hydrogen bonding amide compounds achieved a greater agonist response than the ester compounds on TRPA1-HEK293 cells.

However, having compared fenamic acid and ketoprofen purely based on the nature of the linking group the position of the carboxylic acid must also be considered and the effect it has on any binding that takes place. It appears that the position of the carboxylic acid group may have an effect on the activation of TRPA1 by DFC. DFC's carboxylic acid group is a phenylacetic acid group which separates the acid group and the phenyl ring by one carbon atom as opposed to fenamic acid which has a benzoic acid group, where the acid group is directly bonded to the phenyl ring. This separation, in DFC, between the acid group and the phenyl ring means that the electron withdrawing effect of the acid group will not be able to take place, which may be the reason why DFC has a lower efficacy and potency of activation than the N-phenylanthranilic acid NSAIDs. The effect of the chloro groups that DFC has and whether they contribute to its lower efficacy has not yet been considered. In chapter 3 the effect of chloro groups was discussed with regards to the ojk01 chloro derivatives. It was shown that chloro groups that are ortho and meta to the linking group increased the potency and efficacy of TRPA1 activation. DFC has two chloro groups; both are ortho to the amine linking group which based on the chapter 3 can be presumed to have a positive effect on the agonist response for DFC. Therefore, there is strong evidence which indicates that the benzoic acid group of the N-phenylanthranilic acid compounds is key to the TRPA1 agonist response, however without a direct comparison to a benzoic acid derivative of DFC (see Figure 135 for structure) this cannot be proved definitively.

phenylacetic acid group

benzoic acid group

Diclofenac
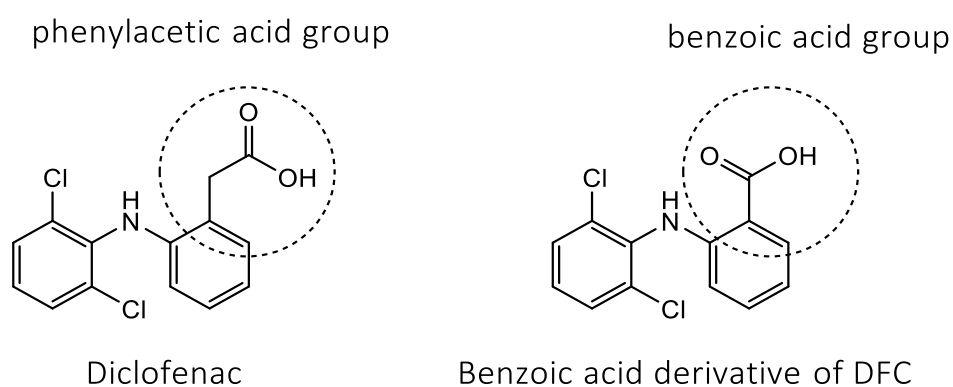
Benzoic acid derivative of DFC

In Table 28 the LogP values of the five compounds assayed can be seen. It is of interest to note that the more potent agonists and antagonists such as flufenamic acid and mefenamic acid have a higher LogP value. The lower potency of DFC and ketoprofen compared to FFA and MFA maybe due to a lower LogP value. It may be the case that TRPA1 activation occurs inside the cell and a lower plasma membrane penetration would lead to lower potency.

Compound	LogP
Fenamic acid	4.4
Flufenamic acid	5.25
Mefenamic acid	5.12
Diclofenac	4.51
Ketoprofen	3.12

Table 28 LogP values for fenamic acid based NSAIDs, values taken from PubChem

Hu *et al.* (141) commented on FFA desensitising TRPA1 after initial activation, yet they did not report any comprehensive results. I have reported full concentration effect curves for the desensitisation of TRPA1 by fenamic based NSAIDs, and the results show that desensitisation may occur through an independent mechanism of activation. The results from the antagonist assay show that FFA, MFA, DFC have a strong desensitising effect on TRPA1, fenamic acid has also been shown to have a desensitising effect but was found to be a lot less potent. Ketoprofen was not found to have a desensitising effect on TRPA1 over the concentrations tested. The comparison of the concentration effect curves from the antagonist assay can be seen in Figure 134.

With regards to the discussion above it was mentioned that the lower LogP value of DFC meant that it was unable to cross the plasma membrane to the same degree as FFA and MFA and therefore was found to be a weaker agonist of TRPA1. However, the results from the antagonist assay do not show the same degree of difference in response between DFC and FFA. This may be due to several factors, firstly the site of interaction with TRPA1 which produces the desensitisation may be outside of the cell, therefore there is no need for DFC to pass through the plasma membrane. Secondly, it could be that the incubation time which is part of the method allows DFC to fully dissolve across the plasma membrane and reach its equilibrium and therefore the full desensitisation effect of DFC has been recorded.

Thirdly, it could be the case that DFC has a greater binding affinity to the TRPA1 site at which desensitisation occurs than FFA and MFA but this is masked because of DFCs inability to fully diffuse across the plasma membrane.

FFA and DFC may both desensitise through the same mechanism as A96 and AP-18 to inhibit TRPA1 as all compounds have aryl halide groups, except FFA which has a trifluoromethyl group bonded to a phenyl ring. Similarly, to the chloro derivatives of ojk01, ojk06 and ok07 which have been discussed in chapter 3. As for MFA, it may desensitise through the same mechanism as FFA and DFC or it could be through a different mechanism altogether. At this point it is unsure and further research is required. What can be concluded from these results is that alterations to the core fenamic acid structure increases the TRPA1 desensitisation effect.

4.3.2 Novel synthetic derivatives of fenamic acid

In results section 4.2.3, a group of novel synthesised derivatives of fenamic acid were screened for agonist and antagonist properties in calcium signalling assays using TRPA1-HEK293 cells. From this screening process, several of the compounds were found to have an agonist response and several others were found to show an antagonist response against TRPA1. All of the compounds screened can be seen in Figure 136, with the agonist hits circled in green and the antagonist hits circled in red. These compounds have been previously tested on TRPC4/5 and TRPM2 and have shown that slight variations in the structure have a great effect on the modulations on these channels. The results found in section 4.2.4 also show that small variations in chemical structure have a great effect on the modulation of TRPA1(152,208).
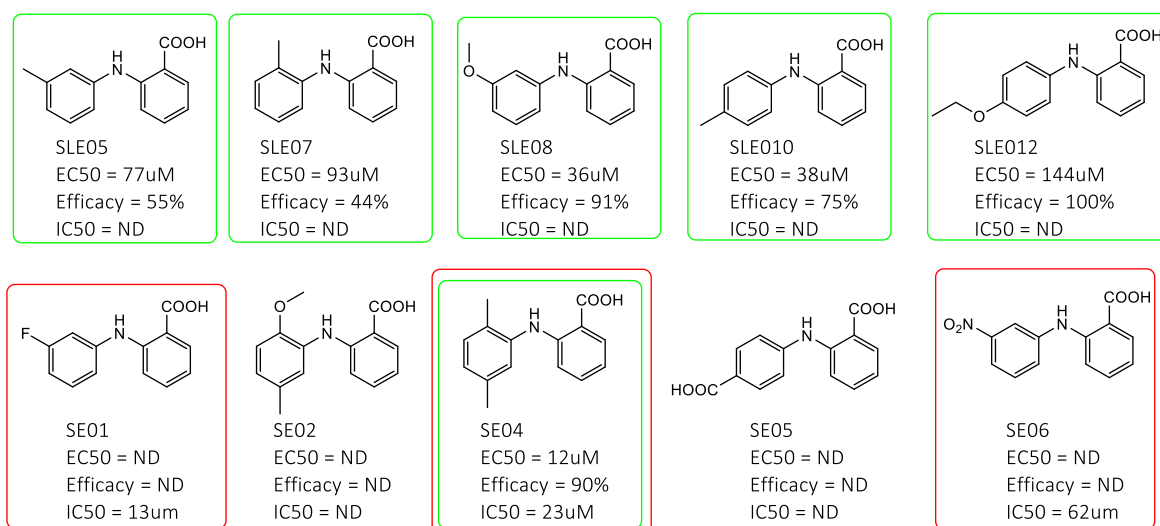
Figure 136 Chemical structures and assay result summary for fenamic acid derivatives

The following sections will discuss the results obtained from these novel synthetic fenamic acid derivatives with regards to structure activity relationships, comparisons to the NSAIDs TRPA1 assay results (discussed in section 4.3.1) and to similar results reported in the literature.

4.3.2.1   Comparison of methyl fenamic acid derivatives

The effect on TRPA1 by the methyl derivatives of fenamic acid have been shown in Figure 137. From the results, it can be seen that fenamic acid has the highest efficacy of the four compounds and is the only one to have a desensitising effect after the initial activation. The ortho methyl derivative, SLE07, has the lowest potency and efficacy. This may be due to the effect of the methyl group on the amine linker; it may prevent hydrogen bonding due to the steric effects of the methyl group; also it will reduce the conformational freedom of the amine linker therefore preventing conformations which may be beneficial to binding. The efficacy and potency increases as the distance between the methyl group and the amine group increases with SLE010, the para methyl derivative, being the most potent of the four compounds. Yet still SLE010 has a lower efficacy than fenamic acid, the reason for the difference in efficacy between these two compounds is unclear, as previously discussed in section 4.3.1 differences in efficacy may arise from the ability of the compound to cross the plasma membrane, in this instance this is not the case as both fenamic acid and SLE010 will have very similar LogP values, with SLE010 being slightly more lipophilic.

Fenamic acid
EC50 = 71uM
Efficacy = 96%
IC50 = 151uM

SLE05
EC50 = 77uM
Efficacy = 55%
IC50 = ND

SLE07
EC50 = 93uM
Efficacy = 44%
IC50 = ND

SLE010
EC50 = 38uM
Efficacy = 75%
IC50 = ND
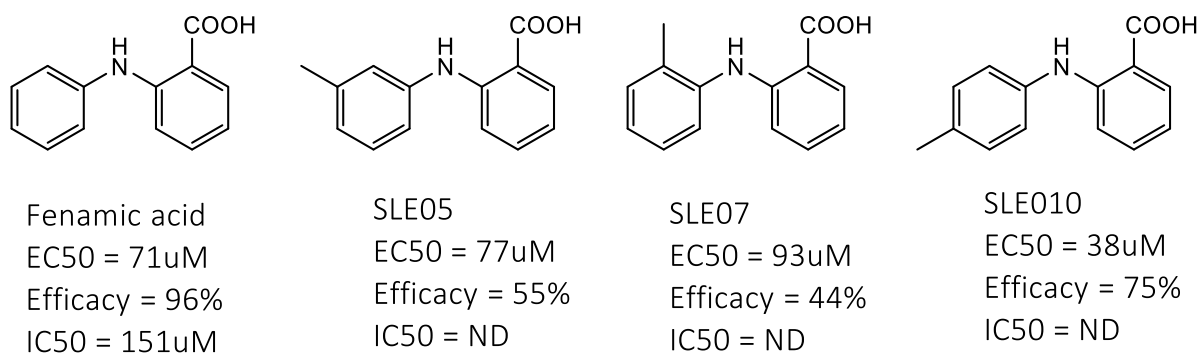
Figure 137 Chemical structures and summary of assay results for methyl derivatives fenamic acid
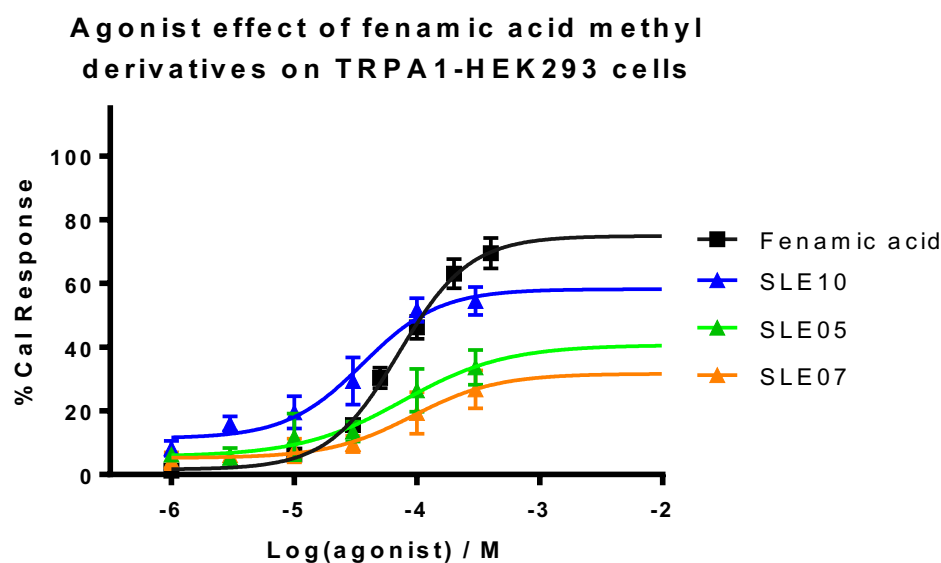
Figure 138 Comparison of agonist concentration effect curves for methyl derivatives of fenamic acid on TRPA1-HEK293 cells. Data points are means±SEM of N = 3 experiments

4.3.2.2   Comparison of di-substituted fenamic acid derivatives

Fenamic acid
EC50 = 71uM
Efficacy = 96%
IC50 = 151uM

Mefenamic acid
EC50 = 34uM
Efficacy = 109%
IC50 = 10uM

SE04
EC50 = 12uM
Efficacy = 90%
IC50 = 23uM

SE02
EC50 = ND
Efficacy = ND
IC50 = ND
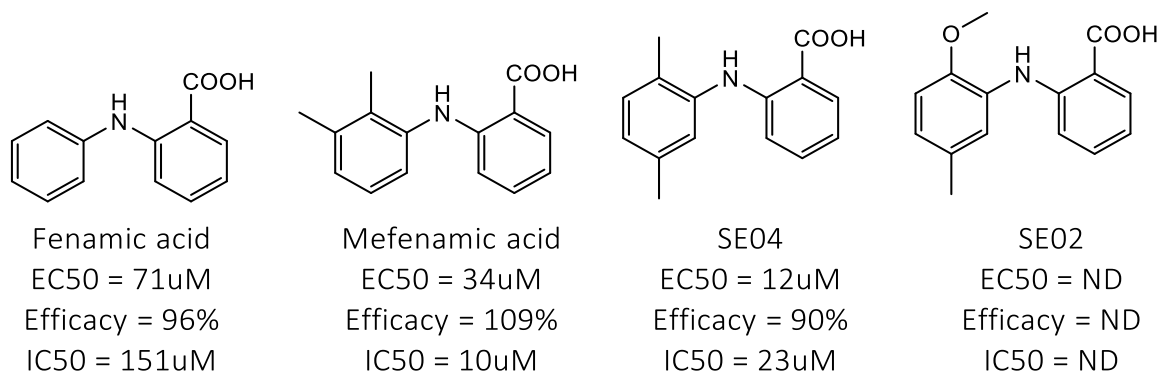
Figure 139 Chemical structures and summary of assay results for di-substituted derivatives of fenamic acid

Two dimethyl derivatives, mefenamic acid and SE04, have been shown to modulate TRPA1. Comparisons of their agonist and antagonist concentration effect curves can be seen in Figure 140 and Figure 141. Both of the dimethyl derivatives show a greater potency of activation and desensitisation of TRPA1 than the parent molecule, fenamic acid. In comparison to the results found for the monomethyl derivatives (see Figure 137) it appears that the dimethyl arrangement has a synergistic effect on the modulation of TRPA1. The results suggest that the 2,3-dimethyl arrangement gives a greater desensitisation effect, whereas in the 2,5-dimethyl arrangement yields a greater agonist effect on TRPA1.

In addition to the two dimethyl derivatives SE02, a 2-methyoxy-5-methyl derivative, has been tested on TRPA1-HEK293 cells results can be seen alongside the two dimethyl derivatives in Figure 139. A comparison of the SE02 and SE04 antagonist concentration effect curves can be seen in Figure 141. It can be seen that SE02 only has a small reduction on the activation of TRPA1 by cinnamaldehyde at the concentrations tested. SE02 did not show a response when carrying out the preliminary screen (see section 4.2.3) and is deemed not to activate TRPA1. SE04 is the most potent agonist of TRPA1 and has one of the strongest desensitising effects. The only difference between the two compounds is that SE02 has a 2-methoxy group and SE04 has a 2-methyl group instead. As previously mentioned in section 4.3.1 and chapter 3 the nature of the linking group and its ability to hydrogen bond is crucial to the modulation of TRPA1 by these double phenyl ring structures. It appears that the greater bulk of the methoxy group of SE02 may have a negative effect on the amine group with regards to its interaction with TRPA1. The results from SLE07 which is a 2-methyl derivative seem to confirm this hypothesis as the agonist response observed by SLE07 is weaker than that of fenamic acid and SE02, with its larger 2-methoxy group, does not activate TRPA1 at all.

Agonist effect of di-substituted derivatives of fenamic acid on TRPA1-HEK293 cells
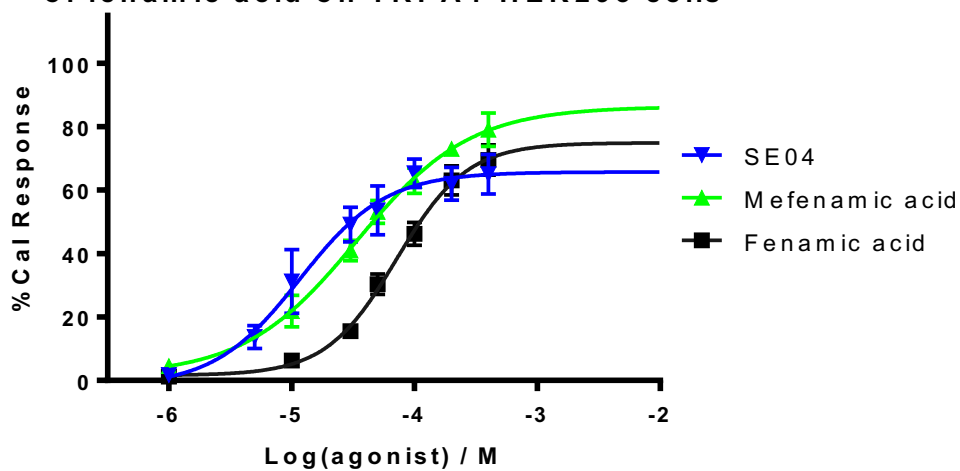
Figure 140 Comparison of agonist concentration effect curves for dimethyl derivatives of fenamic acid on TRPA1-HEK293 cells. Data points are means±SEM of N = 3 experiments

Inhibitory effect of di-substituted fenamic acid derivatives on TRPA1-HEK293 cells
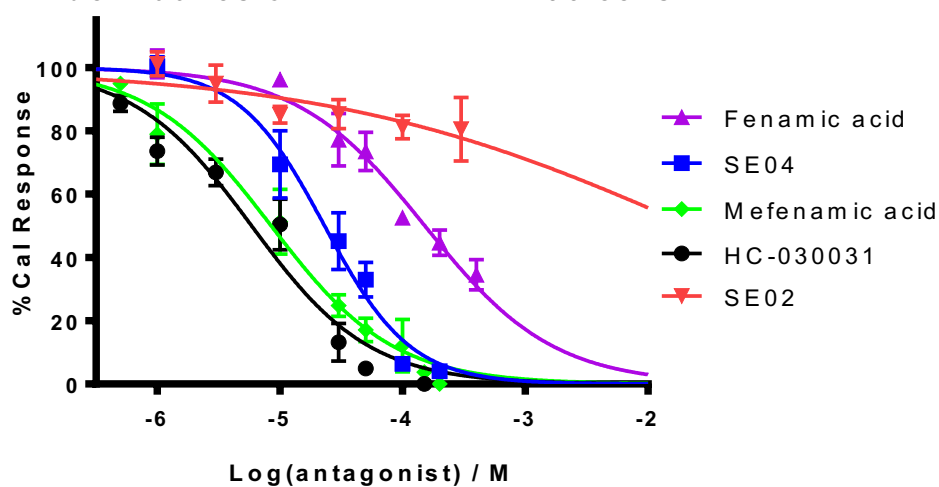
Figure 141 Comparison of antagonist concentration effect curves for dimethyl derivatives of fenamic acid on TRPA1-HEK293 cells. Data points are means±SEM of N = 3 experiments
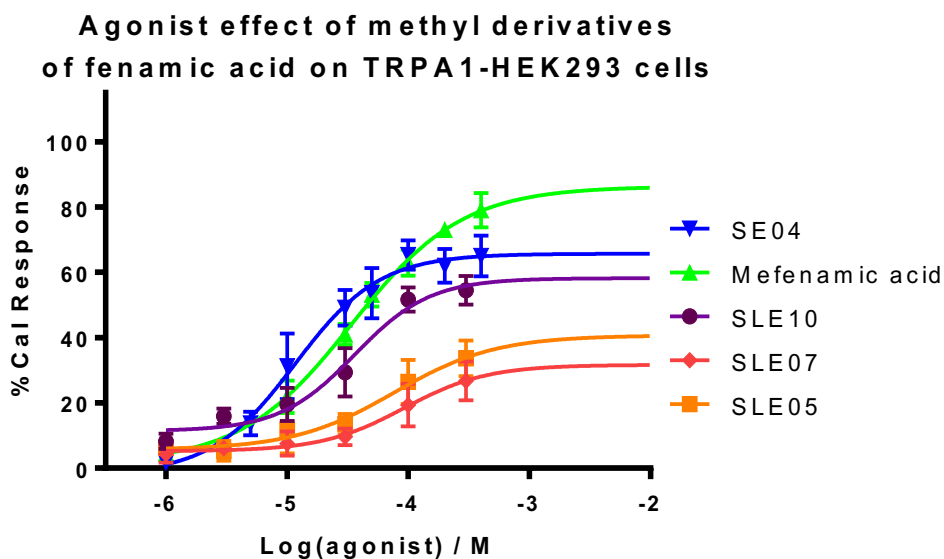
Figure 142 Comparison of agonist concentration effect curves for SE04 vs. methyl derivatives of fenamic acid on TRPA1-HEK293 cells. Data points are means±SEM of N = 3 experiments

4.3.2.3   Comparison of fenamic acid derivatives with substitutions in the meta position
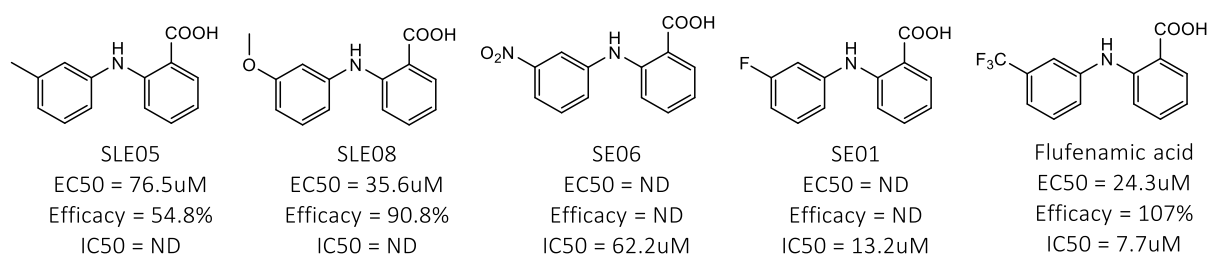
Figure 143 Chemical structures and summary of assay results for derivatives of fenamic acid with substitutions in the meta position

Of the ten fenamic acid derivatives screened four all had substitutions in the 3-position, meta to the amine group. Including flufenamic acid, these five derivatives display an interesting range of effects on TRPA1. From being a full agonist of TRPA1 with no desensitisation such as SLE08 to SE01 which is a potent antagonist of TRPA1. It is clear from the results that substitutions in the meta position strongly influences how the compound modulates TRPA1.

SLE05 and Flufenamic acid are both very similar in terms of size; both methyl and trifluoromethyl group are almost the exact same size. The difference between the two

molecules lies solely in the differing electronic effects of their substitutions. The methyl group of SLE05 is an electron donating group which occurs through an inductive effect, whereas the trifluoromethyl group of FFA is an electron withdrawing group which also occurs through an inductive effect. SLE05 is a weak partial agonist of TRPA1 and FFA is a potent full agonist which potently desensitises TRPA1.

On the other hand, SE01 and FFA have substitutions which are similar in terms of electronic effects but differ with regards to the steric effects. SE01 has the smaller fluoro group which has an electron withdrawing effect which occurs through inductive effects, and FFA has the larger trifluoromethyl group which has an electron withdrawing effect which occurs through inductive effects. SE01 is a potent inhibitor of TRPA1 and shows no activation, whereas FFA is a potent agonist TRPA1 which also potently desensitises TRPA1 to further activation. It may be the case that the greater size of the trifluoromethyl group allows FFA to interact with the agonist binding site of TRPA1 yet still, due to the electronic effects of the group, is able to interact with TRPA1 in a way that desensitises the channel to further activation. SE01, with its smaller fluoro group is not able to interact with the agonist binding site of TRPA1 but maintains its ability to have an inhibitory effect. Taking into account the nitro derivative, SE06, then the reasoning of the greater steric bulk of the trifluoromethyl group of FFA allows it to activate TRPA1 does not agree with the results. However, the case of SE06 is not as simple as it may first seem as the nitro group is an electron withdrawing group which occurs via both inductive and resonance effects, it is also weakly acidic due to the tautomerism of nitro groups to an azinitro form. With these considerations, any binding interaction with TRPA1 by SE06 is even more complex. However, it may be the case that the nitro group is a highly polar group and therefore it is repelled from a potentially hydrophobic agonist binding pocket.
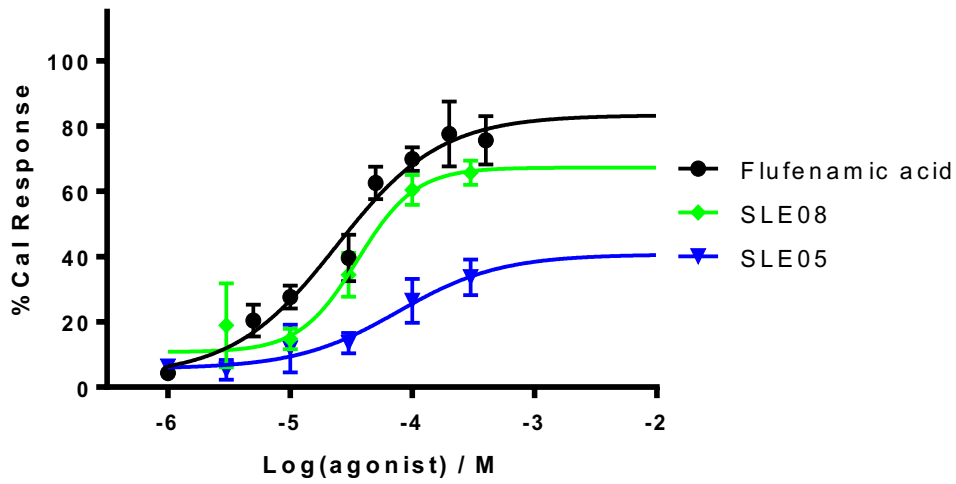
Figure 144 Comparison of agonist concentration effect curves for meta substituent derivatives of fenamic acid on TRPA1-HEK293 cells. Data points are means±SEM of N = 3 experiments
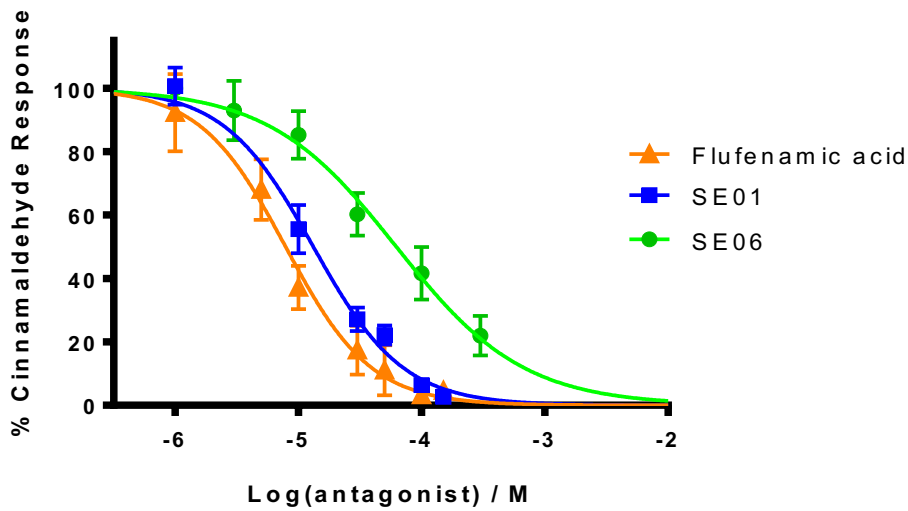
Figure 145 Comparison of antagonist concentration effect curves for meta substituent derivatives of fenamic acid on TRPA1-HEK293 cells. Data points are means±SEM of N = 3 experiments

4.3.2.4   Comparison of fenamic acid derivatives with para substitutions

SLE010
EC50 = 38uM
Efficacy = 75%
IC50 = ND

SLE012
EC50 = 144uM
Efficacy = ~100%
IC50 = ND

SE05
EC50 = ND
Efficacy = ND
IC50 = ND
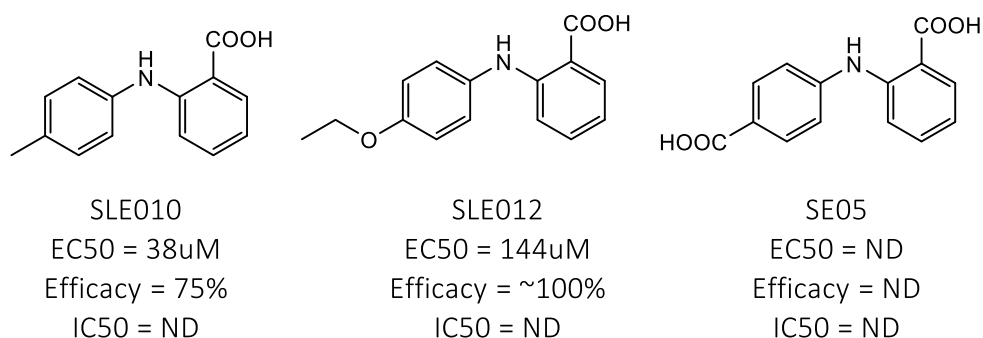
Figure 146 Chemical structures and summary of assay results for derivatives of fenamic acid with para substitutions

The para derivatives of fenamic acid have been shown to have a range of different responses on TRPA1 (summarised in Figure 146). Both SLE010 and SLE012 show agonist response with no desensitisation on TRPA1. SLE012 is a lot less potent than SLE010 and the parent fenamic acid compound. This may be due to the steric effects of the ethoxy group. In contrast, SE05 shows only a weak inhibitor response at high micromolar concentrations; the second carboxylic acid group may make it difficult for the compound to penetrate the plasma membrane in order to bind with TRPA1 due to an increased hydrophilic nature.
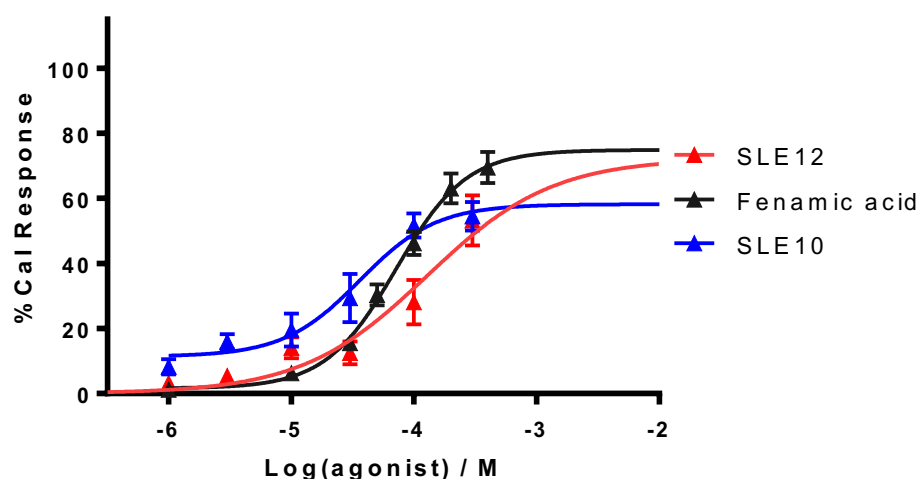
Figure 147 Comparison of agonist concentration effect curves for para substituent derivatives of fenamic acid on TRPA1-HEK293 cells. Data points are means±SEM of N = 3 experiments

4.3.2.5   Comparison of phenoxy fenamic acid derivatives

Fenamic acid	SLE08	SLE012	SE02
EC50 = 71uM	EC50 = 36uM	EC50 = 144uM	EC50 = ND
Efficacy = 96%	Efficacy = 91%	Efficacy = ~100%	Efficacy = ND
IC50 = 151uM	IC50 = ND	IC50 = ND	IC50 = ND
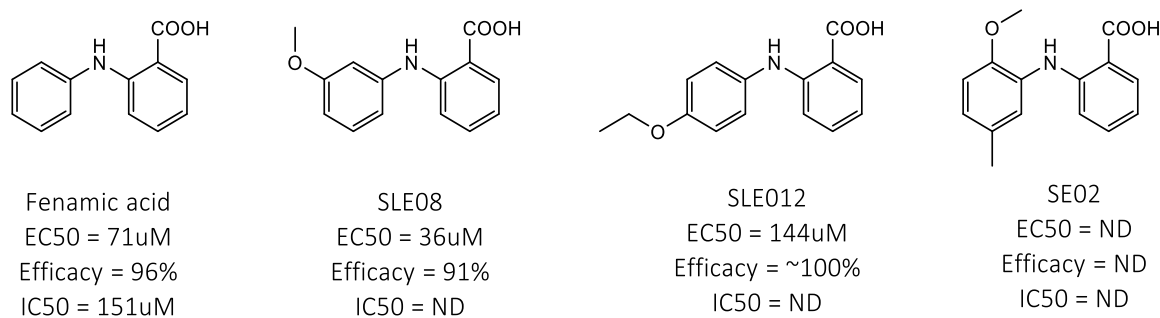
Figure 148 Chemical structures and summary of assay results for phenoxy derivatives of fenamic acid

Of the fenamic acid derivatives that have been assayed for TRPA1 activity, three are phenoxy derivatives. A summary of the results for these compounds can be seen in Figure 148. A comparison of the agonist concentration effect curves can be seen in Figure 149. From these results, it can be seen that the 2-methoxy group of SE02 has a negative impact on the compounds ability to interact with TRPA1. This has been discussed in section 4.3.2.2 when SE02 was compared to the 2,5-dimethyl derivative SE04, and it was determined that the 2-methoxy group was responsible for SE02 not affecting TRPA1 in the calcium signalling assays. This was thought to be because the group hinders the amine's ability to hydrogen bond efficiently with the binding site due to its negative effect on the conformational freedom of the amine linker. The other two phenoxy derivatives only share SE02's inability to inhibit or desensitise TRPA1, both SLE08 and SLE012 have been found to activate TRPA1 is a concentration dependent manner. It appears that the phenoxy groups in general have a negative effect on inhibition or desensitisation of TRPA1 and dependent on the size and position of the group alter the TRPA1 agonist potential of the compound. The results for SLE012 show a lower potency than its parent compound fenamic acid, this may be due to the position of the ethoxy group and the interactions that the electronegative oxygen atom can or cannot carry out, or the size of the group. SLE08 on the other hand, has a greater potency with regards to activation of TRPA1 than its parent compound. This may be due to the electronic effects of the group and as seen with FFA which has a trifluoromethyl group in the same ring position enhances the activation of TRPA1 over fenamic acid. What is interesting is that SLE08 has not been seen to have a desensitising effect after the initial activation like FFA exhibits. These results do show that electronegative groups in the 3-position seem to enhance the nature of the binding with TRPA1.

210
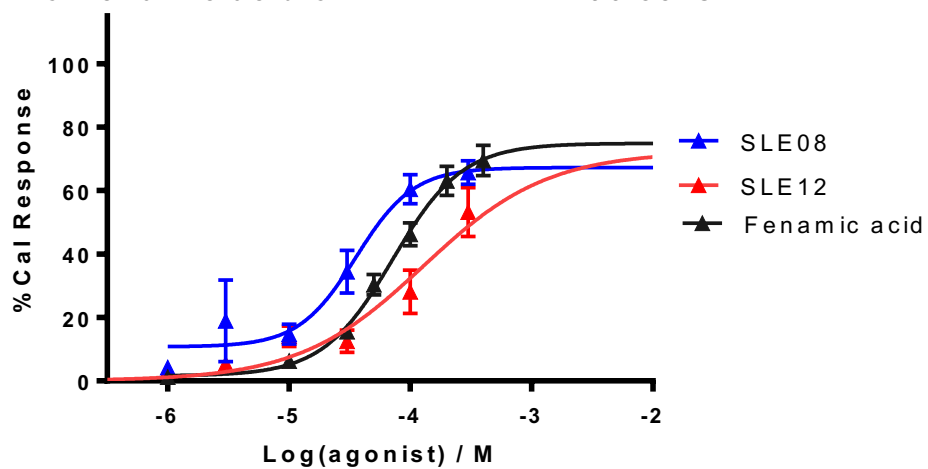
Figure 149 Comparison of agonist concentration effect curves for phenoxy derivatives of fenamic acid on TRPA1-HEK293 cells. Data points are means±SEM of N = 3 experiments

4.4 Summary and Conclusion

In this results chapter several fenamic acids and closely related NSAIDs have been assayed for activity against human TRPA1-HEK293 cells in calcium signalling assays. The results obtained from these compounds displayed similar trends to those reported by Hu *et al.*(141), therefore this confirms the validity of their results and confirms that my assay method is fit for purpose. My results also characterised the nature of the desensitising effect of these compounds unlike Hu *et al.*(141) who mentioned desensitisation of TRPA1 briefly. My results showed FFA and MFA to be potent agonists which desensitised TRPA1, with increased potency. It may be the case that the mechanism of activation is related to the desensitisation effect. DFC showed that at concentrations lower than ~30 µM it acted purely as an inhibitor of TRPA1; above this concentration DFC was shown to act as a partial agonist, possibly due to a lower LogP value than FFA and MFA. It was also determined that the N-phenylanthranilic acid structure is key to the interaction with TRPA1 as ketoprofen which has a ketone linker group and a phenylacetic acid group was found to be a poor agonist of TRPA1 and showed no antagonism of the channel either.

Following on from the results reported for the fenamic acid like NSAIDs a group of ten fenamic acid derivatives, previously assayed for TRPC4/5 and TRPM2 activity, were assayed for TRPA1 activity(152,208). The results obtained for these derivatives show that small changes in the substitutions on the phenyl ring can have a large effect on the interaction with TRPA1. For example, SE01 the 3-fluoro derivative showed a strong inhibitory effect on TRPA1 whereas FFA was a strong agonist of TRPA1 with a subsequent desensitising effect. The effect of the 2-methoxy group of SE02 was shown to interrupt any potential activities with TRPA1 hypothesised to be due to the group's effect on the amine linking group.

The results that have been reported in this chapter detail how biologically diverse fenamic acid based compounds are, especially with regards to TRP channel modulation. With regards to TRPA1 modulation, these compounds have shown that small changes in the structure have a diverse effect on the activation and inhibition of the channel. The compounds that have been tested show potential to be used as pharmacological tools in research to further understand the complexities of TRPA1. Also, due to the fact that there

are several fenamic acid based licensed drugs some of these compounds, SE01 for example, may provide a good starting point to develop a drug that targets TRPA1.

5 The activation of TRPA1 by NDGA and Terameprocol

5.1 Introduction

5.1.1   Nordihydroguaiaretic acid

The use of plants for medicinal purposes has occurred throughout human history. Civilisations across the world have been utilising the herbs and plants at their disposal to treat all kinds of ailments. In recent times the physiological effects of herbal remedies have been studied and key active ingredients discovered to be effective treatments. This method of research is a proven drug discovery route with the most famous example being salicylic acid, an extract of willow tree bark, and its derivative aspirin, which is one of the most used drugs worldwide. Today many people still look to herbs and plants as medical therapies, the World Health Organisation in 1985 estimated that 65-80 % of the world's population relies on herbs for their medical needs(209). It is clear that much can still be learned from the natural world. One recent example is the use of the plant *Larrera tridentata* to treat a myriad of ailments throughout indigenous civilisations around the Central America and the south-west of Northern America, where the plant can most commonly be found. It has been thought that one of the extracts of *Larrera tridentata,* Nordihydroguaiaretic acid (NDGA) may be responsible for the therapeutic effect that medicinal preparations of *Larrera tridentata* may have(210). Many studies have reported the physiological effects of NDGA and highlighted its strong antioxidant, antineoplastic, antiviral and anti-inflammatory properties(210).

Larrera tridentata is commonly known as creosote bush on account of its strong odour. In the United States it is known as chapparal or greasewood (Figure 150). It grows abundantly throughout the desert areas of northern Mexico, and the south-west states of the USA such as Arizona, California, Nevada, Texas and New Mexico, (see Figure 151 for where the creosote bush can be commonly found in the USA)(210). It has been an important medicinal plant for many of the indigenous tribes of North America. They used a variety of methods to extract and prepare the creosote bush to use as treatments for many ailments such as chicken pox, skin sores, diabetes, kidney and gallbladder stones, cancer, colds and rheumatism(211). The most common preparation was an aqueous extraction of the leaves referred to as chaparral tea, which is reported to effectively dissolve kidney and gallbladder stones(211)(210).
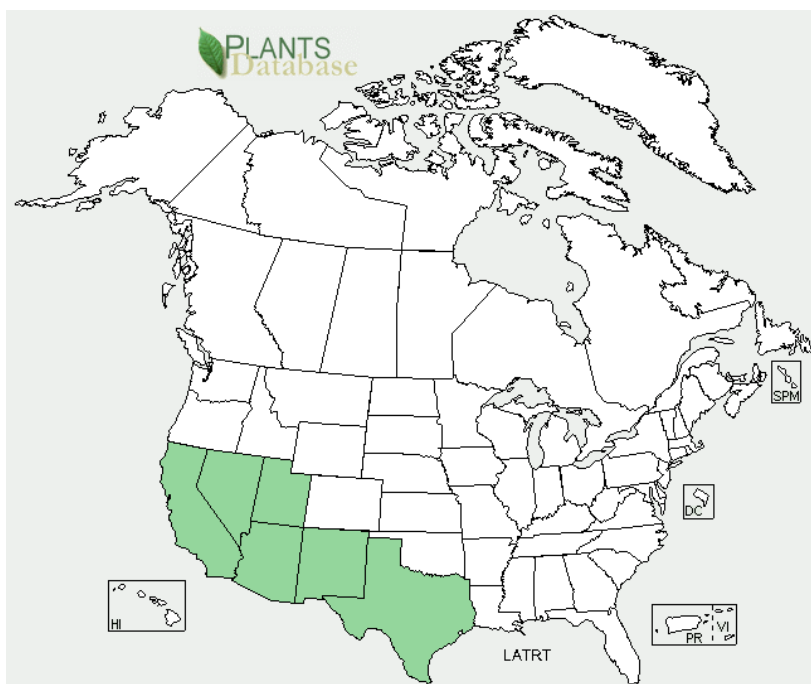
Many different natural products can be extracted from the creosote bush's leaves in good yield; approximately 50 % of the leaves' dry weight is extractable matter. The leaves are shiny with a thick resin coating, which discharges a strong odour, which is reminiscent of creosote hence its common name, and a sour flavour. NDGA is extracted from the leaves, accounting for 5-10 % of the leaves' dry weight, alongside multiple flavonoid aglycones, essential oils, halogenic alkaloids and several lignans(212). NDGA is found in the thick resin that coats the leaves and serves to protect the leaves, due to its possible antimicrobial properties. In addition it protects against UV radiation and water loss, both of which are important to the survival of the species in the harsh desert conditions.

Nordihydroguiaretic acid
(NDGA)
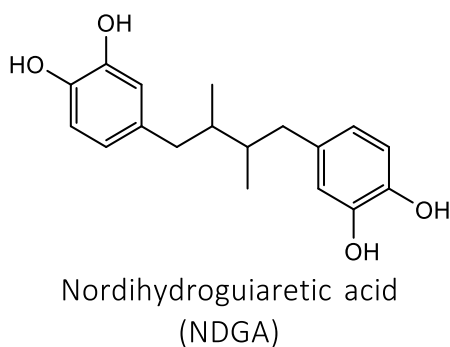
Figure 152 NDGA structure

The structure of NDGA can be seen in Figure 152. It is a polyphenol-bearing o-dihydroxy structure, or catechol structure. NDGA has been highlighted as a strong antioxidant. When compared to other known antioxidants, such as uric acid, glutathione, penicillamine and mannitol, NDGA was found to be more efficient at scavenging the reactive oxygen species (ROS) $ONOO^-$, $^1O_2$, $\bullet OH$ and $O_2^{-\bullet}$(213). The two catechol groups act as reducing agents and therefore one molecule of NDGA can reduce four equivalent ROS. The strong antioxidant properties of NDGA suggests that it may be used in the fight against cardiovascular disease as regulation of free radical levels can potentially play a role in the development of disease in the vasculature. Several groups have noted the vasoprotective effects of NDGA. They have observed the enhanced expression of endothelial nitric oxide synthase (eNOS) in cultured endothelial cells when treated with NDGA. Increases in the bioavailability of eNOS have been observed to substantially reduce endothelial dysfunction (214–217).

NDGA has recently been identified to have a significant role in cancer therapy. NDGA application has shown inhibition of growth in a variety of cell lines and animal models(210,218–221) and has been shown to suppress lung cancer growth in cell lines(222). The nature of the mechanism through which NDGA is anti-tumorigenic has yet to be fully elucidated. *In vivo* studies have shown that NDGA suppresses tumour growth by inhibiting metabolic enzymes as well as RTK phosphorylation, which is overexpressed in some cancer cell lines(223).

Due to NDGA's antioxidant properties research has been carried out to find out its effectiveness in treating neurological disorders such as cerebral ischemia and Alzheimer's disease as it is believed free radicals are responsible for neuronal injury(224). A study has shown the effectiveness of NDGA in preventing neuronal injury of cultured hippocampal neurons from rats(225). The study concluded that NDGA's neuroprotective role was likely linked to its lipoxygenase inhibition and antioxidant properties.

Although NDGA has been used for centuries in herbal medicines and later on in the 20th century as a food preservative, the FDA has generally regarded it as safe until 1968. The use of *Larrera* products appears to be harmless however strong doses have been associated with dermatitis, nephrotoxicity, biliary toxicity, and hepatotoxicity in humans(226–228). Structural modification of NDGA has been seen to reduce the toxicity, for example, the recorded LD50 of NDGA in mice is 75mg/kg, yet the tetramethylated derivative of NDGA,

Terameprocol (M4N)(see Figure 153 for structure) as it is commonly known, is well tolerated by mice with an LD50 dose of 1000mg/kg(226).
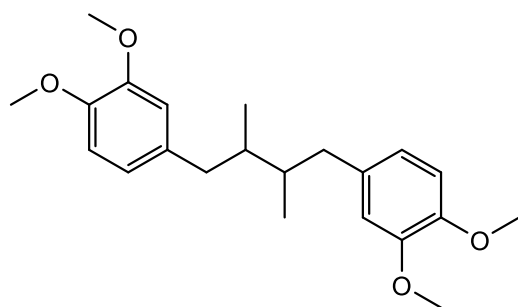
Teremeprocol
(M4N)

Figure 153 Structure of Terameprocol

Due to the toxicity of NDGA its potential for therapeutic use is limited, however research interests have shifted towards M4N, which shows similar properties to NDGA but is far less toxic. M4N has been shown to inhibit the secretion of cytokines, chemokines and inflammatory lipids from activated macrophages in the same way as NDGA does(229–231).

5.1.2   TRPM7 overview

TRPM7, also referred to as TRP-PLIK, ChaK1 or LTRPC7 is a Mg2+ and Ca2+ permeable ion channel, which is covalently bound to an alpha-type Ser/Thr protein kinase domain(232). It has been found to be vital in magnesium homeostasis. It has been found to be expressed in all cells throughout the human body(43,233,234). TRPM7 is 1863 amino acids in length and has been postulated to form a four member multimeric TRPM7 channel complex, the same as the majority of TRP channels(232). Similarly, to the majority of TRP channels, TRPM7 comprises six TM helices with TM5 and TM6 believed to form the channel pore, see Figure 154. TRPM7 shares most similarity to TRPM6, with 49 % primary amino acid sequence similarity. TRPM6 has also been found to be crucial for systemic Mg2+ homeostasis in humans(235).
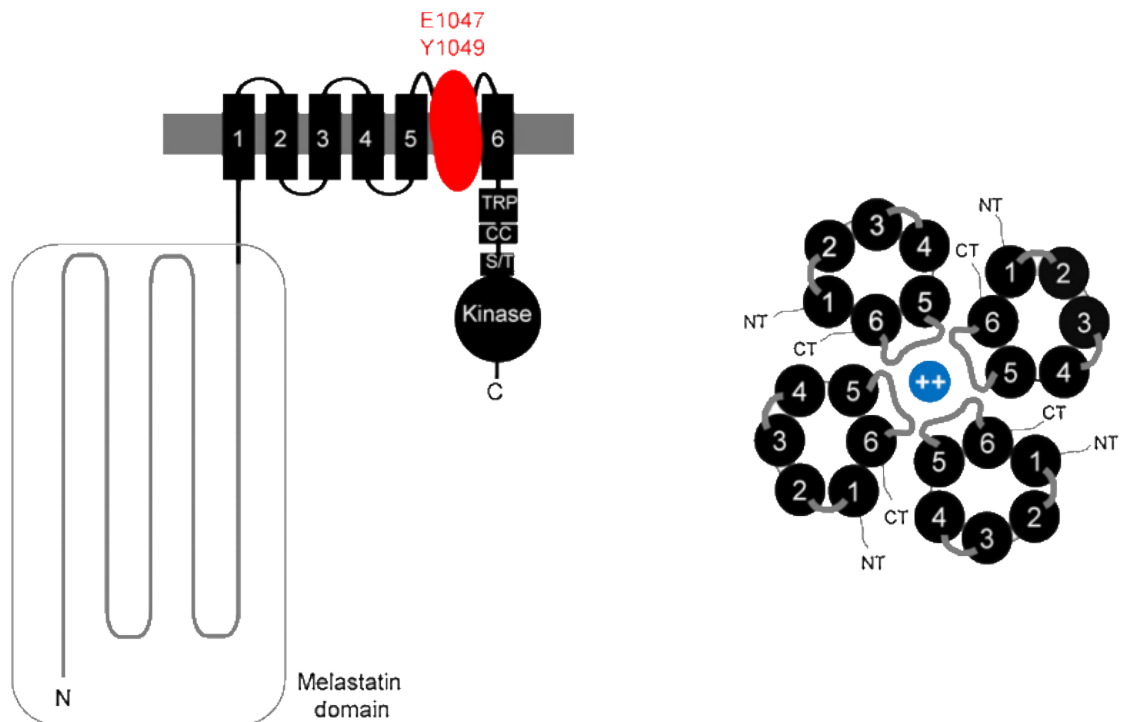
Figure 154 Left: Structure of TRPM7 protein subunit. Right: Top down view of TRPM7 channel with pore domain formed between TM5 and TM6. Image altered from Paravicini et al. 2012(232)

The most notable feature of TRPM7 (and TRPM6) is the protein kinase domain found in the C-terminus. The kinase domain is an alpha kinase that can phosphorylate serine and threonine residues located on alpha helices. A summary of the TRPM7 subunit can be seen Figure 154. Crystallography analysis has shown that the structure of this kinase domain is remarkably similar to that of cAMP-dependent protein kinase A, as it consists of two lobes next to the nucleotide binding site(236).

TRPM7 is a constitutively active channel regulated by intracellular Mg2+ and Mg-ATP. A potential selectivity filter made up of tyrosine and a negatively charged glutamic acid residue can be found in the pore forming loop (E1047 and Y1049 in mouse TRPM7)(237). TRPM7 is regulated by G-protein coupled receptors linked to PLC which acts to cleave PIP2 to produce diacylglycerol and inositol triphosphate. Activation of PLC and PIP2 hydrolysis reduces TRPM7 activity(43). The interaction of the kinase domain with the channel domain, with regards to pore regulation, is poorly understood.

It has been shown that TRPM7 has a role in cellular growth and development, as experiments that have altered the activity of TRPM7 have produced profound effects on

cell growth and development(234). As mentioned previously the channel is involved in Mg2+ homeostasis(238).

Confirmation of *in vitro* results in *in* vivo studies has proved difficult due to the apparent necessity of TRPM7 for maintaining cellular function. TRPM7 gene deletion in mice is lethal with death occurring before embryonic day 7.5(239). Due to TRPM7 being widely expressed and its potential involvement in cellular growth and development as well as Mg^{2+} homeostasis it has been researched with regards to the channels involvement in cancer, ischemic stroke and hypertension. For a full review of the pathophysiologic roles of TRPM7 see Park *et al.* (240).

5.1.3   TRPM7 inhibitors

To date, there are not nearly as many inhibitors of TRPM7 as there are for other TRP channels, particularly the thermo-TRPs. Interest in TRPM7 has been growing in recent years due to it regulating cell proliferation in several cancers and its association with ischemic cell death and vascular smooth muscle cell function(240). As such the number and range of known TRPM7 inhibitors is growing. Some of these inhibitors also have an effect on other TRP channels, including TRPA1. The following is a list of known TRPM7 inhibitors.
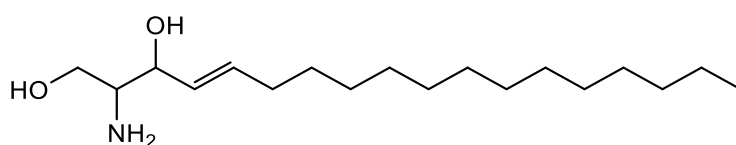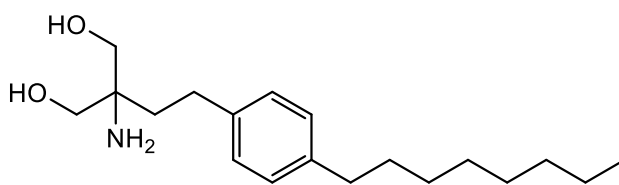
-   Sphingosine and Fingolimod

Figure 155 Chemical structures of Sphingosine and Fingolimod

Qin *et al.* (241) have reported that sphingosine and fingolimod inhibit TRPM7. Using patch clamp techniques, they found that sphingosine and fingolimod inhibited TRPM7 expressed in HEK293 cells with an IC50 of 0.59 and 0.72 μM respectively. These results

220

were confirmed in endogenous TRPM7 cardiac fibroblasts. These two compounds have also been found to activate TRPM2(242).

- 2-aminoethoxydiphenylborate (2-APB)
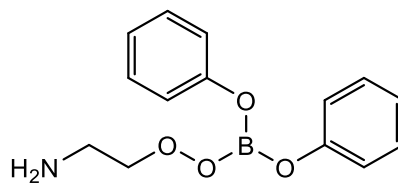
2-aminoethoxydiphenyl borate

Figure 156 Chemical structure of 2-APB

Micromolar concentration levels of 2-APB were found to have a strong inhibitory effect on TRPM7 activation in CHOK1, HEK293 and MDCT expression systems(205). 2-APB has been reported to be a TRPM2 inhibitor and highlighted as a good tool for studying the function of TRPM2(198).

- 5-lipoxygenase inhibitors
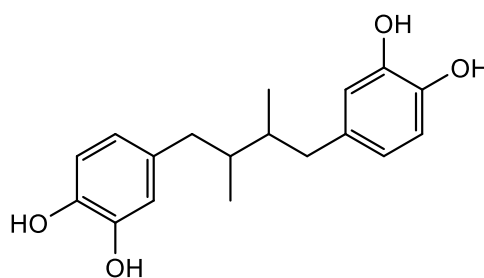
Nordihydroguaiaretic acid
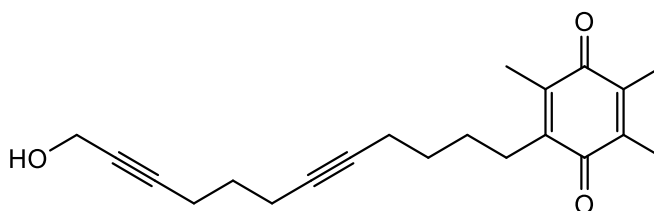
AA-861
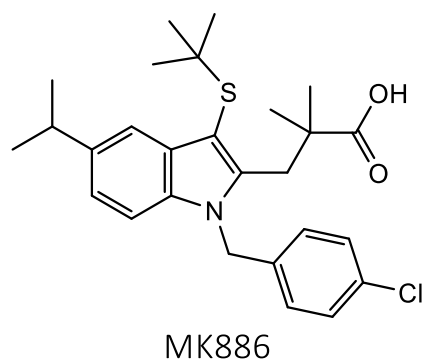
MK886

Figure 157 Chemical structures of 5-lipoxygenase inhibitors; NDGA, AA-861 and MK886

Several 5-lipoxygenase inhibitors, NDGA, AA861 and MK886 have been found to be potent blockers of the TRPM7(243). Using patch clamp cell-based assay methods, Chen *et al.*(243) found that these three compounds potently inhibit TRPM7 channel function in HEK293 cells overexpressing TRPM7 and natively TRPM7 expressing HEK293 cells. They determined that TRPM7 inhibition of these compounds is independent of their 5-lipoxygenase inhibition.

- Nafamostat mesylate

.2CH$_3$SO$_3$H

nafamostat mesylate
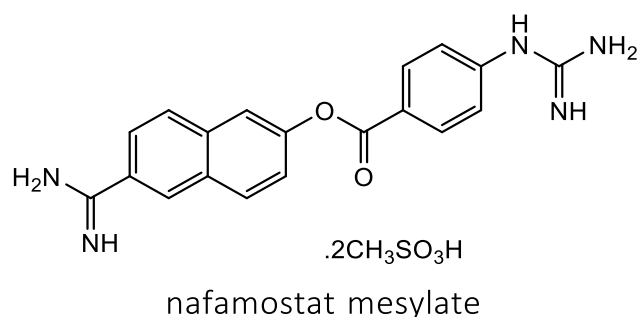
Figure 158 Chemical structure of Nafamostat mesylate

Nafamostat mesylate was found to inhibit TRPM7 function when overexpressed in HEK293 cells with an IC50 of 15 µM(244). This inhibitory function was confirmed in a natural expression system, cultured hippocampal neurons, with an IC50 of 27 µM.

- NS8593
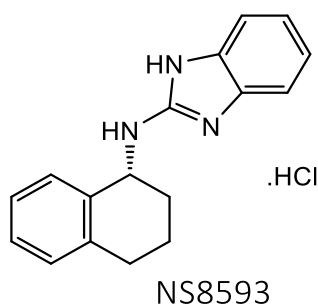
NS8593

A range of modulators of $K_{Ca}2.1$-2.3 channels were found to inhibit TRPM7. Chubanov *et al.*(233) developed an aequorin bioluminescence-based assay to observe TRPM7 channel activity and found that NS8593 was the most potent inhibitor of TRPM7 from the compounds tested with an IC50 of 1.6 μM.
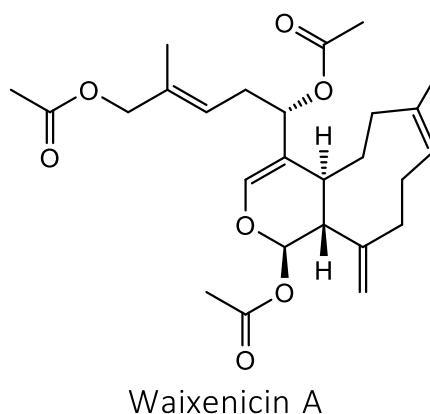
- Waixenicin A

Waixenicin A

Waixencin A is a natural compound from a Hawaiian soft coral which has been reported by Zierler *et al.* (245) to block TRPM7 function when expressed in HEK293 cell lines. Waixencin A was found to block TRPM7 function in patch clamp experiments with an IC50 value of 12 μM. The found waixencin A after screening a chemical library of marine organism-derived extracts.

- Quercetin
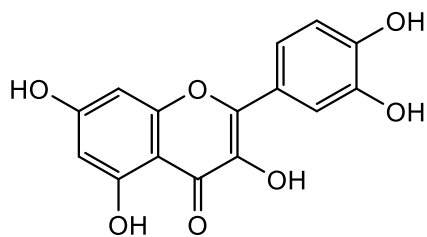
Quercetin

Figure 161 Chemical structure of Quercetin

Quercetin is a bioflavonoid which has been proposed to have anti-cancer properties(246–248). Kim *et al.* (249) sought to determine the nature of the apoptotic mechanisms responsible for the effects of quercetin on AGS cells, which are a commonly used human gastric adenocarcinoma cell line. Quercetin was found to inhibit MAPK signalling pathways and in addition was found to inhibit the function of TRPM7 expressed in AGS cells and when overexpressed in HEK293 cells.

- Midazolam
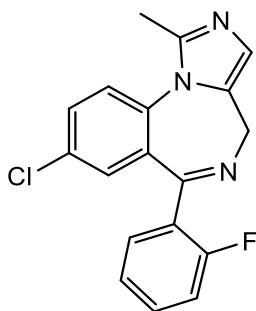
Midazolam

Figure 162 Chemical structure of Midazolam

Midazolam is a benzodiazepine class anaesthetic. It has been reported that it inhibits cancer cell proliferation through the inhibition of TRPM7(250). Midazolam was found to significantly inhibit the growth and proliferation of FaDU human hypopharyngeal squamous cell carcinoma cells. This effect was found to be benzodiazepine receptor independent but TRPM7 dependent.

This list shows the variety of TRPM7 inhibitors that have been identified, from long aliphatic chains in sphingosine, fingolimod and AA-861, to aromatic compounds such as MK886,

nafamostat mesylate and quercetin. It appears that there are no specific structural components that are required for TRPM7 inhibition which is similar to what has been observed for other TRP channels. This further highlights the TRP channels as being complex channels that have a wide array of modulators. Some of the TRPM7 inhibitors have been found to modulate other TRP channels with 2-APB and sphingosine been observed to modulate TRPM2. Several of the compounds share structural similarities to known TRPA1 modulators. MK886 is similar to the structure of the TRPA1 specific antagonist HC-030031. NDGA and quercetin both share structural similarities to phenolic compounds that activate TRPA1. NDGA in particular is of interest with regards to TRPA1 modulation due to its diphenyl structure which is similar to the ojk06, ojk07 and NPPB structures discussed in chapter 3. NDGA contains a 4 atom linker group between its two phenyl groups which is similar in length to the ojk06 and ojk07 compounds as well as NPPB(142).

5.1.4   Inhibition of TRPM7 by carvacrol

Carvacrol is a known TRPA1 agonist, which activates the channel via a non-covalent traditional ligand binding mechanism(130). Parnas *et al.*(251) reported that carvacrol inhibited TRPM7. They demonstrated this in whole cell patch clamp recordings on mammalian TRPM7 heterologously expressed in HEK cells and ectopically expressed in a primary culture of CA3-CA1 hippocampal brain neurons. In the same report they showed that carvacrol inhibited the TRPL channel and decided to examine carvacrol on TRPM7 which shares similar features. TRPM7 has been shown to be constitutively active in the absence of Mg-ATP(234). Carvacrol was observed to inhibit the active state of TRPM7 expressed in HEK293 cells with an IC50 of 306 μM(251). Other TRPA1 agonists were also assayed for inhibition of TRPM7 these include cinnamaldehyde, menthol and borneol, which were all observed to have a small inhibitory effect on TRPM7.

Parnas *et al.* (251) proceeded to determine that the inhibitory effect of carvacrol on TRPM7 was sufficient to block the channels functional effects. They did this by directly monitoring the synaptic vesicle recycling of TRPM7-GFP expressing synapses and control synapses. They found that application of carvacrol, at a concentration of 500 μM, significantly decreased the vesicle release in TRPM7-GFP neurons and had no effect in the control neurons. From the results they suggested that TRP channels may share common

mechanisms of channel modulation. In section 5.1.3 a list of several TRPM7 inhibitors has been compiled. Some of these inhibitors have already been reported to have TRPA1 activity and several have been highlighted as possible TRPA1 modulators.

5.1.5   Hypothesis and Aims

It has been discussed in section 5.1.4 that carvacrol, a TRPA1 agonist, inhibits TRPM7. From a review of the literature and the list of TRPM7 inhibitors, NDGA stood out as a potential TRPA1 modulator due to its similarity to carvacrol and its similarities to the thymol and carvacrol based compounds synthesised and assayed in chapter 3. It is therefore hypothesised that NDGA may modulate TRPA1 possibly through the same mechanism as other alkylated phenol compounds. M4N a semi-synthetic methylated derivative of NDGA shares almost all of NDGA biological functions but is far less toxic than NDGA. Therefore, M4N was also assayed for TRPA1 modulation.

The assay results on TRPA1-HEK293 cells for NDGA and M4N required further investigation to understand the underlying mechanism of action. Firstly, the relationship between the phenol and methoxy functional groups was investigated by comparing the responses for thymol, its methylated derivative. Secondly, I aimed to determine if the potent TRPA1 agonist response by NDGA and M4N was due in part to the symmetrical nature of these compounds. Therefore a group of NDGA and M4N non-symmetrical derivatives, N1-N8, were assayed for TRPA1 modulation.

5.2 Results

In this section the results for the calcium signalling assays have been described in detail.

All the compounds assayed have been tested against mock-transfected HEK293 cells, at the highest concentration used in the agonist and antagonist assays, to determine any effects that the compound has on HEK293 cells. There was no response observed in the mock-transfected HEK293 cells for all of the compounds assayed. Therefore the responses observed in the TRP gene transfected HEK293 cells can be deemed to be via gene product of which the HEK293 cells have been transfected with (see Figure 163 for data traces of responses for selected test compounds from each of the three compound groups).
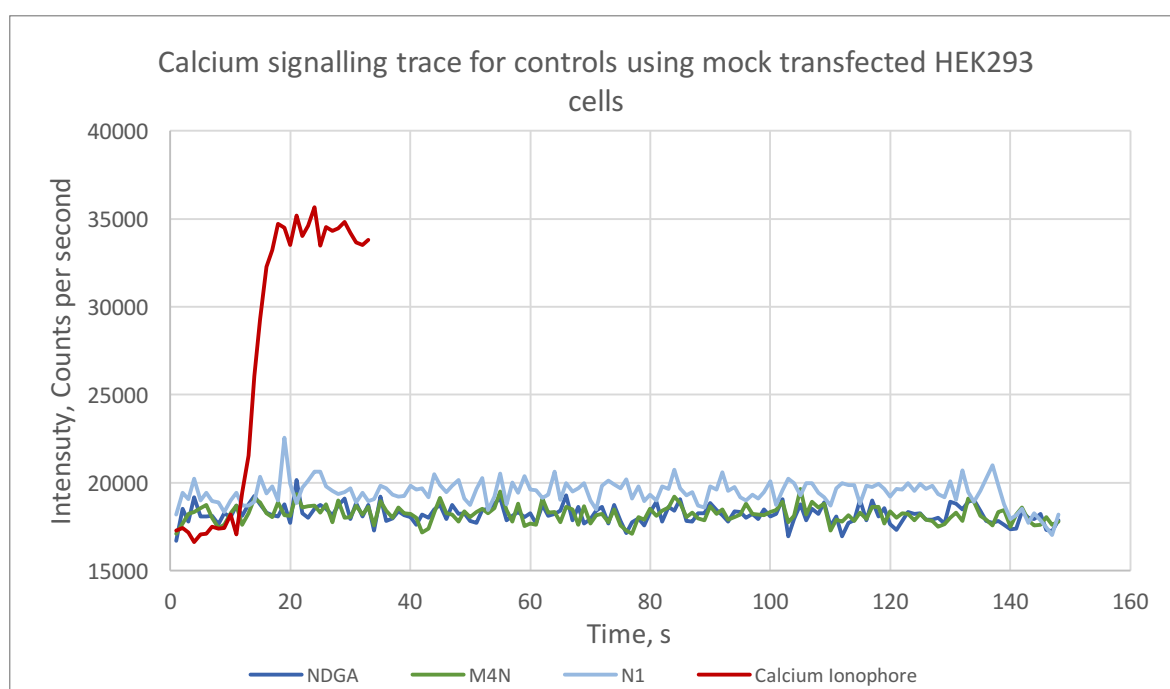
Figure 163 Raw data traces for a selection of test compounds on mock transfected HEK293 cells

5.2.1 Issues with the calcium signalling assay method

In section 3.2.1 any issues with the calcium signaling method and subsequent corrective actions have been explained.

5.2.2 NDGA

Nordihydroguiaretic acid
(NDGA)
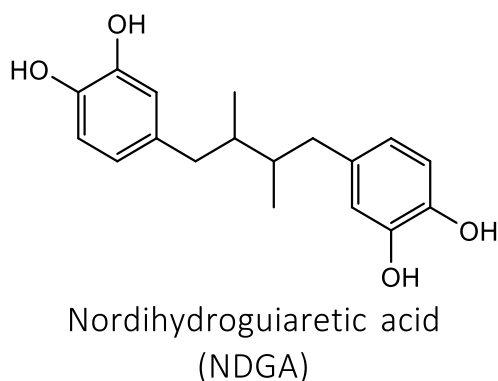
Figure 164 Chemical structure of NDGA

Figure 165 Agonist concentration effect curve for NDGA on TRPA1-HEK293 cells. Data points are means±SEM of N = 3 experiments

NDGA has been assayed using both the agonist and antagonist calcium signalling assays to assess the compound's effect on TRPA1-HEK293 cells. The resulting concentration effect curve can be seen in Figure 165 above.

In the agonist assay a concentration dependent increase in intracellular calcium was observed. This response was inhibited fully by the TRPA1 specific inhibitor HC-030031, therefore this response can be attributed to the gating of TRPA1 channels. NDGA was tested over the concentration range of 0.1 to 400 µM, over this range a typical sigmoidal response was observed. The first significant response was observed at 1 µM with a mean %CaI response of 11. The maximum response was observed at the 200 µM concentration

point with a mean %CaI response of 67. The maximum plateau was observed to occur between the 50 and 100 µM. Non-linear regression analysis was carried out using two different curve fit calculations the best fit was the variable Hill slope four parameter curve which calculated an EC50 value of 23 µM. An efficacy of 92% of the maximum response of cinnamaldehyde (100 µM) on TRPA1-HEK293 cells was calculated. In the antagonist assay no reduction in the response of cinnamaldehyde on TRPA1-HEK293 cells over the concentration range of 1-400 µM of NDGA.

From this analysis of the agonist and antagonist assays of NDGA on TRPA1-HEK293 cells, it can be determined that NDGA is a full agonist of TRPA1 which, unlike Thymol and other agonists tested in chapters 3 and 4, does not show any inhibition or desensitisation of TRPA1 data not shown.

5.2.3 Terameprocol

Teremeprocol
(M4N)

Figure 166 Chemical structure of Terameprocol

Agonist effect of Terameprocol on TRPA1-HEK293 cells

EC50 = 4 µM

Figure 167 Agonist concentration effect curve for Terameprocol on TRPA1-HEK293 cells. Data points are means±SEM of N = 3 experiments

M4N has been assayed using both the agonist and antagonist calcium signalling assays to assess the compound's effect on TRPA1-HEK293 cells. The resulting concentration effect curve can be seen in Figure 167 above. In the agonist assay a concentration dependent increase in intracellular calcium was observed. This response was inhibited fully by the TRPA1 specific inhibitor HC-030031, therefore this response can be attributed to the gating of TRPA1 channels. M4N was tested over the concentration range of 0.1 to 20 µM, over this range a typical sigmoidal response was observed. The first significant response was observed at 1 µM with a mean %Cal response of 20. The maximum response was observed at the 20 µM concentration point with a mean %Cal response of 72. The maximum plateau was observed between 7 and 10 µM. Non-linear regression analysis was carried out using two different curve fit calculations the best fit was the variable Hill slope four parameter curve which calculated an EC50 value of 4 µM. An efficacy of 99% of the maximum response of cinnamaldehyde (100 µM) on TRPA1-HEK293 cells was calculated. In the antagonist assay no reduction in the response of cinnamaldehyde on TRPA1-HEK293 cells over the concentration range of 1-200 µM of M4N, data not shown.

From this analysis of the agonist and antagonist assays of M4N on TRPA1-HEK293 cells, it can be determined that M4N is a full agonist of TRPA1 which unlike Thymol and other agonists tested in chapters 3 and 4, does not show any inhibition or desensitisation of TRPA1, data not shown.

5.2.4 Thymol
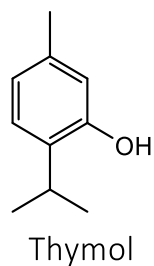
Thymol

Figure 168 Chemical structure of Thymol

Agonist effect of Thymol on TRPA1-HEK293 cells

EC50 = 44 µM

Inhibitory effect of Thymol on TRPA1-HEK293 cells

IC50 = 101 µM

Figure 169 Agonist (above) and antagonist (below) concentration effect curves for Thymol on TRPA1-HEK293 cells. Data points are means±SEM of N = 3 experiments

Thymol has been assayed using both the agonist and antagonist calcium signalling assays to assess the compound's effect on TRPA1-HEK293 cells. The resulting concentration effect curves can be seen in Figure 169 above. In the agonist assay a concentration dependent increase in intracellular calcium was observed. This response was inhibited fully by the TRPA1 specific inhibitor HC-030031 therefore this response can be attributed to the gating of TRPA1 channels. Thymol was tested over the concentration range of 1 to 200 µM, over this range a typical sigmoidal response was observed. The first significant response was observed at 30 µM with a mean %CaI response of 18. The maximum response was observed at the 200 µM concentration point with a mean %CaI response of 66. The maximum plateau occurred between the 100 and 150 µM. Non-linear regression analysis was carried out using two different curve fit calculations the best fit was the variable Hill slope four parameter curve which calculated an EC50 value of 44 µM. An efficacy of 91% of the maximum response of cinnamaldehyde (100 µM) on TRPA1-HEK293 cells was calculated.

In the antagonist assay a concentration dependent decrease in the response of 30 µM of cinnamaldehyde (EC50 concentration of cinnamaldehyde) was observed with increasing concentration of pre-dosed thymol. Thymol was tested over the concentration range of 10-1000 µM over this range a typical inhibition curve was observed. The first decrease in the cinnamaldehyde response was observed at 100 µM with a decrease in cinnamaldehyde response of 54.1 %. The greatest reduction in the cinnamaldehyde response occurred at the 400 µM thymol concentration point with a reduction of 95%, which is deemed to be full inhibition of the cinnamaldehyde response. The plateau was observed between the 200 and 400 µM points. The data points have been fitted with two different non-linear regression analyses, the best fit curve was a four parameter variable slope curve which gave a calculated IC50 value of 101 µM.

From this analysis of the agonist and antagonist assays of Thymol on TRPA1-HEK293 cells, it can be determined that Thymol is a full agonist of TRPA1 which after the initial activation of TRPA1 inhibits further activation via a desensitisation effect.

5.2.5   Carvacrol

Carvacrol

Figure 170 Chemical structure of Carvacrol
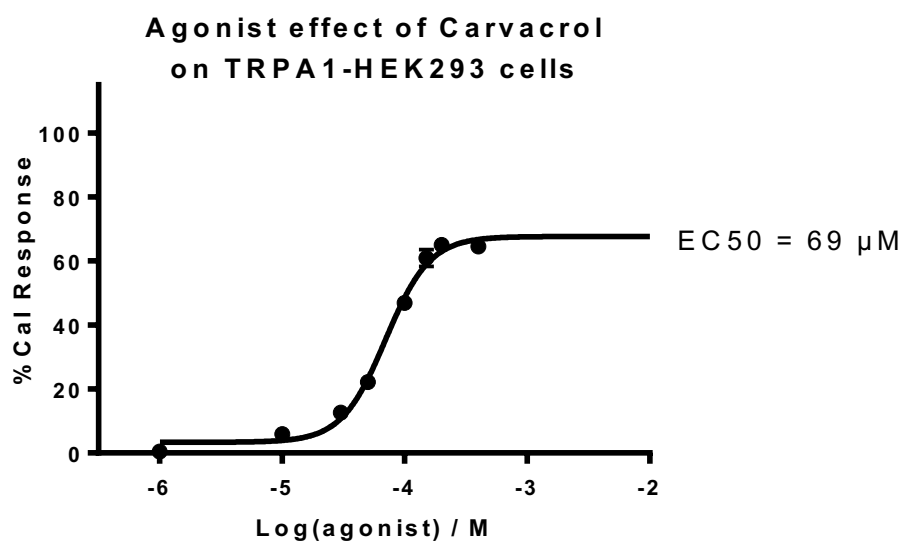
Figure 171 Agonist concentration effect curve for Carvacrol on TRPA1-HEK293 cells. Data points are means±SEM of N = 3 experiments

Concentration, µM	Mean reduction of cinnamaldehyde response, %	SEM
100	59.7	7.08
400	97.5	3.57

Table 29 Antagonist responses for Carvacrol on TRPA1-HEK293 cells. N = 3 experiments

Carvacrol has been assayed using both the agonist calcium signalling assays to assess the compound's effect on TRPA1-HEK293 cells. The resulting concentration effect curve can be seen in Figure 171 above. In the agonist assay a concentration dependent increase in

intracellular calcium was observed. This response was inhibited fully by the TRPA1 specific inhibitor HC-030031 therefore this response can be attributed to the gating of TRPA1 channels. Carvacrol was tested over the concentration range of 1 to 400 µM, over this range a typical sigmoidal response was observed. The first significant response was observed at 30 µM with a mean %CaI response of 13. The maximum response was observed at the 200 µM concentration point with a mean %CaI response of 65. The maximum plateau was observed between the 150 and 200 µM concentration point. Non-linear regression analysis was carried out using two different curve fit calculations the best fit was the variable Hill slope four parameter curve which calculated an EC50 value of 69 µM. An efficacy of 90 % of the maximum response of cinnamaldehyde (100 µM) on TRPA1-HEK293 cells was calculated.

With regards to an antagonist calcium signalling assay of carvacrol, a full concentration effect curve was not carried out. However, two concentration points have been tested, firstly 100 µM, the IC50 concentration for thymol and secondly, 400 µM, the thymol concentration point at which full inhibition for cinnamaldehyde was first observed. The results for this can be seen in Table 29 above. Carvacrol at 100 µM reduced the cinnamaldehyde response by 60 % which was greater than the result obtained for thymol (54%). The result at the 400 µM concentration showed a 98 % reduction in the cinnamaldehyde response which can be deemed to be full inhibition.

From this analysis of the agonist and antagonist assays of carvacrol on TRPA1-HEK293 cells, it can be determined that carvacrol is a full agonist of TRPA1 which after the initial activation of TRPA1 inhibits further activation via a desensitisation effect.

5.2.6   NDGA and Terameprocol derivatives

A range of non-symmetrical compounds similar to the structure of NDGA and M4N have been assayed using the agonist and antagonist calcium signalling methods outlined in section 2.2. The results for each test compound is detailed below.

5.2.6.1   N1
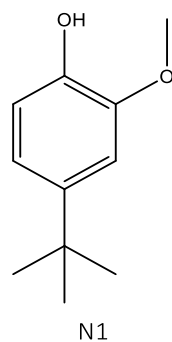
Figure 172 Chemical structure of N1

EC50 = 163 µM

IC50 = 104 µM

Figure 173 Agonist and antagonist concentration effect curves for N1 on TRPA1-HEK293 cells. Data points are means±SEM of N = 3 experiments

N1 has been assayed using both the agonist and antagonist calcium signalling assays to assess the compound's effect on TRPA1-HEK293 cells. The resulting concentration effect curves can be seen in Figure 173 above. In the agonist assay, a concentration dependent increase in intracellular calcium was observed. This response was inhibited fully by the TRPA1 specific inhibitor HC-030031 therefore this response can be attributed to the gating of TRPA1 channels. N1 was tested over the concentration range of 10 to 400 µM, over this range a typical sigmoidal response was observed. The first significant response was observed at 150 µM with a mean %CaI response of 24. The maximum response was observed at the 400 µM concentration point with a mean %CaI response of 53. The maximum plateau occurred between 100 and 150 µM. Non-linear regression analysis was carried out using two different curve fit calculations the best fit was the variable Hill slope four parameter curve which calculated an EC50 value of 163 µM. An efficacy of 73% of the maximum response of cinnamaldehyde (100 µM) on TRPA1-HEK293 cells was calculated.

In the antagonist assay a concentration dependent decrease in the response of 30 µM of cinnamaldehyde (EC50 concentration of cinnamaldehyde) was observed with increasing concentrations of pre-dosed N1. N1 was tested over the concentration range of 3-400 µM. Over this range a typical inhibition curve was observed. The first decrease in the cinnamaldehyde response was observed at 10 µM with a decrease in cinnamaldehyde response of 19 %. The greatest reduction in the cinnamaldehyde response occurred at the 400 µM concentration point with a reduction of 78%. Full inhibition of the cinnamaldehyde response was not observed as testing above a concentration of 400 µM of N1 was not possible as above 400 µM the compound was not completely soluble in the assay media. However, the trend of the data points looks to indicate a full inhibition at higher concentration levels, this is reflected in the curve of best fit which indicates full inhibition at approximately 1000 µM. The curve of best fit was chosen from 4 different models of non-linear regression analysis, the best model was the normalised variable four parameter slope model as it had the highest R^2 value, which was 0.739, the other 3 models were very similar to the one chosen but had slightly lower R^2 values. The calculated IC50 from the normalised variable 4 parameter curve is 104 µM.

From this analysis of the agonist and antagonist assays of N1 on TRPA1-HEK293 cells, it can be determined that N1 is a full agonist of TRPA1 which after the initial activation of TRPA1 inhibits further activation fully via a desensitisation effect.

5.2.6.2   N2
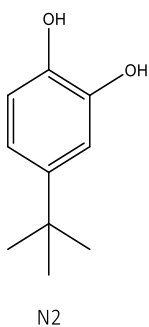
Figure 174 Chemical structure of N2
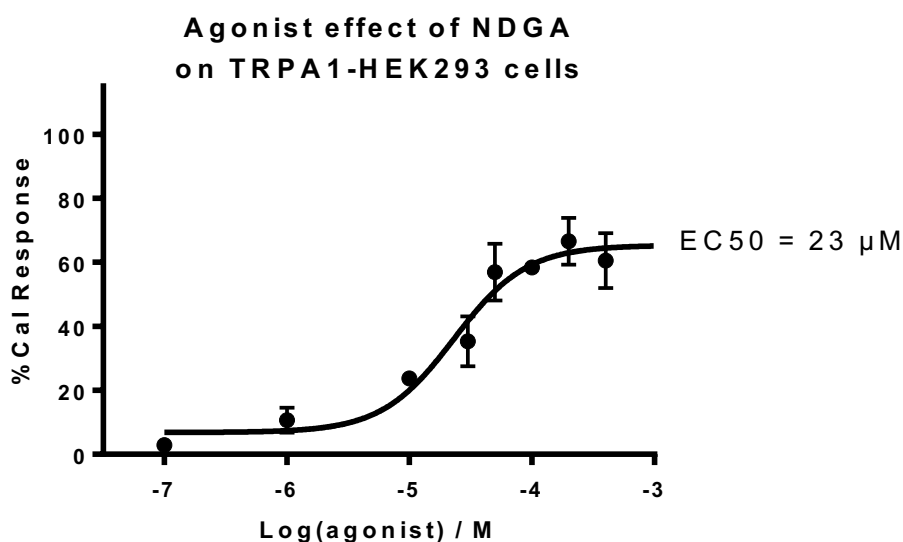

EC50 = 85 µM

IC50 = 57 µM

Figure 175 Agonist and antagonist concentration effect curves for N2 on TRPA1-HEK293 cells. Data points are means±SEM of N = 3 experiments

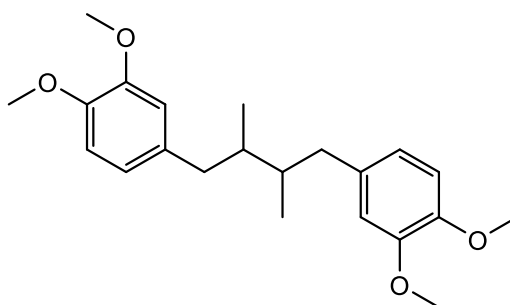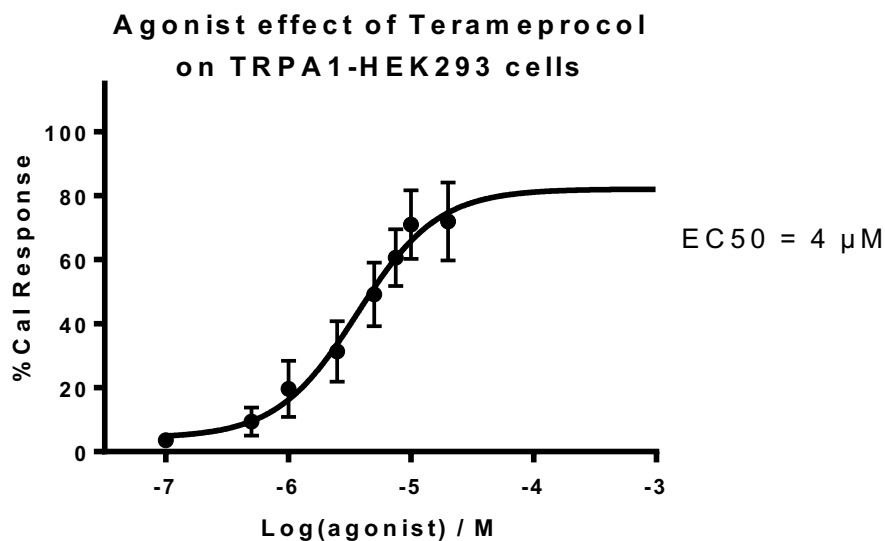N2 has been assayed using both the agonist and antagonist calcium signalling assays to assess the compound's effect on TRPA1-HEK293 cells. The resulting concentration effect curves can be seen in Figure 175 above. In the agonist assay, a concentration dependent increase in intracellular calcium was observed. This response was inhibited fully by the TRPA1 specific inhibitor HC-030031 therefore this response can be attributed to the gating of TRPA1 channels. N2 was tested over the concentration range of 10 to 400 µM, over this range a typical sigmoidal response was observed. The first significant response was observed at 50 µM with a mean %CaI response of 14. The maximum response was observed at the 400 µM concentration point with a mean %CaI response of 58. The maximum plateau occurred between the 200 and 400 µM concentration points. Non-linear regression analysis was carried out using two different curve fit calculations the best fit was the variable Hill slope four parameter curve which calculated an EC50 value of 85 µM. An efficacy of 80 % of the maximum response of cinnamaldehyde (100 µM) on TRPA1-HEK293 cells was calculated.

In the antagonist assay a concentration dependent decrease in the response of 30 µM of cinnamaldehyde (EC50 concentration of cinnamaldehyde) was observed with increasing concentration of pre-dosed N2. N2 was tested over the concentration range of 1-400 µM over this range a typical inhibition curve was observed. The first decrease in the cinnamaldehyde response was observed at 10 µM with a decrease in cinnamaldehyde response of 18 %. The greatest reduction in the cinnamaldehyde response occurred at the 400 µM concentration point with a reduction of 89%. Full inhibition of the cinnamaldehyde response was not observed as testing above a concentration of 400 µM of N2 was not possible as above 400 µM the compound was not completely soluble in the assay media. However, the trend of the data points looks to indicate a full inhibition at higher concentration levels, this is reflected in the curve of best fit which indicates full inhibition at approximately 600 µM. The curve of best fit was chosen from 4 different models of non-linear regression analysis, the best model was the normalised variable four parameter slope model as it had the highest R^2 value, which was 0.8558, the other 3 models were very similar to the one chosen but had slightly lower R^2 values. The calculated IC50 from the normalised variable 4 parameter curve is 57 µM.

From this analysis of the agonist and antagonist assays of N2 on TRPA1-HEK293 cells, it can be determined that N2 is a full agonist of TRPA1 which after the initial activation of TRPA1 inhibits further activation fully via a desensitisation effect.

5.2.6.3   N3

Figure 176 Chemical structure of N3

Agonist effect of N3 on TRPA1-HEK293 cells

EC50 = 123 µM

Inhibitory effect of N3 on TRPA1-HEK293 cells

IC50 = 28 µM
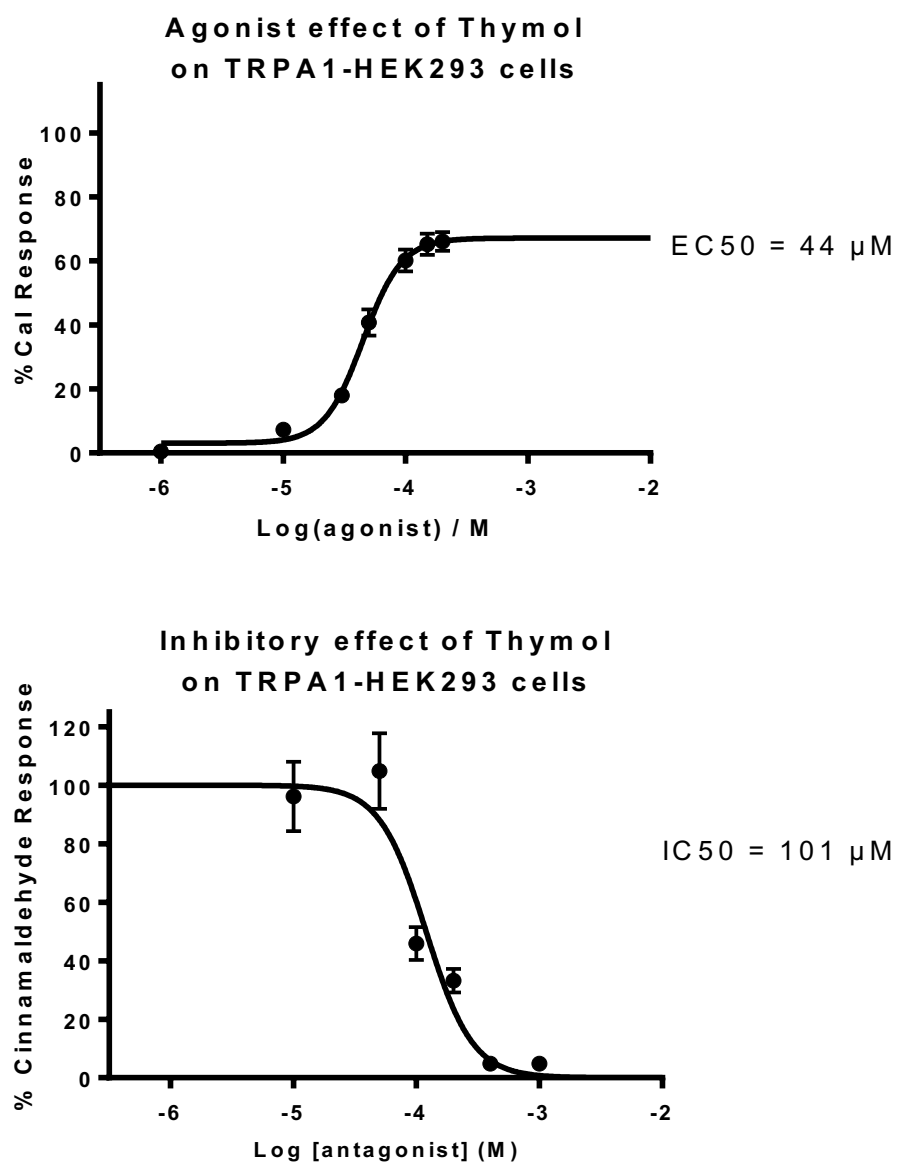
Figure 177 Agonist (above) and antagonist (below) concentration effect curves for N3 on TRPA1-HEK293 cells. Data points are means±SEM of N = 3 experiments

N3 has been assayed using both the agonist and antagonist calcium signalling assays to assess the compound's effect on TRPA1-HEK293 cells. The resulting concentration effect curves can be seen in Figure 177 above. In the agonist assay a concentration dependent increase in intracellular calcium was observed. This response was inhibited fully by the TRPA1 specific inhibitor HC-030031 therefore this response can be attributed to the gating of TRPA1 channels. N3 was tested over the concentration range of 10 to 400 µM, over this range a full sigmoidal agonist response was not observed, however the data trends towards a full sigmoidal concentration effect curve. The first significant response was observed at 30 µM with a mean %CaI response of 12. The maximum response was observed at the

400 μM concentration point with a mean %CaI response of 42. As previously mentioned a maximum plateau was not observed however non-linear regression analysis has been used to fit a curve to the data points which can be used to predict a maximum plateau point. Two models have been used to fit a curve the first assumes a 100 % efficacy, which is the normalised variable slope model, this predicts a maximum plateau around the 15mM concentration. The second model does not assume a 100 % efficacy, this is the variable slope four parameter model, and a maximum value of 55 %CaI was predicted, with a 75 % efficacy, this was assumed to occur at the 1000 μM concentration point. Of the two models, the best fit curve was from the variable slope four parameter model which had a greater R^2 value of 0.8505 and tighter 95 % confidence intervals than the normalised variable slope model. The calculated EC50 value for N3 using the variable slope four parameter model was 123 μM. N3 can be deemed to be a partial agonist of TRPA1.

In the antagonist assay a concentration dependent decrease in the response of 30 μM of cinnamaldehyde (EC50 concentration of cinnamaldehyde) was observed with increasing concentration of pre-dosed N3. N3 was tested over the concentration range of 1-400 μM. Over this range a typical inhibition curve was observed. The first decrease in the cinnamaldehyde response was observed at 10 μM with a decrease in cinnamaldehyde response of 38 %. The greatest reduction in the cinnamaldehyde response occurred at the 400 μM concentration point with a reduction of 92 %, this can be deemed to be full inhibition of the cinnamaldehyde response. A plateau has not been achieved as testing beyond the concentration of 400 μM was not possible due to the insolubility of N3 in the assay media at higher concentrations. However it can be assumed with a reasonable level of certainty that higher concentrations will yield full inhibition of the cinnamaldehyde. Non-linear regression analysis was carried out to produce a curve of best fit, out of the models used the normalised variable slope model was the best fit with an R^2 value of 0.7675, this value shows an adequate level of fit to the data points it is slightly lower when compared to the other compounds tested this is due to the responses at the 30 μM and the 50 μM concentration points which were slightly lower and higher, respectively, than the curve of best fit, however these points have not been deemed to be outliers and therefore have been included. The calculated IC50 using the normalised variable slope model is 27 μM.

From this analysis of the agonist and antagonist assays of N3 on TRPA1-HEK293 cells, it can be determined that N3 is a full agonist of TRPA1 which after the initial activation of TRPA1 inhibits further activation fully via a desensitisation effect.

5.2.6.4   N4
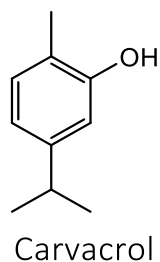

Figure 178 Chemical structure of N4

**Agonist effect of N4
on TRPA1-HEK293 cells**

$EC50 = 130 \ \mu M$

**Inhibitory effect of N4
on TRPA1-HEK293 cells**

$IC50 = 51 \ \mu M$

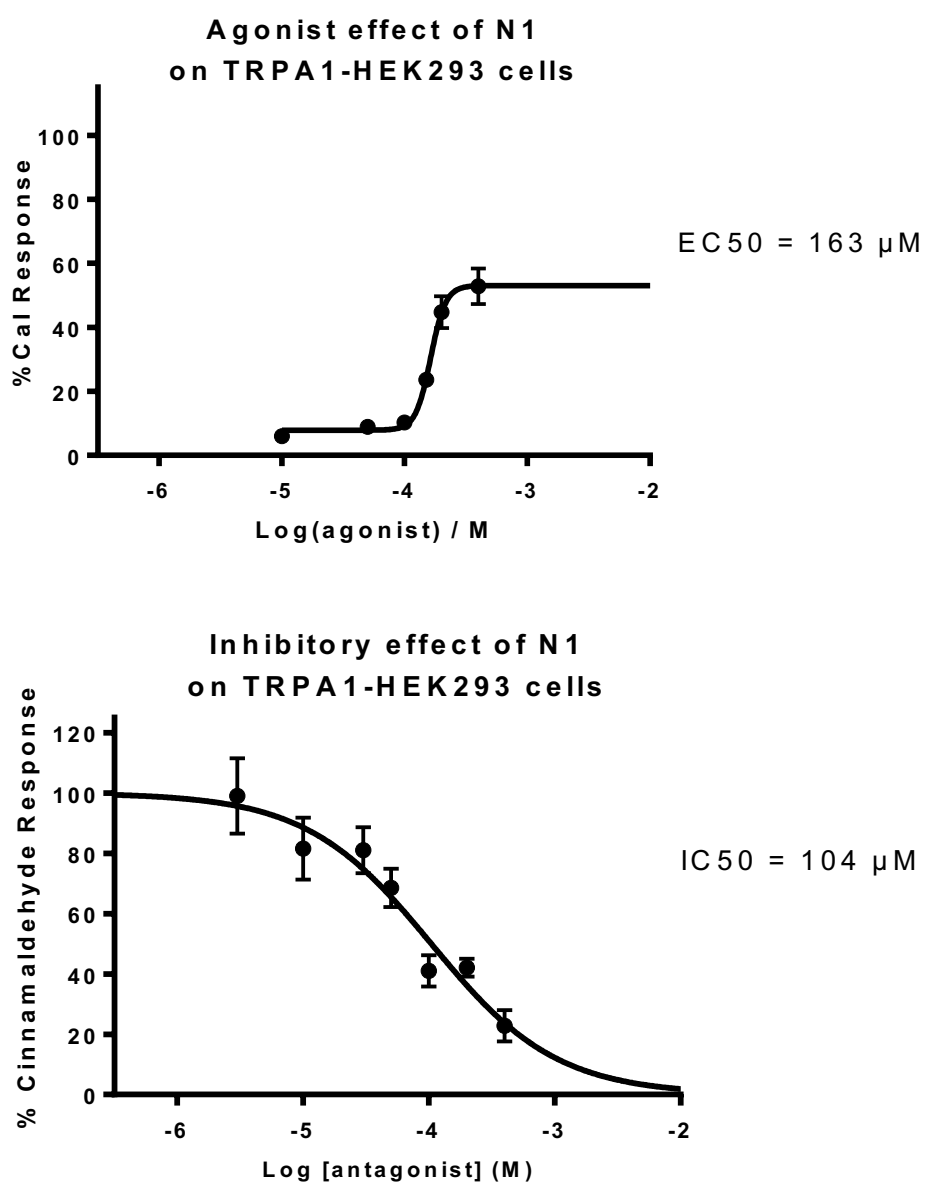*Figure 179 Agonist (above) and antagonist (below) concentration effect curves for N4 on TRPA1-HEK293 cells. Data points are means±SEM of N = 3 experiments*

N4 has been assayed using both the agonist and antagonist calcium signalling assays to assess the compound's effect on TRPA1-HEK293 cells. The resulting concentration effect curves can be seen in Figure 179 above.

In the agonist assay, a concentration dependent increase in intracellular calcium was observed. This response was inhibited fully by the TRPA1 specific inhibitor HC-030031 therefore this response can be attributed to the gating of TRPA1 channels. N4 was tested over the concentration range of 10 to 400 µM, over this range a typical sigmoidal response was observed. The first response was observed at 50 µM with a mean %CaI response of 10. The maximum response was observed at the 400 µM concentration point with a mean %CaI response of 33. A maximum plateau can be observed between the 200 and 400 µM concentration points, however this plateau cannot be fully confirmed as testing above 400 µM was not possible due to the insolubility of N4 in the assay media at higher concentrations.

Non-linear regression analysis was carried out using two different curve fit calculations the best fit was the variable Hill slope four parameter curve with an R^2 value of 0.8225, the normalised variable slope model showed a similarly good fit with an R^2 0.7986. These two models predict different activity profiles for N4 the normalised variable slope model predicts a full agonist, as is the nature of the model which fits the data to a full agonist response (i.e. the maximum response for cinnamaldehyde). This model predicts an EC50 value of 435 µM. The variable slope four parameter model predicts a partial agonist response with an EC50 value of 130 µM and an efficacy of 45 %. As both of these models have very similar R^2 values, it is difficult to decipher which model reflects the interaction between N4 and TRPA1. However, the normalised variable slope model shows a broader concentration effect curve ranging from the first response at 50 µM to the maximum predicted response at approximately 15mM, whereas the variable slope four parameter has a much narrower range which is more in line with other compounds tested and therefore more plausible. The variable slope four parameter has therefore been chosen as the best curve fit model due to a greater R^2 value and a more believable concentration effect range, the final EC50 value for N4 is 130 µM with an efficacy of 45 %.

In the antagonist assay a concentration dependent decrease in the response of 30 µM of cinnamaldehyde (EC50 concentration of cinnamaldehyde) was observed with increasing

concentration of pre-dosed N4. N4 was tested over the concentration range of 10-400 µM over this range a typical inhibition curve was observed. The first decrease in the cinnamaldehyde response was observed at 30 µM with a decrease in cinnamaldehyde response of 30 %. The greatest reduction in the cinnamaldehyde response occurred at 400 µM with a reduction of 93 %, which is deemed to be full inhibition of the cinnamaldehyde response. This full inhibition could not be confirmed at greater concentrations due to the insolubility of N4 in the assay media at higher concentrations, however the data trends heavily towards full inhibition at concentrations of 400 µM and above. The best fit non-linear regression analysis model was the normalised variable slope model which has an R^2 value of 0.9037, the calculated IC50 value for this model is 51 µM.

From this analysis of the agonist and antagonist assays of N4 on TRPA1-HEK293 cells, it can be determined that N4 is a partial agonist of TRPA1 which after the initial activation of TRPA1 inhibits further activation fully via a desensitisation effect.
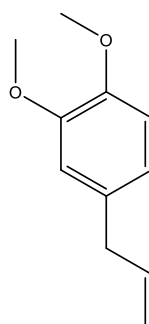
Figure 180 Chemical structure of N5


Agonist effect of N5
on TRPA1-HEK293 cells

EC50 = 314 µM

Inhibitory effect of N5
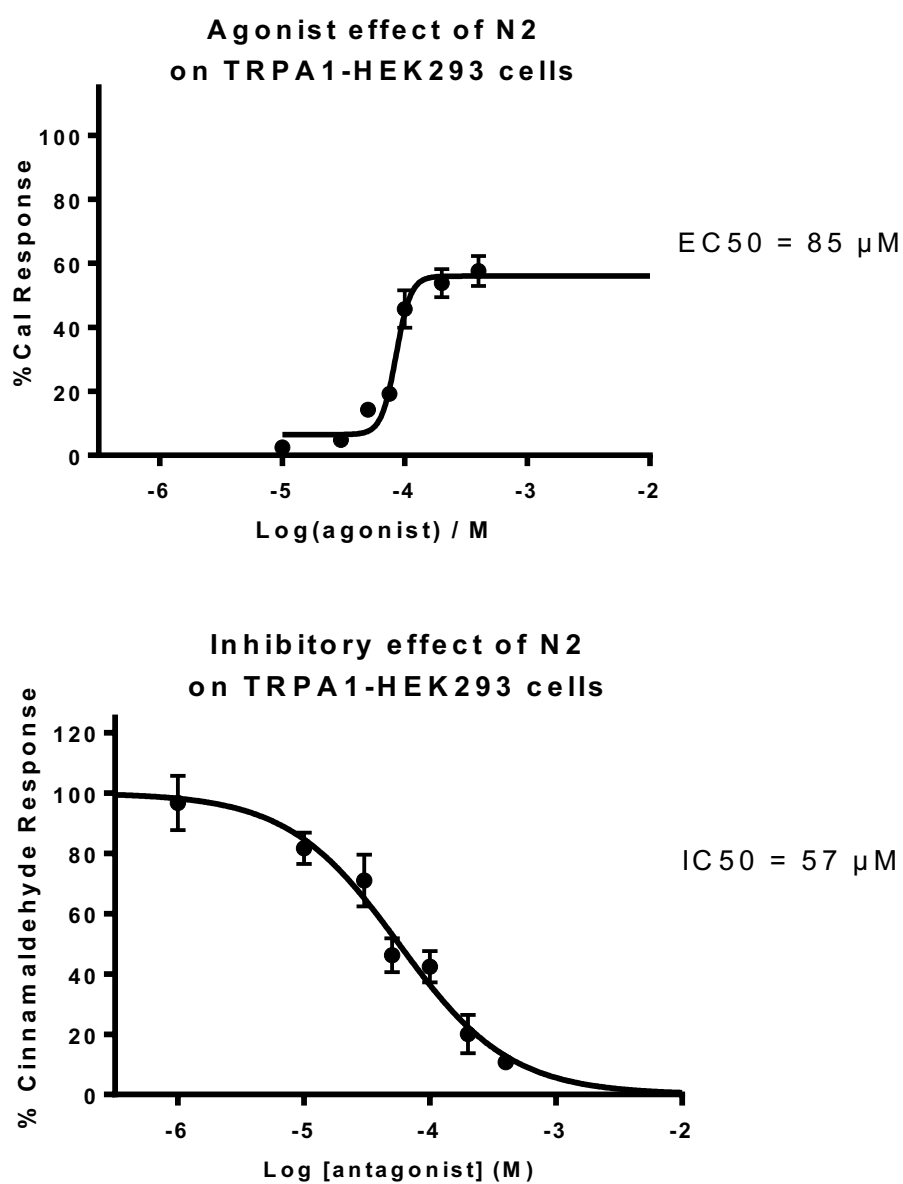**on TRPA1-HEK293 cells**

IC50 = ND µM

Figure 181 Agonist (above) and antagonist (below) concentration effect curves for N5 on TRPA1-HEK293 cells. Data points are means±SEM of N = 3 experiments

247

N5 has been assayed using both the agonist and antagonist calcium signalling assays to assess the compound's effect on TRPA1-HEK293 cells. The resulting concentration effect curves can be seen in Figure 181 above.

In the agonist assay, a concentration dependent increase in intracellular calcium was observed. This response was inhibited fully by the TRPA1 specific inhibitor HC-030031 therefore this response can be attributed to the gating of TRPA1 channels. N5 was tested over the concentration range of 50 to 600 µM, over this range a typical sigmoidal response was observed. The first significant response was observed at 400 µM with a mean %CaI response of 41. The maximum response was observed at the 600 µM concentration point with a mean %CaI response of 49. A maximum plateau was not observed within the data range tested however the best fit curve, created using the variable slope four parameter model, predicts a plateau forming at the 600 µM concentration point. As previously mentioned the best fit curve was created using the variable slope four parameter with an R^2 value of 0.8929 the calculated EC50 from this curve fit model is 314 µM and an efficacy of 68 % of the maximum cinnamaldehyde response. N5 can therefore be deemed to be a low potency partial agonist of TRPA1.

In the antagonist assay a slight concentration dependent decrease in the response of 30 µM of cinnamaldehyde (EC50 concentration of cinnamaldehyde) was observed with increasing concentration of pre-dosed N5. N5 was tested over the concentration range of 1-400 µM over this range no significant trend in the reduction of the cinnamaldehyde response was observed. The first decrease in the cinnamaldehyde response was observed at 10 µM with a decrease in cinnamaldehyde response of 20 %. The greatest reduction in the cinnamaldehyde response occurred at the 100 µM concentration point with a reduction of 30 %. After the 100 µM concentration point there was no further reduction in the cinnamaldehyde response, in fact the average reduction in cinnamaldehyde response for the 200 µM and 400 µM was less than at the 100 µM with 24% and 24% reductions respectively. As the inhibition observed was so small over the concentration range tested fitting a curve to the data points gave no further insight into the inhibitory interactions between N5 and TRPA1.

From this analysis of the agonist and antagonist assays of N5 on TRPA1-HEK293 cells, it can be determined that N5 is a partial agonist of TRPA1 which after the initial activation of

TRPA1 has a slight inhibitory effect on further activation via either a desensitisation or a direct antagonistic effect.

5.2.6.6   N6

N6
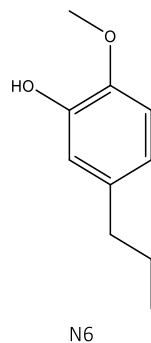
Figure 182 Chemical structure of N6

Agonist effect of N6 on TRPA1-HEK293 cells

EC50 = 294 µM

Inhibitory effect of N6 on TRPA1-HEK293 cells
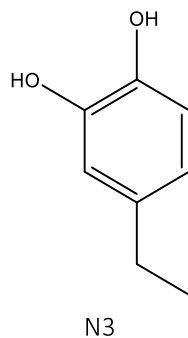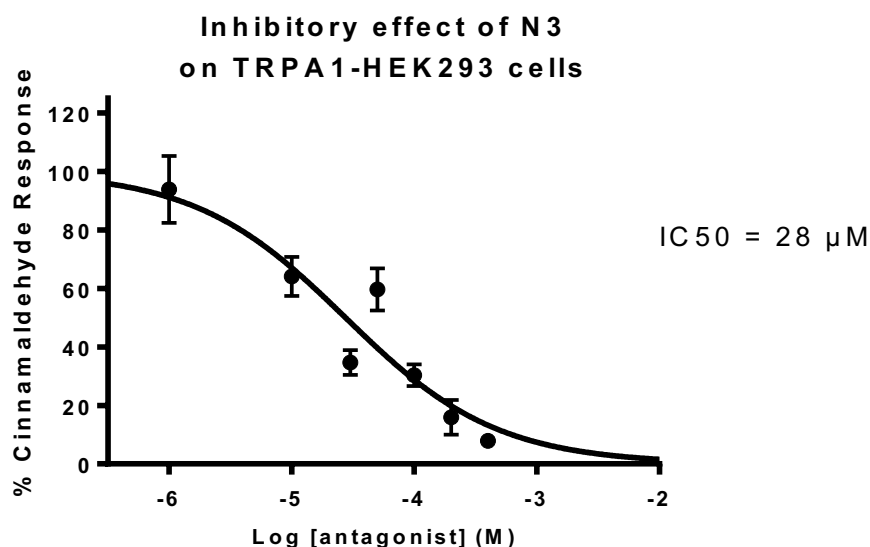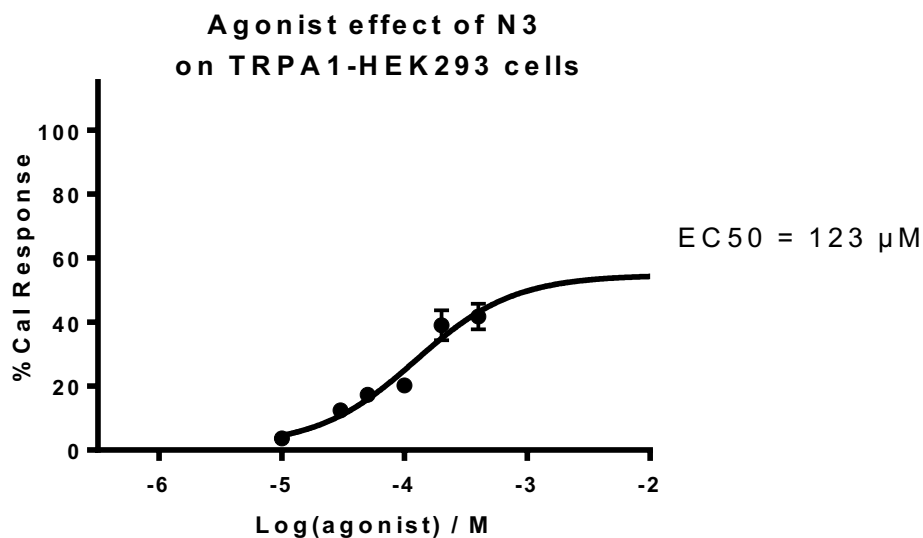
IC50 = ND
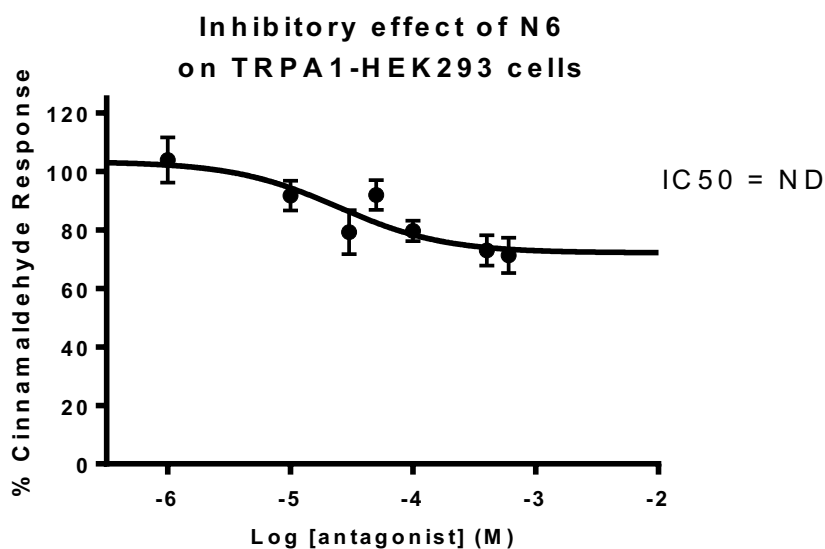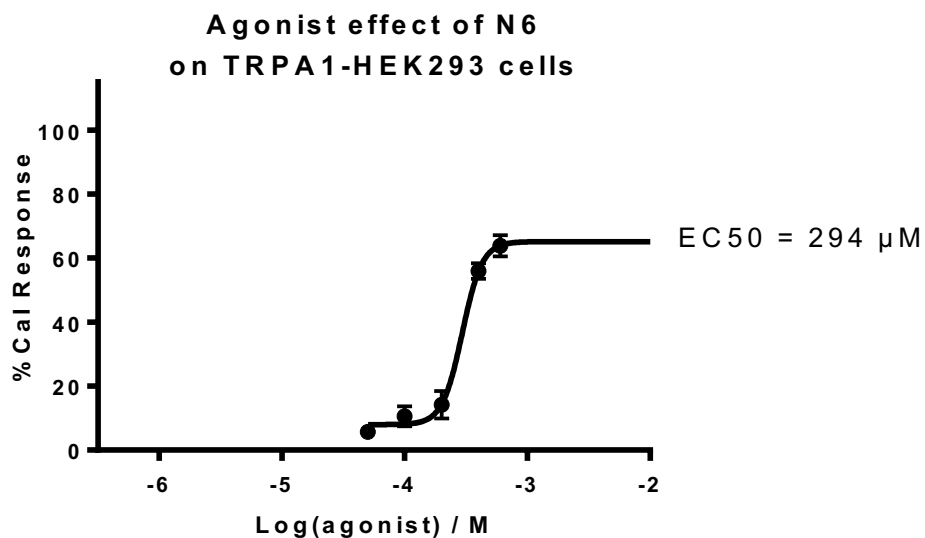
Figure 183 Agonist (above) and antagonist (below) concentration effect curves for N6 on TRPA1-HEK293 cells. Data points are means±SEM of N = 3 experiments

N6 has been assayed using both the agonist and antagonist calcium signalling assays to assess the compound's effect on TRPA1-HEK293 cells. The resulting concentration effect curves can be seen in Figure 183 above.

In the agonist assay, a concentration dependent increase in intracellular calcium was observed. This response was inhibited fully by the TRPA1 specific inhibitor HC-030031 therefore this response can be attributed to the gating of TRPA1 channels. N6 was tested over the concentration range of 50 to 600 µM, over this range a typical sigmoidal response was observed. The first significant response was observed at 100 µM with a mean %Cal

response of 11. The maximum response was observed at the 600 µM concentration point with a mean %CaI response of 64. A maximum plateau was not observed within the data range tested however the best fit curve, created using the variable slope four parameter model, predicts a plateau forming at the 600 µM concentration point. As previously mentioned the best fit curve was created using the variable slope four parameter with an R^2 value of 0.9506 the calculated EC50 from this curve fit model is 294 µM and an efficacy of 88% of the maximum cinnamaldehyde response. N6 can therefore be deemed to be a low potency full agonist of TRPA1.

In the antagonist assay a small concentration dependent decrease in the response of 30 µM of cinnamaldehyde (EC50 concentration of cinnamaldehyde) was observed with increasing concentration of pre-dosed N6. N6 was tested over the concentration range of 1-400 µM over this range no great significant reduction in the cinnamaldehyde response was observed only a small downward trend in cinnamaldehyde response was observed. The first decrease in the cinnamaldehyde response was observed at 30 µM with a decrease in cinnamaldehyde response of 21 %. The greatest reduction in the cinnamaldehyde response occurred at the 400 µMwith a reduction of 27%. Full inhibition of the cinnamaldehyde response was not observed over the concentration range tested. Non-linear regression analysis using a normalised model yielded curves which were not sensible i.e. they predicted full inhibition at concentrations above 1M. The variable four parameter slope, which is not normalised to a full inhibitory effect, predicted a partial antagonistic effect however it was a poor fit for the data points, with an R^2 value of 0.4135, and therefore not very reliable. Without a reliable curve an IC50 value cannot be assigned.

From this analysis of the agonist and antagonist assays of N6 on TRPA1-HEK293 cells, it can be determined that N6 is a full agonist of TRPA1 which after the initial activation of TRPA1 has a slight inhibitory effect on further activation via either a desensitisation or a direct antagonistic effect.

5.2.6.7   N7
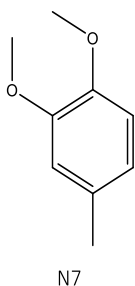
Figure 184 Chemical structure of N7

Agonist effect of N7 on TRPA1-HEK293 cells

EC50 = 139 µM

Inhibitory effect of N7 on TRPA1-HEK293 cells
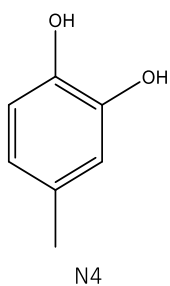
IC50 = ND
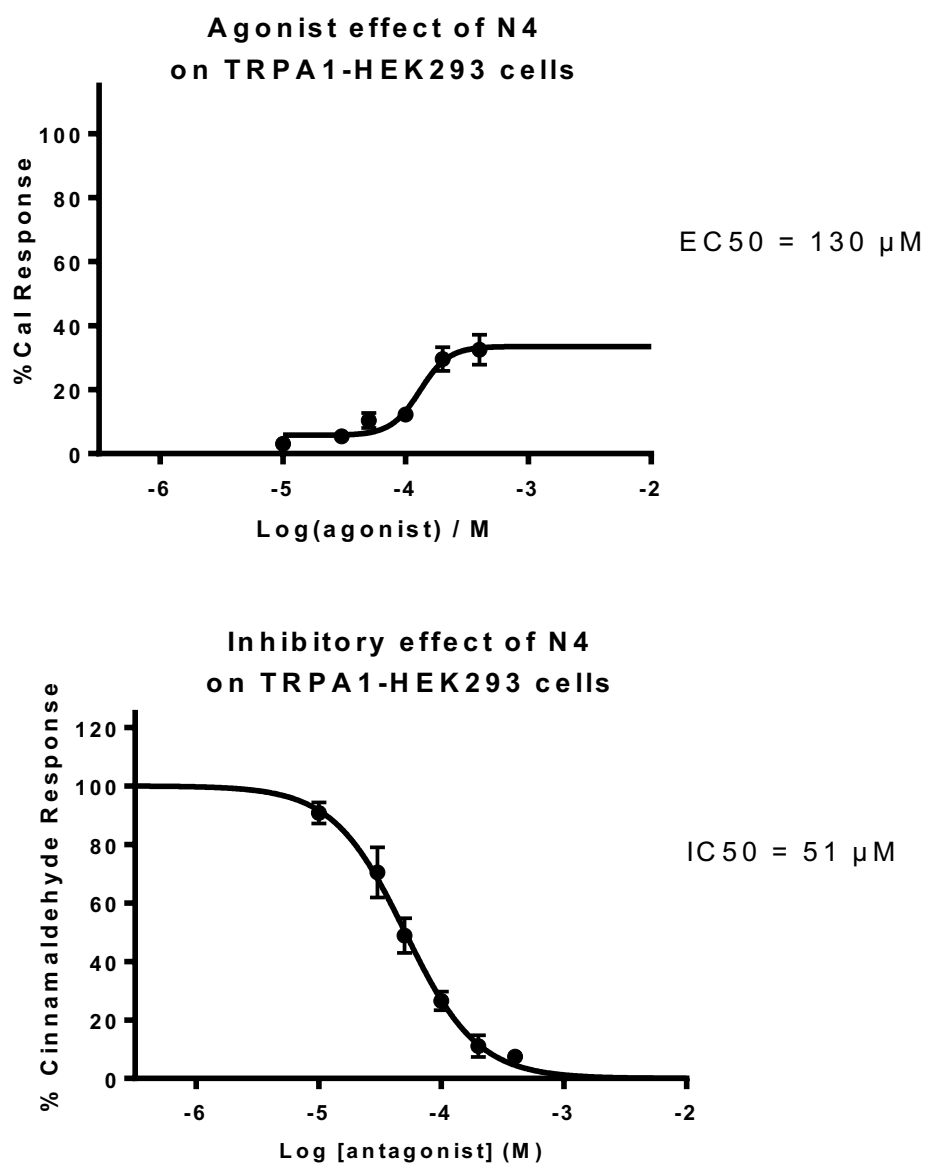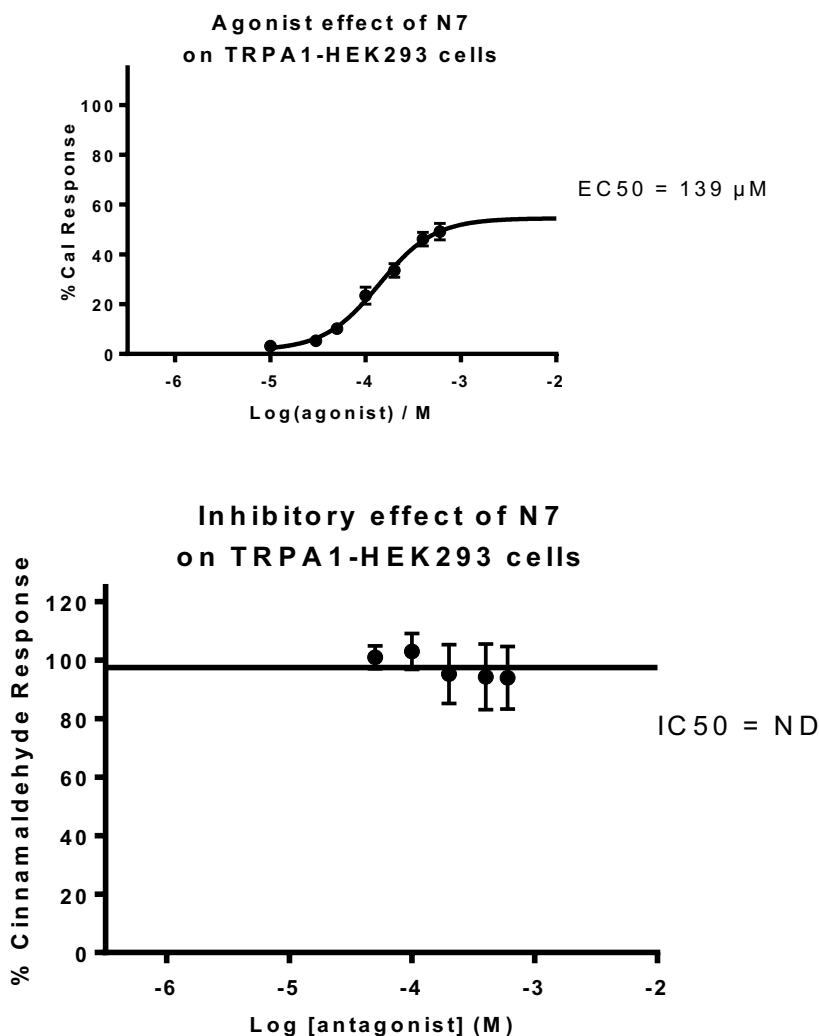
Figure 185 Agonist (above) and antagonist (below) concentration effect curves for N7 on TRPA1-HEK293 cells. Data points are means±SEM of N = 3 experiments

N7 has been assayed using both the agonist and antagonist calcium signalling assays to assess the compound's effect on TRPA1-HEK293 cells. The resulting concentration effect curves can be seen in Figure 185 above.

In the agonist assay, a concentration dependent increase in intracellular calcium was observed. This response was inhibited fully by the TRPA1 specific inhibitor HC-030031 therefore this response can be attributed to the gating of TRPA1 channels. N7 was tested over the concentration range of 100 to 600 µM, over this range a typical sigmoidal response was observed. The first significant response was observed at 50 µM with a mean %CaI response of 10. The maximum response was observed at the 600 µM concentration point with a mean %CaI response of 49. A maximum plateau was not observed within the data range tested however the best fit curve predicts a plateau at around 700 µM. Non-linear regression analysis was carried out using two different curve fit calculations the best fit was the variable Hill slope four parameter curve which calculated an EC50 value of 139 µM. An efficacy of 68 % of the maximum response of cinnamaldehyde (100 µM) on TRPA1-HEK293 cells was calculated, therefore N7 can be deemed a partial agonist.

In the antagonist assay no decrease in the response of 30 µM of cinnamaldehyde (EC50 concentration of cinnamaldehyde) even at the top concentration of 600 µM. Therefore, N7 does not have a desensitising effect on TRPA1.

From this analysis of the agonist and antagonist assays of N7 on TRPA1-HEK293 cells, it can be determined that N7 is a partial agonist of TRPA1 which does not show a desensitisation effect after the initial activation.

5.2.6.8   N8

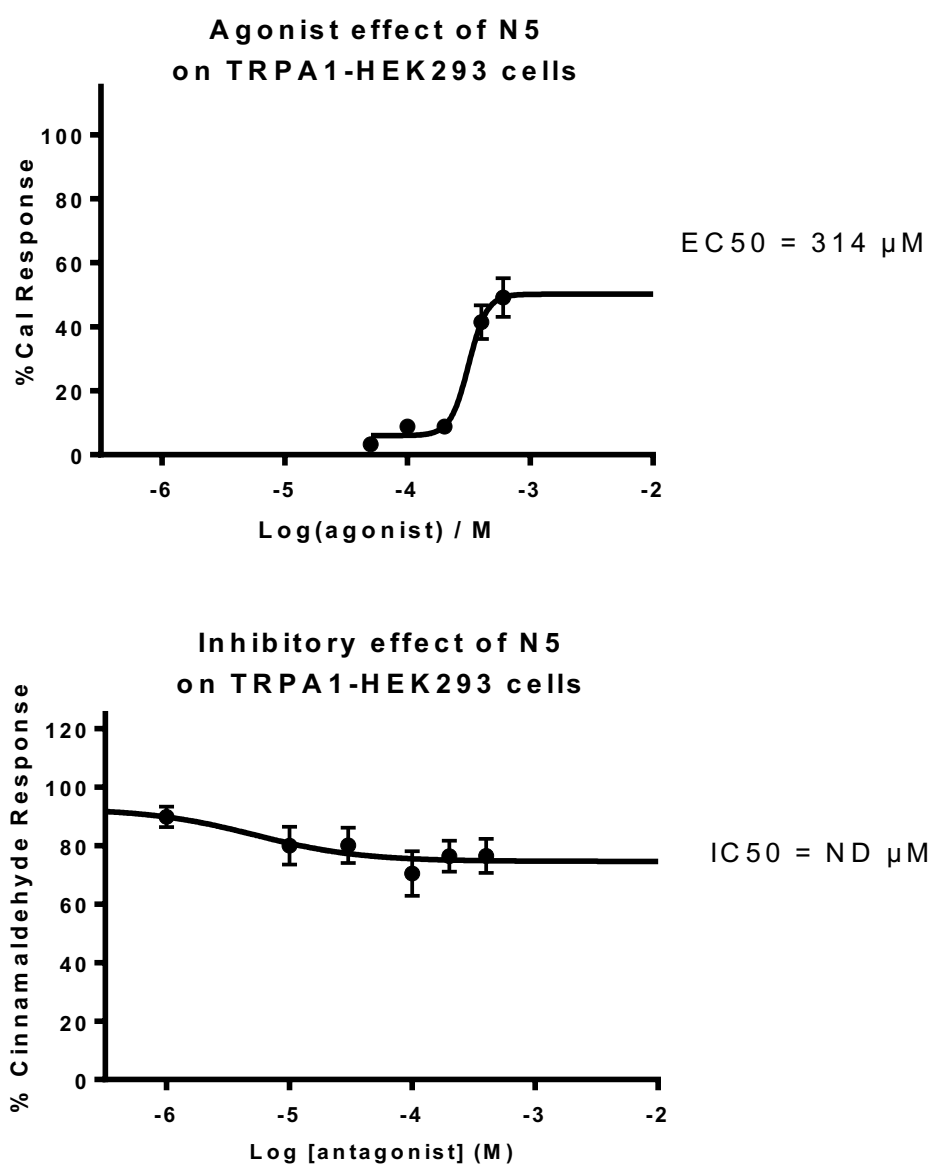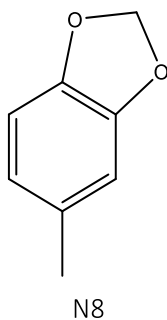Figure 186 Chemical structure of N8

$EC50 = 248 \, \mu M$

$IC50 = ND$
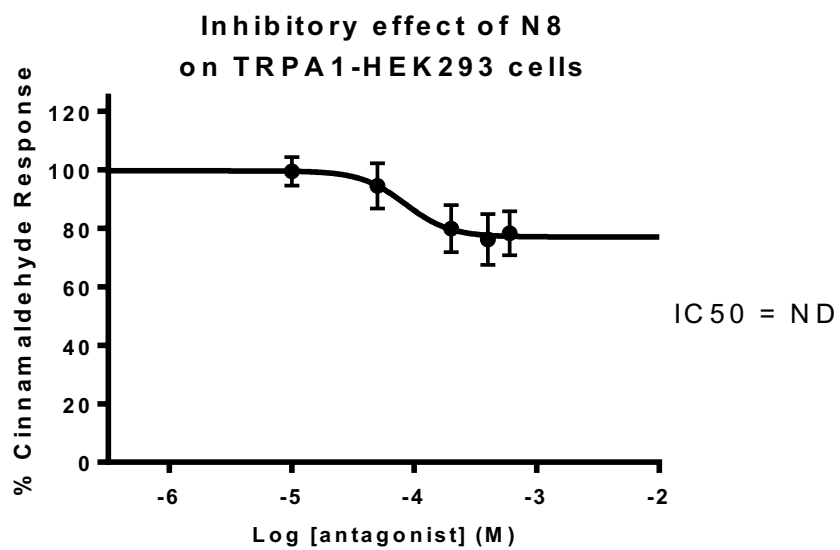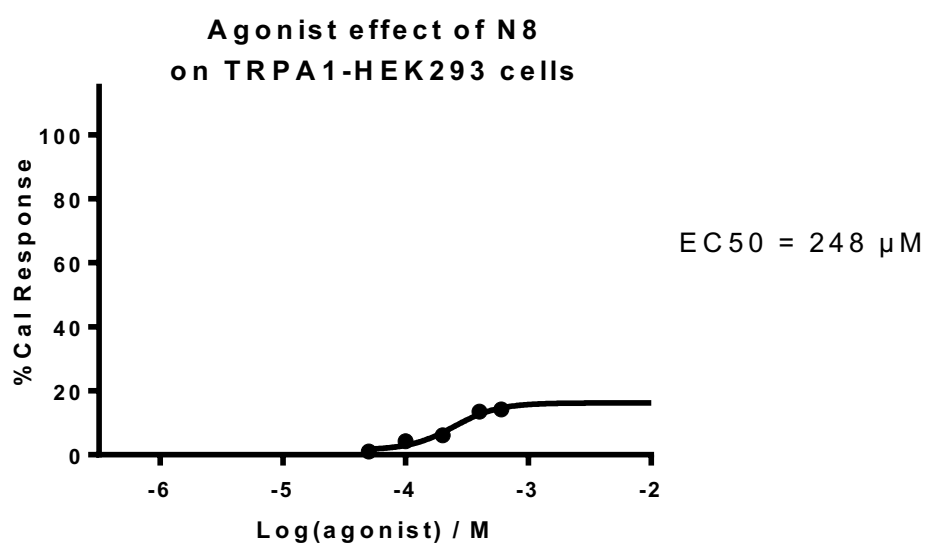
Figure 187 Agonist (above) and antagonist (below) concentration effect curves for N8 on TRPA1-HEK293 cells. Data points are means±SEM of N = 3 experiments

N8 has been assayed using both the agonist and antagonist calcium signalling assays to assess the compound's effect on TRPA1-HEK293 cells. The resulting concentration effect curves can be seen in Figure 187 above.

In the agonist assay a concentration dependent increase in intracellular calcium was observed. This response was inhibited fully by the TRPA1 specific inhibitor HC-030031 therefore this response can be attributed to the gating of TRPA1 channels. N8 was tested over the concentration range of 10 to 600 µM. The first significant response was observed at 400 µM with a mean %CaI response of 14. The maximum response was observed at the 600 µM concentration point with a mean %CaI response of 14. As can be seen, the agonist response of N8 over the concentration range tested is very small, predictions as to what the trend will be after the 600 µM concentration is difficult to determine, however the 400 µM and 600 µM responses are very similar which may indicate a plateau. This plateau at such a low response agrees with the variable slope four parameter non-linear regression analysis model which was the best fit model. Therefore it can be considered that N8 has low efficacy and potency (efficacy of 20 % of the maximum response of cinnamaldehyde and an EC50 value of 248 µM).

In the antagonist assay a concentration dependent decrease in the response of 30 µM of cinnamaldehyde (EC50 concentration of cinnamaldehyde) was observed with increasing concentration of pre-dosed N8. N8 was again tested over the concentration range of 10-600 µM. The first decrease in the cinnamaldehyde response was observed at 200 µM with a decrease in cinnamaldehyde response of 20%. The greatest reduction in the cinnamaldehyde response occurred at the 400 µM concentration point with a reduction of 24 %. Full inhibition of the cinnamaldehyde response was not observed as testing above a concentration of 600 µM of N8 was not possible due to poor solubility in the assay media at higher concentrations. However, the trend of the data points does not seem to indicate a full inhibition of TRPA1 at a relevant pharmacological concentration, it does seem to indicate a partial inhibition as the reduction in the cinnamaldehyde response at the 600 µM is less than that of the 400 µM concentration point. This is indicated by the variable slope four parameter curve fit model which was the best fit curve, but the fit is very poor with an R^2 value of 0.3569 so the prediction of the response beyond the concentration tested cannot be taken with any great certainty.

From this analysis of the agonist and antagonist assays of N8 on TRPA1-HEK293 cells, it can be determined that N8 has a small agonist effect on TRPA1 which after the initial activation of TRPA1 slightly inhibits further activation via a desensitisation effect.

5.2.6.9　Methylated thymol
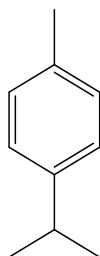
Methylated Thymol

Figure 188 Chemical structure of methylated thymol
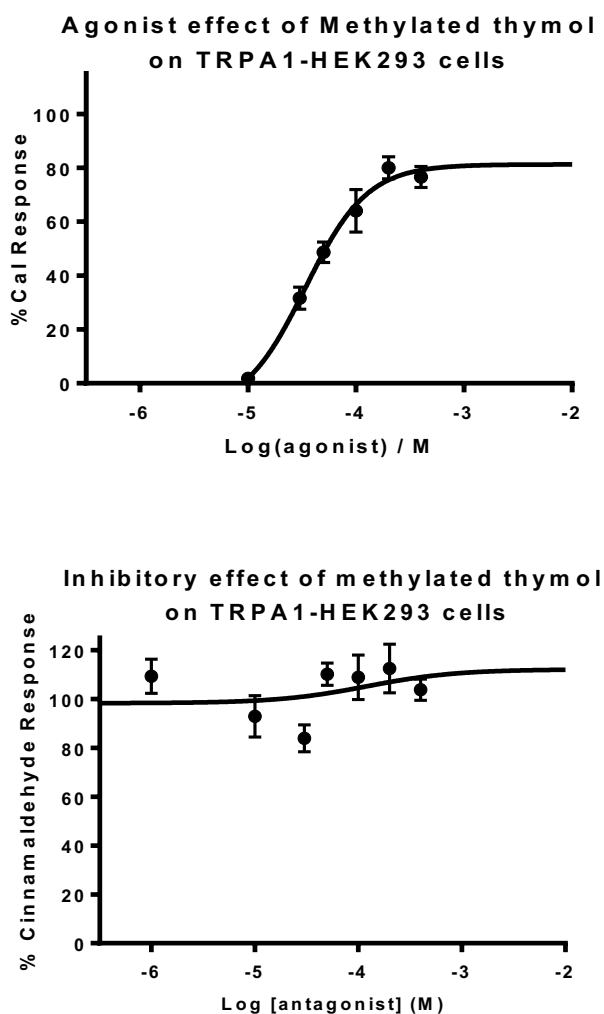
Figure 189 Agonist (above) and antagonist (below) concentration effect curves for N8 on TRPA1-HEK293 cells. Data points are means±SEM of N = 3 experiments

Methylated thymol has been assayed using both the agonist and antagonist calcium signalling assays to assess the compound's effect on TRPA1-HEK293 cells. The resulting concentration effect curves can be seen in Figure 189 above.

In the agonist assay, a concentration dependent increase in intracellular calcium was observed. This response was inhibited fully by the TRPA1 specific inhibitor HC-030031 therefore this response can be attributed to the gating of TRPA1 channels. Methylated thymol was tested over the concentration range of 10 to 400 µM. The first significant response was observed at 30 µM with a mean %CaI response of 28. The maximum response was observed at the 200 µM concentration point with a mean %CaI response of 80. A maximum plateau was observed between 100 and 200 µM, this was confirmed be the curve of best fit. Non-linear regression analysis has been carried out using two different models, the best fit curve was created using the variable slope four parameter model, which has an R^2 value of 0.8368, this model as previously mentions confirms when the response reaches its maximum plateau. The calculated EC50 for methylated thymol using the variable slope four parameter model is 33 µM with an efficacy of 111% of the maximum cinnamaldehyde response.

In the antagonist assay no inhibitory trend was observed over the concentration range tested, 1 to 400 µM, methylated thymol does not inhibit the activation of TRPA1 by cinnamaldehyde.

From this analysis of the agonist and antagonist assays of methylated thymol on TRPA1-HEK293 cells, it can be determined that methylated thymol is a full agonist of TRPA1 which does not inhibit further activation of TRPA1.

5.3 Discussion

The following will discuss in depth the results reported in this chapter.

5.3.1 Effect of NDGA and M4N on TRPA1-HEK293 cells

In section 5.2, the results from the agonist and antagonist assay for both NDGA and M4N are described in detail. A comparison of the concentration effect curves for both NDGA and M4N can be seen in Figure 190. NDGA and M4N have been found to be potent full agonists of TRPA1. M4N was found to be the more potent of the two compounds and also showed a slightly higher efficacy of activation. Both compounds showed no desensitisation of TRPA1 at the concentrations tested.
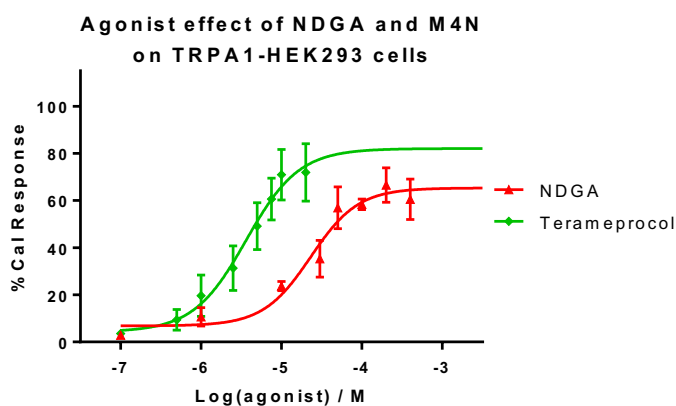
Figure 190 Comparison of agonist concentration effect curves for NDGA and M4N on TRPA1-HEK293 cells. Data points are means±SEM of N = 3 experiments

NDGA became the subject of interest via a literature review of TRPM7 inhibitors brought about by results which reported that carvacrol, a TRPA1 agonist, was an inhibitor of TRPM7(251). As carvacrol and its interaction with TRPA1 was already of interest as some of the compounds in chapter 3 are based on the carvacrol structure, it was a natural route of investigation to look further into TRPM7 and other inhibitors of the channel. Of the inhibitors reviewed in section 5.1.3, NDGA stood out due to its catechol structure and because of its linked phenyl rings. Lee *et al.* (130) had reported thymol, carvacrol and some related monophenol structures activated TRPA1. In the report they hypothesised that phenols that had alkyl substitutions would activate TRPA1 with compounds which had a

higher logP value being more potent. They did not report any results for catecahol-like structures such as NDGA. Also, in chapter 3 it was discussed that compounds with two phenyl groups showed increased modulation of TRPA1 with increasing separation of the two phenyl rings. This has also been shown in the results reported by Liu *et al.*(142). NDGA has a 4 carbon alkyl chain which links the two phenyl rings. Both NDGA's catechol structure and its diphenyl arrangement were points of interest with regards to a possible interaction with TRPA1 therefore it was decided that NDGA should be taken forward to be tested via the calcium signalling assays (described in section 2.2) for TRPA1 modulation. As previously mentioned it was found that NDGA was a full agonist of TRPA1 with an EC50 of 23 µM and unlike the compounds in chapter 3 did not have a desensitising effect after the initial activation. This agonist effect by NDGA was inhibited fully by HC-030031, a specific TRPA1 antagonist. As was described in section 5.1.1, M4N shares a lot of similarities to NDGA with regards to biological activity yet does not suffer the same toxicity issues. Therefore, M4N was also tested and was found to be a full agonist of TRPA1, more potent than NDGA with an EC50 of 4 µM and with a slightly greater efficacy, M4N also did not desensitise TRPA1 after initial activation. The agonist effect of M4N was also found to be fully inhibited by the TRPA1 specific antagonist HC-030031.

Whilst my results were being collected, another research group reported the activation of human TRPA1 by NDGA and M4N with M4N being the more potent of the two(252). In their results the difference in the EC50 values of NDGA and M4N (5.4 µM and 4.5 µM, respectively) were not as great as I have observed, however they also noted that M4N gave a greater maximum response than NDGA, which is in line with what I have reported. Redmond *et al.*(252) stumbled across NDGA and its interaction with TRPA1 when looking into the effects of arachidonic acid and its potential metabolites on TRPA1. They used NDGA as a lipoxygenase inhibitor as part of their assay method and discovered that NDGA increased intracellular calcium concentration in TRPA1-HEK293 cells. Upon following up this discovery they found M4N to have a similar effect. Site directed mutagenesis of the TRPA1 channel was carried out by Redmond *et al.*(252) in order to reveal more information with regards to the mechanism of activation by NDGA and M4N. They carried out the mutation of three cysteine groups, Cys621, Cys641 and Cys 665 to serine, essentially converting the thiol group of cysteine to an alcohol group. The activation of NDGA and M4N

in the 3xCys mutant of TRPA1 was found to be weaker than that determined for the wild type TRPA1. They concluded that this shows that the mechanism of action for NDGA and M4N acts through Cys621, Cys641 and Cys665. While this mutation knocks out activation via covalent modification by electrophilic compounds fully as first reported by Hinman *et al.*(64), it has been noted that these mutations may play a role in the general mechanism of gating as it has been reported that a variety of different agonists all showed a lower potency of activation of TRPA1 with these three cysteine mutations(142). So, it is uncertain as to where NDGA and M4N bind to TRPA1, possibly it may be through the menthol active site situated in the TM5 domain highlighted by Xiao *et al.* (55), as is the case for thymol and carvacrol.

5.3.2 Effect of methylation of phenol groups on TRPA1 activity

M4N is the tetramethylated derivative of NDGA as discussed in section 5.3.1. It was found that M4N was both more potent and showed a slightly greater efficacy. The effect of methylating the four phenol groups are that the methyl groups add extra bulk to the compound and that methoxy groups cannot act as hydrogen bond donors and acceptors just hydrogen bond acceptors due to the lone pair electrons present on the oxygen atoms. The electronic effects of the methoxy and alcohol groups on the phenyl rings are pretty much similar.

Figure 191 Comparison of agonist concentration effect curves for Thymol and methylated thymol on TRPA1-HEK293 cells. Data points are means±SEM of N = 3 experiments

Figure 192 Comparison of antagonist concentration effect curves for Thymol and methylated thymol on TRPA1-HEK293 cells. Data points are means±SEM of N = 3 experiments

A hypothesis was made that methylation of phenol groups of agonists which activated TRPA1 would lead to a greater agonist response. In order to prove this hypothesis thymol and the methylated derivative of thymol were assayed using the calcium signalling assays found in section 2.2. The resulting concentration effect curves have been compared in Figure 191 and Figure 192. As can be seen from the comparison graphs the effect of methylation of the phenol group has seen an increase in potency and efficacy, similar to that seen between NDGA and M4N (see Figure 190). However, the difference in agonist properties is not to the same degree as NDGA and M4N which saw a big difference in EC50 values (23 µM and 3.6 µM respectively) compared to thymol and methylated thymol (44 µM and 33 µM respectively). This smaller difference may be attributed to the number of phenol/methoxy groups.

The reason as to why this alteration in structure has a positive effect on the activation of TRPA1 by NDGA and thymol cannot be fully determined at this point in time. It may be that the extra reach of the methyl groups allows for greater interaction with the binding site. Alternatively, it may be due to the lipophilicity of the compounds, Lee *et al.*(130) when they reported that thymol activated TRPA1 mentioned how in general the greater the lipophilic nature of alkylated phenols the greater the potency of activation. The *in silico* calculated LogP values for NDGA, M4N, thymol and methylated thymol can be found in Table 30. These values have been calculated using the LogP v14.04 software as part of ACD Chemsketch software. As can be seen from these values is that the methylated derivatives

have a greater LogP value and the difference between NDGA and M4N is much greater than for thymol and methylated thymol. This agrees with the observation that Lee *et al.* (130) reported. An observation that can also be made is that the hydrogen bonding acceptor nature of the methoxy derivatives must still be capable of interacting with the binding site similar to that of the phenols.

Compound	LogP
NDGA	3.71 ±0.26
M4N	5.86 ±0.30
Thymol	3.28 ±0.20
Methylated thymol	3.93 ±0.22

Table 30 LogP values for NDGA, M4N, thymol and methylated thymol. Calculated using ACD chemsketch LogP v14.04 software

Another interesting point to note is the desensitising effect of thymol on TRPA1 is not observed with the methylated derivative. The reason for this is unclear as not much is known with regards to the mechanisms of desensitisation but from the results reported in this chapter and those in chapter 3 and 4 it does appear that this mechanism behaves independently of the mechanism of activation.

5.3.3 Effects of N1-N8 on TRPA1 and relation to NDGA and M4N effects on TRPA1

N1	N2	N3	N4
EC50 = 163.1uM	EC50 = 84.8uM	EC50 = 122.8uM	EC50 = 130.4uM
Efficacy = 73.0%	Efficacy = 79.6%	Efficacy = 75%	Efficacy = 45%
IC50 = 104.4uM	IC50 = 56.6uM	IC50 = 27.5uM	IC50 = 50.6uM

N5	N6	N7	N8
EC50 = 314.4uM	EC50 = 294.4uM	EC50 = 138.9uM	EC50 = 247.9uM
Efficacy = 67.9%	Efficacy = 88.3%	Efficacy = 67.9%	Efficacy = 19.6%
IC50 = ND	IC50 = ND	IC50 = ND	IC50 = ND
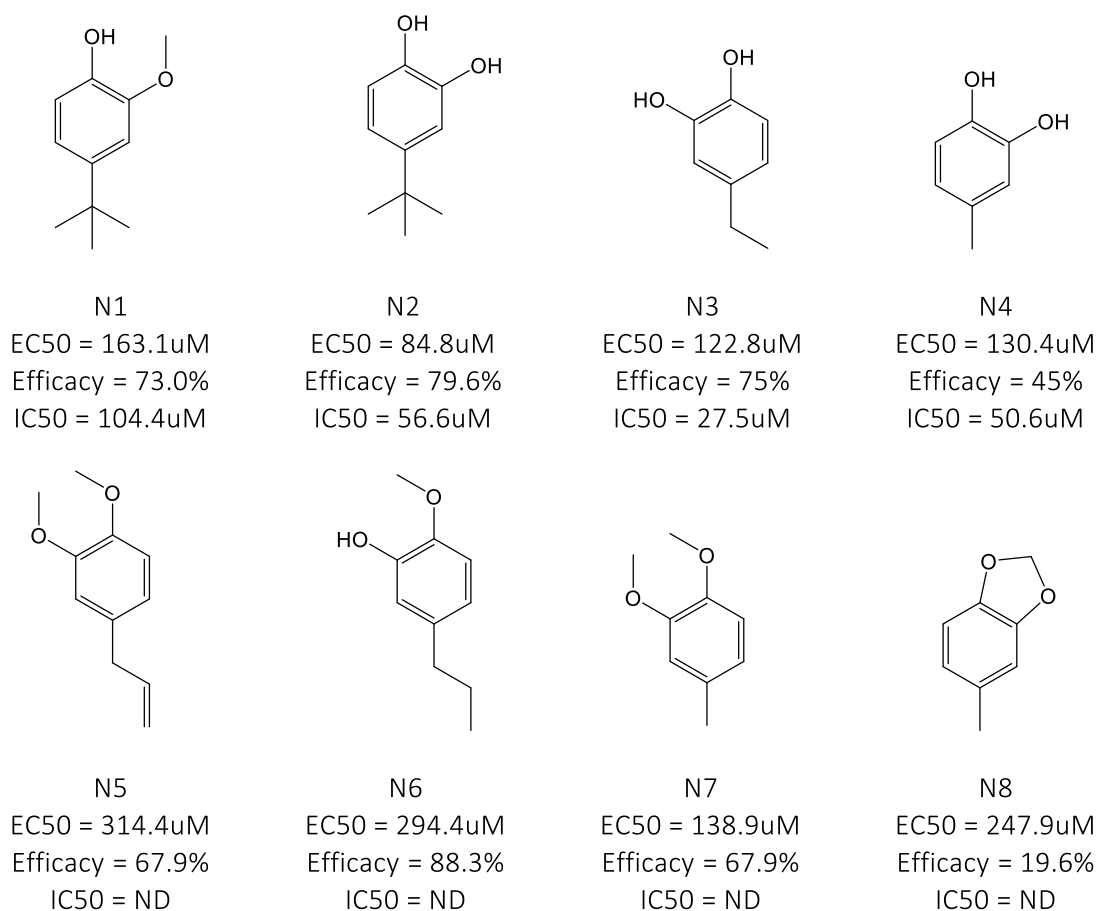
Figure 193 Chemical structures and summary of assay results for N1-N8

Due to the structure of NDGA and M4N being symmetrical it brought into question the reason for its enhanced potency in the activation of TRPA1. Was it due to the fact that there are two pharmacophores i.e. the two substituted phenyl rings which increases the potential for the compound to bind with the binding site. Or, are the enhanced agonist properties due to the three-dimensional conformation of NDGA and M4N. In order to give an indication to this eight compounds similar to one half of NDGA and M4N have been assayed in the agonist and antagonist calcium signalling assays (see section 2.2 for method details) the structures and summary of the assay results can be seen in Figure 193.

The results show that alkylated catechol and methylated derivatives modulate TRPA1 although the potency of these interactions are not as potent as for NDGA, M4N, thymol and methylated thymol. As can be seen from the results N2 was the most potent agonist

of TRPA1 with an EC50 of 85 µM. NDGA is approximately four times more potent than N2 and much more potent than the other compounds tested. Also none of the compounds showed an efficacy greater than NDGA, with N6 being the closest with an efficacy of 88% of the maximum cinnamaldehyde response. These results may suggest the possibility of two close proximity binding sites that the catechol pharmacophores can bind to. With the increased potency of NDGA and M4N being explained by the fact that the binding of one of the catechol pharmacophore brings the second catechol group into close proximity to the second binding site, and therefore increasing its local concentration and probability of interaction with the binding site. This effect is commonly referred to as 'avidity'. Alternatively, NDGA and M4N both have a freely rotating alkyl chain linking the two phenyl groups together which allows a wide range of flexibility, possibly allowing some form of pi-stacking to occur possibly accounting for the lowest energy conformation which may bind to a single activation site of TRPA1 effectively. Ho *et al.* (253) have synthesised a range of M4N derivatives that seek to restrain the flexibility of the molecule. They then assayed these derivatives and some of which showed greater growth inhibitory values on several different cancer cell lines including malignant pancreatic BxPC-3. The derivatives which showed the greatest growth inhibitory values were structures which mimicked the lowest energy conformation of M4N. They had determined that M4N in its lowest energy conformation adopted a T-shaped pi-stacking arrangement, the most potent derivatives, shown in Figure 194 in three-dimensional space imitate this lowest energy conformation of M4N. It was therefore hypothesised that the lowest energy conformation was responsible for M4Ns growth inhibitory action. It may be the case that similar analogs for NDGA and M4N that restrain the flexibility of the molecule may show greater activation of TRPA1.
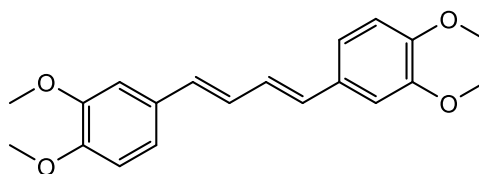
Compound 1a

(1*E*,3*E*)-1,4-bis(3,4-dimethoxyphenyl)buta-1,3-diene
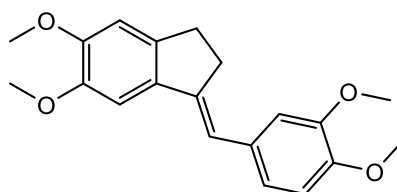
Compound 7

(*E*)-1-(3,4-dimethoxybenzylidene)-5,6-dimethoxy-2,3-dihydro-1 *H*-indene

Figure 194 Chemical structures of rigid derivatives of M4N from Ho et al. 2013(253)

There are several comparisons to be made from the N1-N8 compounds. Starting with N5, N7 and N8, these three compounds all have ether groups and no phenol groups. They were all observed to activate TRPA1 in a concentration dependent manner. As can be seen from the comparison graphs in Figure 195 and Figure 196. N7 is the most potent agonist and has the highest efficacy, along with N5. N5 is the weakest with regards to potency and N8 has the lowest efficacy of the three compounds. None of the compounds display a desensitisation effect over the concentration ranges tested.
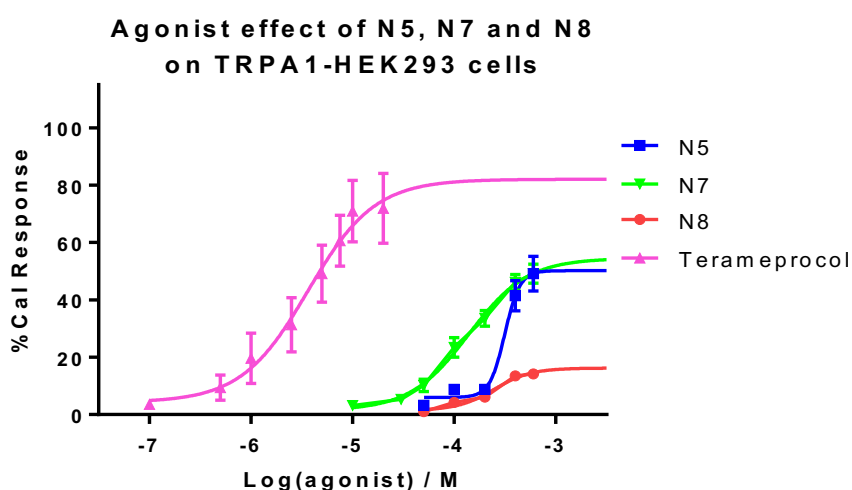
Figure 195 Comparison of agonist concentration effect curves for N5, N7 and N8 on TRPA1-HEK293 cells. Data points are means±SEM of N = 3 experiments

265
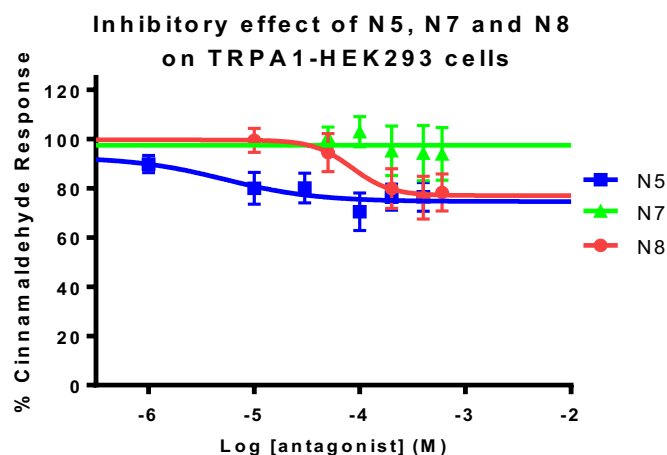
Figure 196 Comparison of antagonist concentration effect curves for N5, N7 and N8 on TRPA1-HEK293 cells. Data points are means±SEM of N = 3 experiments

N8 showed a very poor activation potency and efficacy of TRPA1. This may be due to the restricted nature of the dioxole ring affecting the binding of the compound to the TRPA1 activation site. The three-dimensional structures of N7 and N8 can be seen in Figure 197, these structures were produced in Chem3D 15.1 and a standard MM2 energy minimisation calculation was carried out to predict the lowest energy conformation. From the structures it can be seen that the arrangement of the two methoxy groups covers more space as opposed to the dioxole ring. The dioxole ring is similar in structure to the highest energy conformation for N7 where the two methyl groups are within close proximity.
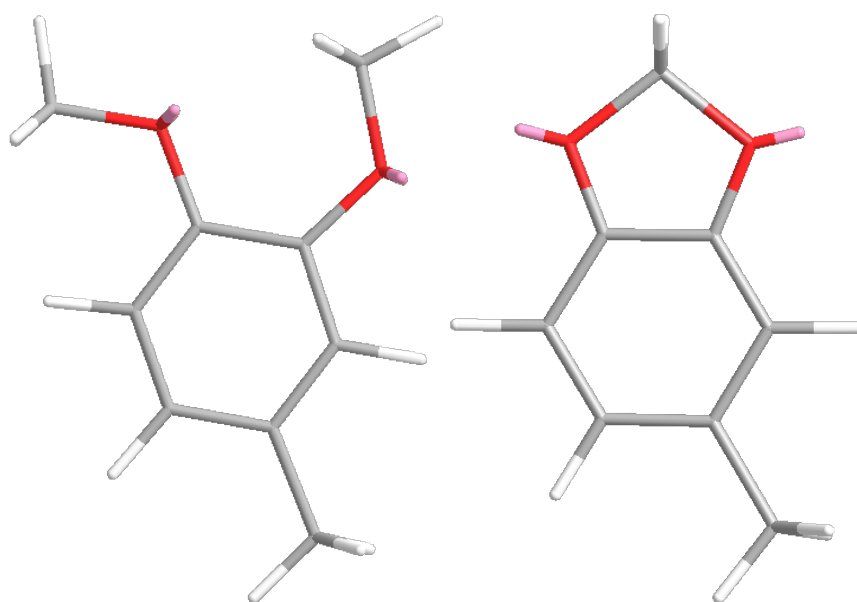
Figure 197 Three-dimensional structures of N7 (left) and N8 (right). Structures are the lowest energy conformations for N7 and N8, calculated using Chem3d v15.1 MM2 calculation.

These results are in line with what was observed with M4N and methylated thymol. M4N and methylated thymol activated TRPA1 and did not desensitise the channel after the initial activation which has been replicated in the results observed for N5, N7 and N8.
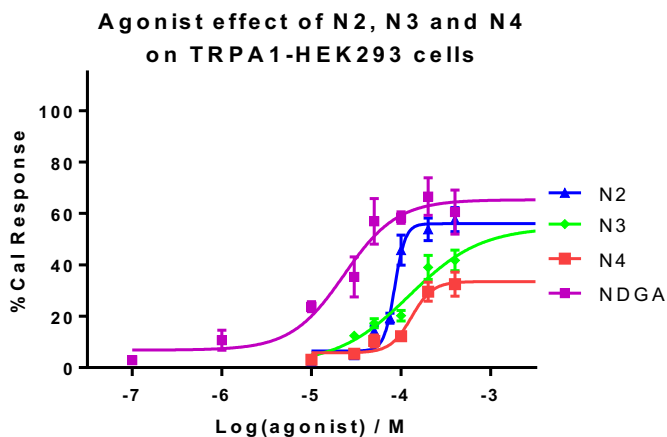
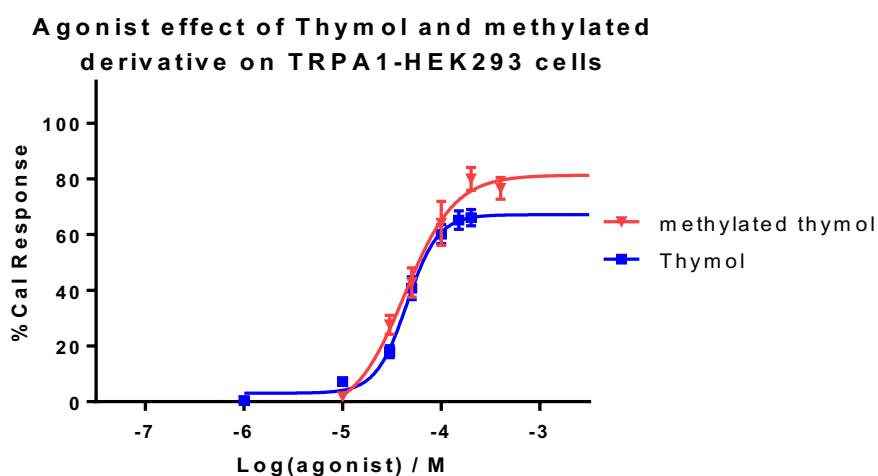Figure 198 Comparison of agonist concentration effect curves for N2, N3 and N4 on TRPA1-HEK293 cells. Data points are means±SEM of N = 3 experiments
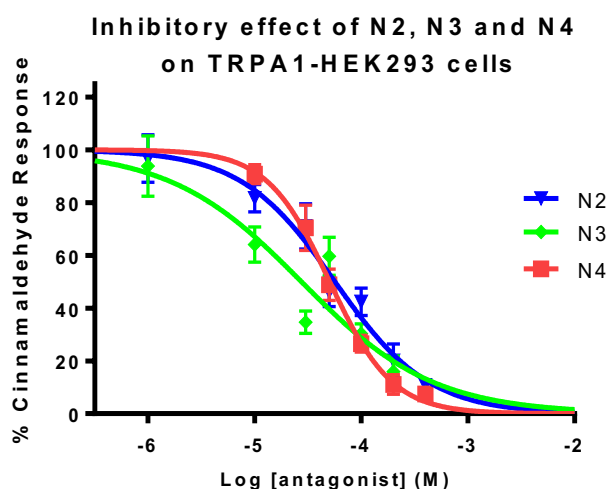
Figure 199 Comparison of antagonist concentration effect curves for N2, N3 and N4 on TRPA1-HEK293 cells. Data points are means±SEM of N = 3 experiments

N2, N3 and N4 are all diphenol compounds, and their concentration effect curves in from the TRPA1 agonist and antagonist calcium signalling assays have been compared in Figure 198 and Figure 199. Each of the compounds showed similar agonist and antagonist properties. They all displayed an agonist effect, with similar potencies and varying efficacy, they also were all found to desensitise TRPA1 to further activation by cinnamaldehyde in a concentration dependent manner.

The order of activation potency and efficacy for N2, N3 and N4 on TRPA1 followed the hypothesis outlined by Lee *et al.* (130) which stated that the TRPA1 agonist effect of alkylated phenols increases with increasing lipophilicity. This opposes what has been observed with the dimethoxy compounds N5, N7 and N8. These observations are not enough to prove or disprove a link between lipophilicity and TRPA1 activation especially considering the overall weak potencies and efficacies of these compounds, as well as the lack of direct comparisons.
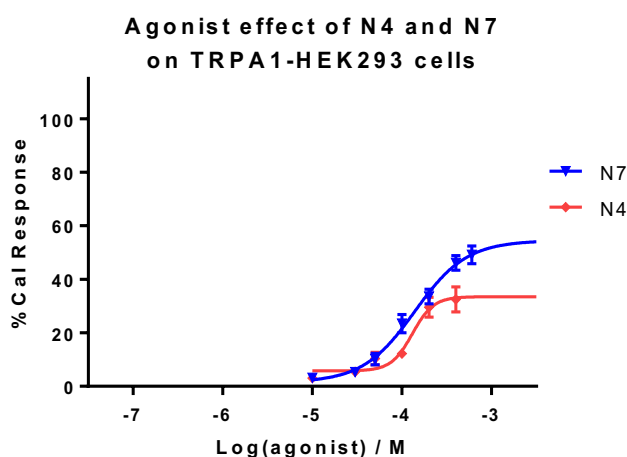
Figure 200 Comparison of agonist concentration effect curves for N4 and N7 on TRPA1-HEK293 cells. Data points are means±SEM of N = 3 experiments

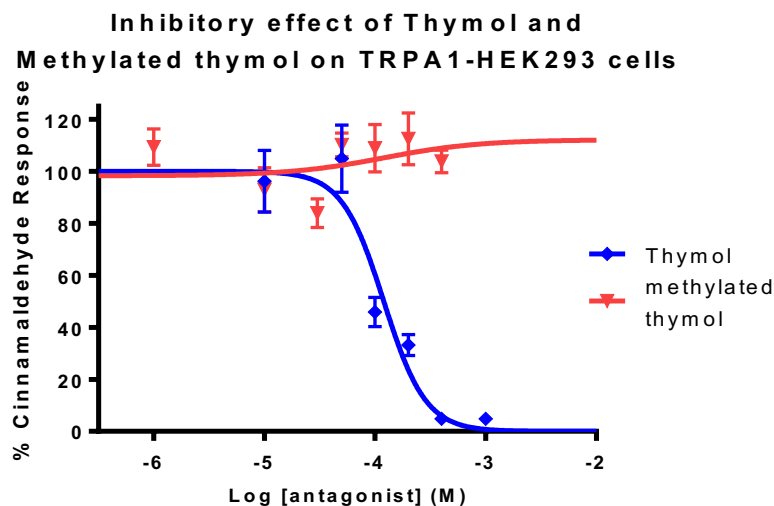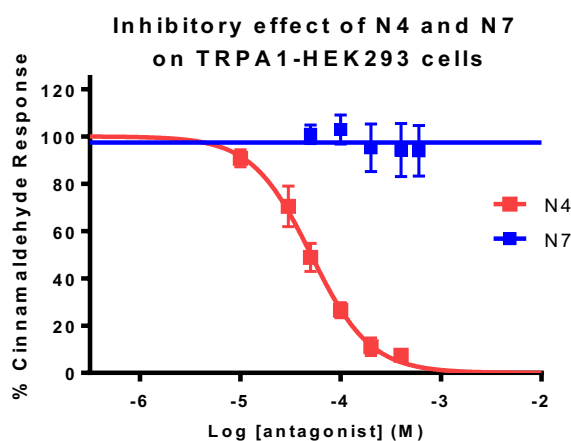*Figure 201 Comparison of antagonist concentration effect curves for N4 and N7 on TRPA1-HEK293 cells. Data points are means±SEM of N = 3 experiments*

The only true direct comparison between diphenol and dimethoxy compounds of the series of phenyl compounds is between N4 and N7. The comparison of the concentration effect curves from the TRPA1 agonist and antagonist calcium signalling assays can be seen in

Figure 200 and Figure 201. From the comparison graphs it can be seen that N7, the dimethoxy compound, is a more potent and efficacious agonist than its diphenol analog which is the same as that observed for NDGA and M4N. The results obtained from the antagonist assay show that N7 does not have a desensitising effect on further activation of TRPA1 whereas N4 does show a full desensitisation effect. This follows the trend observed for the N1-8 compounds all of the diphenols showed some form of desensitisation of TRPA1 over the concentration range tested whereas the dimethoxy compounds did not. It may be the case that the dimethoxy compounds have a desensitisation effect on TRPA1 at higher concentrations than those tested. This trend is observed in thymol and its methylated derivative. The trend is not observed with NDGA and M4N as both have been shown to not have a desensitisation effect on TRPA1. This indicates that the structure of these two compounds inhibits the desensitisation effect on TRPA1, it also indicates that desensitisation of the channel may occur through a different mechanism than activation and is not necessarily a downstream effect of activation of TRPA1.

5.4 Summary and Conclusion

The results presented in this chapter highlight NDGA and its semi-synthetic methylated derivative M4N as potent agonists of TRPA1 which do not desensitise TRPA1 to further activation, unlike other non-covalent agonists of TRPA1. NDGA was highlighted as a potential modulator of TRPA1 through a literature review of TRPM7 inhibitors. Interest in TRPM7 inhibitors came about due to a report that had shown carvacrol, a TRPA1 agonist and a compound of interest to my research, was found to inhibit TRPM7(251). It may be the case that TRPM7 and TRPA1, due to the interactions of both channels with carvacrol, may share a similar form of active site.

There was a stark difference between the response of M4N and NDGA which was replicated with thymol and methylated thymol as well as with the agonist responses observed for N4 and N7. The methylated compounds all showed a greater potency and efficacy with regards to their agonist response on TRPA1. Also, it was observed that the methylated compounds did not inhibit the response of cinnamaldehyde in the antagonist assay and were deemed not to have a desensitising effect whereas the phenol compounds did desensitise TRPA1 to further activation by cinnamaldehyde, all except NDGA. It is thought that the larger folded structure of NDGA may prevent interaction with the channel in a way that causes the desensitising effect. Further research with a variety of compounds is required to fully understand the exact nature of the differences between the modulation of TRPA1 by the two functional groups.

The N1-N8 compounds were assayed with the primary purpose to decipher if the responses observed for NDGA and M4N were due to them both having two pharmacophores or are the potent agonist responses due to the overall effect of the three dimensional structure. All of the N1-N8 compounds were chosen to imitate one half of the symmetrical structure of NDGA and M4N. The assay results showed that the potent agonist response for NDGA and M4N were due to the three dimensional structure of the two compounds. It has been highlighted that restraining the flexibility of the linking group of NDGA and M4N may increase the potency of the TRPA1 agonist response similar to that reported by Ho *et al.* (253). As interest in NDGA and particularly M4N increases with regards to drug development for their anti-cancer properties, their effect on TRPA1 must be considered

due to the channels involvement in pain and inflammation. NDGA and M4N can be used as alternative pharmacological tools when researching TRPA1 and may be a useful starting point in drug development projects targeting TRPA1.

6 Final Discussion

TRPA1, the non-specific ion channel, is formed from four TRPA1 subunits and has been found to have a role in a wide variety of biological functions (see section 1.2.5). This is in part due to the channel's complex nature, as is evident from the wide range of chemically diverse agonists and antagonists that have been reported(64,129,130,136,139,141,142,176,252,254). The diversity of TRPA1 modulators indicates that there are multiple binding sites, this is backed up by multiple mutagenesis studies which detail a number of key amino acid residues that are crucial for certain agonists and antagonist interactions with TRPA1(55,64,128,137,255,256). The results that have been reported as part of chapter 3, 4 and 5 further expand the diversity of TRPA1 modulators and highlight key points with regards to their interaction with TRPA1 which may be of use in drug development.

The calcium signalling methods used to generate the concentration effect curves for the compounds tested described in section 2.2 can be deemed suitable to determine the effect of the test compounds on the TRPA1 protein. TRPA1 is a non-specific ion channel and activation of the channel causes increases in intracellular calcium concentrations(57). The method used uses a fluorescent calcium indicator Fluo-3AM which when applied to the cells is able to diffuse through the plasma membrane once inside the cell Fluo-3AM is broken down by naturally occurring esterases. The product of this is a fluorescent calcium indicator but is also trapped inside the cell. The increase in fluorescence observed is therefore due to the increase in intracellular calcium. Therefore, changes observed in the fluorescence of the assay media are due to changes in intracellular calcium caused by the gating of TRPA1. In order to ensure that the responses of the test compounds were specific to TRPA1 and the response was not caused by other cellular interactions each compound which showed a response in TRPA1-HEK293 cells was assayed at their maximum effective concentration on mock-transfected HEK293 cells. As mentioned in results sections 3.2, 4.2 and 5.2 none of the active test compounds showed any increase in intracellular calcium concentration and therefore the responses observed in TRPA1-HEK293 cells can be deemed to be via the TRPA1 protein.

TRPA1 transfected HEK293 cells have been used in each of the assays and each experiment a number of controls were carried out to ensure that the cells used were suitable produced reproducible results. The controls carried out were calcium ionophore, a solvent control (DMSO), an agonist control (cinnamaldehyde) and an antagonist control (HC-030031 a specific and potent TRPA1 antagonist). The calcium ionophore control was carried out at the start, middle and end of each experiment and gave an indication of cell viability, if the response differed significantly throughout the course of the experiment then results were not used. The solvent control determined if there was any interaction between the solvent used to dissolve the test compounds and TRPA1-HEK293 cells which would give a false positive result. The specific solvent used to dissolve the test compound was used as the solvent control; this was to determine if there was any contamination which gave a response. The agonist control was carried out at the start middle and end of the experiment to determine the expression of the TRPA1 and to ensure it was consistent throughout the experiment. If the agonist control differed from what was expected, then the experiment was repeated. The antagonist control was carried out in much a similar way to that of the agonist control.

There are several advantages of the fluorescent based calcium signalling assay used. The assay uses the reversible calcium indicator Fluo-3 which allows for the tracking of increases and decreases in intracellular calcium concentrations. Fluo-3 requires excitation and emission wavelengths of 506 and 526 nm respectively; these wavelengths are relatively high compared to some other calcium indicators available; therefore, reducing any potential damage to the cells. The assay method records the response of a population of cells in suspension, which provides greater reliability in the results recorded over single cell assay methods. However, there are limitations to this method as it only records the effects of channel gating i.e. changes to intracellular calcium levels. The effect of the test compound on the cells cannot be truly identified as direct binding to the TRPA1 or TRPM8; they may indirectly modulate calcium influx via other mechanisms e.g. via activation of GPCRs that in turn activate TRPA1. False positive and negative results may also occur using the method used. Test compounds may interfere with Fluo-3 activation, especially the ester based compounds which maybe hydrolysed by the same esterases that breakdown the Fluo-3AM. These compounds may then bind to calcium and not fluoresce in the same

manner as Fluo-3 producing a false positive or negative result dependent on the assay type. Also the spectral properties of the test compounds may have interfered with the readout therefore effecting the result obtained. In order to further understand the effects of the compounds tested other assay methods should be carried out which do not have the same limitations. A patch clamp based assay method would be ideal to be used alongside a fluorescent based assay method as any fluorescent based issues would be non-existent in a patch clamp based method.

In chapter 3 three groups of compounds were assayed for TRPA1 activity. All three groups of compounds are derivatives of thymol and carvacrol which are known TRPA1 agonists(130). The first group, ojk01, was made up of 2-isopropylphenol and 2-isopropylamine that have been linked via an ester and amide bonds to a substituted phenyl ring. This group of compounds highlighted that the amide linking bonding was necessary for interaction with TRPA1 rather than the ester bond. It was hypothesised that the amide compounds were able to hydrogen-bond to crucial amino acid residues in order to anchor the rest of the molecule into the binding site, to allow pi-pi interactions to occur between the two phenyl rings of the ojk01 compounds and the amino acid residues which make up the binding site. The effect that was observed for ojk0107; which is a benzyl derivative, was the first indication that the length between the two phenyl rings was important to the modulation of TRPA1. This effect has also been shown in greater detail by Liu *et al.* 2010(142) when they showed that an increasing alkyl chain length between the two phenyl rings of NPB resulted in a greater potency of TRPA1 activation. From the ojk01 the effect of chloro groups on the second phenyl was observed, it was found that the closer the chloro group was the greater the potency of activation and desensitisation of TRPA1. This has been hypothesised to be due to the electronic effects of the amide and chloro group working in tandem to have a greater interaction with the TRPA1 binding site.

The second and third groups from chapter 3 are the ojk06 and ojk07 groups which are derivatives of carvacrol and thymol respectively. Both groups contain compounds which contain acetamide linking groups which link a carvacrol/thymol moiety to a substituted phenyl ring. These compounds backed up the hypothesis from the ojk01 compounds showing that the greater the length between the two phenyl rings, the greater the interaction with TRPA1. A direct comparison could not be made between the ojk01 and

ojk06/7 compounds as other structural differences may play a part in the binding interactions. The ojk06 and ojk07 compounds all showed a potent agonist response with varying levels of efficacy; they also showed a strong desensitisation effect on TRPA1 to further activation. The desensitisation effect seems to be independent of the activation of TRPA1 as there appeared to be no increase in desensitisation with an increase in agonist potency. It may be that these compounds interact with two different sites, one of which produces an agonist response, the other produces an inhibitory response. This theory supported by the fact that generally the ojk06 compounds were more potent desensitisers than the ojk07 compounds and that the ojk07 compounds were more potent agonists. This trend is most probably due to the effect of the linking group attaching in a different position for the two groups therefore producing different three dimensional structures. In chapter 5 the three dimensional structure of NDGA and M4N was discussed and how the two phenyl rings interacted in a T-shaped fashion due to the flexibility of the alkyl linking group, NDGA and M4N were both potent agonists of TRPA1 and did not have a subsequent desensitisation effect. The absence of desensitisation was postulated to be due to the folded nature of the lowest energy conformation of the two compounds. In comparison the ojk06 and ojk07 compounds display a much more rigid linking group which will produce a much more linear three dimensional structure, which may be responsible for the desensitisation effect of the ojk06 and ojk07 compounds. Alternatively, it has been proposed that the ether group in the ojk06 compounds is less sterically hindered and therefore is more open to forming intermolecular bonds with the binding site, which may be of greater importance to the desensitisation effect. The ojk06 and ojk07 compounds have been compared with regards to their substituent groups on the second phenyl group. It was found that in general the methyl derivatives were more potent agonists of TRPA1 and isopropyl derivatives were the more potent desensitisers. The ring position of these groups was also compared and varying results were observed dependent on the group. The differences between the chloro derivatives and the alkyl derivatives was also discussed. It was suggested that the chloro derivatives may desensitise TRPA1 via a different mechanism than the other ojk06 and ojk07 derivatives due to the fact it did not fit with the trends observed for the other derivatives. The different mechanism was believed to be similar to that of A96 and AP-18 which are potent TRPA1 antagonists both of which are aryl halide compounds. It has been shown that amino acid residues located within the fifth

275

transmembrane domain are key to the inhibitory effect of A96 and AP-18(180). The inhibitory action of HC-030031 was not affected by the deletion of the same amino acid residues in a separate study(55). It was therefore hypothesised that the chloro derivatives may inhibit TRPA1 via a A96 like mechanism and that the other alkyl derivatives inhibited via a HC-030031 like mechanism, possibly similar to that of caffeine(137).

In chapter 4 the effect of fenamic acid related NSAIDs and fenamic acid derivatives on TRPA1 was reported. It was observed that small changes in the structure of these derivatives significantly altered the effect of the compounds on TRPA1. For example, the difference between SE01 and FFA, SE01 a 3-fluoro derivative of fenamic acid whereas FFA is a 3-trifluoromethyl. This seemingly small change in structure is translated to SE01 being an antagonist of TRPA1 and FFA being a potent agonist and desensitiser of TRPA1. It appears that the electronic nature of the substituent phenyl functional groups had a major effect on how the compounds interacted with TRPA1. The alkyl derivatives of fenamic acid did not produce potent agonist or antagonist responses except from the di-substituted alkyl derivatives such as SE04 and MFA. The addition of an extra methyl group has been reported to increase both the agonist and desensitising properties. The reason for this is unclear, however it may be due to an increase in lipophilicity. The effect of lipophilicity has been discussed in all the results chapters. In general, a more lipophilic compound tends to have an increased potency of interaction with TRPA1. This may be due to an enhanced ability to diffuse into the cell, or it could be due to the lipophilic nature of the TRPA1 binding sites. The results for chapter 4 also indicate the importance of the amine linking group of fenamic acid as key to the interactions with TRPA1. Firstly, it was seen that ketoprofen was a weak agonist of TRPA1 especially compared to the amine linked derivatives. Secondly, the effect of SE02 further indicated the importance of the amine group. SE02 was found to have no effect on TRPA1; this was deemed to be due to a potential steric hindrance of the amine group by the 2-methoxy ring substitution. As SE02 did not show an agonist or antagonist response it can be deemed that the amine group is important for both agonist and inhibitory responses. This relates to the importance of the amide group in ojk01, ojk06 and ojk07 compounds from chapter 3.

In chapter 5, NDGA and M4N were found to have a potent TRPA1 agonist response and did not show a subsequent desensitising effect which has been observed for the majority of

non-covalent agonists of TRPA1 that have been tested as part of this thesis. The lack of a desensitising effect for NDGA and M4N as mentioned earlier may be due to the conformation of the molecules which have been reported to be in a folded arrangement(253). It has also been shown that the TRPA1 agonist potency for NDGA and M4N is in part due to their three dimensional structure and not due to the compounds having two pharmacophores in the form of two catechol rings. Also it has been established in chapter 5 that the methylation of phenol groups abolishes any form of desensitisation as was observed with the results for methylated thymol and the N1-N8 compounds as none of the methylated compounds showed a desensitising effect. This effect has also been in part observed in chapter 4 with regards to the methoxy and ethoxy derivatives of fenamic acid all of which showed no TRPA1 inhibition. The underlying mechanism of this trend cannot be pinpointed at the moment, however it may be due to a combination of effects such as the electronic effects these groups have on phenyl rings and also the hydrogen bonding capabilities of ether groups i.e. they can only act as hydrogen bond acceptors.

The results that have been reported and discussed in this thesis extends the range of non-covalent modulators of TRPA1. They highlight the complexity of the TRPA1 channel due to the variety of responses observed for very similar compounds. These compounds can be used as pharmacological tools for carrying out research on TRPA1 due to the differing effects observed by very similar compounds. The results also highlight key points that can be used to develop TRPA1 targeting drugs. SE01 has stood out as a potential starting point to develop a new novel TRPA1 inhibitor when considering it is a close derivative to FFA which is already a marketed drug.

7 Summary and Conclusion

The effects of several groups of chemical compounds on TRPA1 have been reported and discussed as part of chapter 3, 4 and 5. They have added to the ever growing, especially in recent years, group of non-covalent modulators of TRPA1. The compounds tested as part of this thesis have shown the complexity of the binding sites of TRPA1 as seemingly small changes to structure have had great effects on the modulation of the channel. These effects have been discussed in detail and underlying mechanisms have been proposed. Several key points have been highlighted with regards to their importance to the binding interaction with TRPA1 summarised in the final discussion in chapter6. A selection of my results have been repeated by other research groups and published. Comparisons of these results have been carried out in their relevant chapters and my results confirm what has already been reported in the literature and therefore also confirm the validity of the assay methods that has been used throughout this thesis.

Several compounds that have been assayed have shown potential to be used as pharmacological tools when researching TRPA1 as they have shown to be potent agonist or antagonists which have complementary compounds which have the opposite effect. In the discussion the effect of key functional groups has been compared and important structural features of the compounds tested have been highlighted and compared to the literature. These key structural features can be of use for drug development. SE01 has stood out as a potential drug lead due to its similarity to marketed drugs and its potent TRPA1 antagonist response.

The research that has been presented as part of this thesis highlights the potential for development of new and novel TRPA1 modulators, further research is required to advance the understanding of the mechanisms of binding with TRPA1. For example, in chapter 5 it was discussed how restraining the flexibility of the linking group of NDGA and M4N may produce an even more potent TRPA1 agonist response. Also it was noted that extending the length between the phenyl rings of the fenamic acid derivatives may induce more potent binding interactions.

8 References

1.   Andrade EL, Meotti FC, Calixto JB. TRPA1 antagonists as potential analgesic drugs. Pharmacol Ther. Elsevier B.V.; 2012 Feb;133(2):189–204.

2.   Geppetti P, Patacchini R, Nassini R, Materazzi S. Cough: The Emerging Role of the TRPA1 Channel. Lung. 2010 Jan;188 Suppl:S63-8.

3.   Cosens DJ, Manning A. Abnormal electroretinogram from a Drosophila mutant. Nature. 1969 Oct 18;224(5216):285–7.

4.   Montell C, Rubin GM. Molecular characterization of the Drosophila trp locus: a putative integral membrane protein required for phototransduction. Neuron. 1989 Apr;2(4):1313–23.

5.   Hardie RC, Minke B. The trp gene is essential for a light-activated Ca2+ channel in Drosophila photoreceptors. Neuron. 1992 Apr;8(4):643–51.

6.   Venkatachalam K, Montell C. TRP channels. Annu Rev Biochem. 2007 Jan;76:387–417.

7.   Clapham DE. TRP channels as cellular sensors. Nature. 2003 Dec 4;426(6966):517–24.

8.   Kang K, Pulver SR, Panzano VC, Chang EC, Griffith LC, Theobald DL, et al. Analysis of Drosophila TRPA1 reveals an ancient origin for human chemical nociception. Nature. 2010 Mar 25;464(7288):597–600.

9.   Nilius B, Owsianik G. The transient receptor potential family of ion channels. Genome Biol. 2011 Jan;12(3):218.

10.   Kedei N, Szabo T, Lile JD, Treanor JJ, Olah Z, Iadarola MJ, et al. Analysis of the Ntive Quaternary Structure of Vanilloid Receptor 1. J Biol Chem. 2001;276(30):28613–9.

11.   Hoenderop JGJ, Voets T, Hoefs S, Weidema F, Prenen J, Nilius B, et al. Homo- and heterotetrameric architecture of the epithelial Ca2+ channels TRPV5 and TRPV6. EMBO J. 2003 Feb 17;22(4):776–85.

12.   Erler I, Hirnet D, Wissenbach U, Flockerzi V, Niemeyer BA. Ca2+-selective Transient Receptor Potential V Channel Architecture and Function Require a Specific Ankyrin Repeat. J Biol Chem. 2004;279(33):34456–63.

13.   Lintschinger B, Balzer-Geldsetzer M, Baskaran T, Graier WF, Romanin C, Zhu MX, et al. Coassembly of Trp1 and Trp3 proteins generates diacylglycerol- and Ca2+-sensitive cation channels. J Biol Chem. 2000 Sep 8;275(36):27799–805.

14.   Strübing C, Krapivinsky G, Krapivinsky L, Clapham DE. TRPC1 and TRPC5 form a novel cation channel in mammalian brain. Neuron. 2001 Mar;29(3):645–55.

15. Tang Y, Tang J, Chen Z, Trost C, Flockerzi V, Li M, et al. Association of mammalian trp4 and phospholipase C isozymes with a PDZ domain-containing protein, NHERF. J Biol Chem. 2000 Dec 1;275(48):37559–64.

16. Okada T, Shimizu S, Wakamori M, Maeda A, Kurosaki T, Takada N, et al. Molecular cloning and functional characterization of a novel receptor-activated TRP Ca2+ channel from mouse brain. J Biol Chem. 1998 Apr 24;273(17):10279–87.

17. Schaefer M, Plant TD, Obukhov AG, Hofmann T, Gudermann T, Schultz G. Receptor-mediated regulation of the nonselective cation channels TRPC4 and TRPC5. J Biol Chem. 2000 Jun 9;275(23):17517–26.

18. Blair NT, Kaczmarek JS, Clapham DE. Intracellular calcium strongly potentiates agonist-activated TRPC5 channels. J Gen Physiol. 2009 May;133(5):525–46.

19. Liu X, Cheng KT, Bandyopadhyay BC, Pani B, Dietrich A, Paria BC, et al. Attenuation of store-operated Ca2+ current impairs salivary gland fluid secretion in TRPC1(-/-) mice. Proc Natl Acad Sci U S A. 2007 Oct 30;104(44):17542–7.

20. Munsch T, Freichel M, Flockerzi V, Pape H-C. Contribution of transient receptor potential channels to the control of GABA release from dendrites. Proc Natl Acad Sci U S A. 2003 Dec 23;100(26):16065–70.

21. Riccio A, Li Y, Moon J, Kim K-S, Smith KS, Rudolph U, et al. Essential role for TRPC5 in amygdala function and fear-related behavior. Cell. 2009 May 15;137(4):761–72.

22. Okada T, Inoue R, Yamazaki K, Maeda A, Kurosaki T, Yamakuni T, et al. Molecular and functional characterization of a novel mouse transient receptor potential protein homologue TRP7. Ca(2+)-permeable cation channel that is constitutively activated and enhanced by stimulation of G protein-coupled receptor. J Biol Chem. 1999 Sep 24;274(39):27359–70.

23. Strübing C, Krapivinsky G, Krapivinsky L, Clapham DE. Formation of novel TRPC channels by complex subunit interactions in embryonic brain. J Biol Chem. 2003 Oct 3;278(40):39014–9.

24. Li HS, Xu XZ, Montell C. Activation of a TRPC3-dependent cation current through the neurotrophin BDNF. Neuron. 1999 Sep;24(1):261–73.

25. Amaral MD, Pozzo-Miller L. BDNF induces calcium elevations associated with IBDNF, a nonselective cationic current mediated by TRPC channels. J Neurophysiol. 2007 Oct;98(4):2476–82.

26. Dietrich A, Gudermann T. TRPC6. Handb Exp Pharmacol. 2007 Jan;(179):125–41.

27. Numaga T, Wakamori M, Mori Y. TRPC7. Handb Exp Pharmacol. 2007 Jan;(179):143–51.

28. Hartmann J, Dragicevic E, Adelsberger H, Henning HA, Sumser M, Abramowitz J, et al. TRPC3 channels

are required for synaptic transmission and motor coordination. Neuron. 2008 Aug 14;59(3):392–8.

29. Dietrich A, Mederos Y Schnitzler M, Gollasch M, Gross V, Storch U, Dubrovska G, et al. Increased vascular smooth muscle contractility in TRPC6-/- mice. Mol Cell Biol. 2005 Aug;25(16):6980–9.

30. Jia Y, Zhou J, Tai Y, Wang Y. TRPC channels promote cerebellar granule neuron survival. Nat Neurosci. 2007 May;10(5):559–67.

31. Zhou J, Du W, Zhou K, Tai Y, Yao H, Jia Y, et al. Critical role of TRPC6 channels in the formation of excitatory synapses. Nat Neurosci. 2008 Jul;11(7):741–3.

32. Caterina MJ, Schumacher MA, Tominaga M, Rosen TA, Levine JD, Julius D. The capsaicin receptor: a heat-activated ion channel in the pain pathway. Nature. 1997 Oct 23;389(6653):816–24.

33. Phelps CB, Wang RR, Choo SS, Gaudet R. Differential regulation of TRPV1, TRPV3, and TRPV4 sensitivity through a conserved binding site on the ankyrin repeat domain. J Biol Chem. 2010 Jan 1;285(1):731–40.

34. Hu H-Z, Gu Q, Wang C, Colton CK, Tang J, Kinoshita-Kawada M, et al. 2-aminoethoxydiphenyl borate is a common activator of TRPV1, TRPV2, and TRPV3. J Biol Chem. 2004 Aug 20;279(34):35741–8.

35. Chung M-K, Lee H, Mizuno A, Suzuki M, Caterina MJ. 2-aminoethoxydiphenyl borate activates and sensitizes the heat-gated ion channel TRPV3. J Neurosci. 2004 Jun 2;24(22):5177–82.

36. Benham CD, Davis JB, Randall AD. Vanilloid and TRP channels: a family of lipid-gated cation channels. Neuropharmacology. 2002 Jun;42(7):873–88.

37. Todaka H, Taniguchi J, Satoh J, Mizuno A, Suzuki M. Warm temperature-sensitive transient receptor potential vanilloid 4 (TRPV4) plays an essential role in thermal hyperalgesia. J Biol Chem. 2004 Aug 20;279(34):35133–8.

38. Niemeyer BA. Structure-function analysis of TRPV channels. Naunyn Schmiedebergs Arch Pharmacol. 2005 Apr;371(4):285–94.

39. Hoenderop JGJ, Nilius B, Bindels RJM. Molecular mechanism of active Ca2+ reabsorption in the distal nephron. Annu Rev Physiol. 2002;64:529–49.

40. Nijenhuis T, Hoenderop JGJ, van der Kemp AWCM, Bindels RJM. Localization and regulation of the epithelial Ca2+ channel TRPV6 in the kidney. J Am Soc Nephrol. 2003 Nov;14(11):2731–40.

41. Peng JB, Chen XZ, Berger U V, Vassilev PM, Tsukaguchi H, Brown EM, et al. Molecular cloning and characterization of a channel-like transporter mediating intestinal calcium absorption. J Biol Chem. 1999 Aug 6;274(32):22739–46.

42. Irie S, Furukawa T. TRPM1. Handb Exp Pharmacol. 2014;222:387–402.

43. Runnels LW, Yue L, Clapham DE. TRP-PLIK, a bifunctional protein with kinase and ion channel activities. Science. 2001 Feb 9;291(5506):1043–7.

44. Scharenberg AM. TRPM2 and TRPM7: channel/enzyme fusions to generate novel intracellular sensors. Pflügers Arch Eur J Physiol. 2005 Oct;451(1):220–7.

45. Uemura T, Kudoh J, Noda S, Kanba S, Shimizu N. Characterization of human and mouse TRPM2 genes: identification of a novel N-terminal truncated protein specifically expressed in human striatum. Biochem Biophys Res Commun. 2005 Mar 25;328(4):1232–43.

46. Koike C, Numata T, Ueda H, Mori Y, Furukawa T. TRPM1: a vertebrate TRP channel responsible for retinal ON bipolar function. Cell Calcium. 48(2–3):95–101.

47. Vriens J, Owsianik G, Hofmann T, Philipp SE, Stab J, Chen X, et al. TRPM3 is a nociceptor channel involved in the detection of noxious heat. Neuron. 2011 May 12;70(3):482–94.

48. Oberwinkler J. TRPM3, a biophysical enigma? Biochem Soc Trans. 2007 Feb;35(Pt 1):89–90.

49. Zeevi DA, Frumkin A, Bach G. TRPML and lysosomal function. Biochim Biophys Acta. 2007 Aug;1772(8):851–8.

50. Puertollano R, Kiselyov K. TRPMLs: in sickness and in health. Am J Physiol Renal Physiol. 2009 Jun;296(6):F1245-54.

51. Sun L, Hua Y, Vergarajauregui S, Diab HI, Puertollano R. Novel Role of TRPML2 in the Regulation of the Innate Immune Response. J Immunol. 2015;

52. Delmas P. Polycystins: polymodal receptor/ion-channel cellular sensors. Pflügers Arch Eur J Physiol. 2005 Oct;451(1):264–76.

53. Jaquemar D, Schenker T, Trueb B. An ankyrin-like protein with transmembrane domains is specifically lost after oncogenic transformation of human fibroblasts. J Biol Chem. 1999 Mar 12;274(11):7325–33.

54. Bandell M, Story GM, Hwang SW, Viswanath V, Eid SR, Petrus MJ, et al. Noxious cold ion channel TRPA1 is activated by pungent compounds and bradykinin. Neuron. 2004 Mar 25;41(6):849–57.

55. Xiao B, Dubin AE, Bursulaya B, Viswanath V, Jegla TJ, Patapoutian A. Identification of transmembrane domain 5 as a critical molecular determinant of menthol sensitivity in mammalian TRPA1 channels. J Neurosci. 2008 Sep 24;28(39):9640–51.

56. Hamada FN, Rosenzweig M, Kang K, Pulver SR, Ghezzi A, Jegla TJ, et al. An internal thermal sensor controlling temperature preference in Drosophila. Nature. 2008 Jul 10;454(7201):217–20.

57. Nilius B, Appendino G, Owsianik G. The transient receptor potential channel TRPA1: from gene to pathophysiology. Pflugers Arch. 2012 Nov;464(5):425–58.

58.   Nilius B, Prenen J, Owsianik G. Irritating Channels : the case of TRPA1. J Physiol. 2011;

59.   Liu C, Montell C. Forcing open TRP channels: Mechanical gating as a unifying activation mechanism. Biochem Biophys Res Commun. 2015 Apr;460(1):22–5.

60.   Zurborg S, Yurgionas B, Jira JA, Caspani O, Heppenstall PA. Direct activation of the ion channel TRPA1 by Ca2+. Nat Neurosci. 2007 Mar;10(3):277–9.

61.   Doerner JF, Gisselmann G, Hatt H, Wetzel CH. Transient receptor potential channel A1 is directly gated by calcium ions. J Biol Chem. 2007 May 4;282(18):13180–9.

62.   Zayats V, Samad A, Minofar B, Roelofs KE, Stockner T, Ettrich R. Regulation of the transient receptor potential channel TRPA1 by its N-terminal ankyrin repeat domain. J Mol Model. 2013 Nov;19(11):4689–700.

63.   Macpherson LJ, Dubin AE, Evans MJ, Marr F, Schultz PG, Cravatt BF, et al. Noxious compounds activate TRPA1 ion channels through covalent modification of cysteines. Nature. 2007 Feb 1;445(7127):541–5.

64.   Hinman A, Chuang H-H, Bautista DM, Julius D. TRP channel activation by reversible covalent modification. Proc Natl Acad Sci U S A. 2006 Dec 19;103(51):19564–8.

65.   Takahashi N, Mizuno Y, Kozai D, Yamamoto S, Kiyonaka S, Shibata T, et al. Molecular characterization of TRPA1 channel activation by cysteine-reactive inflammatory mediators. Channels. 2014 Oct 27;2(4):287–98.

66.   Cvetkov TL, Huynh KW, Cohen MR, Moiseenkova-Bell VY. Molecular architecture and subunit organization of TRPA1 ion channel revealed by electron microscopy. J Biol Chem. 2011 Nov 4;286(44):38168–76.

67.   Caterina MJ. Chemical biology: sticky spices. Nature. 2007 Feb 1;445(7127):491–2.

68.   Bautista DM, Movahed P, Hinman A, Axelsson HE, Sterner O, Högestätt ED, et al. Pungent products from garlic activate the sensory ion channel TRPA1. Proc Natl Acad Sci U S A. 2005 Aug 23;102(34):12248–52.

69.   Story GM, Peier AM, Reeve AJ, Eid SR, Mosbacher J, Hricik TR, et al. ANKTM1, a TRP-like channel expressed in nociceptive neurons, is activated by cold temperatures. Cell. 2003 Mar 21;112(6):819–29.

70.   Nagata K, Duggan A, Kumar G, García-Añoveros J. Nociceptor and hair cell transducer properties of TRPA1, a channel for pain and hearing. J Neurosci. 2005 Apr 20;25(16):4052–61.

71.   Stokes A, Wakano C, Koblan-Huberson M, Adra CN, Fleig A, Turner H. TRPA1 is a substrate for de-ubiquitination by the tumor suppressor CYLD. Cell Signal. 2006 Oct;18(10):1584–94.

283

72. Smith MP, Beacham D, Ensor E, Koltzenburg M. Cold-sensitive, menthol-insensitive neurons in the murine sympathetic nervous system. Neuroreport. 2004 Jun 28;15(9):1399–403.

73. Brozmanova M, Ru F, Surdenikova L, Mazurova L, Taylor-Clark T, Kollarik M. Preferential activation of the vagal nodose nociceptive subtype by TRPA1 agonists in the guinea pig esophagus. Neurogastroenterol Motil. 2011 Oct;23(10):e437-45.

74. Kollarik M, Brozmanova M. Cough and gastroesophageal reflux: insights from animal models. Pulm Pharmacol Ther. 2009 Apr;22(2):130–4.

75. Yu S, Ouyang A. TRPA1 in bradykinin-induced mechanical hypersensitivity of vagal C fibers in guinea pig esophagus. Am J Physiol Gastrointest Liver Physiol. 2009 Feb;296(2):G255-65.

76. Taylor-Clark TE, Undem BJ. Sensing pulmonary oxidative stress by lung vagal afferents. Respir Physiol Neurobiol. 2011 Sep 30;178(3):406–13.

77. Andrè E, Gatti R, Trevisani M, Preti D, Baraldi PG, Patacchini R, et al. Transient receptor potential ankyrin receptor 1 is a novel target for pro-tussive agents. Br J Pharmacol. 2009 Nov;158(6):1621–8.

78. Belvisi MG, Dubuis E, Birrell MA. Transient receptor potential A1 channels: insights into cough and airway inflammatory disease. Chest. American College of Chest Physicians; 2011 Oct 1;140(4):1040–7.

79. Zhou Y, Sun B, Li Q, Luo P, Dong L, Rong W. Sensitivity of bronchopulmonary receptors to cold and heat mediated by transient receptor potential cation channel subtypes in an ex vivo rat lung preparation. Respir Physiol Neurobiol. 2011 Aug 15;177(3):327–32.

80. Poole DP, Pelayo JC, Cattaruzza F, Kuo Y-M, Gai G, Chiu J V, et al. Transient receptor potential ankyrin 1 is expressed by inhibitory motoneurons of the mouse intestine. Gastroenterology. 2011 Aug;141(2):565–75, 575-4.

81. Du S, Araki I, Yoshiyama M, Nomura T, Takeda M. Transient receptor potential channel A1 involved in sensory transduction of rat urinary bladder through C-fiber pathway. Urology. 2007 Oct;70(4):826–31.

82. Gratzke C, Weinhold P, Reich O, Seitz M, Schlenker B, Stief CG, et al. Transient receptor potential A1 and cannabinoid receptor activity in human normal and hyperplastic prostate: relation to nerves and interstitial cells. Eur Urol. 2010 May;57(5):902–10.

83. Koch M, Kreutz S, Böttger C, Grabiec U, Ghadban C, Korf H-W, et al. The cannabinoid WIN 55,212-2-mediated protection of dentate gyrus granule cells is driven by CB1 receptors and modulated by TRPA1 and Cav 2.2 channels. Hippocampus. 2011 May;21(5):554–64.

84. Yokoyama T, Ohbuchi T, Saito T, Sudo Y, Fujihara H, Minami K, et al. Allyl isothiocyanates and cinnamaldehyde potentiate miniature excitatory postsynaptic inputs in the supraoptic nucleus in rats.

Eur J Pharmacol. 2011 Mar 25;655(1–3):31–7.

85. Sun B, Bang S-I, Jin Y-H. Transient receptor potential A1 increase glutamate release on brain stem neurons. Neuroreport. 2009 Jul 15;20(11):1002–6.

86. Corey DP, García-Añoveros J, Holt JR, Kwan KY, Lin S-Y, Vollrath MA, et al. TRPA1 is a candidate for the mechanosensitive transduction channel of vertebrate hair cells. Nature. 2004 Dec 9;432(7018):723–30.

87. Stepanyan RS, Indzhykulian AA, Vélez-Ortega AC, Boger ET, Steyger PS, Friedman TB, et al. TRPA1-mediated accumulation of aminoglycosides in mouse cochlear outer hair cells. J Assoc Res Otolaryngol. 2011 Dec;12(6):729–40.

88. Takumida M, Ishibashi T, Hamamoto T, Hirakawa K, Anniko M. Expression of transient receptor potential channel melastin (TRPM) 1-8 and TRPA1 (ankyrin) in mouse inner ear. Acta Otolaryngol. 2009 Oct;129(10):1050–60.

89. Earley S. TRPA1 channels in the vasculature. Br J Pharmacol. 2012 Sep;167(1):13–22.

90. Qian X, Francis M, Solodushko V, Earley S, Taylor MS. Recruitment of dynamic endothelial Ca2+ signals by the TRPA1 channel activator AITC in rat cerebral arteries. Microcirculation. 2013 Feb;20(2):138–48.

91. Kaji I, Karaki S, Kuwahara A. Effects of luminal thymol on epithelial transport in human and rat colon. Am J Physiol Gastrointest Liver Physiol. 2011 Jun;300(6):G1132-43.

92. Alenmyr L, Herrmann A, Högestätt ED, Greiff L, Zygmunt PM. TRPV1 and TRPA1 stimulation induces MUC5B secretion in the human nasal airway in vivo. Clin Physiol Funct Imaging. 2011 Nov;31(6):435–44.

93. Caceres AI, Brackmann M, Elia MD, Bessac BF, del Camino D, D'Amours M, et al. A sensory neuronal ion channel essential for airway inflammation and hyperreactivity in asthma. Proc Natl Acad Sci U S A. 2009 Jun 2;106(22):9099–104.

94. Atoyan R, Shander D, Botchkareva N V. Non-neuronal expression of transient receptor potential type A1 (TRPA1) in human skin. J Invest Dermatol. 2009 Sep;129(9):2312–5.

95. Kim YS, Jung HK, Kwon TK, Kim CS, Cho JH, Ahn DK, et al. Expression of transient receptor potential ankyrin 1 in human dental pulp. J Endod. 2012 Aug;38(8):1087–92.

96. Jordt S-E, Bautista DM, Chuang H-H, McKemy DD, Zygmunt PM, Högestätt ED, et al. Mustard oils and cannabinoids excite sensory nerve fibres through the TRP channel ANKTM1. Nature. 2004 Jan 15;427(6971):260–5.

97. Kwan KY, Allchorne AJ, Vollrath MA, Christensen AP, Zhang D-S, Woolf CJ, et al. TRPA1 contributes to

cold, mechanical, and chemical nociception but is not essential for hair-cell transduction. Neuron. 2006 Apr 20;50(2):277–89.

98. Bautista DM, Jordt S-E, Nikai T, Tsuruda PR, Read AJ, Poblete J, et al. TRPA1 mediates the inflammatory actions of environmental irritants and proalgesic agents. Cell. 2006 Mar 24;124(6):1269–82.

99. Eid SR, Crown ED, Moore EL, Liang H a, Choong K-C, Dima S, et al. HC-030031, a TRPA1 selective antagonist, attenuates inflammatory- and neuropathy-induced mechanical hypersensitivity. Mol Pain. 2008 Jan;4:48.

100. Trevisani M, Siemens J, Materazzi S, Bautista DM, Nassini R, Campi B, et al. 4-Hydroxynonenal, an endogenous aldehyde, causes pain and neurogenic inflammation through activation of the irritant receptor TRPA1. Proc Natl Acad Sci U S A. 2007 Aug 14;104(33):13519–24.

101. Taylor-Clark TE, McAlexander MA, Nassenstein C, Sheardown SA, Wilson S, Thornton J, et al. Relative contributions of TRPA1 and TRPV1 channels in the activation of vagal bronchopulmonary C-fibres by the endogenous autacoid 4-oxononenal. J Physiol. 2008 Jul 15;586(14):3447–59.

102. Cruz-Orengo L, Dhaka A, Heuermann RJ, Young TJ, Montana MC, Cavanaugh EJ, et al. Cutaneous nociception evoked by 15-delta PGJ2 via activation of ion channel TRPA1. Mol Pain. 2008 Jan;4:30.

103. Taylor-Clark TE, Undem BJ, Macglashan DW, Ghatta S, Carr MJ, McAlexander MA. Prostaglandin-induced activation of nociceptive neurons via direct interaction with transient receptor potential A1 (TRPA1). Mol Pharmacol. 2008 Feb;73(2):274–81.

104. Petrus M, Peier AM, Bandell M, Hwang SW, Huynh T, Olney N, et al. A role of TRPA1 in mechanical hyperalgesia is revealed by pharmacological inhibition. Mol Pain. 2007 Jan;3:40.

105. Namer B, Seifert F, Handwerker HO, Maihöfner C. TRPA1 and TRPM8 activation in humans: effects of cinnamaldehyde and menthol. Neuroreport. 2005 Jun 21;16(9):955–9.

106. Chang JC, Barrow CS. Sensory irritation tolerance and cross-tolerance in F-344 rats exposed to chlorine or formaldehyde gas. Toxicol Appl Pharmacol. 1984 Nov;76(2):319–27.

107. Babiuk C, Steinhagen WH, Barrow CS. Sensory irritation response to inhaled aldehydes after formaldehyde pretreatment. Toxicol Appl Pharmacol. 1985 Jun 15;79(1):143–9.

108. Mukhopadhyay I, Gomes P, Aranake S, Shetty M, Karnik P, Damle M, et al. Expression of functional TRPA1 receptor on human lung fibroblast and epithelial cells. J Recept Signal Transduct Res. 2011 Oct;31(5):350–8.

109. Brooks SM. Irritant-induced chronic cough: irritant-induced TRPpathy. Lung. 2008 Jan;186 Suppl(December 2007):S88-93.

110. Baraniuk JN, Kim D. Nasonasal reflexes, the nasal cycle, and sneeze. Curr Allergy Asthma Rep. 2007 May;7(2):105–11.

111. Baraniuk JN, Lundgren JD, Goff J, Mullol J, Castellino S, Merida M, et al. Calcitonin gene-related peptide in human nasal mucosa. Am J Physiol. 1990 Feb;258(2 Pt 1):L81-8.

112. Undem BJ, McAlexander M, Hunter DD. Neurobiology of the upper and lower airways. Allergy. 1999 Jan;54 Suppl 5:81–93.

113. Brooks SM. Perspective on the human cough reflex. Cough. 2011 Jan;7:10.

114. Canning BJ, Mori N, Mazzone SB. Vagal afferent nerves regulating the cough reflex. Respir Physiol Neurobiol. 2006 Jul 28;152(3):223–42.

115. Laude EA, Higgins KS, Morice AH. A comparative study of the effects of citric acid, capsaicin and resiniferatoxin on the cough challenge in guinea-pig and man. Pulm Pharmacol. 1993 Sep;6(3):171–5.

116. Lalloo UG, Fox AJ, Belvisi MG, Chung KF, Barnes PJ. Capsazepine inhibits cough induced by capsaicin and citric acid but not by hypertonic saline in guinea pigs. J Appl Physiol. 1995 Oct;79(4):1082–7.

117. Andrè E, Campi B, Materazzi S, Trevisani M, Amadesi S, Massi D, et al. Cigarette smoke-induced neurogenic inflammation is mediated by alpha,beta-unsaturated aldehydes and the TRPA1 receptor in rodents. J Clin Invest. 2008 Jul;118(7):2574–82.

118. Birrell MA, Belvisi MG, Grace M, Sadofsky L, Faruqi S, Hele DJ, et al. TRPA1 agonists evoke coughing in guinea pig and human volunteers. Am J Respir Crit Care Med. 2009 Dec 1;180(11):1042–7.

119. Kremeyer B, Lopera F, Cox JJ, Momin A, Rugiero F, Marsh S, et al. A gain-of-function mutation in TRPA1 causes familial episodic pain syndrome. Neuron. 2010 Jun 10;66(5):671–80.

120. del Camino D, Murphy S, Heiry M, Barrett LB, Earley TJ, Cook CA, et al. TRPA1 contributes to cold hypersensitivity. J Neurosci. 2010 Nov 10;30(45):15165–74.

121. Karashima Y, Talavera K, Everaerts W, Janssens A, Kwan KY, Vennekens R, et al. TRPA1 acts as a cold sensor in vitro and in vivo. Proc Natl Acad Sci U S A. 2009 Jan 27;106(4):1273–8.

122. Sawada Y, Hosokawa H, Hori A, Matsumura K, Kobayashi S. Cold sensitivity of recombinant TRPA1 channels. Brain Res. 2007 Jul 30;1160:39–46.

123. Cordero-Morales JF, Gracheva EO, Julius D. Cytoplasmic ankyrin repeats of transient receptor potential A1 (TRPA1) dictate sensitivity to thermal and chemical stimuli. Proc Natl Acad Sci U S A. 2011 Nov 15;108(46):E1184-91.

124. Gracheva EO, Ingolia NT, Kelly YM, Cordero-Morales JF, Hollopeter G, Chesler AT, et al. Molecular basis of infrared detection by snakes. Nature. 2010 Apr 15;464(7291):1006–11.

125. Kang K, Panzano VC, Chang EC, Ni L, Dainis AM, Jenkins AM, et al. Modulation of TRPA1 thermal sensitivity enables sensory discrimination in Drosophila. Nature. 2012 Jan 5;481(7379):76–80.

126. Viswanath V, Story GM, Peier AM, Petrus MJ, Lee VM, Hwang SW, et al. Opposite thermosensor in fruitfly and mouse. Nature. 2003 Jun 19;423(6942):822–3.

127. Saito S, Nakatsuka K, Takahashi K, Fukuta N, Imagawa T, Ohta T, et al. Analysis of transient receptor potential ankyrin 1 (TRPA1) in frogs and lizards illuminates both nociceptive heat and chemical sensitivities and coexpression with TRP vanilloid 1 (TRPV1) in ancestral vertebrates. J Biol Chem. 2012 Aug 31;287(36):30743–54.

128. Chen J, Kang D, Xu J, Lake M, Hogan JO, Sun C, et al. Species differences and molecular determinant of TRPA1 cold sensitivity. Nat Commun. Nature Publishing Group; 2013 Jan;4:2501.

129. Sadofsky LR, Boa AN, Maher S a, Birrell M a, Belvisi MG, Morice AH. TRPA1 is activated by direct addition of cysteine residues to the N-hydroxysuccinyl esters of acrylic and cinnamic acids. Pharmacol Res. Elsevier Ltd; 2011 Jan;63(1):30–6.

130. Lee SP, Buber MT, Yang Q, Cerne R, Cortés RY, Sprous DG, et al. Thymol and related alkyl phenols activate the hTRPA1 channel. Br J Pharmacol. 2008 Apr;153(8):1739–49.

131. Komatsu T, Uchida K, Fujita F, Zhou Y, Tominaga M. Primary alcohols activate human TRPA1 channel in a carbon chain length-dependent manner. Pflugers Arch. 2012 Apr;463(4):549–59.

132. Ortar G, Morera L, Moriello AS, Morera E, Nalli M, Di Marzo V, et al. Modulation of thermo-transient receptor potential (thermo-TRP) channels by thymol-based compounds. Bioorg Med Chem Lett. Elsevier Ltd; 2012 May 15;22(10):3535–9.

133. McKemy DD, Neuhausser WM, Julius D. Identification of a cold receptor reveals a general role for TRP channels in thermosensation. Nature. 2002 Mar 7;416(6876):52–8.

134. Karashima Y, Damann N, Prenen J, Talavera K, Segal A, Voets T, et al. Bimodal action of menthol on the transient receptor potential channel TRPA1. J Neurosci. 2007 Sep 12;27(37):9874–84.

135. Macpherson LJ, Hwang SW, Miyamoto T, Dubin AE, Patapoutian A, Story GM. More than cool: promiscuous relationships of menthol and other sensory compounds. Mol Cell Neurosci. 2006 Aug;32(4):335–43.

136. Nagatomo K, Kubo Y. Caffeine activates mouse TRPA1 channels but suppresses human TRPA1 channels. Proc Natl Acad Sci U S A. 2008 Nov 11;105(45):17373–8.

137. Nagatomo K, Ishii H, Yamamoto T, Nakajo K, Kubo Y. The Met268Pro mutation of mouse TRPA1 changes the effect of caffeine from activation to suppression. Biophys J. Biophysical Society; 2010 Dec 1;99(11):3609–18.

138. Zhong J, Pollastro F, Prenen J, Zhu Z, Appendino G, Nilius B. Ligustilide: a novel TRPA1 modulator. Pflugers Arch. 2011 Dec;462(6):841–9.

139. Ortar G, Schiano Moriello A, Morera E, Nalli M, Di Marzo V, De Petrocellis L. 3-Ylidenephthalides as a new class of transient receptor potential channel TRPA1 and TRPM8 modulators. Bioorg Med Chem Lett. Elsevier Ltd; 2013 Oct 15;23(20):5614–8.

140. Talavera K, Gees M, Karashima Y, Meseguer VM, Vanoirbeek JAJ, Damann N, et al. Nicotine activates the chemosensory cation channel TRPA1. Nat Neurosci. 2009 Oct;12(10):1293–9.

141. Hu H, Tian J, Zhu Y, Wang C, Xiao R, Herz JM, et al. Activation of TRPA1 channels by fenamate nonsteroidal anti-inflammatory drugs. Pflugers Arch. 2010 Mar;459(4):579–92.

142. Liu K, Samuel M, Ho M, Harrison RK, Paslay JW. NPPB structure-specifically activates TRPA1 channels. Biochem Pharmacol. Elsevier Inc.; 2010 Jul 1;80(1):113–21.

143. Fischer MJM, Leffler A, Niedermirtl F, Kistner K, Eberhardt M, Reeh PW, et al. The general anesthetic propofol excites nociceptors by activating TRPV1 and TRPA1 rather than GABAA receptors. J Biol Chem. 2010 Nov 5;285(45):34781–92.

144. Matta JA, Cornett PM, Miyares RL, Abe K, Sahibzada N, Ahern GP. General anesthetics activate a nociceptive ion channel to enhance pain and inflammation. Proc Natl Acad Sci U S A. 2008 Jun 24;105(25):8784–9.

145. Leffler A, Lattrell A, Kronewald S, Niedermirtl F, Nau C. Activation of TRPA1 by membrane permeable local anesthetics. Mol Pain. BioMed Central Ltd; 2011 Jan;7(1):62.

146. Moran MM, McAlexander MA, Bíró T, Szallasi A. Transient receptor potential channels as therapeutic targets. Nat Rev Drug Discov. 2011 Aug;10(8):601–20.

147. Fanger CMC, Camino D del, Moran MM. TRPA1 as an analgesic target. Open Drug Discov J. 2010;2(2):64–70.

148. Nilius B, Szallasi A. Transient receptor potential channels as drug targets: from the science of basic research to the art of medicine. Pharmacol Rev. 2014 Jul;66(3):676–814.

149. Baraldi PG, Preti D, Materazzi S, Geppetti P. Transient receptor potential ankyrin 1 (TRPA1) channel as emerging target for novel analgesics and anti-inflammatory agents. J Med Chem. 2010 Jul 22;53(14):5085–107.

150. Defalco J, Steiger D, Gustafson A, Emerling DE, Kelly MG, Duncton MAJ. Oxime derivatives related to AP18: Agonists and antagonists of the TRPA1 receptor. Bioorg Med Chem Lett. 2010 Jan 1;20(1):276–9.

151. Preti D, Saponaro G, Szallasi A. Transient receptor potential ankyrin 1 (TRPA1) antagonists. Pharm Pat

Anal. 2015;4(2):75–94.

152.   Jiang H, Zeng B, Chen G-L, Bot D, Eastmond S, Elsenussi SE, et al. Effect of non-steroidal anti-inflammatory drugs and new fenamate analogues on TRPC4 and TRPC5 channels. Biochem Pharmacol. 2012 Apr 1;83(7):923–31.

153.   Sadofsky LR, Campi B, Trevisani M, Compton SJ, Morice AH. Transient receptor potential vanilloid-1-mediated calcium responses are inhibited by the alkylamine antihistamines dexbrompheniramine and chlorpheniramine. Exp Lung Res. Informa UK Ltd UK; 2008 Dec 2;34(10):681–93.

154.   Hüsnü K, Başer C, Demirci F. Chemistry of Essential Oils. Flavours and Fragrances. Berlin, Heidelberg: Springer Berlin Heidelberg; 2007. p. 43–86.

155.   Cane DE. 2.01 – Isoprenoid Biosynthesis: Overview. Comprehensive Natural Products Chemistry. 1999. p. 1–13.

156.   Zuzarte M, Salgueiro L. Essential Oils Chemistry. Bioactive Essential Oils and Cancer. Cham: Springer International Publishing; 2015. p. 19–61.

157.   Baser KHC. Biological and pharmacological activities of carvacrol and carvacrol bearing essential oils. Curr Pharm Des. 2008;14(29):3106–19.

158.   Marchese A, Orhan IE, Daglia M, Barbieri R, Di Lorenzo A, Nabavi SF, et al. Antibacterial and antifungal activities of thymol: A brief review of the literature. Food Chem. Elsevier Ltd; 2016;210:402–14.

159.   Marino M, Bersani C, Comi G. Antimicrobial activity of the essential oils of Thymus vulgaris L. measured using a bioimpedometric method. J Food Prot. 1999 Sep;62(9):1017–23.

160.   Olasupo NA, Fitzgerald DJ, Gasson MJ, Narbad A. Activity of natural antimicrobial compounds against Escherichia coli and Salmonella enterica serovar Typhimurium. Lett Appl Microbiol. 2003;37(6):448–51.

161.   Hernández-Hernández E, Regalado-González C, Vázquez-Landaverde P, Guerrero-Legarreta I, García-Almendárez BE, Hernández-Hernández E, et al. Microencapsulation, chemical characterization, and antimicrobial activity of Mexican (Lippia graveolens H.B.K.) and European (Origanum vulgare L.) oregano essential oils. ScientificWorldJournal. Hindawi Publishing Corporation; 2014;2014:641814.

162.   Koparal AT, Zeytinoglu M. Effects of Carvacrol on a Human Non-Small Cell Lung Cancer (NSCLC) Cell Line, A549. Cytotechnology. 2003 Nov;43(1–3):149–54.

163.   Kang S-H, Kim Y-S, Kim E-K, Hwang J-W, Jeong J-H, Dong X, et al. Anticancer Effect of Thymol on AGS Human Gastric Carcinoma Cells. J Microbiol Biotechnol. 2016 Jan;26(1):28–37.

164.   Prieto JM, Iacopini P, Cioni P, Chericoni S. In vitro activity of the essential oils of Origanum vulgare,

Satureja montana and their main constituents in peroxynitrite-induced oxidative processes. Food Chem. 2007;104(3):889–95.

165.   Yanishlieva N V, Marinova EM, Gordon MH, Raneva VG. Antioxidant activity and mechanism of action of thymol and carvacrol in two lipid systems. Food Chem. 1999;64(1):59–66.

166.   Lee S-J, Umano K, Shibamoto T, Lee K-G. Identification of volatile components in basil (Ocimum basilicum L.) and thyme leaves (Thymus vulgaris L.) and their antioxidant properties. Food Chem. 2005;91(1):131–7.

167.   Džamić AM, Nikolić BJ, Giweli AA, Mitić-Ćulafić DS, Soković MD, Ristić MS, et al. Libyan Thymus capitatus essential oil: antioxidant, antimicrobial, cytotoxic and colon pathogen adhesion-inhibition properties. J Appl Microbiol. 2015 Aug;119(2):389–99.

168.   Mendes SS, Bomfim RR, Jesus HCR, Alves PB, Blank AF, Estevam CS, et al. Evaluation of the analgesic and anti-inflammatory effects of the essential oil of Lippia gracilis leaves. J Ethnopharmacol. 2010 Jun 16;129(3):391–7.

169.   Wagner H, Wierer M, Bauer R. [In vitro inhibition of prostaglandin biosynthesis by essential oils and phenolic compounds]. Planta Med. 1986 Jun;(3):184–7.

170.   Nagle PS, Pawar YA, Sonawane AE, Bhosale SM, More DH. Synthesis and evaluation of antioxidant and antimicrobial properties of thymol containing pyridone moieties. Med Chem Res. 2012;21(7):1395–402.

171.   Huang M-H, Liao L-F, Kuo S-H, Chen C-L, Shen A-Y. Effects of 4-piperidinomethyl-2-isopropyl-5-methylphenol on oxidative stress and calcium current. J Pharm Pharmacol. Blackwell Publishing Ltd; 2005 Sep;57(9):1191–7.

172.   Kulabaş N, Tatar E, Bingöl Özakpınar Ö, Özsavcı D, Pannecouque C, De Clercq E, et al. Synthesis and antiproliferative evaluation of novel 2-(4H-1,2,4-triazole-3-ylthio)acetamide derivatives as inducers of apoptosis in cancer cells. Eur J Med Chem. 2016 Oct 4;121:58–70.

173.   James Bound D, Murthy PS, Srinivas P. 2,3-Dideoxyglucosides of selected terpene phenols and alcohols as potent antifungal compounds. Food Chem. 2016 Nov 1;210:371–80.

174.   Kang HH, Rho HS, Hwang JS, Oh S-G. Depigmenting activity and low cytotoxicity of alkoxy benzoates or alkoxy cinnamte in cultured melanocytes. Chem Pharm Bull (Tokyo). 2003 Sep;51(9):1085–8.

175.   Xu H, Delling M, Jun JC, Clapham DE. Oregano, thyme and clove-derived flavors and skin sensitizers activate specific TRP channels. Nat Neurosci. 2006;9(5):628–35.

176.   Ortar G, De Petrocellis L, Morera L, Moriello AS, Orlando P, Morera E, et al. (-)-Menthylamine derivatives as potent and selective antagonists of transient receptor potential melastatin type-8 (TRPM8) channels. Bioorg Med Chem Lett. Elsevier Ltd; 2010 May 1;20(9):2729–32.

177. Sherkheli MA, Vogt-Eisele AK, Bura D, Beltrán Márques LR, Gisselmann G, Hatt H. Characterization of selective TRPM8 ligands and their structure activity response (S.A.R) relationship. J Pharm Pharm Sci a Publ Can Soc Pharm Sci Société Can des Sci Pharm. 2010;13(2):242–53.

178. Ortar G, Morera L, Moriello AS. Modulation of thermo-transient receptor potential (thermo-TRP) channels by thymol-based compounds. Bioorganic Med …. Elsevier Ltd; 2012 May 15;22(10):3535–9.

179. Chen J, Kym PR. TRPA1: the species difference. J Gen Physiol. 2009 Jun;133(6):623–5.

180. Nakatsuka K, Gupta R, Saito S, Banzawa N, Takahashi K, Tominaga M, et al. Identification of Molecular Determinants for a Potent Mammalian TRPA1 Antagonist by Utilizing Species Differences. J Mol Neurosci. 2013 Jul 20;

181. Klement G, Eisele L, Malinowsky D, Nolting A, Svensson M, Terp G, et al. Characterization of a Ligand Binding Site in the Human Transient Receptor Potential Ankyrin 1 Pore. Biophys J. 2013 Feb 19;104(4):798–806.

182. Mcgaraughty S, Chu KL, Perner RJ, Didomenico S, Kort ME, Kym PR. TRPA1 modulation of spontaneous and mechanically evoked firing of spinal neurons in uninjured, osteoarthritic, and inflamed rats.

183. Behrendt H-J, Germann T, Gillen C, Hatt H, Jostock R. Characterization of the mouse cold-menthol receptor TRPM8 and vanilloid receptor type-1 VR1 using a fluorometric imaging plate reader (FLIPR) assay. Br J Pharmacol. Wiley-Blackwell; 2004 Feb;141(4):737–45.

184. Hawkey CJ. COX-2 chronology. Gut. 2005 Nov;54(11):1509–14.

185. Vonkeman HE, van de Laar MAFJ. Nonsteroidal anti-inflammatory drugs: adverse effects and their prevention. Semin Arthritis Rheum. 2010 Feb;39(4):294–312.

186. Flower R, Gryglewski R, Herbaczyńska-Cedro K, Vane JR. Effects of anti-inflammatory drugs on prostaglandin biosynthesis. Nat New Biol. 1972 Jul 26;238(82):104–6.

187. WINDER C V, WAX J, SERRANO B, JONES EM, McPHEE ML. Anti-inflammatory and antipyretic properties of N-(alpha,alpha,alpha-trifluoro-m-tolyl) anthranilic acid (CI-440; flufenamic acid). Arthritis Rheum. 1963 Feb;6:36–47.

188. WINDER C V, WAX J, SCOTTI L, SCHERRER RA, JONES EM, SHORT FW. Anti-inflammatory, antipyretic and antinociceptive properties of N-(2,3-xylyl)anthranilic acid (mefenamic acid). J Pharmacol Exp Ther. 1962 Dec;138:405–13.

189. Lentjes EG, van Ginneken CA. Pharmacokinetics of flufenamic acid in man. Int J Clin Pharmacol Ther Toxicol. 1987 Apr;25(4):185–7.

190. Famaey JP, Whitehouse MW. Effects of nonsteroidal anti-inflammatory drugs on the uptake of various cations by lymphoid cells. Arch Int Physiol Biochim. 1976 Oct;84(4):719–34.

191.   Yamada K, Waniishi Y, Inoue R, Ito Y. Fenamates potentiate the alpha 1-adrenoceptor-activated nonselective cation channels in rabbit portal vein smooth muscle. Jpn J Pharmacol. 1996 Jan;70(1):81–4.

192.   Inoue R, Okada T, Onoue H, Hara Y, Shimizu S, Naitoh S, et al. The Transient Receptor Potential Protein Homologue TRP6 Is the Essential Component of Vascular 1-Adrenoceptor-Activated Ca2+-Permeable Cation Channel. Circ Res. 2001 Feb 16;88(3):325–32.

193.   Foster RR, Zadeh MAH, Welsh GI, Satchell SC, Ye Y, Mathieson PW, et al. Flufenamic acid is a tool for investigating TRPC6-mediated calcium signalling in human conditionally immortalised podocytes and HEK293 cells. Cell Calcium. 2009 Apr;45(4):384–90.

194.   Klose C, Straub I, Riehle M, Ranta F, Krautwurst D, Ullrich S, et al. Fenamates as TRP channel blockers: mefenamic acid selectively blocks TRPM3. Br J Pharmacol. 2011 Apr;162(8):1757–69.

195.   Albert AP, Pucovsky V, Prestwich SA, Large WA. TRPC3 properties of a native constitutively active Ca2+-permeable cation channel in rabbit ear artery myocytes. J Physiol. 2006 Mar 1;571(Pt 2):361–9.

196.   Lee YM, Kim BJ, Kim HJ, Yang DK, Zhu MH, Lee KP, et al. TRPC5 as a candidate for the nonselective cation channel activated by muscarinic stimulation in murine stomach. Am J Physiol Gastrointest Liver Physiol. 2003 Apr;284(4):G604-16.

197.   Hill K, Benham CD, McNulty S, Randall AD. Flufenamic acid is a pH-dependent antagonist of TRPM2 channels. Neuropharmacology. 2004 Sep;47(3):450–60.

198.   Togashi K, Inada H, Tominaga M. Inhibition of the transient receptor potential cation channel TRPM2 by 2-aminoethoxydiphenyl borate (2-APB). Br J Pharmacol. 2008 Mar;153(6):1324–30.

199.   Guinamard R, Sallé L, Simard C. The non-selective monovalent cationic channels TRPM4 and TRPM5. Adv Exp Med Biol. 2011 Jan;704:147–71.

200.   Liman ER. TRPM5 and taste transduction. Handb Exp Pharmacol. 2007 Jan;(179):287–98.

201.   Guinamard R, Demion M, Magaud C, Potreau D, Bois P. Functional expression of the TRPM4 cationic current in ventricular cardiomyocytes from spontaneously hypertensive rats. Hypertension. 2006 Oct;48(4):587–94.

202.   Ullrich ND, Voets T, Prenen J, Vennekens R, Talavera K, Droogmans G, et al. Comparison of functional properties of the Ca2+-activated cation channels TRPM4 and TRPM5 from mice. Cell Calcium. 2005 Mar;37(3):267–78.

203.   Aly FA, Al-Tamimi SA, Alwarthan AA. Determination of flufenamic acid and mefenamic acid in pharmaceutical preparations and biological fluids using flow injection analysis with tris(2,2'-bipyridyl)ruthenium(II) chemiluminescence detection. Anal Chim Acta. 2000 Jul;416(1):87–96.

204. Jiang X, Newell EW, Schlichter LC. Regulation of a TRPM7-like current in rat brain microglia. J Biol Chem. 2003 Oct 31;278(44):42867–76.

205. Guilbert A, Gautier M, Dhennin-Duthille I, Haren N, Sevestre H, Ouadid-Ahidouch H. Evidence that TRPM7 is required for breast cancer cell proliferation. Am J Physiol Cell Physiol. 2009 Sep;297(3):C493-502.

206. Guinamard R, Paulais M, Lourdel S, Teulon J. A calcium-permeable non-selective cation channel in the thick ascending limb apical membrane of the mouse kidney. Biochim Biophys Acta. 2012 May;1818(5):1135–41.

207. Wang S, Lee J, Ro JY, Chung M-K. Warmth suppresses and desensitizes damage-sensing ion channel TRPA1. Mol Pain. 2012 Jan;8:22.

208. Chen G-L, Zeng B, Eastmond S, Elsenussi SE, Boa AN, Xu S-Z. Pharmacological comparison of novel synthetic fenamate analogues with econazole and 2-APB on the inhibition of TRPM2 channels. Br J Pharmacol. 2012 Nov;167(6):1232–43.

209. Pribitkin E deAzevedo, Boger G. Herbal Therapy: What Every Facial Plastic Surgeon Must Know. Arch Facial Plast Surg. American Medical Association; 2001 Apr 1;3(2):127–32.

210. Arteaga S, Andrade-Cetto A, Cárdenas R. Larrea tridentata (Creosote bush), an abundant plant of Mexican and US-American deserts and its metabolite nordihydroguaiaretic acid. J Ethnopharmacol. 2005 Apr 26;98(3):231–9.

211. Lia V V, Confalonieri VA, Comas CI, Hunziker JH. Molecular phylogeny of Larrea and its allies (Zygophyllaceae): reticulate evolution and the probable time of creosote bush arrival to North America. Mol Phylogenet Evol. 2001 Nov;21(2):309–20.

212. Konno C, Lu ZZ, Xue HZ, Erdelmeier CA, Meksuriyen D, Che CT, et al. Furanoid lignans from Larrea tridentata. J Nat Prod. Jan;53(2):396–406.

213. Floriano-Sánchez E, Villanueva C, Medina-Campos ON, Rocha D, Sánchez-González DJ, Cárdenas-Rodríguez N, et al. Nordihydroguaiaretic acid is a potent in vitro scavenger of peroxynitrite, singlet oxygen, hydroxyl radical, superoxide anion and hypochlorous acid and prevents in vivo ozone-induced tyrosine nitration in lungs. Free Radic Res. Informa UK Ltd UK; 2006 May 7;40(5):523–33.

214. Zhou W, Chai H, Courson A, Lin PH, Lumsden AB, Yao Q, et al. Ginkgolide A attenuates homocysteine-induced endothelial dysfunction in porcine coronary arteries. J Vasc Surg. Elsevier; 2006 Oct 10;44(4):853–62.

215. Ramasamy S, Drummond GR, Ahn J, Storek M, Pohl J, Parthasarathy S, et al. Modulation of Expression of Endothelial Nitric Oxide Synthase by Nordihydroguaiaretic Acid, a Phenolic Antioxidant in Cultured Endothelial Cells. Mol Pharmacol. 1999 Jul 1;56(1):116–23.

216. Bismuth J, Chai H, Lin PH, Yao Q, Chen C. Lactosylceramide causes endothelial dysfunction in porcine coronary arteries and human coronary artery endothelial cells. Med Sci Monit. 2009 Sep;15(9):BR270-4.

217. Kumar S, Wedgwood S, Black SM. Nordihydroguaiaretic acid increases endothelial nitric oxide synthase expression via the transcription factor AP-1. DNA Cell Biol. Mary Ann Liebert, Inc. 140 Huguenot Street, 3rd Floor New Rochelle, NY 10801 USA; 2007 Dec 14;26(12):853–62.

218. Ansar S, Iqbal M, Athar M. Nordihydroguairetic acid is a potent inhibitor of ferric-nitrilotriacetate-mediated hepatic and renal toxicity, and renal tumour promotion, in mice. Carcinogenesis. 1999 Apr;20(4):599–606.

219. Huang J-K, Chen W-C, Huang C-J, Hsu S-S, Chen J-S, Cheng H-H, et al. Nordihydroguaiaretic acid-induced Ca2+ handling and cytotoxicity in human prostate cancer cells. Life Sci. 2004 Sep 24;75(19):2341–51.

220. Hofmanová J, Soucek K, Pacherník J, Kovaríková M, Hoferová Z, Minksová K, et al. Lipoxygenase inhibitors induce arrest of tumor cells in S-phase of the cell cycle. Neoplasma. 2002 Jan;49(6):362–7.

221. Moody TW, Leyton J, Martinez A, Hong S, Malkinson A, Mulshine JL. Lipoxygenase inhibitors prevent lung carcinogenesis and inhibit non-small cell lung cancer growth. Exp Lung Res. Jan;24(4):617–28.

222. Soriano AF, Helfrich B, Chan DC, Heasley LE, Bunn PA. J, Chou T-C. Synergistic Effects of New Chemopreventive Agents and Conventional Cytotoxic Agents against Human Lung Cancer Cell Lines. Cancer Res. 1999 Dec 1;59(24):6178–84.

223. Blecha JE, Anderson MO, Chow JM, Guevarra CC, Pender C, Penaranda C, et al. Inhibition of IGF-1R and lipoxygenase by nordihydroguaiaretic acid (NDGA) analogs. Bioorg Med Chem Lett. 2007 Jul 15;17(14):4026–9.

224. Noor R, Mittal S, Iqbal J. Superoxide dismutase--applications and relevance to human diseases. Med Sci Monit. 2002 Sep;8(9):RA210-5.

225. Goodman Y, Steiner MR, Steiner SM, Mattson MP. Nordihydroguaiaretic acid protects hippocampal neurons against amyloid β-peptide toxicity, and attenuates free radical and calcium accumulation. Brain Res. 1994 Aug;654(1):171–6.

226. Lambert JD, Zhao D, Meyers RO, Kuester RK, Timmermann BN, Dorr RT. Nordihydroguaiaretic acid: hepatotoxicity and detoxification in the mouse. Toxicon. 2002 Dec;40(12):1701–8.

227. Obermeyer WR, Musser SM, Betz JM, Casey RE, Pohland AE, Page SW. Chemical studies of phytoestrogens and related compounds in dietary supplements: flax and chaparral. Proc Soc Exp Biol Med. 1995 Jan;208(1):6–12.

228. Alderman S, Kailas S, Goldfarb S, Singaram C, Malone DG. Cholestatic hepatitis after ingestion of

chaparral leaf: confirmation by endoscopic retrograde cholangiopancreatography and liver biopsy. J Clin Gastroenterol. 1994 Oct;19(3):242–7.

229. Meyer AN, McAndrew CW, Donoghue DJ. Nordihydroguaiaretic acid inhibits an activated fibroblast growth factor receptor 3 mutant and blocks downstream signaling in multiple myeloma cells. Cancer Res. 2008 Sep 15;68(18):7362–70.

230. Eads D, Hansen R, Oyegunwa A, Cecil C, Culver C, Scholle F, et al. Terameprocol, a methylated derivative of nordihydroguaiaretic acid, inhibits production of prostaglandins and several key inflammatory cytokines and chemokines. J Inflamm (Lond). 2009 Jan;6:2.

231. Wang L, Yang L, Gao L, Gao TW, Li W, Liu YF. A functional promoter polymorphism in monocyte chemoattractant protein-1 is associated with psoriasis. Int J Immunogenet. 2008 Feb;35(1):45–9.

232. Paravicini TM, Chubanov V, Gudermann T. TRPM7: a unique channel involved in magnesium homeostasis. Int J Biochem Cell Biol. Elsevier Ltd; 2012 Aug;44(8):1381–4.

233. Chubanov V, Mederos y Schnitzler M, Meißner M, Schäfer S, Abstiens K, Hofmann T, et al. Natural and synthetic modulators of SK (K(ca)2) potassium channels inhibit magnesium-dependent activity of the kinase-coupled cation channel TRPM7. Br J Pharmacol. 2012 Jun;166(4):1357–76.

234. Nadler MJ, Hermosura MC, Inabe K, Perraud AL, Zhu Q, Stokes AJ, et al. LTRPC7 is a Mg.ATP-regulated divalent cation channel required for cell viability. Nature. 2001 May 31;411(6837):590–5.

235. Schlingmann KP, Waldegger S, Konrad M, Chubanov V, Gudermann T. TRPM6 and TRPM7--Gatekeepers of human magnesium metabolism. Biochim Biophys Acta. 2007 Aug;1772(8):813–21.

236. Yamaguchi H, Matsushita M, Nairn AC, Kuriyan J. Crystal structure of the atypical protein kinase domain of a TRP channel with phosphotransferase activity. Mol Cell. 2001 May;7(5):1047–57.

237. Mederos y Schnitzler M, Wäring J, Gudermann T, Chubanov V. Evolutionary determinants of divergent calcium selectivity of TRPM channels. FASEB J. 2008 May;22(5):1540–51.

238. Schmitz C, Perraud A-L, Johnson CO, Inabe K, Smith MK, Penner R, et al. Regulation of vertebrate cellular Mg2+ homeostasis by TRPM7. Cell. 2003 Jul 25;114(2):191–200.

239. Jin J, Desai BN, Navarro B, Donovan A, Andrews NC, Clapham DE. Deletion of Trpm7 disrupts embryonic development and thymopoiesis without altering Mg2+ homeostasis. Science. 2008 Oct 31;322(5902):756–60.

240. Park HS, Hong C, Kim BJ, So I. The Pathophysiologic Roles of TRPM7 Channel. Korean J Physiol Pharmacol. 2014 Feb;18(1):15–23.

241. Qin X, Yue Z, Sun B, Yang W, Xie J, Ni E, et al. Sphingosine and FTY720 are potent inhibitors of the transient receptor potential melastatin 7 (TRPM7) channels. Br J Pharmacol. 2013 Mar;168(6):1294–

312.

242.   Grimm C, Kraft R, Schultz G, Harteneck C. Activation of the melastatin-related cation channel TRPM3 by D-erythro-sphingosine [corrected]. Mol Pharmacol. 2005 Mar;67(3):798–805.

243.   Chen H-C, Xie J, Zhang Z, Su L-T, Yue L, Runnels LW. Blockade of TRPM7 channel activity and cell death by inhibitors of 5-lipoxygenase. PLoS One. 2010 Jan;5(6):e11161.

244.   Chen X, Numata T, Li M, Mori Y, Orser B a, Jackson MF, et al. The modulation of TRPM7 currents by nafamostat mesilate depends directly upon extracellular concentrations of divalent cations. Mol Brain. BioMed Central Ltd; 2010 Jan;3(1):38.

245.   Zierler S, Yao G, Zhang Z, Kuo WC, Pörzgen P, Penner R, et al. Waixenicin A inhibits cell proliferation through magnesium-dependent block of transient receptor potential melastatin 7 (TRPM7) channels. J Biol Chem. 2011 Nov 11;286(45):39328–35.

246.   Stefani ED, Boffetta P, Deneo-Pellegrini H, Mendilaharsu M, Carzoglio JC, Ronco A, et al. Dietary antioxidants and lung cancer risk: a case-control study in Uruguay. Nutr Cancer. 1999;34(1):100–10.

247.   van Erk MJ, Roepman P, van der Lende TR, Stierum RH, Aarts JMMJG, van Bladeren PJ, et al. Integrated assessment by multiple gene expression analysis of quercetin bioactivity on anticancer-related mechanisms in colon cancer cells in vitro. Eur J Nutr. 2005 Mar;44(3):143–56.

248.   Dihal AA, de Boer VCJ, van der Woude H, Tilburgs C, Bruijntjes JP, Alink GM, et al. Quercetin, but not its glycosidated conjugate rutin, inhibits azoxymethane-induced colorectal carcinogenesis in F344 rats. J Nutr. 2006 Nov;136(11):2862–7.

249.   Kim MC, Lee HJ, Lim B, Ha K-T, Kim SY, So I, et al. Quercetin induces apoptosis by inhibiting MAPKs and TRPM7 channels in AGS cells. Int J Mol Med. 2014 Jun;33(6):1657–63.

250.   Dou Y, Li Y, Chen J, Wu S, Xiao X, Xie S, et al. Inhibition of cancer cell proliferation by midazolam by targeting transient receptor potential melastatin 7. Oncol Lett. 2013 Mar;5(3):1010–6.

251.   Parnas M, Peters M, Dadon D, Lev S, Vertkin I, Slutsky I, et al. Carvacrol is a novel inhibitor of Drosophila TRPL and mammalian TRPM7 channels. Cell Calcium. 2009 Mar;45(3):300–9.

252.   Redmond WJ, Camo M, Mitchell V, Vaughan CW, Connor M. Nordihydroguaiaretic acid activates hTRPA1 and modulates behavioral responses to noxious cold in mice. Pharmacol Res Perspect. 2014 Dec;2(6):e00079.

253.   Ho SSH, Go ML. Restraining the flexibility of the central linker in terameprocol results in constrained analogs with improved growth inhibitory activity. Bioorg Med Chem Lett. 2013 Nov 15;23(22):6127–33.

254.   Ortar G, Morera L, Moriello AS. Modulation of thermo-transient receptor potential (thermo-TRP)

channels by thymol-based compounds. Bioorganic Med …. 2012 Apr;153(8):1739–49.

255. Takahashi N, Mizuno Y, Kozai D, Yamamoto S, Kiyonaka S, Shibata T, et al. Molecular characterization of TRPA1 channel activation by cysteine-reactive inflammatory mediators. Channels. 2008;2(4):287–98.

256. Zurborg S, Yurgionas B, Jira J a, Caspani O, Heppenstall P a. Direct activation of the ion channel TRPA1 by Ca2+. Nat Neurosci. 2007;10(3):277–9.